UNIVERSITAT DE BARCELONA

Detection of early cerebral amyloid-β deposition by PET imaging and its downstream effect

Gemma Salvadó Blasco

Detection of early cerebral amyloid-β deposition by PET imaging and its downstream effects

Gemma Salvadó Blasco

UNIVERSITAT DE BARCELONA

barcelonaβeta
BRAIN RESEARCH CENTER

Detection of early cerebral amyloid-β deposition by PET imaging and its downstream effects

Thesis presented by:

Gemma Salvadó Blasco

Supervisors:

Dr. Juan Domingo Gispert López & Dr. José Luis Molinuevo Guix

Tutor:

Dra. Roser Sala Llonch

Dr. Juan Domingo Gispert López *Dr. José Luis Molinuevo Guix*

Dra. Roser Sala Llonch

Barcelonaβeta Brain Research Center - Pasqual Maragall Foundation

Doctoral Programme in Biomedicine

University of Barcelona

April 2021

Caminante, son tus huellas
el camino y nada más;
Caminante, no hay camino,
se hace camino al andar.
Al andar se hace el camino,
y al volver la vista atrás
se ve la senda que nunca
se ha de volver a pisar.
Caminante no hay camino
sino estelas en la mar[1]

Antonio Machado

[1] Wanderer, it is your footprints
winding down, and nothing more;
Wanderer, no roads lie waiting,
roads you make as you explore,
Step by step your road is charted,
and behind your turning head
lies the path that you have trodden,
not again for you to tread.
Wanderer, there are no roadways,
only wakes upon the sea

LIST OF ABREVIATIONS

AA: Alzheimer's Association

Aβ: amyloid-β

AD: Alzheimer's disease

ADAD: autosomal dominant Alzheimer's disease

ADNC: Alzheimer's disease neuropathologic change

ALFA: Alzheimer and Families

AMYPAD: Amyloid Imaging to Prevent Alzheimer's Disease

***APOE*:** apolipoprotein E

APP: amyloid precursor protein

A4: Anti-Amyloid Treatment in Asymptomatic Alzheimer's Disease

BBRC: Barcelonaβeta Brain Research Center

CERAD: Consortium to Establish a Registry for Alzheimer's Disease

CL: Centiloid

CSF: cerebrospinal fluid

DIAN: Dominantly Inherited Alzheimer Network

DIAN-TU: Dominantly Inherited Alzheimer Network - Trials Unit

EMA: European Medicines Agency

ERC: entorhinal cortex

EYO: estimated years of onset

FDA: Food and Drug Administration

FDG: fluorodeoxyglucose

FINGER: Finnish Geriatric Intervention Study to Prevent Cognitive Impairment and Disability

GFAP: glial fibrillary acidic protein

GM: gray matter

GWAS: genome-wide association study

IL-6: interleukin 6

MCI: mild cognitive impairment

MRI: magnetic resonance imaging

MTL: medial temporal lobe

NfL: neurofilament light

NFT: neurofibrillary tau tangles

NIA: National Institute on Aging

OR: odds ratio

PET: positron emission tomography

PIB: Pittsburgh Compound-B

PSEN: presenilin

p-tau: phosphorylated tau

ROI: region of interest

sTREM2: soluble triggering receptor on myeloid cells 2

SUVR: standardized uptake value ratio

SV2A: synaptic vesicle protein 2A

TDP-43: TAR DNA-binding protein 43

TREM2: triggering receptor expressed on myeloid cells 2

TSPO: translocator protein

t-tau: total tau

VR: visual read

ABSTRACT

Alzheimer's disease (AD) is the leading cause of dementia worldwide. This disease, however, starts decades before any clinical symptom appears with the accumulation in the brain of aggregates of two main proteins: amyloid-β (Aβ) and tau. In recent years, the appearance of *in vivo* biomarkers capable to track biological changes has boosted the research interest to earlier phases of the disease. With these concepts in mind, the general objective of this thesis was to investigate Aβ deposition and its downstream effects in the earliest stages of the Alzheimer's *continuum*. To this aim, the four studies of the thesis include participants of the ALFA (from Alzheimer and Families) cohort, who are characterized as being cognitively unimpaired, (late) middle-aged, and to be enriched in risk factors for AD. Thus, increasing the probability of incorporating participants with low-intermediate burden of Aβ.

In the first two studies of this thesis, our focus was set on the early detection of Aβ deposition using PET scans. We first used automated quantification methods, as typically done in the research setting and, second, we used visual assessment, which is more often used in the clinical context. Our results lead to the identification of quantitative thresholds for the detection of early abnormalities in amyloid PET scans significantly lower than previously proposed. We also concluded that visual inspection of Aβ PET scans is sensitive to detect and grade early Aβ deposition in the brain.

In the third study, Aβ PET images were used to investigate whether risk factors for Alzheimer's dementia promoted the deposition of insoluble, fibrillar aggregates of Aβ in the brain for similar levels of Aβ in the cerebrospinal fluid (CSF), reflecting the production/clearance rate of soluble Aβ species. We found that that the main unmodifiable risk factors for Alzheimer's dementia -older age, female sex, and *APOE-ε4* allele carriership- increased deposited fibrillar Aβ for similar levels of soluble Aβ as measured in the CSF. However, while older age and female sex promoted the deposition in typical AD-related areas, thus suggesting an

additive effect, *APOE-ε4* allele facilitated the spread of Aβ in the entorhinal area, which has been described as an area vulnerable to tau deposition. This result suggests that *APOE-ε4* allele-related mechanisms might accelerate the propagation of Aβ pathology to these areas, facilitating the spread of tau through the neocortex and thus, contributing to raise the risk of developing AD.

Finally, in our last study, we investigated Aβ-downstream effects in the earliest stages of the Alzheimer's *continuum*. To this aim, we analysed core and novel AD CSF biomarkers. These included: Aβ42/40 and phosphorylated tau (p-tau) as markers of Aβ and tau pathology, respectively; total tau (t-tau) and neurofilament light (NfL) as markers of neurodegeneration; neurogranin for synaptic dysfunction; glial fibrillary acidic protein (GFAP), YKL-40, soluble triggering receptor on myeloid cells 2 (sTREM2), S100b, interleukin 6 (IL-6) as glial activity biomarkers and, total α-synuclein as marker of α-synuclein pathology. We observed that, although studying participants with low Aβ load, many pathophysiological pathways, such as inflammation, were already altered. Of note, our results suggest a direct link between Aβ deposition in the brain and neurodegeneration that is independent of tau pathology. Further, we described their direct and/or indirect associations with Aβ deposition, as well as the moderation effects of some Alzheimer’s dementia risk factors on these relationships.

RESUM

La malaltia d'Alzheimer és la causa principal de demència en tot el món. Aquesta malaltia però, comença dècades abans de l'aparició de qualsevol símptoma clínic amb l'acumulació en el cervell de l'agregat de dues proteïnes: l'amiloide-β (Aβ) i la tau. En els últims anys, l'aparició de biomarcadors *in vivo* capaços de monitoritzar aquests, entre d'altres, canvis biològics ha estimulat l'interès cap a etapes més inicials de la malaltia. Amb aquests conceptes en ment, l'objectiu general d'aquesta tesis era el d'investigar l'acumulació d'Aβ i els seus efectes derivats en les etapes més incipients del continu de la malaltia d'Alzheimer. Amb aquest objectiu, els quatre estudis d'aquesta tesis inclouen participants de la cohort ALFA (per Alzheimer i Famílies), els quals es caracteritzen per ser cognitivament sans, ser de mitjana edat avançada i per estar prioritàriament seleccionats per tenir factors de risc per l'Alzheimer. Incrementant, d'aquesta manera, la possibilitat d'incorporar participants amb càrrega baixa o intermitja d'Aβ.

En els primers dos estudis d'aquesta tesis, el nostre focus era la detecció precoç de l'acumulació d'Aβ utilitzant imatges PET. Primer utilitzant mètodes de quantificació automàtica, típicament utilitzats en la recerca i, segon, mitjançant l'avaluació visual, que és més sovint utilitzada en el context clínic. Els nostres resultats ens van portar a la identificació de llindars quantitatius per a la detecció precoç d'anormalitats en les imatges PET d'Aβ significativament inferiors als prèviament proposats. A més, també vam concloure que la inspecció visual d'aquestes imatges és sensible per detectar i qualificar el dipòsit inicial d'Aβ en el cervell.

En el tercer estudi, les imatges PET d'Aβ van ser utilitzades per investigar si factors de risc per la demència d'Alzheimer promovien l'acumulació d'agregats fibril·lars insolubles d'Aβ en el cervell per nivells similars d'Aβ mesurat en el líquid cefalorraquidi (LCR), els quals reflecteixen el rati de producció/eliminació d'espècies solubles d'Aβ. La nostra conclusió en aquest estudi és que els tres principals factors de risc no modificables per

a la demència d'Alzheimer -edat avançada, sexe femení i ser portador de l'al·lel *APOE-ε4*- incrementen la càrrega fibril·lar d'Aβ dipositat per nivells similars d'Aβ soluble mesurat en el LCR. Tanmateix, mentre que l'edat avançada i el sexe femení promouen el dipòsit d'Aβ en àrees típiques de la malaltia d'Alzheimer i, per tant, suggereixen un efecte additiu; l'al·lel *APOE-ε4* facilita l'expansió de l'Aβ en l'escorça entorínica, que ha sigut descrita per ser especialment vulnerable al dipòsit de la proteïna tau. Aquest últim resultat suggereix que, els mecanismes relacionats amb l'al·lel *APOE-ε4* podrien accelerar la propagació de la patologia Aβ a aquestes àrees, facilitant la futura propagació de la proteïna tau pel neocòrtex i contribuir així, a l'augment de risc de desenvolupar la malaltia d'Alzheimer.

Finalment, en el nostre últim estudi, vam investigar els efectes derivats de l'acumulació d'Aβ en les primeres etapes del continu de la malaltia d'Alzheimer. Amb aquest objectiu, vam analitzar marcadors bàsics i novells en LCR de la malaltia d'Alzheimer. Aquests inclouen: Aβ42/40 i tau fosforilat (p-tau) com a marcadors de patologia Aβ i tau, respectivament; tau total (t-tau) i neurofilament lleuger (NfL) com a biomarcadors de neurodegeneració; neurogranina per disfunció sinàptica; GFAP, YKL-40, sTREM2, S100b i IL-6 com marcadors d'activitat glial i, α-synucleïna total com a marcador de patologia d'α-synucleïna. Val a destacar que els nostres resultats suggereixen una relació directe entre el dipòsit d'Aβ en el cervell i la neurodegeneració que és independent de la patologia tau. A més, també vam descriure les associacions directes i/o indirectes amb la càrrega d'Aβ, així com l'efecte moderador d'alguns factors de risc en aquestes relacions.

CONTENT

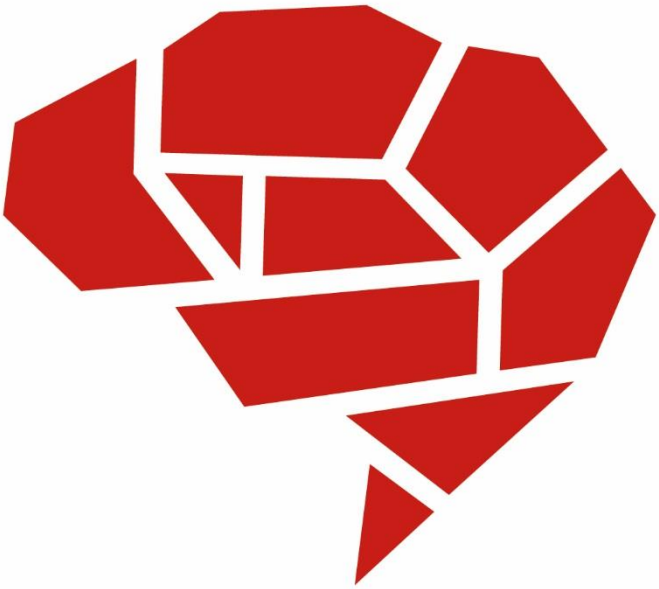

INTRODUCTION

INTRODUCTION

■ ALZHEIMER'S DISEASE

Alzheimer's disease (AD) is a neurodegenerative disorder that is clinically characterized by progressive cognitive decline, which ultimately leads to dementia. Memory impairment is one of the most well-known traits of AD, however, other cognitive domains, such as executive function or visuospatial abilities, are also impaired during the course of the disease (Weintraub *et al.*, 2012; Mortamais *et al.*, 2017). AD affects approximately 40 million people in the world but it is thought to reach 115.4 million patients by the year 2050 due to the increase in life expectancy (Prince *et al.*, 2013). At present, there is no treatment capable to cure, stop or even slow down the progression of the disease. For this reason, it is of utmost importance to study and to understand the pathophysiological events that occur during the Alzheimer's *continuum* to design interventions that can modify the course of this disease. Ideally, it has been suggested that these interventions should be applied in preclinical stages to prevent the start of cognitive decline.

Main pathophysiological events in AD

AD is characterized by two main pathological hallmarks: senile plaques of amyloid-β (Aβ) and neurofibrillary tau tangles (NFT; **Figure 1**). Aβ plaques are aggregations of Aβ fibrils that accumulate outside neurons in dense formation. And tau tangles are found within the neuron body and consist of aggregations of hyperphosphorylated tau protein (Selkoe and Hardy, 2016). The accumulation of these two proteins is thought to cause neural death, which leads to neurodegeneration and consequently causes cognitive impairment of the subjects.

Aβ and tau accumulation in the brain were already described by Alois Alzheimer when he reported the first case of AD, subsequently named after

him (Alzheimer, 1907; Stelzmann *et al.*, 1995). Both proteins can be measured in *post mortem* neuropathological studies, which until some years ago was the only way to establish a definitive diagnosis of AD. However, in recent years many *in vivo* biomarkers have been developed for both proteins and a more accurate diagnosis of AD can be performed before death. These biomarkers include neuroimaging biomarkers, such as positron emission tomography (PET) (Masdeu, 2017; Jagust, 2018), or soluble biomarkers, such as the level of certain proteins measured in the cerebrospinal fluid (CSF) and in the plasma (Molinuevo *et al.*, 2018*a*; Milà-Alomà *et al.*, 2019; Zetterberg and Bendlin, 2020; Zetterberg and Blennow, 2021).

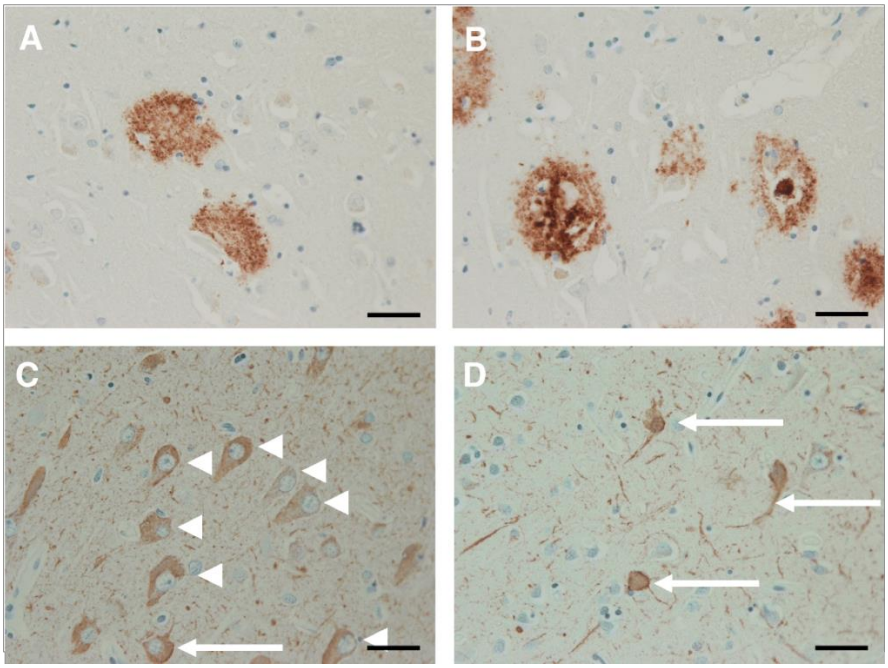

Figure 1: Aβ senile plaques and neurofibrillary tau tangles seen with immunohistochemistry. Upper row shows diffuse (A) and dense (B) Aβ senile plaques. Lower row show NFT of both pre-tangles (arrowheads, C) and mature tangles (arrows, D). Modified from (Deture and Dickson, 2019).

Parallel to Aβ and tau accumulation, AD is characterized by many other alterations in the brain. The most common and well-known is neurodegeneration. AD-related neurodegeneration is characterized by

atrophy in particular areas of the brain, such as the hippocampus and entorhinal cortex (ERC), which has been described as the Alzheimer's signature (Dickerson *et al.*, 2009). This neurodegeneration can be measured through neuroimaging techniques such as structural magnetic resonance imaging (MRI) and fluorodeoxyglucose (FDG) PET (Reiman and Jagust, 2012; Jagust, 2018), but also using fluid biomarkers such as total tau (t-tau) and neurofilament light (NfL) levels which can be measured in CSF and plasma (Molinuevo *et al.*, 2018*a*; Milà-Alomà *et al.*, 2019; Zetterberg and Bendlin, 2020). Other pathophysiological mechanisms altered in AD are neuroinflammation and synaptic function which can be also measured through specific imaging techniques and soluble biomarkers (Heneka *et al.*, 2015; Lagarde *et al.*, 2018; Milà-Alomà *et al.*, 2019; Zetterberg and Bendlin, 2020).

Temporal evolution of AD pathophysiological events

The alterations mentioned above, however, do not occur all at the same time (**Figure 2A**). The Alzheimer's *continuum* spans a long period, in which different pathophysiological events appear at different moments. For instance, Aβ PET burden needs more than 30 years to achieve the levels typically observed in AD patients from those in healthy controls (Villemagne *et al.*, 2013; Wang *et al.*, 2020) (**Figure 2B**). Autosomal dominant AD (ADAD) is the familiar version of AD. Given that it shows a similar pattern of events than sporadic AD, it has been used to understand the preclinical stage of the disease. In ADAD, CSF Aβ levels decline up to 25 years before the estimated years of onset (EYO) (Bateman *et al.*, 2012*a*). Also in the familiar version of AD, Aβ accumulation can be detected using PET, after CSF Aβ levels alterations, and up to 15 years before EYO. This is followed by changes in phosphorylated tau (p-tau) and brain atrophy, around 15 years before EYO, and finally, hypometabolism is detected in FDG PET together with episodic memory decline of the patients, 10 years before EYO (Bateman *et al.*, 2012*a*). In non-autosomal dominant AD, a similar ordering was found, with CSF Aβ becoming abnormal first, followed by increases in Aβ PET burden, then increases in CSF p-tau, followed by abnormalities in

MRI and FDG biomarkers of neurodegeneration and, finally, cognitive impairment (Jack *et al.*, 2013*a*).

More recently, other biomarkers have also shown alterations early in the Alzheimer's *continuum*. In this sense, the soluble triggering receptor on myeloid cells 2 (sTREM2) is a marker of microglial activation that can be measured in CSF. The CSF levels of sTREM2 are increased after Aβ accumulation and neuronal injury but before clinical onset (Suárez-Calvet *et al.*, 2016). Also biomarkers of synaptic dysfunction, and astroglial-response have shown increases after Aβ and tau changes (Palmqvist *et al.*, 2019*a*, Milà-Alomà *et al.*, 2020*a*) (See "Other AD biomarkers" section).

Spatial evolution of AD pathophysiological events

It is also important to note, that Aβ and tau follow different spatio-temporal patterns of accumulation in the brain (**Figure 3**). Some models have been proposed to depict the spread of these two proteins across the brain using *post-mortem* neuropathological data. Historically, tau accumulation was the first to be described using a staging model. This model divided the spread of tau into six stages that are called the Braak and Braak stages (Braak and Braak, 1991). These stages included: transentorhinal area as the first to become affected (stage I), followed by the ERC and the hippocampus (stage II), temporal preneocortex (stage III), adjoining neocortex areas and the insula cortex (stage IV), that evolve to superior-lateral areas (stage V) and, finally, primary areas of the neocortex (stage VI) (Braak *et al.*, 2006, 2011). Then, staging methods for Aβ accumulation appeared first mainly focusing its attention on medial temporal lobe (MTL) areas (Braak and Braak, 1997; Thal *et al.*, 2000), but were followed by a more global model, including its spread across the whole brain (Thal *et al.*, 2002). According to this model, Aβ accumulation starts in the neocortex (phase 1), followed by the involvement in the allocortical regions (phase 2). Afterwards, the regions affected by Aβ accumulation are diencephalic nuclei, the striatum, and the cholinergic nuclei of the basal forebrain (phase 3). And, finally, Aβ accumulates in several nuclei of the brainstem (phase 4) and the cerebellum (phase 5).

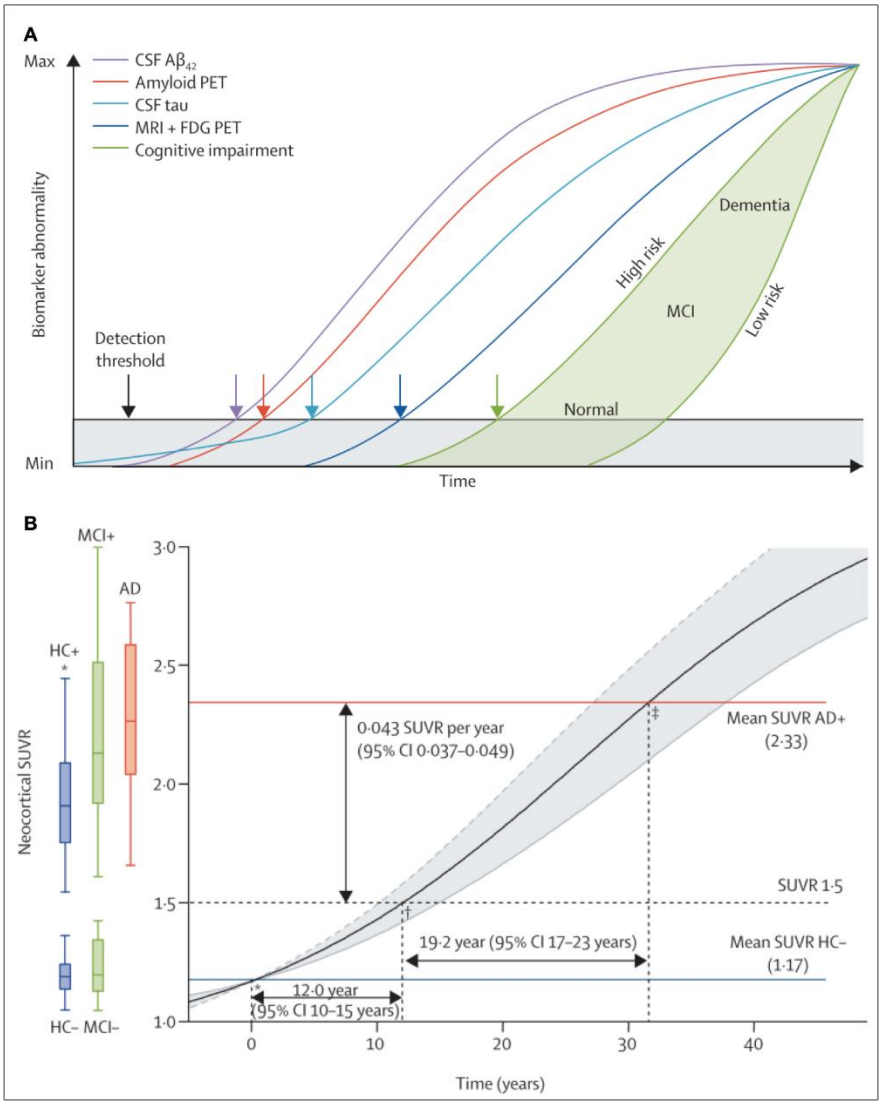

Figure 2: Biomarkers progression across the AD *continuum.* Hypothetical evolution of different AD biomarkers is shown in (A). Subfigure (B) shows the Aβ accumulation over time as well as the expected rates and time to progression in different stages of the disease. Modified from(Jack *et al.*, 2013*a*; Villemagne *et al.*, 2013)

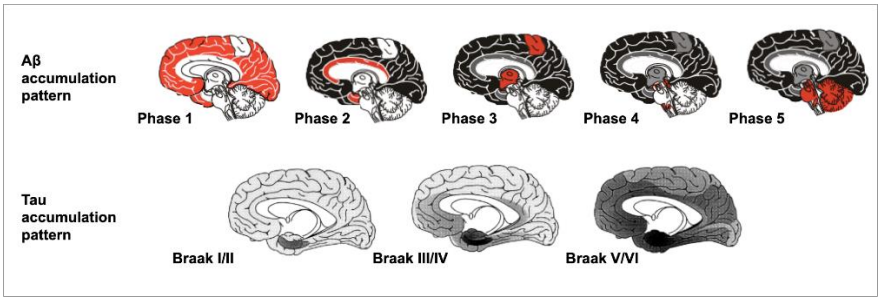

Figure 3: Aβ and tau accumulation patterns. Upper row show the Aβ accumulation pattern and lower row show tau accumulation pattern. Modified from (Braak and Braak, 1997; Thal *et al.*, 2018).

CORE AD BIOMARKERS

The field of AD biomarkers experimented a revolution in the last few years, which has influenced both the clinical and the research settings. In the following section, we describe the main biomarkers currently available for Aβ, tau and neurodegeneration. Then, we comment on the relationships between them and, to finalize, we detail some of the implications that these developments have entailed in the research of AD.

Amyloid-β pathology

In recent years many different Aβ biomarkers have been developed (Cohen *et al.*, 2019). They can be grouped into two big categories: neuroimaging Aβ biomarkers and fluid Aβ biomarkers. The latter can also be divided into those that measure Aβ concentrations in the CSF and in the blood. Apart from these general divisions, each biomarker has its characteristics, with its advantages and disadvantages, and measure different forms of Aβ. In this section, we will summarize the main characteristics of each of these biomarkers and their inter-relationships.

Aβ has different species (*e.g.* $A\beta_{42}$, $A\beta_{40}$, $A\beta_{38}$) depending on their length that have been related to different levels of toxicity in the brain (Molinuevo

et al., 2018*a*). Whilst $A\beta_{42}$, is a minor component in the CSF and plasma in physiological conditions, it is the major component of Aβ plaques (Iwatsubo *et al.*, 1994). For this reason maybe, CSF $A\beta_{42}$ was the first Aβ biomarker to be developed (Motter *et al.*, 1995; Galasko *et al.*, 1998; Andreasen *et al.*, 1999). Already in the first studies, it showed decreased levels in AD individuals compared to normal controls. As $A\beta_{42}$ was known to be deposited in Aβ plaques in the brain (Roher *et al.*, 1993; Iwatsubo *et al.*, 1994), it was hypothesized that the lower clearance in AD patients may result in lower $A\beta_{42}$ levels in the CSF (Motter *et al.*, 1995). Nowadays, CSF $A\beta_{42}$ levels are often normalized to $A\beta_{40}$ levels, which seems not as pathogenic as $A\beta_{42}$, to account for inter-individual Aβ production differences and other technical factors. This procedure has shown advantages above CSF $A\beta_{42}$ alone in the differentiation of AD patients (Hansson *et al.*, 2019).

Another Aβ biomarker usually used in clinical and research settings is Aβ PET (Rowe and Villemagne, 2013; Meyer *et al.*, 2019), which refers to the amount of Aβ deposited in the brain by means of an specific radiotracer and a PET scan (**Figure 4**). The first Aβ tracer to be developed was the ^{11}C-Pittsburgh compound B (PIB), which was administered for the first time to a human subject in 2002. In the first study with humans, PIB showed good discrimination between AD subjects and healthy controls, with high retention of the tracer in areas known to accumulate Aβ in AD patients compared to healthy controls (Klunk *et al.*, 2004). The main caveat of PIB is that is labelled with ^{11}C, which has a very short half-life and, therefore, reduces its usability only to PET centers with an on-site cyclotron. To overcome this limitation, ^{18}F-labelled tracers, with a longer half-life, were developed a few years later. At this moment, three ^{18}F-labelled Aβ tracers are approved by the Food and Drug Administration (FDA) and the European Medicines Agency (EMA): [^{18}F]flutemetamol (Vandenberghe *et al.*, 2010), [^{18}F]florbetaben (Rowe *et al.*, 2008; Barthel *et al.*, 2011; Villemagne *et al.*, 2011) and [^{18}F]florbetapir (Wong *et al.*, 2010; Clark *et al.*, 2011). All have shown good accuracy to differentiate between AD patients and healthy controls (Morris *et al.*, 2016) and, more importantly, have been validated against pathology (Clark *et al.*, 2011; Sabri *et al.*, 2015; Ikonomovic *et al.*, 2016). In addition, a study compared two of the fluorinated tracers with PIB measures showing a very high correlation (Landau *et al.*, 2014).

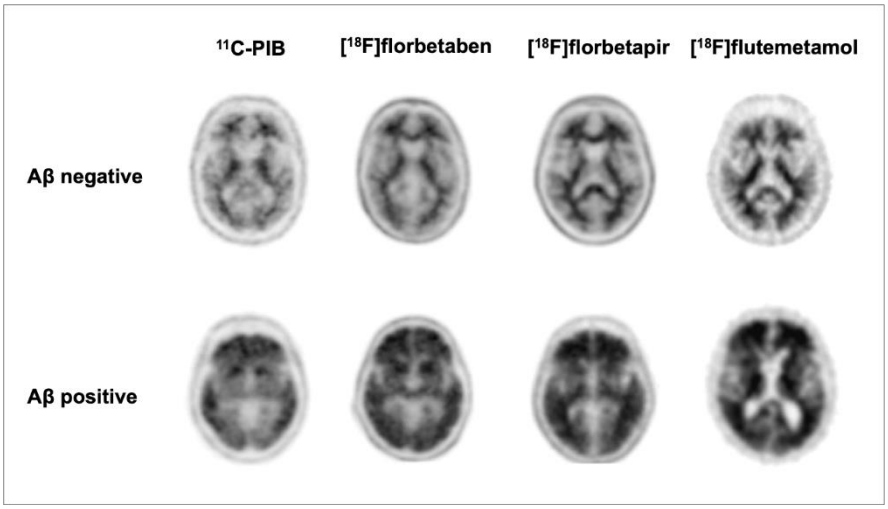

Figure 4: Aβ PET imaging with different tracers. This figure shows Aβ negative (upper row) and Aβ positive (lower row) PET scans with different tracers (columns). Modified from (Rowe and Villemagne, 2013)

In research, the most widely-used methodology to assess an Aβ PET scan is quantification. In static PET scans, which are the most commonly used, the metric most often utilised is the standardized uptake value ratio (SUVR). This is a measure of tracer binding in a region of interest (ROI) that is normalized to the uptake in a reference region, which is supposed not to have any specific binding. It is important to note, though, that this measure can be highly affected by the preprocesing methods and the definition of ROIs used to quantify the images, the selection of the reference region, or when using different tracers (Schwarz *et al.*, 2017). To overcome this issue, the Centiloid project was designed (Klunk *et al.*, 2015). It aimed to standardize the Aβ PET quantification in a way that measures of different centers and tracers could be directly compared using the Centiloid scale (CL). This scale, as the Centigrade scale, has two anchor points: one at 0 CL, which represents the mean Aβ retention of young controls, and another at 100 CL, which is the average Aβ retention of typical AD patients. The Centiloid project also proposed a standard processing pipeline to quantify the images, as well as a standard set of ROIs as target and four different reference regions, which are all publicly available (www.gaain.org/centiloid-

project). Importantly, the Centiloid group has also proposed a method to validate any other non-standard Centiloid quantification method making use of alternative processing pipelines or ROIs. Thus, one could use their method to quantify their Aβ PET images and then transform the measure into CL, which will be more comparable to CL of other centers than their original SUVRs.

While quantification of Aβ PET scans provides a continuous measure, in some cases it might be of interest to simply classify subjects into Aβ positive or negative, especially for decision making (*i.e.* who should enter in a clinical trial). In the clinical routine, Aβ PET quantification is barely used and scans are classified as positive or negative by visual read (VR) by a trained nuclear physician or radiologist. VR is the only FDA- and EMA-approved method to classify participants into Aβ positive or negative. This method has been validated against neuropathological Aβ measures, considered to be standard of truth (Clark *et al.*, 2011; Sabri *et al.*, 2015; Ikonomovic *et al.*, 2016; Salloway *et al.*, 2017). It has been claimed that VR is a conservative measure as it was developed to indicate moderate-to-frequent plaques as evaluated using the CERAD classification (Mirra *et al.*, 1991; Salloway *et al.*, 2017), which may lead to a lack of sensitivity in early cases where Aβ accumulation is still low. Few studies have derived CL thresholds against VR positivity, but those that had have found high CL thresholds (around 40 CL) (Battle *et al.*, 2019; Hanseeuw *et al.*, 2020). Therefore, it is fair to assume that there is still room for improvement as regards the applicability of VR assessment to early disease stages, which is especially important for clinical trials targeting preclinical subjects.

Although CSF Aβ and Aβ PET quantification have been used as Aβ biomarkers interchangeably in the research setting, their exact correspondence is not straightforward. In dichotomic classification, both CSF Aβ and Aβ PET have shown good accuracy in classifying subjects (Landau *et al.*, 2013; Palmqvist *et al.*, 2014, 2015). Nonetheless, its different criteria to derive cut-offs for positivity (Jack *et al.*, 2017) can lead to different conclusions (Milà-Alomà *et al.*, 2020*b*). It is important to note that CSF Aβ and Aβ PET measure different pools of Aβ (Roberts *et al.*, 2017); CSF Aβ is thought to measure the product of Aβ production and clearance, whereas Aβ

PET tracers are known to bind only to dense fibrillar Aβ plaques and have low affinity to diffuse Aβ plaques or soluble Aβ (Rowe and Villemagne, 2013). Moreover, CSF Aβ and Aβ PET have a negative association, as CSF decreases and Aβ PET binding increases in AD patients (Fagan *et al.*, 2006). In addition, this association is highly non-linear (Toledo *et al.*, 2015) (**Figure 5**), being characterized by a larger dynamic range of CSF Aβ measures in the lower range of Aβ PET values that later on *plateaus* at the upper range of Aβ PET values. Altogether these characteristics result in an earlier detectability of abnormality in CSF Aβ than Aβ PET measures (Palmqvist *et al.*, 2016), which suggests that CSF Aβ more suitable for an early and sensitive measure of Aβ pathology. However, it has also pointed out that the usual Aβ PET thresholds for positivity may be too high to detect this early/subtle amyloidosis and that lowering them may result in a more sensitive measure (Villeneuve *et al.*, 2015).

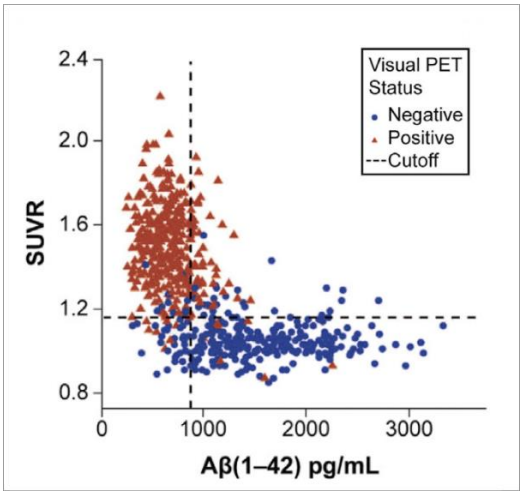

Figure 5: Association between CSF Aβ and Aβ PET measures. Relationship between CSF Aβ levels and Aβ PET SUVR in a sample of 646 participants covering the whole Alzheimer's *continuum*. Blue dots represent Aβ negative subjects and red triangles represent Aβ positive subjects as classified by visual assessment of Aβ PET. Modified from (Hansson *et al.*, 2018)

Both CSF and PET have advantages and drawbacks as Aβ biomarkers. One of the main advantages of measuring Aβ in CSF is that its collection

allows the measurement of other proteins in the same exam. Further, it is more available and cheaper to perform than Aβ PET, although it is also an invasive technique. Another of its caveats is the low comparability of quantitative levels between different laboratories and even batch-to-batch (Mattsson *et al.*, 2013; Kuhlmann *et al.*, 2017). To overcome this, the Elecsys β-amyloid (1–42) assay (Roche Diagnostics), a fully automated electrochemiluminescence immunoassay, was recently developed (Bittner *et al.*, 2016). This Aβ essay relies on the automatization and the use of reference measurement procedures to produce replicable results across laboratories and lots. Although its recent development, it has already shown high concordance with Aβ PET and generalizable cut-offs for Aβ positivity have been derived (Hansson *et al.*, 2018; Schindler *et al.*, 2018; Shaw *et al.*, 2018).

The regional information, on the other hand, is the main advantage of PET imaging compared to soluble biomarkers. This regional information has shown multiple clinical implications (Grothe *et al.*, 2017; Hanseeuw *et al.*, 2018; Mattsson *et al.*, 2019; Collij *et al.*, 2020; Jelistratova *et al.*, 2020). In particular, staging models including regional Aβ information to classify participants have shown improved predictive capacity for cognitive decline and atrophy compared to global Aβ classification (Hanseeuw *et al.*, 2018; Mattsson *et al.*, 2019; Collij *et al.*, 2020). Furthermore, these regional staging methods have also proven their value for earlier Aβ detection (Grothe *et al.*, 2017; Collij *et al.*, 2020; Jelistratova *et al.*, 2020), and showed its association to regional neuropathological markers of Aβ pathology (Teipel *et al.*, 2020). However, all these regional staging methods rely on quantification methods only. Although many of the VR criteria are based on regional assessment, the final classification often omits this information, leading to a final positive or negative without exploiting the extension of Aβ accumulation. Thus, including regional information into VR assessment could lead to an earlier and more precise characterization of the progression of the disease.

Finally, blood-based Aβ biomarkers are the most recent development in this field (Zetterberg *et al.*, 2011; Janelidze *et al.*, 2016; Nakamura *et al.*, 2018). The main and huge advantage of this type of biomarker is that is a non-

invasive technique, suitable for screening the general population. This, together with a projected lower cost compared to the other two techniques, will allow more generalizable testing, which may in turn help earlier Aβ detection and enable preventive intervention strategies. However, there is still a lot to work to do to assess its validity, especially in the general population. Further, plasma biomarker do not give any regional information, which, as explained above, has been proven useful.

Altogether, we can say that all Aβ biomarkers have their advantages and caveats. Moreover, although they are usually used indistinguishably, especially in the clinics, they are measuring different signs of Aβ dysmetabolism and their relationship may be complex.

Tau pathology

Together with Aβ, NFT are the other pathological hallmark of AD. Tau pathology can be also measured using both neuroimaging and soluble biomarkers. In the CSF, the most widely studied markers of tau pathology are p-tau (181) and t-tau, which were developed more than twenty years ago (Blennow *et al.*, 1995). While p-tau measures the phosphorylated amount of tau, specific of AD, t-tau levels give an assessment of the total amount of tau, which can be related to other neurodegenerative diseases (Milà-Alomà *et al.*, 2019). For this reason, t-tau has been sometimes proposed as a neurodegeneration marker. In the last few years other CSF p-tau biomarkers have appeared, measuring at different phosphorylation sites (*e.g.* 217 or 231) and in different fragments (*e.g.* mid-region, N-terminal) with promising future applications (Barthélemy *et al.*, 2020, Janelidze *et al.*, 2020*b*; Suárez-Calvet *et al.*, 2020). CSF tau is elevated in AD patients compared to healthy controls (Hansson *et al.*, 2006; Mattsson *et al.*, 2009; Shaw *et al.*, 2009; Olsson *et al.*, 2016), and it already shows altered levels in the preclinical stage (Hansson *et al.*, 2006; Shaw *et al.*, 2009, Bateman *et al.*, 2012*a*). Thus, it is used to stage subjects in the Alzheimer's *continuum* (Fagan *et al.*, 2014; McDade *et al.*, 2018; Schindler *et al.*, 2019). Similar to Aβ, fully automated CSF p-tau and t-tau biomarkers have been developed to minimize lot-to-lot variability (Blennow *et al.*, 2019; Lifke *et al.*, 2019).

On the other hand, tau PET tracers have only a few years of life. Although multiple tau PET tracers have shown their power to detect NFT *in vivo* (Marquié *et al.*, 2017; Okamura *et al.*, 2018; Leuzy *et al.*, 2019), currently there is only one, [^{18}F]flortaucipir, approved by the FDA for clinical purposes. The main advantage of tau PET over CSF biomarkers, as with Aβ PET, is that they provide topographical information. In tau PET, this information is usually analysed looking at Braak-like regions (Cho *et al.*, 2016; Schöll *et al.*, 2016) which can be used to stage participants (Pascoal *et al.*, 2020). Moreover, it has shown a tight association with neurodegeneration and cognitive decline (Schöll *et al.*, 2016; Bejanin *et al.*, 2017; Maass *et al.*, 2017; Pascoal *et al.*, 2020).

In the field of plasma biomarkers, there has been a recent revolution regarding tau measurements. Recent studies have shown a very high association with tau PET and CSF tau measures (Mielke *et al.*, 2018, Palmqvist *et al.*, 2019*b*), showing elevated levels shortly after the first changes in CSF Aβ but before reaching Aβ PET positivity. These results have been validated to multiple other pathological measures of AD including neuropathological data (Janelidze *et al.*, 2020*a*; Thijssen *et al.*, 2020).

Neurodegeneration

Multiple biomarkers are currently used to measure neurodegeneration in the AD field. As previously stated, structural MRI is one of the most convenient and widely-used ways to measure neurodegeneration. This was typically done using visual ratings (Scheltens *et al.*, 1992), but several quantitative methods have appeared to measure gray matter (GM) volumes and/or thickness (Dickerson *et al.*, 2009, Jack *et al.*, 2015*a*). Another widely accepted imaging biomarker for neurodegeneration FDG PET scan which measures glucose metabolism (Minoshima *et al.*, 1997, Jack *et al.*, 2015*a*), although it can also be related to synaptic and metabolic dysfunction (Reiman, 2011). This can also be assessed either by visual inspection or by quantification.

As for soluble biomarkers, CSF t-tau has been used as a marker of neurodegeneration in the past, but recent studies suggest that the novel

CSF NfL might be superior for this purpose (Kern *et al.*, 2019; Mattsson-Carlgren *et al.*, 2020). Neurofilaments are abundant in the axons of the neurons, and of all types, NfL has shown to be the best biomarker of neurodegeneration as it leaks into the CSF when there is neuronal and axonal damage (Milà-Alomà *et al.*, 2019), irrespective of cause (Khalil *et al.*, 2018). NfL levels increase in mild cognitive impairment (MCI) and Alzheimer's dementia stages (Sjögren *et al.*, 2001; Zetterberg *et al.*, 2016; Alcolea *et al.*, 2017). More importantly, NfL, either in blood or in CSF, has demonstrated its capacity as a staging biomarker, as its levels continuously increase during the progression of the disease, and it is already elevated in preclinical AD and as early as a decade before symptoms in ADAD subjects (Weston *et al.*, 2017, 2019; Bos *et al.*, 2019; Preische *et al.*, 2019). More precisely, in a recent study of our group, we showed that CSF NfL levels were associated with CSF Aβ already in cognitively unimpaired participants (Milà-Alomà *et al.*, 2020*a*), which was also replicated in a coetaneous independent study (Andersson *et al.*, 2020). Altogether, NfL is a good biomarker for early neurodegeneration although it is important to note that it is unspecific for AD, as its levels increase in other neurodegenerative diseases with axonal loss (*e.g.* Parkinson's disease, frontotemporal dementia or vascular dementia) (Skillbäck *et al.*, 2014; Lin *et al.*, 2019).

Relationship between core AD biomarkers

Although the temporal and the spatial sequences of these pathophysiological events are well accepted, the mechanistic links between them as well as their drivers are still unknown. One of the hypotheses behind the pathophysiological alterations observed in AD is the so-called ‘Aβ cascade hypothesis’ (Hardy and Higgins, 1992). This hypothesis, which has been revised in the recent years (Selkoe and Hardy, 2016), states that Aβ deposition leads to tau tangle formation and subsequent cell death. However, there are some studies of neuropathological data (Braak and Braak, 1997), that show that tau tangles may appear years, or even decades, before Aβ in specific subcortical nuclei (Braak and Del Tredici, 2011).

Recently, another explanation regarding Aβ and tau interaction in the course of AD has been proposed. It has been suggested that the accumulation of tau filaments in the ERC is one of the first alterations to appear but may be only a consequence of aging (Braak and Braak, 1991). Supporting this, some studies have found this kind of accumulation in older subjects without cognitive impairment nor Aβ deposition (Braak and Braak, 1997; Arnsten *et al.*, 2020). However, Aβ deposition might be necessary for the spreading of tau to cortical areas, or at least it may facilitate it (Price and Morris, 1999; Musiek and Holtzman, 2012; Mungas *et al.*, 2014; Pontecorvo *et al.*, 2017; He *et al.*, 2018). Some studies support that this spread occurs via cell-to-cell connections, similar to prion disease and that it is accelerated in those areas with previous Aβ deposition (Vogel *et al.*, 2020). However, this theory is still under debate and other studies suggest distinct types of interactions between tau and Aβ, such as tau, and not Aβ, being the initiating factor of the disease (Arnsten *et al.*, 2020).

The temporal and regional association between Aβ and tau accumulation and neurodegeneration is much clearer. On one hand, regional Aβ accumulation is not strongly associated with specific GM atrophy or FDG hypometabolism (Lehmann *et al.*, 2013; Jagust, 2016; Iaccarino *et al.*, 2018; La Joie *et al.*, 2020) of any specific region. On the other hand, there are multiple studies relating regional tau deposition with subsequent GM atrophy (Whitwell *et al.*, 2008; Iaccarino *et al.*, 2018; La Joie *et al.*, 2020) or FDG hypometabolism (Ossenkoppele *et al.*, 2015, 2016*a*; Bischof *et al.*, 2016) in the same or adjacent regions. The hypothesis is that tau accumulation within the neurons causes their death, provoking the later atrophy (Duyckaerts *et al.*, 2009).

Associations between the previously mentioned pathophysiological events during AD and cognitive decline are also well understood. Tau deposition, but not Aβ, is related to cognitive decline both as shown in *post-mortem* neuropathological as well as *in vivo* studies (Arriagada *et al.*, 1992; Gómez-Isla *et al.*, 1997; Giannakopoulos *et al.*, 2003; Brier *et al.*, 2016). Higher density and extension of NFT are associated with decreased cognitive status in neuropathological studies (Nelson *et al.*, 2012). Studies using tau PET have also confirmed these findings and revealed that the specific

areas affected by tau were also associated with the specific cognitive domains impaired (Ossenkoppele *et al.*, 2016*b*; Schöll *et al.*, 2016), as was also previously suggested by neuropathological data (Mitchell *et al.*, 2002; Guillozet *et al.*, 2003). As expected by the aforementioned relationship between tau accumulation and GM volume, neurodegeneration is also strongly associated with cognitive decline (Chetelat *et al.*, 2003; Jack *et al.*, 2009; Saint-Aubert *et al.*, 2016; Bejanin *et al.*, 2017). Interestingly, GM atrophy partly mediates the association between tau accumulation and cognitive decline, suggesting that tau effect on cognition is partly, but not only, explained by its effects on GM volume (Bejanin *et al.*, 2017).

Implications of AD biomarkers on research

The widespread utilisation of biomarkers in AD research has had consequences at multiple facets. One of the most important in the research setting is the development of new research criteria for the definition of AD, which moved from a syndromic definition to a more biological-based one. In this research framework, created by the National Institute on Aging (NIA) and the Alzheimer's Association (AA), subjects are classified using the A/T/(N) criteria (Jack *et al.*, 2016). According to these criteria, participants are grouped as a function of their binary AD biomarker status (A for Aβ, T for tau and N for neurodegeneration) into three general categories: normal AD biomarkers (A-T-(N)-); Alzheimer's *continuum* (those that are A+ regardless of the other AD biomarkers status) and; non-AD pathological change (those that are T+ and/or N+ without being A+; **Table 1**). Under this framework, AD is defined as the presence of abnormal biomarkers of Aβ and tau, irrespective of cognitive status. Moreover, any subject with signs of tau and/or neurodegeneration without Aβ positivity will be considered to be outside the Alzheimer's *continuum*, even though they may enter into it if Aβ abnormalities can be detected later on.

The availability AD biomarkers has also influenced the design of clinical trials. For some time now, it has been suggested that clinical trials against AD would benefit from focusing on the earliest stages of the disease (Sperling *et al.*, 2011*a*). Knowledge that both Aβ and tau accumulation start years, even decades, before any clinical symptom opens a window of

treatment opportunity for therapeutic intervention before widespread damage in the brain. Within this period, stopping or slowing the accumulation of these proteins may also help in preventing future cognitive symptoms. Two examples of these early intervention trials are: the Dominantly Inherited Alzheimer Network (DIAN) trials unit (DIAN-TU) for ADAD participants (Mills *et al.*, 2013) and the Anti-Amyloid Treatment in Asymptomatic Alzheimer's Disease (A4) for normal individuals identified "at-risk" for progression towards Alzheimer's dementia (Sperling *et al.*, 2014*c*; Insel *et al.*, 2020). However, it is important to note that current clinical trials for AD are becoming more diversified including also inflammatory response, neuronal and synapse protection as target mechanisms of action (Cummings *et al.*, 2020); or non-pharmacological interventions such as the Finnish Geriatric Intervention Study to Prevent Cognitive Impairment and Disability (FINGER), which is a multidomain approach involving diet, exercise cognitive training and vascular risk monitoring (Ngandu *et al.*, 2015).

AT(N) profiles	**Biomarker category**	
A-T-(N)-	Normal AD biomarkers	
A+T-(N)-	Alzheimer's pathologic change	Alzheimer's *continuum*
A+T+(N)-	Alzheimer's disease	
A+T+(N)+	Alzheimer's disease	
A+T-(N)+	Alzheimer's and concomitant suspected non Alzheimer's pathologic change	
A-T+(N)-	Non-AD pathologic change	
A-T-(N)+	Non-AD pathologic change	
A-T+(N)+	Non-AD pathologic change	

Table 1: Categorization of participants using the NIA-AA criterion by the AT(N) profile. Extracted from (Jack *et al.*, 2018)

In conclusion, the development of AD biomarkers in recent years has had a huge repercussion on the way we think about AD (Molinuevo *et al.*, 2018*c*). This change of view has influenced AD research in the way we

stage individuals, how clinical trials are designed, and has allowed us to understand many pathophysiological mechanisms in the course of the disease. However, this development has also revealed several unknown aspects and highlighted that focusing on the earliest stages of the disease may be of utmost importance to understand and prevent later consequences in the course of the Alzheimer's *continuum*.

OTHER BIOMARKERS RELATED TO PATHOPHYSIOLOGICAL MECHANISMS IN AD

On top of the aforementioned Aβ and tau deposition and neurodegeneration, multiple other pathophysiological mechanisms are altered during the Alzheimer's *continuum*. In recent years, there has been an increasing interest in developing biomarkers targeting these pathways (Blennow and Zetterberg, 2018, Molinuevo et al., 2018b; Milà-Alomà et al., 2019; Zetterberg and Bendlin, 2020) (See **Figure 6**). In this section, their main characteristics will be reviewed. See **Table 2** for a review of the whole list of biomarkers included in this thesis.

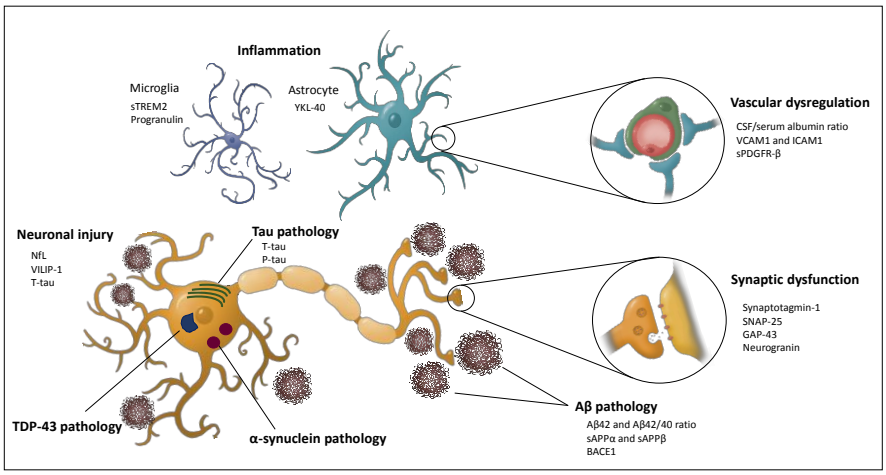

Figure 6: Summary of the pathological events in Alzheimer's disease and their corresponding fluid biomarkers. Extracted from (Milà-Alomà *et al.*, 2019).

	Pathological mechanism	Biomarker	AD vs HC
Core AD biomarkers	Aβ pathology	Aβ PET	↑
		CSF Aβ42/40	↓
	Tau pathology	CSF p-tau	↑
		CSF t-tau	↑
	Neurodegeneration	CSF NfL	↑
Other AD biomarkers	Synaptic dysfunction	CSF Neurogranin	↑
	Inflammation	CSF YKL-40	↑
		CSF GFAP	≈
		CSF sTREM2	↑
		CSF IL-6	↑
		CSF S100b	≈
	α-synuclein pathology	CSF α-synuclein	≈

Table 2: Summary of biomarkers included in this thesis. The table depicts the changes observed in AD compared with healthy controls (HC) as follows: ↑ increased or ↓ decreased levels in most or all studies; ≈ inconsistent results.

Synaptic dysfunction

Another event that occurs in the early stages of AD is synaptic dysfunction (Masliah *et al.*, 1994), which historically has been pointed as the best correlate to cognitive decline (Terry *et al.*, 1991). With respect of neuroimaging markers, the PET tracer [^{11}C]UCB-J was developed to detect synaptic loss measuring synaptic vesicle protein 2A (SV2A), which, as its name suggests, is a protein expressed in synapses. Another protein related to synapse activity is neurogranin, which is a dendritic protein involved in post-synaptic signalling pathways. Neurogranin has also been proposed as a biomarker of this pathologic change, in this case, measured in the CSF (Thorsell *et al.*, 2010). Similar to NfL, neurogranin levels are elevated in AD

and MCI patients (Kester *et al.*, 2015; Portelius *et al.*, 2015). Moreover, neurogranin has shown a tight correlation with cognition (Casaletto *et al.*, 2017) and has also been related to disease progression even in cognitively unimpaired participants (Tarawneh *et al.*, 2016). It is also highly correlated with p-tau and t-tau levels and it is quite specific for AD as other non-AD dementias show normal or even slightly low levels of neurogranin (Kvartsberg *et al.*, 2015; Wellington *et al.*, 2016). Further, our group has also recently shown that it is associated with CSF Aβ levels in positive Aβ subjects without cognitive impairment (Milà-Alomà *et al.*, 2020*a*).

Inflammation

Neuroinflammation is another pathophysiological mechanism altered in AD that apprears to be related to disease progression and severity (Heneka *et al.*, 2015). Inflammation in the brain is mainly related to two cells: microglia and astroglia; however, it encompasses a broad variety of complex biological processes. For many years, neuroinflammation was thought of as a passive consequence after Aβ and/or tau started to accumulate. Nonetheless, many recent studies suggest their active role in the course of the disease.

Genetic studies were one of the main reasons behind this change of mind (Bradshaw *et al.*, 2013; Guerreiro *et al.*, 2013). For instance, genome-wide association studies (GWAS) observed that some rare variants of the triggering receptor expressed on myeloid cells 2 (TREM2) gene, which is highly expressed in microglia, increased from two- to fourfold the risk of AD, similar to what happens with *APOE-ε4* heterozygotes (Gratuze *et al.*, 2018). These results suggested that microglia in particular, but also neuroinflammation in general, are an active player in the course of AD (Heneka *et al.*, 2015).

However, there is still some controversy whether neuroinflammation is a protective or detrimental factor in AD. It is currently thought that the role of inflammation may highly depend on the stage of progression in the course of the disease, which may permit to have either positive or negative

consequences. For instance, when activated, microglia can show a wide range of phenotypes going from pro-inflammatory to non-inflammatory, which can lead to opposite effects (Lyman *et al.*, 2014). Furthermore, these phenotypes may shift from one to another depending on their environment and the stage of the disease (Varnum and Ikezu, 2012; Cai *et al.*, 2014).

Apart from the different microglial phenotypes across the Alzheimer's *continuum*, it is nowadays acknowledged that its activation does not follow a monotonic evolution. It is believed that microglial activation has two different peaks during AD (Fan *et al.*, 2017). Recent studies suggest that there would be the first microglial activation peak in the MCI stage as a response to neuronal injury (Suárez-Calvet *et al.*, 2016; Suárez-Calvet *et al.*, 2016). However, as the neuronal injury increases, microglia may lose their beneficial role and become over-activated, provoking a chronic inflammation process. This second peak of microglial activation may occur at the dementia stage of the disease and seems to be associated with neurodegeneration (Fan *et al.*, 2015, 2017).

Multiple inflammatory biomarkers are currently available. Imaging biomarkers of neuroinflammation are usually related to PET tracers that bind to the translocator protein (TSPO), which is expressed by in the pro-inflammatory activated microglia. However, the availability of this type of tracers is quite reduced. More diversity is found in soluble markers of inflammation. Preclinical studies have shown that functions of TREM2 may include Aβ plaque compaction, clustering of microglia around plaques and activation and proliferation of these cells (Gratuze *et al.*, 2018). Moving to human studies, a study covering the whole AD *continuum* revealed that CSF sTREM2 is elevated in early stages of symptomatic AD (*i.e.* MCI), and closely correlated with markers of tau pathology (Suárez-Calvet *et al.*, 2016). Further, in a continuation study with ADAD participants, the same group showed that mutation carriers had higher levels of sTREM2 five years before the expected symptom onset and that was posterior to Aβ and tau pathology cascade (Suárez-Calvet *et al.*, 2016). Finally, sTREM2 has also been related to cognitive decline, showing that those MCI and AD participants with higher sTREM2 levels presented slower rates of cognitive decline, suggesting that TREM2-mediated microglial activity could be a

good target for AD clinical trials (Ewers *et al.*, 2019). However, other studies have reported a deleterious effect of sTREM2 on neurodegeneration in cognitively unimpaired subjects (Halaas *et al.*, 2020).

Together with activated microglia, reactive astrocytes are also found close to Aβ plaques (Medeiros and LaFerla, 2013). Regarding measuring astroglial function, there are multiple candidate biomarkers, although the most commonly used is CSF YKL-40 (Craig-Schapiro *et al.*, 2010). Similar to what has been found with sTREM2, CSF YKL-40 is elevated in AD patients as well as in late preclinical AD stages and it is associated with tau pathology and markers of neurodegeneration (Alcolea *et al.*, 2015*b*; Gispert *et al.*, 2016, 2017, Molinuevo *et al.*, 2018*a*; Milà-Alomà *et al.*, 2019). Another promising astroglial biomarker is glial fibrillary acidic protein (GFAP) but its potential to differentiate AD patients from controls is still to be resolved (Olsson *et al.*, 2016). However, a recent study conducted in our group found elevated CSF GFAP levels in A+T+ cognitively unimpaired participants compared to T-, regardless of the Aβ status, suggesting an association with tau pathology (Milà-Alomà *et al.*, 2020*a*). In the same study, we also reported higher levels of another astrocytic marker, S100b, in A+T+ compared to A-T- subjects (Milà-Alomà *et al.*, 2020*a*). Finally, interleukin-6 (IL6), has also been suggested as a neuroinflammatory marker, which showed increased levels in AD patients in a meta-analysis of cytokines related to AD (Swardfager *et al.*, 2010).

Other proteinopathies

Some other biomarkers interesting in the AD research field are those related to common AD co-pathologies. Examples of these are TAR DNA-binding protein 43 (TDP-43) and α-synuclein (Zetterberg and Bendlin, 2020). TDP-43 is a protein that is usually seen in some frontotemporal dementias, amyotrophic lateral sclerosis, and the recently categorized limbic-predominant age-related TDP-43 encephalopathy (LATE) (Nelson *et al.*, 2019). In its turn, α-synuclein has a main role in multiple neurodegenerative diseases such as Parkinson's disease and dementia with Lewy bodies and multiple system atrophy.

In summary, the recent development of multiple biomarkers directly or indirectly related to AD provide novel opportunities for research. First of all, the study of their dynamics across the disease, as well as their relationship with other biomarkers will help us understand a disease, AD, that has been proven to be very complex. Furthermore, the development of AD biomarkers not directly related to Aβ and tau pathology also enables intervention studies targeting alternative mechanisms (Honig *et al.*, 2018; Selkoe, 2019).

RISK FACTORS FOR ALZHEIMER'S DEMENTIA

Another important factor in the study of AD and more particularly at the early stages refers to the risk factors that contribute to the disease. There are many risk factors for Alzheimer's dementia and there exists several ways of categorizing them. One of the most obvious classification criteria is the one based on our capacity to modify them. In this regard, we could consider as modifiable risk factors, as those we can affect, like education, body mass index, or cardiovascular health (Norton *et al.*, 2014; de Bruijn *et al.*, 2015; Vemuri *et al.*, 2017; Livingston *et al.*, 2020). Non-modifiable risk factors, include those which we cannot escape of (Zhao *et al.*, 2020) such as age (Hebert *et al.*, 2013), sex (Ferretti *et al.*, 2018; Fisher *et al.*, 2018) and apolipoprotein E (*APOE*) genotype (Liu *et al.*, 2013). In this chapter, we will focus on the non-modifiable risk factors giving that a better knowledge on their role in the AD evolution may help us to better understand the biological processes that occur during the disease.

Increasing age is the most important risk factor of AD (Hebert *et al.*, 2013). The main pathological events in the Alzheimer's *continuum* have been related to older ages, including Aβ deposition (Jansen *et al.*, 2015), tau pathology, especially in the MTL (Braak and Braak, 1997; Schöll *et al.*, 2016; Arnsten *et al.*, 2020), and neurodegeneration (DeCarli *et al.*, 2005; Raz *et al.*, 2005, Jack *et al.*, 2013*a*, Milà-Alomà *et al.*, 2020*a*). However, tau accumulation rates seem to decrease in older ages (Whitwell *et al.*,

2019; Jack *et al.*, 2020). Further, other brain-related measures, such as white matter integrity or functional activity, and cognitive-related measures also worsen with older age (Hedden and Gabrieli, 2004; Van der Elst *et al.*, 2005). Additionally, multiple other pathophysiological mechanisms of AD, such as inflammation, have shown a direct association with age (Falcon *et al.*, 2019, Milà-Alomà *et al.*, 2020*a*). Finally, it has also been recently shown that older age is related to the presence of comorbidities in a neuropathological study (Spina *et al.*, 2020), which can contribute to a higher susceptibility to AD (Boyle *et al.*, 2019).

The *ε4* allele of *APOE* is the major genetic risk factor for non-autosomal dominant AD (Corder *et al.*, 1994; Farrer *et al.*, 1997; Belloy *et al.*, 2019; Reiman *et al.*, 2020). The *APOE* gene has three main alleles (*i.e. ε2*, *ε3* and *ε4*), which result in six possible genotypes. Having one or two copies of the *APOE-ε4* increases the odds of developing AD (allelic dose odds ratio (OR) [95% confidence interval(CI)]: 6.00[5.06-7.12]), whereas the *APOE-ε2* allele is related to a lower risk of AD (allelic dose OR[95%CI]: 0.38[0.30-0.48]) (Bu, 2009; Liu *et al.*, 2013; Reiman *et al.*, 2020). The apoE protein has many roles in the brain, among them cholesterol delivery, key to the maintenance of neurons; but it also plays a signalling role for the immune system to remove amyloid from the brain. Thus, *APOE-ε4* carriers, who have the less efficient apoE isoform (*i.e.* apoE4), have an increased Aβ deposition compared to *APOE-ε3* homozygotes (reference group) (Reiman *et al.*, 2009; Jansen *et al.*, 2015). *APOE-ε4* carriers have also shown higher levels of tau pathology (Nagy *et al.*, 1995; Oyama *et al.*, 1995) and neurodegeneration (Reiman *et al.*, 2005; Shi *et al.*, 2017; Cacciaglia *et al.*, 2018), although it has been suggested that these effects are mediated by their elevated Aβ levels (Mungas *et al.*, 2014; Serrano-Pozo *et al.*, 2015; Farfel *et al.*, 2016; van der Kant *et al.*, 2020; Salvadó *et al.*, 2021).

Finally, sex has also been suggested to have a major effect on the development of Alzheimer's dementia, with women having greater risk. However, the underlying mechanisms are not well understood (Ferretti *et al.*, 2018, 2020; Fisher *et al.*, 2018). In this regard, multiple studies have shown no apparent differences in Aβ deposition between men and women (Jack et al., 2015b; Buckley et al., 2018), although downstream effects on

cognitive decline seem to be more deleterious in women (Buckley et al., 2018). On the other hand, women do present higher tau pathology than men (Buckley *et al.*, 2019*b*, 2020), which seems to contribute to the observed higher cognitive decline (Buckley et al., 2020). Further, a GWAS investigated sex-specific genetic associations with AD features, showing a novel locus protective against tau pathology only in men (Dumitrescu *et al.*, 2019). However, the increased risk of AD in women is still under debate because the higher prevalence of AD in women may also be due to their longer life expectancy. In another direction, another hypothesis suggests that the AD risk is the same for both sexes, but that the clinical manifestation, age of onset and regional vulnerability are different by sexes (Liesinger *et al.*, 2018).

Although there is no consensus regarding the consideration of female sex as a risk for AD, its interaction with other AD risk factors are well accepted. In this regard, multiple studies have shown the increased deleterious effect of *APOE-ε4* in women (Farrer *et al.*, 1997; Altmann *et al.*, 2014). Concerning Aβ and tau pathology, women that are *APOE-ε4* carriers have more Aβ plaques before 80 years old (Ghebremedhin *et al.*, 2001); higher levels of tau pathology (Damoiseaux *et al.*, 2012; Altmann *et al.*, 2014; Hohman *et al.*, 2018); and higher tau accumulation for the same levels of Aβ pathology (Buckley *et al.*, 2019*a*). Moreover, they also show a more pronounced hypometabolism and cortical thinning (Sampedro *et al.*, 2015); and faster cognitive decline when they were also Aβ positive (Buckley *et al.*, 2018). Nevertheless, some of these relationships may depend on age or the disease stage in AD (Neu *et al.*, 2017; Mofrad *et al.*, 2020).

Other studies have also investigated the interaction between other AD risk factors. For example, the AD risk associated with the *APOE-ε4* allele seems to vary with age being higher in younger ages (Farrer *et al.*, 1997), which may be in part related to the different age-dependent prevalence of Aβ positivity of *APOE-ε4* carriers (Jansen *et al.*, 2015). The interaction between sex and age has also shown an impact on AD course. In a neuropathological study, NFT, especially in the hippocampus, showed a higher prevalence in women than in men in older ages (Liesinger *et al.*, 2018).

In summary, age, sex and *APOE-ε4* allele, alone or in combination have shown an important impact on the risk and/or development of AD. Elucidating how these risk factors modify the course of the disease would help us to better understand its mechanisms and develop precision medicine in the AD field (Ferretti *et al.*, 2018).

THE ALFA PROJECT

As aforementioned, the development of AD biomarkers has influenced our thinking about AD. Being able to monitor the development of pathophysiological events *in vivo* has allowed us to study the evolution of the disease many years before the appearance of any symptom. This has also modified the AD field on its approach to intervening in the disease's course, which has progressively moved towards performing research to enable preventive strategies (Sperling *et al.*, 2014*a*). In this regard, current clinical trials are including participants in earlier stages of the disease including some MCI and mild AD patients (https://clinicaltrials.gov/ct2/show/NCT03639987,https://clinicaltrials.gov/ct2/show/NCT02477800) or even in cognitively unimpaired participants (Sperling *et al.*, 2014*c*). Also in the research field, nowadays more and more research settings are focused on the study of preclinical participants, such as the ALFA project (for ALzheimer's and FAmilies).

The ALFA project was designed as an infrastructure to investigate the pathophysiology and pathogenic factors in the earliest stages of AD (Molinuevo *et al.*, 2016). To this aim, the Barcelonaβeta Brain Research Center (BBRC) recruited the ALFA parent cohort, which consists of 2,743 cognitively unimpaired participants aged between 45 and 75 years old, almost half of them offspring of AD patients. In their initial visit, ALFA participants were clinically and cognitively assessed. BBRC also collected their medical history, information about their lifestyle and a blood sample to genetically characterize them. These ALFA participants had been included in different research studies including both observational and interventional approaches.

For more detailed phenotyping, the ALFA+ study was created as a subsample of the ALFA parent cohort, to perform thorough research in participants within the Alzheimer's *continuum*. These participants were carefully selected to cover the full AD risk spectrum, thus preferentially including participants with a family history of AD or being *APOE-ε4* carriers. ALFA+ participants underwent a more thorough characterization including MRI, Aβ and FDG PET scans, blood and CSF sampling and, extensive cognitive tests and lifestyle questionnaires, among others. Further, some of these tests will also be performed longitudinally to assess the evolution of the ALFA+ participants. A summary of their main baseline demographic characteristics is shown in **Table 3**.

n = 381	
Age (years old), mean(SD) [range]	61.2 (4.7) [49.3 - 73.6]
Women, n(%)	232 (60.9)
Education (years), mean(SD)	13.4 (3.5)
***APOE-ε4* carriers, n(%)**	201 (52.8)
Family history of AD, n(%)	184 (48.3)
Aβ positive (by CSF), n(%)	131 (34.4)

Table 3: Basic demographics of ALFA+ participants.

In summary, the ALFA+ cohort provides a splendid opportunity to investigate the earliest pathophysiological events of AD. On one hand, participants have been deeply characterized, thus allowing a multi-modal and multi-focal research approach. On the other, ALFA+ participants are at increased risk of AD but they are still cognitively unimpaired, increasing the prevalence of preclinical AD.

HYPOTHESES AND OBJECTIVES

HYPOTHESES AND OBJECTIVES

STATEMENT OF THE PROBLEM

The research in AD has been progressively moving its attention towards earlier stages of the disease. This focus in initial phases has been fostered by the increasing development of *in vivo* biomarkers. Furthermore, the negative results in clinical trials, suggest that drugs seem to be administered too late. In this regard, some recent studies have proved drug capacity to remove Aβ plaques. However, the clinical value of this Aβ removal is still to be demonstrated, with current trials showing low or no efficacy at all. One of the hypotheses for this lack of change in the cognitive progression is that these treatments have been administered in advanced stages of the disease, when Aβ is no longer the driver of the pathological events. On the other hand, the rise of *in vivo* biomarkers for AD has allowed studying participants years, even decades, before they have any clinical symptom. Thus, providing more information about the events in the early Alzheimer's *continuum*, which may, in turn, help improving drug targets and inform the design of clinical trials.

As has been presented, Aβ deposition in the brain is hypothesized to be the earliest, or one of the earliest, pathophysiological events in the Alzheimer's *continuum*. Thus, and given the increasing interest for initial AD stages, detection methods of early Aβ deposition are a clear need of the field. Some studies have proposed CSF Aβ as the best biomarker to detect the earliest signs of Aβ alterations. However, some other studies have also suggested that detection of low Aβ load using PET may have room for improvement. One of the proposals to improve this sensitivity was performing studies in participants with lower Aβ load, instead of in the typical clinical cohorts.

Apart from its detection, there are many other topics related to early Aβ deposition that deserve further attention. For instance, it is known that several factors impact the risk of developing AD. However the relationship between some of them and Aβ deposition is not fully understood, especially in the early Alzheimer's *continuum*. Investigating these relationships may improve our understanding of the biological mechanisms behind early pathogenic events.

Finally, it is well established that Aβ deposition is associated with tau accumulation over time, which, in turn, promotes neurodegeneration and, ultimately, cognitive dysfunction. Nonetheless, many other pathophysiological mechanisms are altered during the disease, even in its earliest stages. The development of many novel biomarkers for these mechanisms has increased our understanding of some of them. However, the knowledge about their role in this disease as well as their relationship to the main hallmarks of AD is still limited. Filling this gap of knowledge will be of utmost importance to the whole AD research field, but in particular to future drug development.

HYPOTHESIS

1. Lower than previously assumed thresholds of Aβ PET can specifically detect early Aβ deposition.

2. Visual reading of Aβ PET scans, which is the only EMA- and FDA-approved method to assess Aβ PET positivity, is able to detect early Aβ deposition.

3. Established risk factors for Alzheimer's dementia, namely, older age, female sex and *APOE-ε4* carriership, promote Aβ deposition in the brain for any given level of soluble Aβ dyshomeostais.

4. Multiple pathophysiological mechanisms are linked to the earliest Aβ deposition in the brain.

MAIN AND SPECIFIC OBJECTIVES

The overarching goal of this PhD Thesis is:

> To investigate Aβ deposition in its earliest stages of the Alzheimer's *continuum* and its downstream effects.

To this end, specific objectives are:

1. To set sensitive thresholds for abnormal cerebral Aβ deposition using Aβ PET quantification.
2. To assess the accuracy and sensitivity of the visual assessment of Aβ PET scans to detect early signs of cerebral Aβ deposition.
3. To investigate differences between soluble Aβ dyshomeostasis and Aβ deposition related to established Alzheimer's dementia risk factors.
4. To describe pathophysiological mechanisms downstream to early cerebral Aβ deposition using novel CSF biomarkers.

RESULTS

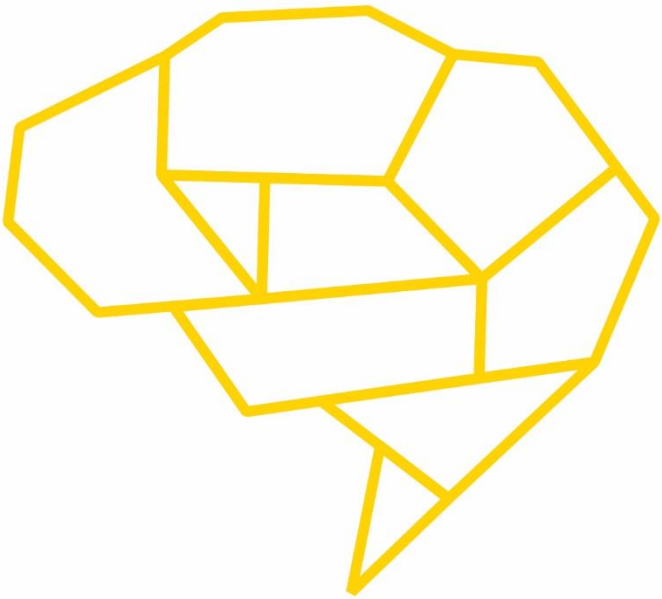

FIRST STUDY:

Centiloid cut-off values for optimal agreement between PET and CSF core AD biomarkers

Salvadó et al. Alzheimer's Research & Therapy (2019) 11:27
https://doi.org/10.1186/s13195-019-0478-z

Alzheimer's Research & Therapy

RESEARCH Open Access

Centiloid cut-off values for optimal agreement between PET and CSF core AD biomarkers

Gemma Salvadó[1], José Luis Molinuevo[1,2,3*], Anna Brugulat-Serrat[1], Carles Falcon[1,4], Oriol Grau-Rivera[1], Marc Suárez-Calvet[1], Javier Pavia[4,5,6], Aida Niñerola-Baizán[5], Andrés Perissinotti[5], Francisco Lomeña[5], Carolina Minguillon[1,2], Karine Fauria[1,2], Henrik Zetterberg[7,8,9,10], Kaj Blennow[7,8], Juan Domingo Gispert[1,3,4*] and for the Alzheimer's Disease Neuroimaging Initiative, for the ALFA Study

Abstract

Background: The Centiloid scale has been developed to standardize measurements of amyloid PET imaging. Reference cut-off values of this continuous measurement enable the consistent operationalization of decision-making for multicentre research studies and clinical trials. In this study, we aimed at deriving reference Centiloid thresholds that maximize the agreement against core Alzheimer's disease (AD) cerebrospinal fluid (CSF) biomarkers in two large independent cohorts.

Methods: A total of 516 participants of the ALFA+ Study ($N = 205$) and ADNI ($N = 311$) underwent amyloid PET imaging ([^{18}F]flutemetamol and [^{18}F]florbetapir, respectively) and core AD CSF biomarker determination using Elecsys® tests. Tracer uptake was quantified in Centiloid units (CL). Optimal Centiloid cut-offs were sought that maximize the agreement between PET and dichotomous determinations based on CSF levels of $A\beta_{42}$, tTau, pTau, and their ratios, using pre-established reference cut-off values. To this end, a receiver operating characteristic analysis (ROC) was conducted, and Centiloid cut-offs were calculated as those that maximized the Youden's J Index or the overall percentage agreement recorded.

Results: All Centiloid cut-offs fell within the range of 25–35, except for CSF $A\beta_{42}$ that rendered an optimal cut-off value of 12 CL. As expected, the agreement of tau/$A\beta_{42}$ ratios was higher than that of CSF $A\beta_{42}$. Centiloid cut-off robustness was confirmed even when established in an independent cohort and against variations of CSF cut-offs.

Conclusions: A cut-off of 12 CL matches previously reported values derived against postmortem measures of AD neuropathology. Together with these previous findings, our results flag two relevant inflection points that would serve as boundary of different stages of amyloid pathology: one around 12 CL that marks the transition from the absence of pathology to subtle pathology and another one around 30 CL indicating the presence of established pathology. The derivation of robust and generalizable cut-offs for core AD biomarkers requires cohorts with adequate representation of intermediate levels.

Trial registration: ALFA+ Study, NCT02485730
ALFA PET Sub-study, NCT02685969

Keywords: AD pathophysiology, Biomarker concordance, Threshold, Positivity, Preclinical, Early detection, Positron emission tomography, Phosphorylated tau, Biomarker categorization

* Correspondence: jlmolinuevo@barcelonabeta.org; jdgispert@barcelonabeta.org
[1]BarcelonaβetaBrain Research Center (BBRC), Pasqual Maragall Foundation, Wellington 30, 08005 Barcelona, Spain
Full list of author information is available at the end of the article

Introduction

Aggregation of β-amyloid (Aβ) is a neuropathological hallmark of Alzheimer disease (AD) and occurs decades before the onset of clinical symptoms occur [1, 2]. Both amyloid positron emission tomography (PET) and cerebrospinal fluid (CSF) $A\beta_{42}$ measurement are established biomarkers of Aβ deposition that highly correlate with post-mortem [3, 4] and brain biopsy findings [5] and serving as in vivo proxies of AD pathological findings that can be assessed in vivo. They are included as part of the biological definition of AD in the recent NIA-AA 2018 research framework [6] for the definition of preclinical stages of AD [7] and as well as inclusion criteria in clinical trials [8]. CSF $A\beta_{42}$ and amyloid PET show a high degree of agreement [9–19], even though they probably measure two different pools of amyloid. While the signal detected by amyloid PET may reflect fibrillary amyloid [20], the decrease of CSF $A\beta_{42}$ levels more likely reflects both fibrillar and non-fibrillar Aβ deposits. Another difference is that CSF $A\beta_{42}$ may become abnormal before amyloid PET [21, 22], while amyloid PET has been suggested to be superior for grading early symptomatic AD stages [19].

For diagnostic purposes, three ^{18}F-labelled PET radiotracers have been granted marketing authorizations and are being used: [^{18}F]flutemetamol (Vizamyl; GE Healthcare), [^{18}F]florbetaben (Neuraceq; Life Molecular Imaging), and [^{18}F]florbetapir (Amyvid, Eli Lilly). In the clinical setting, PET scans are visually read by trained specialists and are categorized as either positive or negative [23]. For quantitative purposes, the three different tracers show considerable variability when measured using the typical standardized update value ratios (SUVRs). To improve the comparability of the retention measurements across tracers, the Centiloid method has been proposed [24]. This method linearly scales the measurement of a particular tracer from 0 to 100 scale, where '0' represents the average uptake in young controls and '100' corresponds to the average uptake in typical AD patients at the dementia stage. To apply the Centiloid conversion, reference datasets, quantification pipelines, and regions of interest and reference are available publically from http://www.gaain.org/centiloid-project. When expressed in Centiloids (CL), optimal thresholds for positivity against visual reads typically fall within the range between 25 and 35 CL [25–27].

The applicability of CSF $A\beta_{42}$ determinations with enzyme-linked immunosorbent assays (ELISAs) has been limited by several preanalytical and analytical factors, resulting in lot-to-lot and between-laboratory variability. These issues are expected to be improved by the availability of certified reference materials [28], and the problem with analytical variation is expected to be overcome with fully automated systems, such as the novel Elecsys® CSF immunoassay [29]. Using this system, core AD biomarkers in CSF have been compared to Aβ PET [22, 30, 31] and a CSF cut-off against PET visual read has been established by receiver operating characteristic (ROC) analysis and validated against an independent sample. The resulting areas under the curve (AUC) of CSF $A\beta_{42}$ against Aβ PET visual read ranged from 0.85 to 0.92. Interestingly, in these studies, tau/$A\beta_{42}$ ratios showed a higher agreement against PET visual reading (AUCs 0.94–0.96) than CSF $A\beta_{42}$ alone.

During the last years, investigators have started interventions before the onset of clinical symptoms, when $A\beta_{42}$ changes are detectable using CSF and amyloid PET biomarkers [32–34]. Amyloid positivity is often recognized as the earliest detectable pathophysiological abnormality in AD. Typically, positivity has been operationalized as a positive visual read in an amyloid PET scan. Accordingly, quantitative cut-offs for PET imaging, but also for CSF biomarkers, have been derived against visual reads. However, the question remains of whether lower quantitative cut-offs can be used to detect more subtle amyloid alterations with higher sensitivity, but which still provide good specificity. Such cut-offs are critical for the operationalization of preventive interventions like recruiting cognitively unimpaired individuals into prevention clinical trials. Therefore, there is a need to establish sensitive, reliable and generalizable cut-off values for amyloid PET to detect early amyloid deposition and operationalize decision-making in preventive intervention. In addition, visual inspection of PET scans can render both positive and negative reads throughout a wide range of CL values.

Initial studies to find optimal thresholds have been performed in populations recruited from clinical populations. This translates into samples with extreme values of both CSF $A\beta_{42}$ and amyloid PET, which is AD patients with high amyloid load vs normal cognitive with low amyloid load. This approximation results in defining an optimal cut-off based on a population with low number of individuals with intermediate values around putative threshold values, which may hamper rendering. A critical consideration when deriving such cut-offs is to appropriately populate amyloid values around the cut-offs to derive optimal and robust values. On the other hand, as CSF $A\beta_{42}$ levels start changing earlier than the PET signal, derivation of CL cut-off values against CSF in populations with initial amyloid abnormalities brings the opportunity to derive more sensitive, yet robust and generalizable, CL values associated to early amyloid accumulation.

In this study, we aimed at deriving optimal Centiloid threshold values in amyloid PET that maximize the agreement against established thresholds of CSF core AD biomarkers. To this end, we capitalized on the ALFA+ cohort of cognitively unimpaired individuals enriched for risk factors for AD [35], and in order to improve the generalizability of our results, analogous data from the Alzheimer's Disease Neuroimaging Initiative

(ADNI; http://adni.loni.usc.edu/) was pooled with that originated in the ALFA+ cohort.

Methods

Participants

ALFA+ is a nested longitudinal long-term study of the ALFA (for ALzheimer's and FAmilies) cohort [35]. In brief, the ALFA cohort was established as a research platform to characterize preclinical AD in 2743 cognitively preserved individuals, aged between 45 and 75 years old with increased risk for AD. In the nested ALFA+ study, participants undergo advanced protocols of magnetic resonance imaging (MRI), amyloid PET imaging with [^{18}F]flutemetamol and CSF core AD biomarkers [35]. The first consecutive 205 participants of the ALFA+ study were included in this work.

In order to have generalizable results reflecting the whole AD continuum, 311 participants from ADNI were also included in this study selected according to the following inclusion criteria: (1) AD CSF core biomarkers analysed with the Elecsys® tests available, (2) amyloid PET scan acquired in less than a year from CSF collection available, and (3) MRI acquired with a difference from the time of the PET acquisition of less than a year. All ADNI PET images included were acquired with [^{18}F]florbetapir.

CSF preanalytics of ALFA+ participants

Fresh CSF samples were collected in 15-mL polypropylene tubes (Sarstedt catalog #62.554), the supernatant aliquoted into 0.5-mL polypropylene tubes (Sarstedt catalog #72.730.005), and frozen within 2 h after lumbar puncture. Aliquots were placed into long-term storage boxes and stored at − 80 °C until shipment on dry ice for analysis.

CSF analyses on ALFA+ and ADNI

CSF samples were measured using the Elecsys® β-amyloid(1–42) [29], and the Elecsys® phosphotau (181P) and Elecsys® total-tau immunoassays for CSF on a cobas e 601 analyzer (software version 05.02) at the Clinical Neurochemistry Laboratory, University of Gothenburg, Sweden (ALFA+) or at the Biomarker Research Laboratory, University of Pennsylvania, USA (ADNI), according to the kit manufacturer's instructions and as described in previous studies [29].

Predefined CSF cut-offs against PET visual read

The BioFINDER and ADNI CSF AD core biomarker cut-offs were previously determined against amyloid PET visual read classification [22, 30]. ADNI participants were categorized using ADNI-specific CSF thresholds (please see Additional file 1: Table S1). Given that the ALFA+ study shares the same preanalytical and analytical conditions as BioFINDER, we used the same thresholds previously published for BioFINDER to categorize ALFA+ participants (please, see Additional file 1: Table S1).

On the other hand, we used the previously described conversion factor from BioFINDER to ADNI values [30] in order to pool herein the ALFA+ values with those of ADNI (only for figures, not used for CL cut-offs derivation).

Neuroimage acquisition procedures

Each cohort had its own acquisition protocol. For ALFA+, a T1-weighted MRI and an [^{18}F]flutemetamol PET scan was acquired in all participants (mean time difference 97.1 days; range [14–343]). The T1-weighted 3D-TFE sequence was acquired in a Philips 3 T Ingenia CX scanner with a voxel size of 0.75 × 0.75 × 0.75 mm^3, FOV 240 × 240 × 180 mm^3, sagittal acquisition, flip angle 8°, TR = 9 .9ms, TE = 4 .6ms, TI = 900 ms. PET imaging was conducted in a Siemens Biograph mCT, following a cranial CT scan for attenuation correction. Participants were injected with 185 MBq (range 166.5–203.5 Mbq) of [^{18}F]flutemetamol, and 4 frames of 5 min each were acquired 90 min post-injection. Images were reconstructed with an OSEM3D algorithm using 8 iterations and 21 subsets and with point spread function (PSF) and time of flight (TOF) corrections into a matrix size of 1.02 × 1.02 × 2.03 mm.

The methods for ADNI PET and MRI acquisition methods are described in more detail elsewhere (http://adni.loni.usc.edu/methods/documents/). In brief, all PET images were acquired with [^{18}F]florbetapir, which consisted of 4 frames of 5 min each, acquired at 50 to 70 min post injection. Most of the T1 sequences used for normalization were magnetization-prepared rapid acquisition gradient echo (MPRAGE), acquired with 1 .5T or 3 T scanners. All images, ALFA+ and ADNI, were visually inspected for quality control.

Image processing

All PET images were preprocessed following the Centiloid [24] pipeline using SPM12 (https://www.fil.ion.ucl.ac.uk/spm/software/spm12/). In brief, PET frames were coregistered. Averaged images were then coregistered to corresponding MRI scans. MRIs were then segmented and normalized to the MNI space together with PET images. We calculated the SUVr in MNI space using the target region provided in the GAAIN website (www.gaain.org) and the whole cerebellum as reference region. SUVr values were then transformed to the Centiloid scale as explained in Additional file 1: Supplementary methods.

Statistical analysis

Demographic characteristics of both cohorts were first compared. *T* test for independent samples was used with continuous variables and χ^2 with dichotomous variables. To be able to directly compare Aβ_{42} measures from both cohorts, we had to transform ADNI data to account for pre-analytical conditions [30]. This transformation was only used to perform scatter plots but not to perform

any other analysis, as each dataset had their own cut-offs for the CSF biomarkers (Additional file 1: Table S1).

Optimal Centiloid cut-offs were calculated as those that maximized the Youden's J Index (YI) or the overall percentage agreement (OPA; "accuracy"). YI statistic consists of the summation of the sensitivity and specificity [36], and the OPA reflects the percentage of cases with concordant binary classification with CSF and PET. Both were calculated on the pooled ALFA+ and ADNI data as a function of Centiloid values for $A\beta_{42}$, phosphorylated tau (pTau), total tau (tTau), and pTau/$A\beta_{42}$ and tTau/$A\beta_{42}$ ratios. For each CSF biomarker as binary outcome, optimal cut-offs were selected as those showing the maximum value of one of the statistics after minimally smoothing true-positive, true-negative, false-positive and false-negative curves using the 'smooth' function in Matlab (v2018b) with the 'lowess' method and a span value of 0.1.

On top of YI and OPA, we also calculated the positive percentage agreement (PPA, "sensitivity") and negative percentage agreement (NPA, "specificity") and the area under the curve (AUC) of the receiver operating characteristic (ROC) analysis. All 95% confidence intervals (95% CI) for all statistics were derived using bootstrapping methods ($n = 5000$).

In order to explore the generalizability of the calculated thresholds, we also derived them in each cohort individually. Robustness of the Centiloid cut-offs were assessed by deriving them against more liberal CSF thresholds (higher for $A\beta_{42}$ and lower for tau, Additional file 1: Table S1). With this new CSF categorization, we wanted to include those participants that are close to the threshold but still classified as negative ("grey zone", [GZ]). To calculate these new CSF thresholds, we add (or subtract) the 10% of the original threshold, as this slight variation in the CSF thresholds showed helping to reduce false negatives and to be strongly associated with future $A\beta_{42}$ positivity [37, 38].

Results

Demographic characteristics and CSF and amyloid biomarkers

Table 1 shows demographics and characteristics of CSF and amyloid PET biomarkers in the two cohorts included, i.e. ALFA+ and ADNI, which have some differences. The ALFA+ cohort has younger participants, more women and significantly less proportion of positive participants on all AD CSF core biomarkers, as expected as it includes only cognitively preserved participants. By contrast, ADNI participants are in more advanced stages of the disease, with higher number of *APOE-ε4* carriers and higher frequency of positive core AD CSF biomarkers (Table 1). This also translates into a significant difference in both the mean and average of amyloid PET CL values between both cohorts. As shown in Figs. 2a, 3a and 4a, the ALFA+ cohort covers intermediate CSF and CL values, whereas ADNI participants' CSF and CL measures show a more bimodal pattern. Mean and SD values for CSF biomarkers and Centiloid measures can be found in Additional file 1: Table S2. Scatterplots for pTau and tTau can be found in Additional file 1: Figure S1.

Optimal CL cut-offs

We computed the optimal CL cut-off values to differentiate individuals within the Alzheimer's *continuum* and controls using the AD CSF core biomarkers as a reference. We performed the analysis with CSF $A\beta_{42}$ alone, pTau/$A\beta_{42}$ and tTau/$A\beta_{42}$ ratios and also pTau and tTau

Table 1 Demographics and characteristics of CSF biomarkers and PET quantification measures, overall and by cohort. All the characteristics shown in this table were statistically different ($p < 0.001$) between cohorts

	ALL ($n = 516$)	ALFA+ ($n = 205$)	ADNI ($n = 311$)
Age, mean (SD) [range]	69.13 (9.10) [50–92]	61.01 (4.85) [50–74]	74.48 (7.07) [56–92]
Women, *n* (%)	286 (55.4)	134 (65.4)	152 (48.9)
Education, years mean (SD)	14.98 (3.37)	13.49 (3.58)	15.96 (2.82)
APOE-ε4 carriers, *n* (%)	260 (50.4)	81 (39.5)	179 (57.6)
Positive $A\beta_{42}$, *n* (%)	273 (52.9)	60 (29.3)	213 (68.5)
Positive pTau, *n* (%)	323 (62.6)	56 (27.3)	267 (85.9)
Positive tTau, *n* (%)	294 (57.0)	50 (24.4)	244 (78.5)
Positive pTau/$A\beta_{42}$, *n* (%)	258 (50.0)	24 (11.7)	234 (75.2)
Positive tTau/$A\beta_{42}$, *n* (%)	246 (47.7)	21 (10.2)	225 (72.3)
Diagnostic, *n* (%) CN/MCI/AD	256 / 237 / 23 (49.6)/(45.9)/(4.5)	205 / 0 / 0 (100)/(0)/(0)	36 / 237 / 23 (11.6)/(76.2)/(7.4)
Time difference CSF-PET, days mean (SD) [range]	45.2 (60.3) [0–343]	97.1 (65.1) [14–343]	11.0 (17.2) [0–126]

Aβ β-amyloid, *AD* Alzheimer's disease, *ADNI* Alzheimer's Disease Neuroimaging Initiative, *APOE* Apoliprotein E, *CN* cognitively normal, *MCI* mild cognitive impaired participants, *pTau* phosphorylated tau, *SD* standard deviation, *tTau* total tau

alone. We studied the pooled data from ALFA+ and ADNI cohorts, using cohort-specific CSF thresholds.

Table 2 summarizes the optimal CL values, using the pooled data from ALFA+ and ADNI cohorts, and associated statistical performance against CSF $A\beta_{42}$, pTau/$A\beta_{42}$, tTau/$A\beta_{42}$, pTau and tTau. Figure 1 shows the associated ROC curves.

CSF $A\beta_{42}$

Derivation of Centiloid cut-off against $A\beta_{42}$ is shown in Fig. 2. The resulting cut-offs with this analysis were 12.1 CL with YI's optimization and 11.6 CL OPA's optimizations, which corresponded with maximum values YI of 0.66 (95% CI 0.59–0.72) and OPA of 0.83 (95% CI 0.81–0.86), respectively. The corresponding area under the curve for CSF $A\beta_{42}$ was of 0.87 (95% CI 0.84–0.90). PPA and NPA values for these CL cut-offs are shown in Table 2.

The optimal cut-offs calculated against 10% variation of the CSF threshold were similar (CL = 11.1 CL with OPA, 0.85, and CL = 12.9 with YI, 0.70; Additional file 1: Table S3 and Figure S2), and the AUC was slightly improved AUC = 0.90. When CL cut-offs were derived separately in the two independent cohorts, the AUC for CSF $A\beta_{42}$ was higher in the ADNI cohort than in ALFA+ (0.85 vs 0.76 Additional file 1: Table S4). The optimal threshold for the ALFA+ cohort were slightly lower to the one found in the pooled analysis (CL = 5.4 with YI and CL = 10.7 with OPA, Additional file 1: Table S4 and Figure S3), whereas, for ADNI, the optimal cut-off resulted was significantly higher (CL = 36.2 CL with YI and CL = 33.1 with OPA, Additional file 1: Table S4 and Figure S4).

CSF tau/$A\beta_{42}$ ratios and tau

Very similar results were found in both tau over $A\beta_{42}$ ratios (Figs. 3 and 4). The optimal cut-off derived with both cohorts merged for pTau/$A\beta_{42}$ was 28.8 CL with an AUC of 0.97 [0.96–0.99] with both YI and OPA's maximization and for tTau/$A\beta_{42}$ 29.7CL with YI's maximization and 30.1 CL with OPA's maximization with an AUC of 0.96 [0.94–0.97] (Table 2).

Unlike for CSF $A\beta_{42}$, optimal thresholds against variations of the CSF cut-offs resulted in a reduced optimal threshold of CL = 21.4 for both tau ratios with YI's maximization and CL = 20.6 for both tau ratios with OPA's maximization (Additional file 1: Table S3 and Figure S2). When derived in both cohorts separately, thresholds were again slightly lower in the ALFA+ cohort (CL = 20.0 and CL = 24.8 for pTau ratio and CL = 20.1 and CL = 24.9 for tTau ratio; Additional file 1: Figure S3 and Table S4) and significantly higher for ADNI (CL = 34.4 and CL = 31.5 for pTau ratio and CL = 34.7 and CL = 32.5 for tTau ratio; Additional file 1: Figure S4 and Table S4).

Optimal cut-offs for CSF pTau and tTau were similar to those for the ratios, but with lower AUCs (Table 2). Meanwhile, tTau cut-offs remained relatively stable when using YI or OPA as criterion (CL = 28.6 and CL = 28.8, respectively); pTau cut-offs changed highly (29.3 CL with YI vs 18.7 with OPA; Additional file 1: Table S3). The analysis against 10% CSF variations resulted in similar cut-offs with similar AUCs except for tTau cut-off resulting from OPA's maximization that lowered up to 15.9 CL (Additional file 1: Table S3 and Figure S2). Finally, the behaviour of the cut-offs in the two cohorts separately was quite different with respect to tau over $A\beta_{42}$ ratios and resulted in lower AUCs than the optimal cut-off (Additional file 1: Figure S2, S3 and, Table S4).

Discussion

In this paper, we sought to calculate the optimal Centiloid cut-off values from amyloid PET data to maximize the agreement against previously established thresholds for positivity on core AD CSF biomarkers. At a first glance, this might be regarded as a circular exercise, since these CSF cut-offs were originally derived to maximally concord with positive visual reading of PET scans. Under this rationale, all resulting Centiloid cut-offs would have be expected to fall in the range that optimally discriminates negative from positive visual reads, which is between 25 and 35 CL [25, 26]. On the contrary, optimal agreement for CSF $A\beta_{42}$ was observed for a cut-off of 12 CL. This seemingly unexpected result can be explained by the clearly non-linear relationship between amyloid PET Centiloids and CSF $A\beta_{42}$, as previously reported [39]. Almost all subjects with CSF $A\beta_{42}$ over 1000 pg/ml showed Centiloid values below 20, and only for CSF values < 1000 pg/ml, a linear association could be intuited. This nonlinear association makes goodness criteria (both the Youden's Index and the overall percentage agreement) to plateau between 10 and 40 CL (Fig. 2). Under these circumstances, to derive stable optimal cut-offs, it is critical to make use of a test sample comprising both sufficient concordant positive and negative cases as well as a good representation of individuals falling within intermediate amyloid ranges (10 < CL < 40 and 500 < CSF $A\beta_{42}$ < 1000 pg/ml). In this study, this was achieved by pooling the ADNI and ALFA+ datasets.

The independent derivation of optimal CSF $A\beta_{42}$ cut-offs in the two cohorts confirmed this rationale. In the ADNI sample, optimal values fell in the expected range of visual reads (between 33 and 36 CL) whereas the optimal threshold in the ALFA+ sample is closer to that in the pooled sample (between 5 and 11 CL). This result confirms that the derivation of optimal cut-offs is very sensitive to the recruitment strategy of the reference sample, with clinical ones rendering higher cut-offs than population based ones with a better representation around the range of values where cut-offs are expected to lay. Previous literature has suggested that CSF $A\beta_{42}$

Table 2 Centiloid cut-off against CSF biomarkers. Derivation was done by maximization of YI or OPA. Other statistics for this cut-off have been also derived: PPA, NPA and AUC. 95% CI are shown between brackets. All participants' information was used to derive these cut-offs

Biomarker		YI's derived cut-offs					OPA's derived cut-offs				
	AUC	CL cut-off	YI[a]	OPA	PPA	NPA	CL cut-off	YI	OPA[a]	PPA	NPA
$A\beta_{42}$	0.874 [0.840–0.903]	12.1	0.659 [0.594–0.721]	0.831 [0.798–0.861]	0.852 [0.809–0.892]	0.806 [0.753–0.851]	11.6	0.659 [0.593–0.720]	0.831 [0.798–0.861]	0.855 [0.812–0.895]	0.804 [0.750–0.849]
pTau/$A\beta_{42}$	0.974 [0.956–0.9985]	28.8	0.886 [0.842–0.922]	0.943 [0.921–0.961]	0.941 [0.904–0.964]	0.945 [0.915–0.970]	28.8	0.886 [0.842–0.922]	0.943 [0.921–0.961]	0.941 [0.904–0.964]	0.945 [0.915–0.970]
tTau/$A\beta_{42}$	0.961 [0.940–0.975]	29.7	0.863 [0.818–0.905]	0.931 [0.908–0.952]	0.948 [0.912–0.970]	0.915 [0.882–0.946]	30.1	0.863 [0.818–0.905]	0.931 [0.908–0.952]	0.948 [0.911–0.970]	0.915 [0.882–0.947]
pTau	0.833 [0.793–0.869]	29.3	0.689 [0.629–0.745]	0.822 [0.787–0.853]	0.755 [0.704–0.798]	0.934 [0.898–0.966]	18.7	0.680 [0.610–0.732]	0.823 [0.787–0.852]	0.773 [0.726–0.816]	0.907 [0.856–0.939]
tTau	0.774 [0.727–0.814]	28.6	0.573 [0.505–0.640]	0.781 [0.747–0.815]	0.745 [0.693–0.792]	0.828 [0.779–0.875]	26.7	0.573 [0.502–0.639]	0.781 [0.745–0.815]	0.748 [0.697–0.795]	0.825 [0.773–0.870]

[a]Shows the statistic was used to derive each cut-off

pTau phosphorylated tau, *tTau* total tau, *CL* Centiloids, *OPA* overall percentage agreement ("accuracy"), *YI* Youden's J Index, *PPA* positive percentage agreement ("sensitivity"), *NPA* negative percentage agreement ("specificity"), *AUC* area under the curve

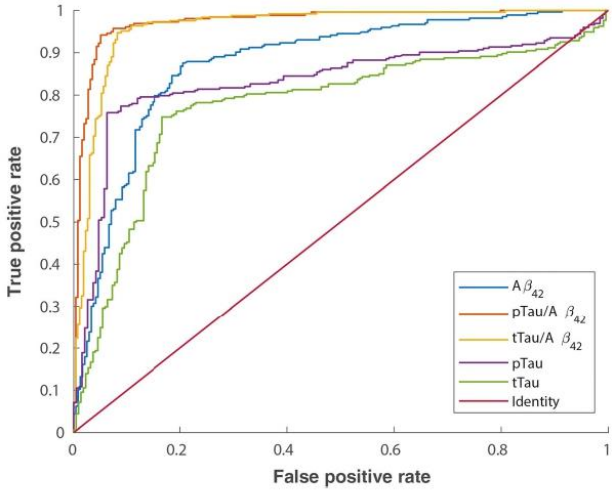

Fig. 1 Summary of ROC curves for Centiloid cut-off derivation against CSF biomarkers. pTau, phosphorylated tau; tTau, total tau; CSF, cerebrospinal fluid; ROC, receiver operating characteristic

values become positive before amyloid PET [21, 22]. This may be related to amyloid PET visual read and SUVRs cut-offs on clinical populations. In these populations, the visual read is performed in patients with either prodromal AD or dementia due to AD; hence, the amyloid load is supposed to have reached its ceiling. By contrast, the ALFA+ population reflects a cohort of early amyloid accumulators at risk for cognitive impairment; therefore, a positive visual read may be reached when amyloid is still not at its peak. Indeed, the threshold of 12 CL is robust against variations in the cut-off for CSF positivity (Additional file 1: Table S3) as well as if only the ALFA+ dataset is used for its derivation.

Although 12 CL may initially be regarded as a low value for amyloid positivity, it matches recent reports of Centiloid cut-offs against postmortem measures of AD neuropathology showing that 12.2 CL optimally detected Consortium to Establish a Registry for Alzheimer's Disease (CERAD) moderate-to-frequent neuritic plaques, whereas 24.4 CL identified intermediate-to-high AD neuropathologic change (ADNC) differences [40]. Another similar study showed that a threshold < 10 CL was optimal for ruling out the presence of amyloid plaques, whereas CL > 20 suggests significant amyloid pathology [26]. However, we would like to point out that we did not want to affirm that the CL cut-offs found show amyloid pathology, but only to find those CL values that maximally agree with those of the CSF core AD biomarkers. The fact that the CL cut-offs derived in this study agree with a previous one done with neuropathological data is only a marker that these values might have an actual biological meaning, more than only a practical one. But this hypothesis should be tested in another work, preferably with longitudinal data.

Unlike CSF $A\beta_{42}$, for tau/CSF $A\beta_{42}$ ratios, the optimal CL cut-offs fell within the expected range (28–30 CL) given the linear relationship between this biomarker and amyloid PET Centiloids. Indeed, tau/CSF $A\beta_{42}$ ratios showed higher AUC versus amyloid PET Centiloids than CSF $A\beta_{42}$, in agreement with the previous reports [22, 27, 30, 31]. The higher capacity of tau/CSF $A\beta_{42}$ ratios to predict Centiloids may be accounted for by two different factors. On the one hand, CSF ratios may provide a more stable measurement than absolute values since they provide an inherent normalization against protein production and release to the CSF, between-individual variations in CSF dynamics, and pre-analytical conditions. Therefore, the lower variability in the CSF ratios may account for better AUCs. On the other hand, CSF $A\beta_{42}$ has been proposed to become abnormal prior to amyloid PET [21, 41]. This fact might stem from the fact that both techniques probe different pools of the amyloid protein. Therefore, the combination of measurements of Aβ with those of tau, a pathological change that is expected to occur later in the AD *continuum* [41], might show better agreement with amyloid PET, which is also expected to become abnormal later than CSF $A\beta_{42}$.

Together with previous studies, the observed thresholds might be useful to flag two different inflection points in preclinical AD stages. A cut-off below 12 CL might be optimal to rule out-amyloid pathology, whereas a cut-off over 29 CL might be denoting established

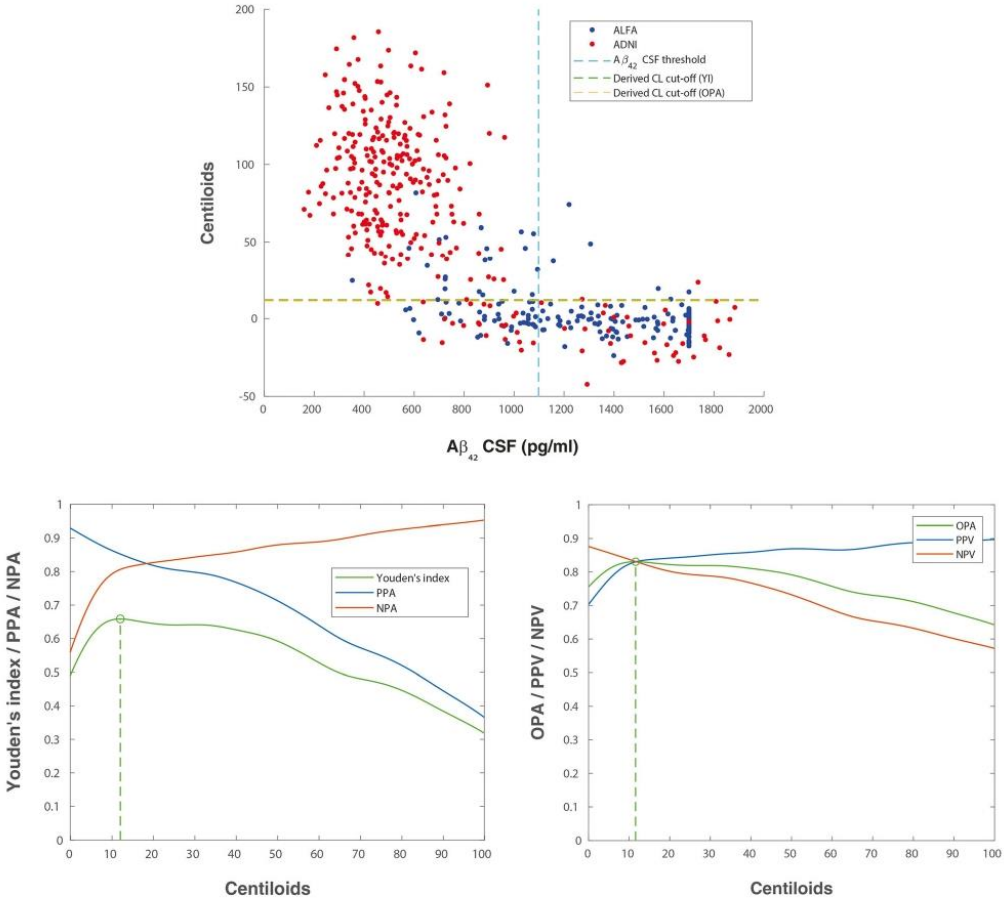

Fig. 2 Derivation of amyloid PET Centiloid cut-offs using $A\beta_{42}$ CSF biomarker. Upper row shows a scatterplot of PET quantitative measures in Centiloids against CSF $A\beta_{42}$ biomarker values for both ALFA+ (blue) and ADNI (red) participants. Vertical lines depict previously published CSF threshold ($A\beta_{42}$ 1098 pg/ml [22, 30]), and horizontal lines depict optimal cut-offs derived in this study (YI derived: green, OPA derived: yellow). Two outliers were excluded of this picture for having CL value higher than 200. Second row shows this cut-offs derivation by the maximization of YI (left) and OPA (right). The YI (green) was calculated from PPA (blue) and NPA (red) values. The OPA (green) was calculated from PPV (blue) and NPV (red) values. Derivation was done with participants of both cohorts merged. Aβ, amyloid; CSF, cerebrospinal fluid; YI, Youden's J index; PPA, positive percentage agreement; NPA, negative percentage agreement; CL, Centiloids

pathology. These kinds of thresholds have typically been used to dichotomize continuous values into two categories for clarity and ease of use. However, alternatives have also been considered and include the score of the severity of each biomarker on a semi-continuous scale as considered, for instance, in the A/T/N scheme [42]. Therefore, an option would be to categorize the full range of variation of biomarker values in three categories: one that excludes any pathology, another intermediate category that would indicate early and developing pathology and a third one that corresponds with established pathology.

Two goodness criteria have been used here to derive optimal cut-offs: the Youden's Index, which balances sensitivity and specificity, and the overall percentage agreement, which is sensitive to the percentages of positives versus negatives in the test sample. Both rendered very similar values and the Centiloid cut-offs proposed here are robust against variations in the threshold values for CSF positivity. Still, the Youden's index showed a more noisy behaviour than the overall percentage agreement, particularly in the analysis of the two individual samples. In order to obtain more robust estimates of

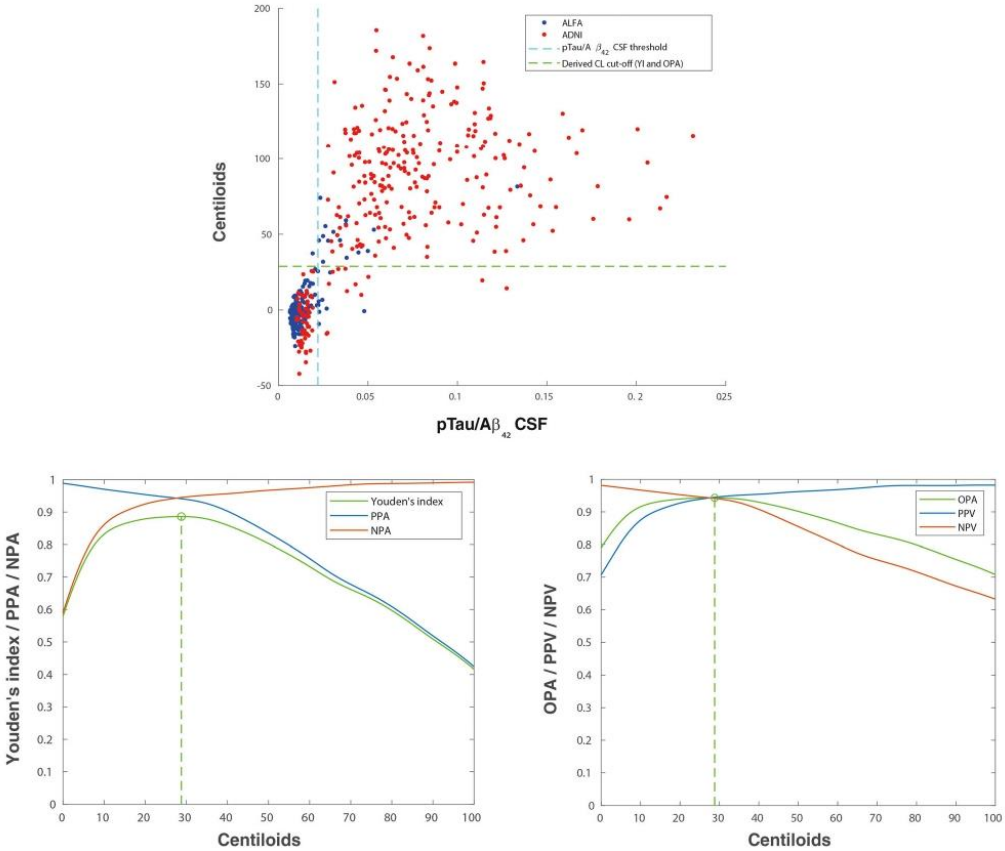

Fig. 3 Derivation of amyloid PET Centiloid cut-offs for CSF pTau/Aβ_{42}. Top row shows scatterplots of PET quantitative measures in Centiloids against CSF pTau/Aβ_{42} biomarker values for both ALFA+ (blue) and ADNI (red) participants. Vertical line depicts previously published CSF thresholds (pTau/Aβ_{42} 0.022 [22, 30]), and horizontal line depicts optimal cut-offs derived in this study (YI and OPA derived cut-offs are equal). Two outliers were excluded of this picture for having CL value higher than 200. Second row shows this cut-off derivation by maximization of YI (left) and OPA (right). The YI (green) was calculated from PPA (blue) and NPA (red) values. The OPA (green) was calculated from PPV (blue) and NPV (red) values. Derivation was done with participants of both cohorts merged. pTau, phosphorylated tau; CSF, cerebrospinal fluid; YI, Youden's J index; PPA, positive percentage agreement; NPA, negative percentage agreement; CL, Centiloids

classification performance, more subjects across the full AD *continuum* would be needed. This is a relevant effect because in previous similar works, the Youden's Index has been typically selected as the reference measurement of agreement [22, 30, 31]. Hansson et al. [30] added reliability measures to performance metrics to derive optimal cut-offs. We handled the noisy behaviour of performance metrics by deriving optimal cut-offs after some minimal smoothing of the data. This approach proved to be efficacious to derive stable cut-offs even in the analysis of the individual cohorts.

Irrespective of the approach to counter the effect of noisy agreement estimates, additional analysis with larger samples might be needed to yield more robust and generalizable cut-offs. To this end, future work will focus on pooling additional samples. In addition to a limited sample size, we rely on the comparability of PET and CSF measures across the two studied samples. While agreement on CSF data is certainly improved with the Elecsys® tests and with the use of the Centiloid method on PET scans, we cannot rule out the presence of a certain degree of sample-dependent bias in the data analysed. Still, when computing the cut-offs solely using the

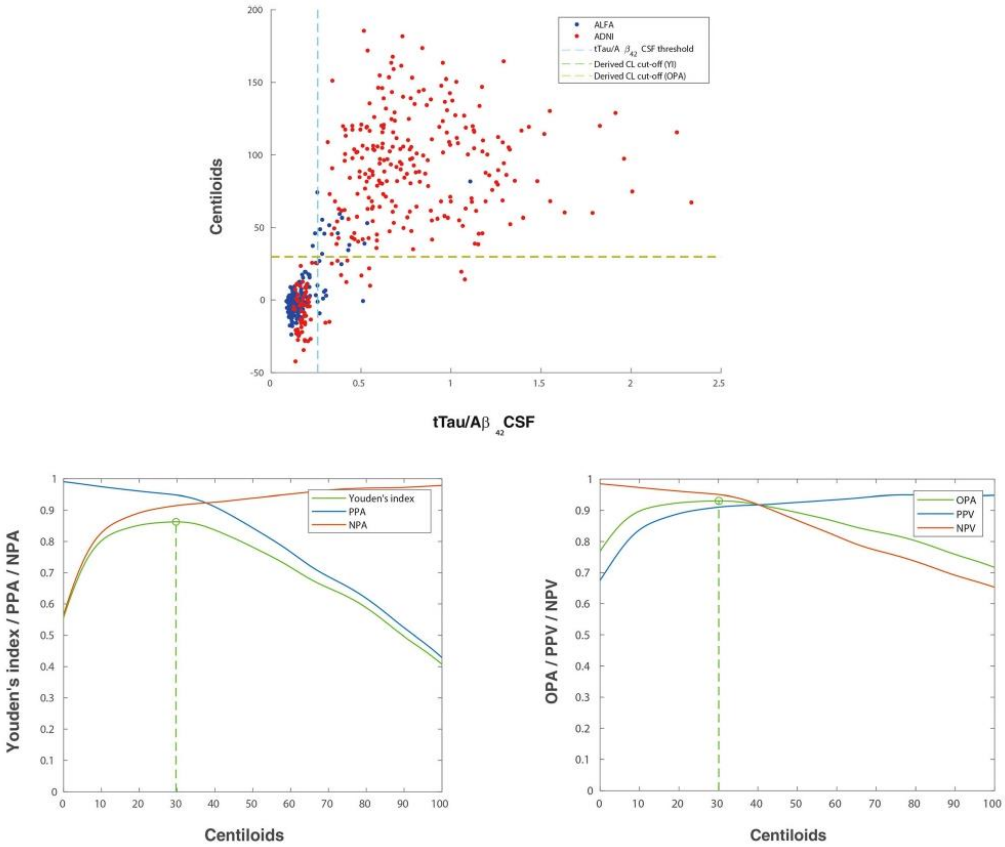

Fig. 4 Derivation of amyloid PET Centiloid cut-offs for CSF tTau/Aβ_{42}. Top row shows scatterplots of PET quantitative measures in Centiloids against CSF tTau/Aβ_{42} biomarker values for both ALFA+ (blue) and ADNI (red) participants. Vertical line depicts previously published CSF thresholds (tTau/Aβ_{42} 0.26 [22, 30]), and horizontal lines depict optimal cut-offs derived in this study (YI derived: green, OPA derived: yellow). Two outliers were excluded of this picture for having CL value higher than 200. Second row shows this cut-off derivation by maximization of YI (left) and OPA (right). The YI (green) was calculated from PPA (blue) and NPA (red) values. The OPA (green) was calculated from PPV (blue) and NPV (red) values. Derivation was done with participants of both cohorts merged. tTau, total tau; CSF, cerebrospinal fluid; YI, Youden's J index; PPA, positive percentage agreement; NPA, negative percentage agreement; CL, Centiloids

ALFA+ cohort results were very similar, thus suggesting that any remaining bias is small and did not have a significant impact on our results. Another limitation may stem from the somewhat limited sample analysed here may not be sufficient to derive robust generalizable cut-off values. Additional analysis with bigger sample sizes and more amyloid PET tracers that the two used here may overcome this limitation.

In summary, we have derived optimal Centiloid values to maximize the agreement against core AD CSF biomarkers. Regarding Aβ, a relatively low value of 12 CL optimally corresponded to CSF Aβ_{42} positivity, in line with Centiloid thresholds derived against post-mortem measures of AD neuropathology. On the other hand, CSF tau/Aβ_{42} ratios were better predicted by a higher Centiloid cut-off of 29 CL, which is in line with those optimally discriminating positive from negative visual reads on PET scans. In agreement with previous reports, CSF tau/Aβ_{42} ratios showed a higher capacity to predict amyloid PET Centiloids than CSF Aβ_{42}. Overall, our results provide reference values in the Centiloid scale and suggest two relevant inflection points the development of early AD pathology across the full AD *continuum*.

Additional file

Additional file 1: Supplementary data including supplementary methods and results. (DOCX 1010 kb)

Abbreviations

AD: Alzheimer's disease; ADNC: AD neuropathologic change; ADNI: Alzheimer's Disease Neuroimaging Initiative; ALFA: Alzheimer and Families; AUC: Area under the curve; Aβ: β-Amyloid; CERAD: Consortium to Establish a Registry for Alzheimer's Disease; CI: Confidence interval; CL: Centiloid; CSF: Cerebrospinal fluid; ELISA: Enzyme-linked immunosorbent assay; GZ: Grey zone; MPRAGE: Magnetization-prepared rapid acquisition gradient echo; MRI: Magnetic resonance imaging; NPA: Negative percentage agreement ("specificity"); OPA: Overall percentage agreement ("accuracy"); PET: Positron emission tomography; PPA: Positive percentage agreement ("sensitivity"); PSF: Point spread function; pTau: Phosphorylated tau; ROC: Receiver operating characteristic; SUVr: Standardized uptake value ratio; TOF: Time of flight; tTau: Total tau; YI: Youden's J index

Acknowledgements

This publication is part of the ALFA study (ALzheimer and FAmilies). The authors would like to express their most sincere gratitude to the ALFA project participants, without whom this research would have not been possible.

Authors would like to thank GE Healthcare for kindly providing ^{18}F-flutemetamol doses of ALFA+ participants and Roche Diagnostics International Ltd. for kindly providing the kits for the CSF analysis of ALFA+ participants. Authors would also like to thank Christopher Foley, Christopher Buckley and Mark Battle for their help on the Centiloid calculation.

Collaborators of the ALFA study are: Jordi Camí, Raffaele Cacciaglia, Marta Crous-Bou, Carme Deulofeu, Ruth Dominguez, Xavi Gotsens, Nina Gramunt, Laura Hernandez, Gema Huesa, Jordi Huguet, María León, Paula Marne, Tania Menchón, Marta Milà, Grégory Operto, Maria Pascual, Albina Polo, Sandra Pradas, Aleix Sala-Vila, Gonzalo Sánchez-Benavides, Sabrina Segundo, Anna Soteras, Laia Tenas, Marc Vilanova, Natalia Vilor-Tejedor.

Data collection and sharing for this project was funded by the Alzheimer's Disease Neuroimaging Initiative (ADNI) (National Institutes of Health Grant U01 AG024904) and DOD ADNI (Department of Defense award number W81XWH-12-2-0012). ADNI is funded by the National Institute on Aging, the National Institute of Biomedical Imaging and Bioengineering, and through generous contributions from the following: AbbVie, Alzheimer's Association; Alzheimer's Drug Discovery Foundation; Araclon Biotech; BioClinica, Inc.; Biogen; Bristol-Myers Squibb Company; CereSpir, Inc.; Cogstate; Eisai Inc.; Elan Pharmaceuticals, Inc.; Eli Lilly and Company; EuroImmun; F. Hoffmann-La Roche Ltd and its affiliated company Genentech, Inc.; Fujirebio; GE Healthcare; IXICO Ltd.; Janssen Alzheimer Immunotherapy Research & Development, LLC.; Johnson & Johnson Pharmaceutical Research & Development LLC.; Lumosity; Lundbeck; Merck & Co., Inc.; Meso Scale Diagnostics, LLC.; NeuroRx Research; Neurotrack Technologies; Novartis Pharmaceuticals Corporation; Pfizer Inc.; Piramal Imaging; Servier; Takeda Pharmaceutical Company; and Transition Therapeutics. The Canadian Institutes of Health Research is providing funds to support ADNI clinical sites in Canada. Private sector contributions are facilitated by the Foundation for the National Institutes of Health (www.fnih.org). The grantee organization is the Northern California Institute for Research and Education, and the study is coordinated by the Alzheimer's Therapeutic Research Institute at the University of Southern California. ADNI data are disseminated by the Laboratory for Neuro Imaging at the University of Southern California.

Data used in precreation of this article were obtained from the Alzheimer's Disease Neuroimaging Initiative (ADNI) database (adni.loni.usc.edu). As such, the investigators within the ADNI contributed to the design and implementation of ADNI and/or provided data but did not participate in analysis or writing of this report. A complete listing of ADNI investigators can be found at (http://adni.loni.usc.edu/wp-content/uploads/how_to_apply/ADNI_Acknowledgement_List.pdf).

Funding

The research leading to these results has received funding from "la Caixa" Foundation (LCF/PR/GN17/10300004) and the Alzheimer's Association and an international anonymous charity foundation through the the TriBEKa Imaging Platform project. JDG holds a 'Ramón y Cajal' fellowship (RYC-2013-13054). MS-C receives funding from the European Union's Horizon 2020 research and innovation programme under the Marie Sklodowska-Curie action grant agreement No 752310. CM is supported by the Spanish Ministry of Economy and Competitiveness (grant n° IEDI-2016-00690). KB holds the Torsten Söderberg Professorship in Medicine at the Royal Swedish Academy of Sciences, and is supported by the Swedish Research Council (#2017-00915), the Swedish Alzheimer Foundation (#AF-742881), Hjämfonden, Sweden (#FO2017-0243), and a grant (#ALFGBG-715986) from the Swedish state under the agreement between the Swedish government and the County Councils, the ALF-agreement.

HZ is a Wallenberg Academy Fellow supported by grants from the Swedish Research Council and the European Research Council.

Availability of data and materials

The datasets generated and/or analysed during the current study are not publicly available.

Authors' contributions

All authors listed (GS, JLM, AB-S, CF, OG-R, MS-C, JP, AN, AP, FL, CM, KF, HZ, KB and JDG) made a substantial contribution to the concept and design, acquisition of data or analysis and interpretation of data; drafted the article or revised it critically for important intellectual content; and approved the final version to be published.

Ethics approval and consent to participate

The ALFA study and the PET sub-study protocols have been approved by an independent Ethics Committee Parc de Salut Mar Barcelona and registered at Clinicaltrials.gov (ALFA Identifier: NCT02485730; PET sub-study Identifier: NCT02685969). Both studies have been conducted in accordance with the directives of the Spanish Law 14/ 2007, of 3rd of July, on Biomedical Research (Ley 14/ 2007 de Investigación Biomédica).

Consent for publication

Not applicable.

Competing interests

JLM is a consultant for the following for-profit companies: Alergan, Roche diagnostics, Genentech, Novartis, Lundbeck, Oryzon, Biogen, Lilly, Janssen, Green Valley, MSD, Eisai, Alector, Raman Health.

Other authors declared no potential conflicts of interest with respect to the research, authorship, and/or publication of this article.

Publisher's Note

Springer Nature remains neutral with regard to jurisdictional claims in published maps and institutional affiliations.

Author details

[1]Barcelonaβeta Brain Research Center (BBRC), Pasqual Maragall Foundation, Wellington 30, 08005 Barcelona, Spain. [2]CIBER Fragilidad y Envejecimiento Saludable (CIBERFES), Madrid, Spain. [3]Universitat Pompeu Fabra, Barcelona, Spain. [4]CIBER de Bioengeniería, Biomateriales y Nanomedicina, Madrid, Spain. [5]Nuclear Medicine Department, Hospital Clínic, Barcelona, Spain. [6]Institut d'Investigacions Biomèdiques August Pi i Sunyer, Barcelona, Spain. [7]Clinical Neurochemistry Laboratory, Sahlgrenska University Hospital, Mölndal, Sweden. [8]Department of Psychiatry and Neurochemistry, Institute of Neuroscience and Physiology, Sahlgrenska Academy at University of Gothenburg, Sahlgrenska University Hospital, Mölndal, Sweden. [9]Department of Neurodegenerative Disease, UCL Institute of Neurology, Queen Square, London, UK. [10]UK Dementia Research Institute at UCL, London, UK.

Received: 10 January 2019 Accepted: 27 February 2019
Published online: 21 March 2019

References

1. Villemagne VL, Burnham S, Bourgeat P, Brown B, Ellis KA, Salvado O, et al. Amyloid β deposition, neurodegeneration, and cognitive decline in sporadic Alzheimer's disease: a prospective cohort study. Lancet Neurol. 2013;12:357–67.

2. Vos SJB, Xiong PC, Visser PJ, Ms MSJ, Hassenstab J, Grant EA, et al. Preclinical Alzheimer's disease and its outcome: a longitudinal cohort study. Lancet Neurol. 2013;12:957–65.
3. Shaw LM, Vanderstichele H, Knapik-Czajka M, Clark CM, Aisen PS, Petersen RC, et al. Cerebrospinal fluid biomarker signature in Alzheimer's disease neuroimaging initiative subjects. Ann Neurol. 2009;65:403–13.
4. Ikonomovic MD, Buckley CJ, Heurling K, Sherwin P, Jones PA, Zanette M, et al. Post-mortem histopathology underlying β-amyloid PET imaging following flutemetamol F 18 injection. Acta Neuropathol Commun. 2016;4:130.
5. Seppälä TT, Nerg O, Koivisto AM, Rummukainen J, Puli L, Zetterberg H, et al. CSF biomarkers for Alzheimer disease correlate with cortical brain biopsy findings. Neurol. 2012;78:1568 LP–1575.
6. Jack CR, Bennett DA, Blennow K, Carrillo MC, Dunn B, Haeberlein SB, et al. NIA-AA Research Framework: toward a biological definition of Alzheimer's disease. Alzheimers Dement. 2018;14:535–62.
7. Sperling RA, Aisen PS, Beckett LA, Bennett DA, Craft S, Fagan AM, et al. Toward defining the preclinical stages of Alzheimer's disease. Alzheimers Dement. 2011;7:280–92.
8. Sperling RA, Mormino EC, Johnson KA. The evolution of preclinical Alzheimer's disease: implications for prevention trials. Neuron. 2014;84:608–22.
9. Fagan AM, Mintun MA, Mach RH, Lee SY, Dence CS, Shah AR, et al. Inverse relation between in vivo amyloid imaging load and cerebrospinal fluid Abeta 42 in humans. Ann Neurol. 2006;59:512–9.
10. Fagan AM, Mintun MA, Shah AR, Aldea P, Roe CM, Mach RH, et al. Cerebrospinal fluid tau and ptau181increase with cortical amyloid deposition in cognitively normal individuals: implications for future clinical trials of Alzheimer's disease. EMBO Mol Med. 2009;1:371–80.
11. Grimmer T, Riemenschneider M, Förstl H, Henriksen G, Klunk WE, Mathis CA, et al. Beta amyloid in Alzheimer's disease: increased deposition in brain is reflected in reduced concentration in cerebrospinal fluid. Biol Psychiatry. 2009;65:927–34.
12. Forsberg A, Almkvist O, Engler H, Wall A, Langstrom B, Nordberg A. High PIB retention in Alzheimers disease is an early event with complex relationship with CSF biomarkers and functional parameters. Curr Alzheimer Res. 2010;7:56–66.
13. Jagust WJ, Landau SM, Shaw LM, Trojanowski JQ, Koeppe RA, Reiman EM, et al. Relationships between biomarkers in aging and dementia. Neurol. 2009;73:1193–9.
14. Koivunen J, Pirttilä T, Kemppainen N, Aalto S, Herukka SK, Jauhianen AM, et al. PET amyloid ligand [11C]PIB uptake and cerebrospinal fluid β-amyloid in mild cognitive impairment. Dement Geriatr Cogn Disord. 2008;26:378–83.
15. Landau SM, Lu M, Joshi AD, Pontecorvo M, Mintun MA, Trojanowski JQ, et al. Comparing positron emission tomography imaging and cerebrospinal fluid measurements of β-amyloid. Ann Neurol. 2013;74:826–36.
16. Tolboom N, van der Flier WM, Yaqub M, Boellaard R, Verwey NA, Blankenstein MA, et al. Relationship of cerebrospinal fluid markers to 11C-PiB and 18F-FDDNP binding. J Nucl Med. 2009;50:1464–70.
17. Weigand SD, Vemuri P, Wiste HJ, Senjem ML, Pankratz VS, Aisen PS, et al. Transforming cerebrospinal fluid Aβ42 measures into calculated Pittsburgh compound B units of brain Aβ amyloid. Alzheimers Dement. 2011;7:133–41.
18. Palmqvist S, Zetterberg H, Mattsson N, Johansson P, Minthon L, Blennow K, et al. Detailed comparison of amyloid PET and CSF biomarkers for identifying early Alzheimer disease. Neurol. 2015;85:1240–9.
19. Palmqvist S, Zetterberg H, Blennow K, Vestberg S, Andreasson U, Brooks DJ, et al. Accuracy of brain amyloid detection in clinical practice using cerebrospinal fluid β-amyloid 42: a cross-validation study against amyloid positron emission tomography. JAMA Neurol. 2014;71:1282–9.
20. Mathis CA, Lopresti BJ, Ikonomovic MD, Klunk WE. Small-molecule PET tracers for imaging proteinopathies; 2017.
21. Palmqvist S, Mattsson N, Hansson O. Cerebrospinal fluid analysis detects cerebral amyloid-β accumulation earlier than positron emission tomography. Brain. 2016;139:1226–36.
22. Schindler SE, Gray JD, Gordon BA, Xiong C, Batrla-Utermann R, Quan M, et al. Cerebrospinal fluid biomarkers measured by Elecsys assays compared to amyloid imaging. Alzheimers Dement. 2018;14(11):1460-469.
23. Morris E, Chalkidou A, Hammers A, Peacock J, Summers J, Keevil S. Diagnostic accuracy of18F amyloid PET tracers for the diagnosis of Alzheimer's disease: a systematic review and meta-analysis. Eur J Nucl Med Mol Imaging. 2016;43:374–85.
24. Klunk WE, Koeppe RA, Price JC, Benzinger TL, Devous MD, Jagust WJ, et al. The Centiloid project: standardizing quantitative amyloid plaque estimation by PET. Alzheimers Dement. 2015;11:1–15.e4.
25. Rowe CC, Doré V, Jones G, Baxendale D, Mulligan RS, Bullich S, et al. 18F-Florbetaben PET beta-amyloid binding expressed in Centiloids. Eur J Nucl Med Mol Imaging. 2017;44:2053–9.
26. Rowe CC, Amadoru S, Dore V, McLean CL, Hinton F, Shepherd C, et al. Correlation of amyloid PET in Centiloid units with neuropathological findings in Alzheimer's disease. J Nucl Med. 2018;59:482.
27. Leuzy A, Chiotis K, Hasselbalch SG, Rinne JO, De Mendonça A, Otto M, et al. Pittsburgh compound B imaging and cerebrospinal fluid amyloid-β in a multicentre European memory clinic study. Brain. 2016;139:2540–53.
28. Kuhlmann J, Andreasson U, Pannee J, Bjerke M, Portelius E, Leinenbach A, et al. CSF Aβ1–42– an excellent but complicated Alzheimer's biomarker – a route to standardisation. Clin Chim Acta. 2017;467:27–33.
29. Bittner T, Zetterberg H, Teunissen CE, Ostlund RE, Militello M, Andreasson U, et al. Technical performance of a novel, fully automated electrochemiluminescence immunoassay for the quantitation of β-amyloid (1–42) in human cerebrospinal fluid. Alzheimers Dement. 2016;12:517–26.
30. Hansson O, Seibyl J, Stomrud E, Zetterberg H, Trojanowski JQ, Bittner T, et al. CSF biomarkers of Alzheimer's disease concord with amyloid-β PET and predict clinical progression: a study of fully automated immunoassays in BioFINDER and ADNI cohorts. Alzheimers Dement. 2018;14(11):1470-481.
31. Shaw LM, Waligorska T, Fields L, Korecka M, Figurski M, Trojanowski JQ, et al. Derivation of cutoffs for the Elecsys * amyloid β (1–42) assay in Alzheimer's disease. Alzheimers Dement Diagnosis Assess Dis Monit. 2018;10:698-705.
32. Ritchie CW, Molinuevo JL, Truyen L, Satlin A, Van der Geyten S, Lovestone S. Development of interventions for the secondary prevention of Alzheimer's dementia: the European Prevention of Alzheimer's Dementia (EPAD) project. Lancet Psychiatry. 2016;3:179–86.
33. Weninger S, Carrillo MC, Dunn B, Aisen PS, Bateman RJ, Kotz JD, et al. Collaboration for Alzheimer's prevention: principles to guide data and sample sharing in preclinical Alzheimer's disease trials. Alzheimers Dement. 2016;12:631–2.
34. McDade E, Bateman RJ. Stop Alzheimer's before it starts. Nature. 2017;547: 153–5.
35. Molinuevo JL, Gramunt N, Gispert JD, Fauria K, Esteller M, Minguillon C, et al. The ALFA project: a research platform to identify early pathophysiological features of Alzheimer's disease. Alzheimers Dement Transl Res Clin Interv. 2016;2:82–92.
36. Youden WJ. Index for rating diagnostic tests. Cancer. 1950;3:32–5.
37. Molinuevo JL, Blennow K, Dubois B, Engelborghs S, Lewczuk P, Perret-Liaudet A, et al. The clinical use of cerebrospinal fluid biomarker testing for Alzheimer's disease diagnosis: a consensus paper from the Alzheimer's biomarkers standardization initiative. Alzheimers Dement. 2014;10:808–17.
38. Mattsson N, Insel PS, Donohue M, Jagust W, Sperling R, Aisen P, et al. Predicting reduction of cerebrospinal fluid β-amyloid 42 in cognitively healthy controls. JAMA Neurol. 2015;72:554–60.
39. Toledo JB, Bjerke M, Da X, Landau SM, Foster NL, Jagust W, et al. Nonlinear association between cerebrospinal fluid and florbetapir F-18 β-amyloid measures across the spectrum of Alzheimer disease. JAMA Neurol. 2015;72:571–81.
40. La Joie R, Ayakta N, Seeley WW, Borys E, Boxer AL, DeCcarli C, et al. Multisite study of the relationships between antemortem [11C]PIB-PET Centiloid values and postmortem measures of Alzheimer's disease neuropathology. Alzheimers Dement. 2018;15(2):205-216.
41. Jack CR, Knopman DS, Jagust WJ, Petersen RC, Weiner MW, Aisen PS, et al. Tracking pathophysiological processes in Alzheimer's disease: An updated hypothetical model of dynamic biomarkers. Lancet Neurol. 2013;12(2):207–16.
42. Jack CR, Bennett DA, Blennow K, Carrillo MC, Feldman HH, Frisoni GB, et al. A/T/N: an unbiased descriptive classification scheme for Alzheimer disease biomarkers. Neurol. 2016;87:539–47.

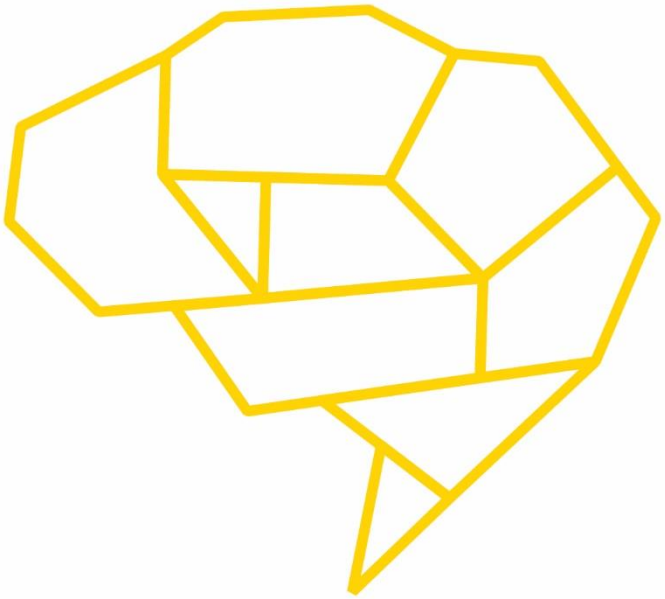

SECOND STUDY:

Visual assessment of flutemetamol PET images can detect early amyloid pathology and grade its extent

European Journal of Nuclear Medicine and Molecular Imaging
https://doi.org/10.1007/s00259-020-05174-2

ORIGINAL ARTICLE

Visual assessment of [^{18}F]flutemetamol PET images can detect early amyloid pathology and grade its extent

Lyduine E. Collij[1] · Gemma Salvadó[2,3] · Mahnaz Shekari[2] · Isadora Lopes Alves[1] · Juhan Reimand[4,5,6] · Alle Meije Wink[1] · Marissa Zwan[4] · Aida Niñerola-Baizán[7] · Andrés Perissinotti[7] · Philip Scheltens[4] · Milos D. Ikonomovic[8,9,10] · Adrian P. L. Smith[11] · Gill Farrar[11] · José Luis Molinuevo[2,3,9,12,13] · Frederik Barkhof[1,14] · Christopher J. Buckley[11] · Bart N. M. van Berckel[1,15] · Juan Domingo Gispert[2,3,9,16,17] · For the ALFA study[13] · On behalf of the AMYPAD consortium[14]

Received: 29 June 2020 / Accepted: 20 December 2020

Abstract

Purpose To investigate the sensitivity of visual read (VR) to detect early amyloid pathology and the overall utility of regional VR.

Methods [^{18}F]Flutemetamol PET images of 497 subjects (ALFA+ $N = 352$; ADC $N = 145$) were included. Scans were visually assessed according to product guidelines, recording the number of positive regions (0–5) and a final negative/positive classification. Scans were quantified using the standard and regional Centiloid (CL) method. The agreement between VR-based classification and published CL-based cut-offs for early (CL = 12) and established (CL = 30) pathology was determined. An optimal CL cut-off maximizing Youden's index was derived. Global and regional CL quantification was compared to VR. Finally, 28 post-mortem cases from the [^{18}F]flutemetamol phase III trial were included to assess the percentage agreement between VR and neuropathological classification of neuritic plaque density.

Results VR showed excellent agreement against CL = 12 ($\kappa = .89$, 95.2%) and CL = 30 ($\kappa = .88$, 95.4%) cut-offs. ROC analysis resulted in an optimal CL = 17 cut-off against VR (sensitivity = 97.9%, specificity = 97.8%). Each additional positive VR region corresponded to a clear increase in global CL. Regional VR was also associated with regional CL quantification. Compared to $mCERAD_{SOT}$-based classification (i.e., any region $mCERAD_{SOT} > 1.5$), VR was in agreement in 89.3% of cases, with 13 true negatives, 12 true positives, and 3 false positives (FP). Regional sparse-to-moderate neuritic and substantial diffuse Aβ plaque was observed in all FP cases. Regional VR was also associated with regional plaque density.

Conclusion VR is an appropriate method for assessing early amyloid pathology and that grading the *extent* of visual amyloid positivity could present clinical value.

Keywords Amyloid PET · [^{18}F]flutemetamol · Regional visual read · Centiloid · Sensitivity · Neuropathology

L. E. Collij and G. Salvadó contributed equally to this work.

The project leading to these results has received funding from "la Caixa" Foundation (ID 100010434), under agreement LCF/PR/GN17/50300004 and the Alzheimer's Association and an international anonymous charity foundation through the TriBEKa Imaging Platform project (TriBEKa-17-519007).

The project leading to this paper has received funding from the Innovative Medicines Initiative 2 Joint Undertaking under grant agreement No 115952. This Joint Undertaking receives the support from the European Union's Horizon 2020 research and innovation programme and EFPIA. This communication reflects the views of the authors and neither IMI nor the European Union and EFPIA are liable for any use that may be made of the information contained herein

This article is part of the Topical Collection on Neurology – Dementia.

✉ Bart N. M. van Berckel
b.berckel@amsterdamumc.nl

✉ Juan Domingo Gispert
jdgispert@barcelonabeta.org

Extended author information available on the last page of the article

Introduction

Positron emission tomography (PET) imaging enables the in vivo assessment and quantification of amyloid-β (Aβ) neuritic plaque density, a pathological hallmark of Alzheimer's disease (AD). In the clinical setting, the approved method for the assessment of amyloid pathology for supporting diagnosis using PET images is the visual read (VR), as described in the product labels of all currently registered amyloid PET tracers. To this end, VR has been validated against neuropathological determinations of amyloid burden [1–3]. However, it has been suggested that VR is a rather conservative method, as it was

Published online: 22 February 2021

developed to indicate moderate-to-frequent plaques as evaluated using the CERAD classification [1, 4]. As a consequence, it is possible that this method misses the detection of early sparse amyloid accumulation, which could be of interest for detecting early amyloid abnormalities [5]. In addition, although several regions-of-interest (ROIs) are visually assessed as in accordance with the reader guidelines, generally only the final classification (i.e., negative/positive) is used in both research and clinical settings, omitting any information regarding the location and extent of amyloid pathology.

Differently than in the clinical routine, amyloid PET (semi-)quantification has mainly been used in the research setting to study both clinical and earlier (preclinical) populations. However, the considerable variability in choice of tracer and (semi-)quantitative methods across centers has challenged the comparability of quantitative outcomes. For that purpose, the recently proposed Centiloid scale has become an increasingly used approach for the harmonization of amyloid PET data. Local processing pipelines can be validated against the original Centiloid method, and tracer-specific metrics such as the standardized uptake value ratio (SUVr) can be converted to a common scale referred to as "Centiloid" (CL). The scale is anchored on [^{11}C]PiB SUVr data and constructed such that CL = 0 represents the mean level of amyloid PET tracer uptake in young controls, while CL = 100 reflects the average signal observed in typical mild-to-moderate AD dementia patients [6]. This method has also been validated against neuropathological data by two independent studies [7, 8]. First, La Joie and colleagues (2019) demonstrated that the earliest detectable [^{11}C]PiB signal occurred at CL = 12, and that a cut-off of CL = 24 best discriminated between subjects with none-to-low Aβ plaque burden and those with intermediate-to-high deposition [7]. Similar CL cut-off values were also identified by Amadoru and colleagues (2020), where CL = 10 was considered an optimal threshold for excluding neuritic plaques, while approximately CL = 21 successfully detected moderate-to-frequent plaque density [8]. In addition, a cut-off of CL = 12 was later also reported by Salvadó and colleagues (2019) to maximize the agreement between [^{18}F]florbetapir and [^{18}F]flutemetamol PET CL values from two different cohorts with respect to amyloid positivity as determined through CSF Aβ_{42} levels. Furthermore, when comparing to CSF p-tau/Aβ_{42} ratio levels as an indication of established AD pathology, the authors identified a cut-off of CL = 30 [9].

In contrast, studies using VR as the reference standard have reported significantly higher CL cut-offs (i.e., up to 42 CL) for determining amyloid abnormality [10–12]. This discrepancy is possibly due to substantial differences in the populations studied, with the number of preclinical individuals being limited or even absent in most VR studies. Preclinical AD participants are more likely to show low levels of amyloid burden in a focal manner [13] and therefore support more sensitive (lower) cut-offs than the specific (higher) ones identified from end-of-life subjects or typical clinical populations. Unfortunately, reports of regional VR are scarce and only available from clinical populations, where focal increase in signal has been visually observed in < 2% of individuals [14, 15]. However, as recent studies highlight the value of quantitative regional amyloid assessments in identifying focal amyloid pathology [16–18], performing systematic regional VR informed by the spatial-temporal evolution of amyloid pathology [19] could bring value to stage the progression of amyloid accumulation.

As stated in the strategic roadmap for an early diagnosis of AD framework, proper evaluation of VR performance in detecting early or focal amyloid deposition and establishing reader guidelines to facilitate such use remains incomplete [20]. Within this context, the aims of this study are twofold. First, we studied the agreement between VR- and CL-based classification of amyloid PET scans using previously proposed cut-offs for early and established amyloid accumulation. Secondly, we characterized and assessed the utility of regional VR positivity to stage amyloid burden across the AD *continuum*. To these ends, we pooled [^{18}F]flutemetamol scans of two complementary cohorts that allowed us to cover both early and established pathology. The pooled cohort was intended to cover the full range of amyloid burden and to have a good representation of intermediate amyloid levels around proposed cut-offs for early amyloid accumulation. We also studied the inter- and intra-reader agreement in a subset of scans with mainly intermediate levels of amyloid burden, to assess the reproducibility of regional VR in the early stages of AD. Finally, we aimed to validate our results using an independent post-mortem data-set, in which (regional) VR was compared to neuropathological scores.

Methods

Subjects

Data from two cohorts were pooled in order to capture amyloid accumulation across the AD *continuum*; the ALFA+ cohort, which is a nested longitudinal long-term study of the ALFA (for ALzheimer's and FAmilies) [21] and the Dutch Flutemetamol study from the Amsterdam Dementia Cohort (ADC) [22, 23]. The ALFA cohort was established as a research platform to characterize preclinical AD in 2743 cognitively unimpaired individuals, aged between 45 and 75 years old with increased risk for AD. The ALFA+ sub-study consists of participants enriched for family history of AD and APOE ε4 carriership and who underwent amyloid PET imaging. The first consecutive 352 participants of the ALFA+ study collected between March 2017 and January 2020 were included in this work. The ADC cohort consisted of cognitively impaired patients (mild cognitive impairment (MCI), AD dementia, and non-AD dementia (e.g., fronto-temporal dementia [FTD], dementia with lewy bodies [DLB]) who underwent standard dementia screening at the VU University Medical Center Amsterdam [22]. In total, 145

PET scans from ADC passed quality control for quantification (e.g., absence of significant lesions, brain parenchyma in field of view, and available high quality T1-weighted MRI) and were therefore included. Thus, a total of 497 [^{18}F]flutemetamol scans were included in this study. Demographics are shown in Table 1.

The ALFA study and the PET sub-study (ALFA+) protocols have been approved by an independent Ethics Committee Parc de Salut Mar Barcelona and registered at Clinicaltrials.gov (ALFA Identifier: NCT02485730; PET sub-study Identifier: NCT02685969). Both studies have been conducted in accordance with the directives of the Spanish Law 14/2007, of 3rd of July, on Biomedical Research (Ley 14/ 2007 de Investigación Biomédica). The medical ethics review committee of the VU University Medical Center approved the Dutch Flutemetamol study (reference number: 2012/302).

Amyloid PET acquisition, processing, and quantification

Scans from the ALFA+ (Siemens Biograph mCT scanner) and ADC (Gemini TF-64PET/CT scanner) cohort consisted of four frames (4 × 5 minutes) acquired 90–110 min post-injection of [^{18}F]flutemetamol (ALFA+: 191 ± 14 MBq; ADC: 191 ± 10 MBq). All scans were pre-processed using a validated standard Centiloid pipeline and converted to the Centiloid scale [6]. To match the intrinsic resolutions between centers, we first smoothed the ALFA+ scans using an isotropic 3D Gaussian Filter with a 4-mm full width at half maximum (FWHM) to match the resolution of the PET scans from the joined cohort (see Sup. Figure 1 for example images before and after the resolution harmonization step). Subsequent steps were equal for both cohorts and have been previously reported [9]. Briefly, images were checked for motion and inter-frame registration was performed when necessary. Then, the four frames from the PET images were first averaged and co-registered to the corresponding T1-weighted scans. Then, the T1-weighted MRI scans were warped to standard space; the same warp was applied to warp the co-registered PET image. These procedures were performed in SPM12. Of note, different T1 protocols were used for each site. Acquisition details can be found in the supplementary material.

PET images were intensity normalized using the whole cerebellum as the reference region using the mask provided by the Centiloid method [6] (http://www.gaain.org/centiloid-project). Cortical Centiloid values were calculated using the standard target region and a previously calibrated conversion equation [9]. Based on their respective Centiloid values, scans were classified as amyloid negative (CL-: CL < 12), gray-zone (CL-GZ: CL = 12–30) or amyloid positive (CL+: CL > 30) [9]. In addition, regional standard uptake value ratios (SUVr) were extracted using the Desikan Killiany atlas [24] and converted to regional Centiloid units using the global conversion equation [6]. Five regions-of-interest (ROIs) were created to reflect the visual assessment guidelines: (1) frontal: rostral and caudal anterior cingulate cortex, medial and lateral orbitofrontal, superior frontal, frontal pole, rostral and caudal middle frontal, pars orbitalis, pars triangularis, and pars opercularis; (2) the precuneus (PC)/posterior cingulate cortex (PCC): precuneus, posterior cingulate cortex, and isthmus cingulate cortex; (3) lateral-parietal: superior parietal, supramarginal, and inferior parietal; (4) lateral temporal: transverse temporal, temporal pole and inferior, middle, and superior temporal cortex; and finally (5) striatum: putamen and caudate nucleus (Sup. Figure 2).

Visual assessment of PET scans

All 497 [^{18}F]flutemetamol scans were initially read by one reader (Reader 1, LEC), who was blinded to clinical details of the individuals, completed the training provided by GE Healthcare [25], and has experience in assessing >1000 scans. For the visual read, image maximum intensity was scaled to 90% of the pons signal using rainbow color scaling and transverse, sagittal, and coronal views were displayed using the software package Vinci 2.56 and assessed together with a

Table 1 Demographics of the visual read cohorts

	Pooled (*N* =497)	ALFA+ CU population (*N* =352)	ADC Clinical Population (*N* =145)	*p* value
Age (years)	61.7±4.9	61.5±4.6	62.2±5.6	n.s.
Sex, Female (%)	281 (56.5%)	215 (61.1%)	66 (45.5%)	<0.01
MMSE	27.2±3.5	29.2±1.0	23.4±3.4	<0.01
APOE ε4 carriership	280 (56.3%)	193 (54.8%)	87 (60.0%)	n.s.
Centiloid	18.7±38.8	2.9±17.2	56.8±48.9	<0.01
VR+	141 (28.4%)	47 (13.4%)	94 (64.8%)	<0.01

ALFA ALzheimer's and Families cohort, *ADC* Amsterdam Dementia Cohort, *CU* cognitively unimpaired, *MMSE* Mini-Mental Estate examination, *VR* visual read

T1-weighted MR scan to assist reading in the presence of atrophy in the visual assessment. Images were rated according to the read criteria as defined by the manufacturer, which included the visual assessment of 5 regions; frontal cortex, PC/PCC, lateral-parietal, lateral temporal, and striatum. In addition to regional reads, the final classification was also available, with images rated as either *positive* (VR+, unilateral binding in one or more cortical brain region or striatum) or *negative* (VR-, predominantly white matter uptake). Reader confidence of the final read was captured on a 5 point scale (1 very low confidence–5 very high confidence).

Intra- and inter-reader agreement

Two additional readers (BvB and CB) were involved at a secondary step, where scans were independently selected (GS) to assess the intra- and inter-reader agreement, with an emphasis on the images with emerging levels of amyloid from the ALFA+ cohort. Scans were selected based on their initial VR assessment by Reader 1 and their Centiloid quantification. The selection criteria were (1) only one region assessed as amyloid positive based on VR ($N = 19$); (2) only the frontal and PC/PCC ROI were assessed as VR+ ($N = 16$); (3) VR assessment with low confidence (i.e., ≤ 3, $N = 8$); (4) discordant classification between VR and Centiloid (cut-off CL 12 [7, 9], $N = 20$); and (5) Centiloid values between 10 and 35 ($N = 26$). This resulted in the selection of 58 scans, as some fell into more than one inclusion category. In addition, 21 clearly negative and 21 clearly positive scans were also included to balance the sample, resulting in the final selection of 100 scans. Importantly, all readers (LEC, BvB, CB) were blinded to these selection parameters as well as to the initial (Reader 1) VR classification of the scans. BvB is a nuclear physician with considerable experience in reading [^{18}F]flutemetamol scans and CB is a medical imaging expert employed at GE Healthcare.

Post-mortem data-set

To further evaluate the utility of regional visual assessment of [^{18}F]flutemetamol scans, we selected a sub-set of the post-mortem [^{18}F]flutemetamol phase III study cases and compared the read of our three readers to the available neuropathological scores [26]. GS randomly selected a sample of 30 subjects from the original study, prioritizing for presence of MRI scans, shortest imaging-autopsy intervals, and intermediate levels of Aβ pathology as determined by CERAD. Also, different combinations of regional Aβ burden based on CERAD were represented. After selection, 2 cases were excluded due to severe vascular burden/lesions and severe atrophy, resulting in a final data-set for analyses of 28 cases. The readers were blinded to the selection. Demographics are shown in Table 2.

We evaluated the VR results against a previously established neuropathological standard of truth (SOT) that was better suited for comparison with a PET study than the traditional CERAD-based classification. This modified CERAD standard of truth ($mCERAD_{SOT}$) approach includes the assessment of neuritic plaque density in 8 neocortical regions (i.e., midfrontal lobe (MFL), middle and superior temporal gyrus (MTG/STG), inferior parietal lobe (IPL), anterior and posterior cingulate gyrus (ACG/PCG), precuneus (PRC), and primary visual cortex) and provides a continuous measure of pathology instead of a binary classification. Per region, a score of 0 = none (no plaques), 1 = sparse (1–5 plaques), 2 = moderate (6–19 plaques), or 3 = frequent (20+ plaques per 100× field of view [FoV]) was given. The scale midpoint of 1.5 represents the threshold between sparse and moderate categories. Thus, a mean score ≤ 1.5 was considered normal, while a mean score of >1.5 was considered abnormal for each region. If any one of the 8 regions was considered abnormal, i.e., any regional $mCERAD_{SOT}$ was >1.5, the whole brain was considered abnormal or Aβ+. See Ikonovomic et al. (2016) for a detailed description of the methodology [27].

Statistical analyses

Statistical Package for the Social Sciences (SPSS) version 26 was used for all statistical analyses, apart from the Kappa statistics, which were computed using R version 3.6.0. For the majority of cases ($N = 397$), only the assessment of Reader 1 was available for analysis. In cases where a majority VR was available ($N = 100$), this classification was used instead for both the global and regional analyses. Baseline demographics were described using simple descriptive statistical analyses.

Global visual read and global Centiloid

The aim of our first set of analyses was to compare global VR assessment to global Centiloid values. Kappa statistics were used to determine the agreement between Centiloid-based classification (cut-offs CL 12 and 30) and VR-based classification. In addition, the sensitivity, specificity, and Youden's J index (sensitivity+specificity-1) of VR compared to CL were reported. Next, we aimed to derive the optimal Centiloid threshold using VR as standard of truth in an receiver operating characteristic (ROC) analyses, maximizing the Youden's J Index.

Regional visual read and global and regional Centiloid

Our second group of main analyses aimed at comparing regional VR assessment and global and regional Centiloid values. First, differences in global CL quantification depending on the number of VR positive regions were assessed using Kruskal-Wallis test. Then, we assessed the difference in

Table 2 Demographics of the post-mortem cohort

	All (N =28)	Non-demented (N = 10)	Demented (N = 18)	p value
Age (years)	79.1±9.3	75.2±9.7	81.28±8.5	.097
Sex, Female (%)	13 (46.4%)	3 (30%)	10 (55.6%)	.184
Delay PET imaging (days)	72.5 (111)	60.0 (311)	72.5 (104)	n.s.
VR+	15 (53.6%)	4 (40%)	11 (61.1%)	n.s.
Mean $mCERAD_{SOT}$	1.08 (1.72)	0.09 (1.67)	1.15 (1.26)	.064

Age is shown in mean ± SD. PET delay and $mCERAD_{SOT}$ are shown in median (IQR). VR: visual read. $mCERAD_{SOT}$ modified CERAD standard of truth

regional quantification (Centiloid and SUVr) by regional VR assessment using Wilcoxon test. Finally, the sensitivity and specificity associated with a maximized Youden index of regional VR compared to regional quantification were reported.

Patterns of regional visual read

Furthermore, as secondary analyses, we aimed to characterize VR stages based on the observed patterns of regional visual positivity. Chi-squared tests were used to assess the distribution of VR stages across CL groups and clinical diagnosis.

Intra- and inter-reader agreement

Finally, intra-reader agreement for Reader 1 and inter-reader agreement among the three readers regarding the final classification (i.e., negative/positive) was determined using Kappa statistics. Agreement was considered poor if κ was less than 0.20, satisfactory if κ was 0.21–0.40, moderate if κ was 0.41–0.60, good if κ was 0.61–0.80, and excellent if κ was more than 0.80. Reader agreement for regional visual read was assessed via percentage agreement, as the imbalance in negative/positive for certain regions affects the kappa statistic.

Visual read and neuropathological scores

First, we assessed the percentage agreement between global VR classification and neuropathological classification of neuritic plaque density (i.e., any region $mCERAD_{SOT} > 1.5$), reporting the number of true positives (TP), false positive (FP), false negatives (FN), and true negatives (TN). Then, we determined the percentage agreement between regional VR and regional $mCERAD_{SOT}$ scores. Finally, we assessed the difference in continuous regional $mCERAD_{SOT}$ score by regional VR assessment of negative/positive using a Wilcoxon test. More specifically, VR assessment of the frontal ROI was compared to neuropathological scores in the ACG and MFL, VR of PC/PCC ROI to PCG and PRC, VR of temporo-parietal to IPL, and VR of lateral temporal to MTG and STG.

Results

Relationship between Centiloid and global visual read

CL values ranged from −27.57 to 171.11, with a mean value of 19.82 (SD = 38.62) across the pooled dataset. After applying the previously established CL cut-offs of 12 and 30, 335 (64.4%) scans were classified as CL-, 44 (8.9%) as CL-GZ, and 118 (23.7%) as CL+. CL-GZ subjects were mostly cognitively unimpaired (N = 33, 75%), APOE ε4 carriers (N = 31, 70.5%), and distributed across a broad age range (M = 62.26,SD = 5.16, range = 49.6–70.6).

Across the pooled dataset, 141 (28.4%) scans were read as amyloid PET positive. Of the ALFA+ cohort (cognitively unimpaired population), 47 (13.4%) scans were read as amyloid positive, compared to 94 (64.8%) of the ADC cohort (cognitively impaired population). Visually amyloid PET positive scans had a significantly higher CL value than those visually negative (VR+: $M_{CL} = 72.41$, $SD_{CL} = 35.09$; VR-: $M_{CL} = -1.00$, $SD_{CL} = 8.06$, $F = 1378.18$, $\eta^2 = 0.74$, $p < 0.01$). In addition, within the VR+ group, quantitative amyloid burden was significantly different between the two cohorts (ALFA+: $M_{CL} = 39.87$, $SD_{CL} = 17.77$; ADC: $M_{CL} = 88.67$, $SD_{CL} = 29.91$, $F = 106.15$, $\eta^2 = 0.43$, $p < 0.01$). In relation to CL groups, scans were read as positive in 0.3%/50.0%/100% of CL-/CL-GZ/CL+ cases, respectively.

Visual read performance compared to Centiloid

First, we investigated the agreement between VR-based classification and Centiloid-based classification of amyloid positivity using the previously proposed CL cut-offs of 12 and 30. VR showed excellent agreement against both the lower bound (CL = 12, κ = .89, 95.2% [473/497]) and upper bound (CL = 30, κ = .88, 95.4% [474/497]) of the gray-zone cut-off, with a sensitivity/specificity of 85.9%/99.7% (PPV = 99.2%; NPV = 93.5%) and 100%/93.9% (PPV = 83.7%; NPV = 100%), respectively.

Subsequently, we performed a ROC analysis with VR as the reference standard to assess whether the optimal CL cut-off in this independent dataset would fall within the previously

reported 12–30 range. The overall agreement between VR and CL values was excellent (area under the curve [AUC] = 0.998; 95% CI: 0.996–1.0). A cut-off value of CL = 17, maximized the Youden's Index (J = 0.956) and was associated with both very high sensitivity (97.9%) and specificity (97.8%) (Fig. 1a). See Sup. Table 1 for ROC results for all coordination points between 85% and 100% specificity. In addition, the sensitivity, specificity, and Youden Index as a function of CL can be found in Sup. Figure 3.

Finally, mean CL values showed a clear increase per additional positive VR region ($\chi^2 = 303.71$, df = 5, $p < .001$, Fig. 1b). Post hoc analyses revealed a statically significant difference in CL values between all consecutive groups based on number of regions read as positive and differences at trend level between 3 and 4 regions visually positive.

Regional visual read and regional Centiloid

The PC/PCC and frontal regions were read positive most often (26.4% and 26.0%), followed by lateral temporal (20.3%), temporo-parietal (18.3%), and striatal region (17.9%). Isolated regional VR+ (one region only) occurred in only 20 subjects (4.0%), where the positive region was frontal in 9 subjects (1.8%) and PC/PCC in 11 subjects (2.2%). Out of 136 subjects that were PC/PCC VR+, 90.8% of them also were frontal VR+. Striatal VR+ always occurred with concomitant frontal VR+ (100%), while only .1% of striatal VR+ cases were not PC/PCC VR+, and around 15% of striatal VR+ cases were not temporo-parietal or lateral temporal VR+ (Sup. Table 2).

Figure 2 shows for each VR ROI the regional amyloid burden quantified in both SUVr and CL units and stratified by VR status. For all regions, VR+ corresponded to significantly higher regional CL values (Frontal: $W = 461$; PC/PCC: $W = 78$; Parietal: $W = 449$; Temporal: $W = 208$; Striatum $W = 791$, $p < 0.001$, Sup. Table 3) and was accompanied with high sensitivity and specificity for all ROIs (frontal: sensitivity = 94.7%, specificity = 97.8%; PC/PCC: sensitivity = 100%, specificity = 96.2%; temporo-parietal: sensitivity = 96.8%, specificity = 95.5%; lateral temporal: sensitivity = 98.1%, specificity = 97.5%; striatum: sensitivity = 97.8%, specificity = 92.1%).

Patterns of regional visual read

Figure 3 shows the distribution of regional VR+, stratified per cohort. The distribution of subjects across the patterns suggests a general order of regions becoming visually amyloid positive; in case of one positive VR region, only the PC/PCC or frontal ROI was assessed as such (VR stage 1), most often (75%) followed by a combination of these regions being read as positive (VR stage 2). Then, further cortical and/or striatal visual positivity becomes apparent (VR stage 3). In the ALFA cohort, generally positivity beyond the PC/PCC and frontal ROIs was initially observed in the lateral temporal region, followed by the temporo-parietal regions, and finally the striatum. Early striatal involvement was more often reported in the cognitively impaired cohort. This could be the result of

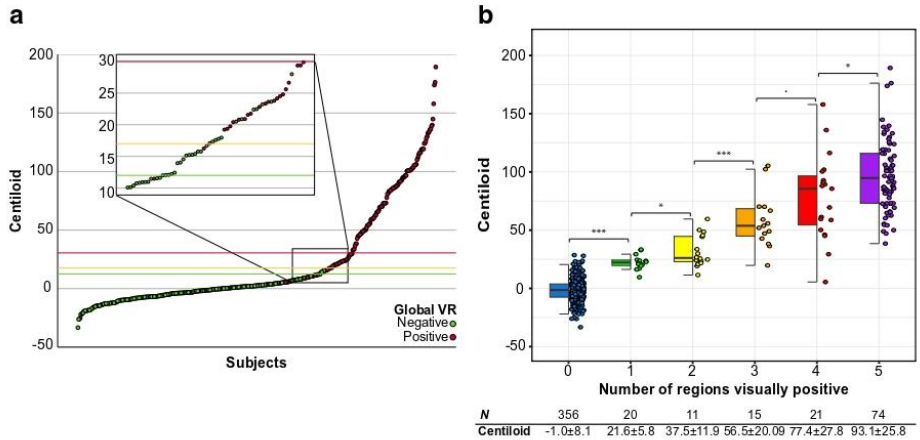

Fig. 1 Visual read against global Centiloid. **a** Plots shows all 497 subjects ordered by global amyloid burden expressed in Centiloid units. The green line illustrates the CL = 12 cut-off as proposed by La Joie and colleagues (2019) based on post-mortem comparison and by Salvadó and colleagues (2019) based on CSF $A\beta_{42}$. The red line illustrates the CL = 30 cut-off as previously proposed by Salvadó and colleagues compared to CSF p-tau/$A\beta_{42}$, which was suggested to indicate the presence of established pathology. Finally, the orange line represents the optimal CL = 17 cut-off according the data-driven ROC analyses of this dataset using the Youden Index. **b** Centiloid values significantly increase per additional visually positive region. Post hoc analyses showed significant differences between all groups. $p < 0.1$; $*p < 0.05$; $**p < 0.01$; $***p < 0.001$

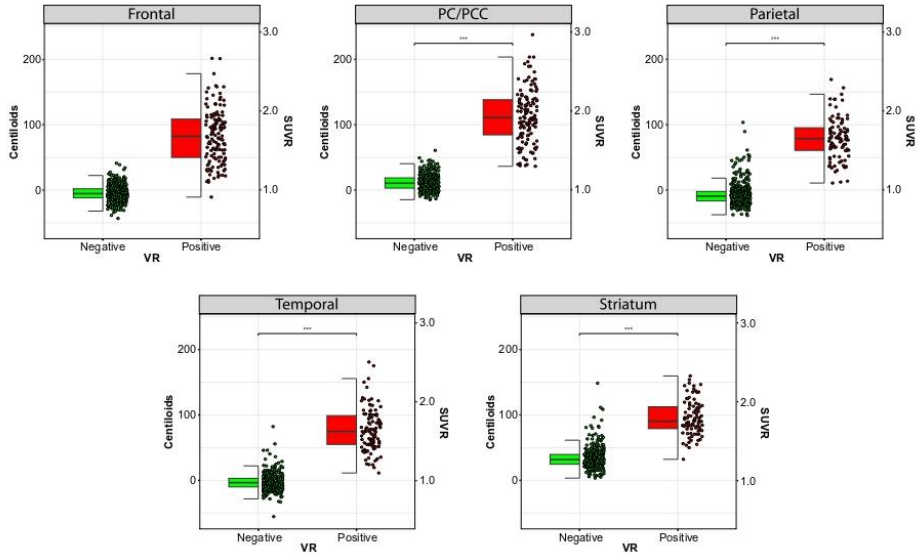

Fig. 2 Regional visual read against regional quantification. Boxplots represent the regional visual assessment against regional amyloid burden, with quantification expressed in both Centiloid (y-axis left) and SUVR (y-axis right) units. PC/PCC: precuneus/posterior cingulate cortex; SUVR: standardized uptake value ratio; VR: visual read

partial volume effects (i.e., atrophy) on the more lateral cortical regions, which is known to have a lesser effect on the striatal region.

Mean CL values were significantly different between all VR stages ($H = 302.55$, $p < .001$), and the ROC analyses revealed the optimal CL cut-offs were CL = 16 (VR- vs. VR+ stage ≥1), CL = 22 (VR stage 0/1 vs. VR+ stage ≥2), and CL = 35 (VR stage 0/1/2 vs. VR+ stage 3), with good to excellent sensitivity/specificity (Table 3). Also, VR stages were associated with CL groups of low, gray-zone, and high amyloid burden ($\chi^2 = 577.16$, $p < 0.01$) and with clinical diagnosis ($\chi^2 = 343.92$, $p < 0.01$), which was made pre-disclosure of PET results. More details can be found in supplementary results and Sup. Figure 4. Figure 4 shows example images following this general pattern of visual amyloid positivity and their accompanying CL values.

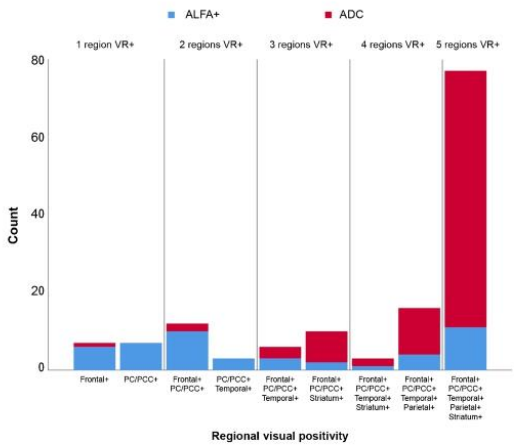

Fig. 3 Patterns of visually positive regions. Bar graph represents number of subjects in each visual read group. In total, 10 combinations of regional amyloid positivity were observed. Blue represents the ALFA+ cognitively unimpaired subjects and red represents the ADC clinical cohort. PC/PCC: precuneus/posterior cingulate cortex; VR: visual read

Intra- and inter-reader agreement

Based on the 100 pre-selected scans focused on the most difficult/borderline cases, intra-reader agreement of Reader 1 (LEC) was considered to be good ($\kappa = .71$). The overall agreement between the 3 readers was also good ($\kappa = .75$, 84%). The highest agreement was seen between Reader 1 and Reader 2 ($\kappa = .78$) and the lowest between Reader 2 and Reader 3 ($\kappa = .72$). Supplementary Table 5 shows all 100 cases ordered by CL burden and their final VR classification per reader. It shows that scans with a CL ~ 20 or higher burden are generally classified as VR+ across all readers. In addition, 4/9 of scans with a CL 17–20 were also classified as VR+ by at least 2 out of 3 readers. Importantly, reader agreement was high and comparable across all ROIs: frontal 74%, PC/PCC 84%, temporo-parietal 80%, lateral temporal 79%, and striatum 73%.

Table 3 VR stages

	VR negative	VR+ stage 1	VR+ stage 2	VR+ stage 3
Number of subjects	356	20	9	110
Centiloid	−1.0±8.1	21.6±5.8	35.4±12.2	85.1±28.3
CL cut-off*	n/a	16	23	35
Sensitivity*	n/a	97.8%	96.7%	97.3%
Specificity*	n/a	96.3%	97.8%	99.2%
Youden Index*	n/a	0.941	0.943	0.965
AUC*	n/a	.995	.992	.996
		(.992-.999)	(.992–1.00)	(.992–1.00)

*Compared to lower stage(s)

Regional visual read and regional neuropathological scores

Compared to $mCERAD_{SOT}$-based classification (i.e., any region $mCERAD_{SOT} > 1.5$) of neuritic plaque density, VR classification was in agreement in 89.3% [25/28] of cases, with 13 TN, 12 TP, and 3 FP. Interestingly, all FP cases had a mean $mCERAD_{SOT}$ above 1 and at least one region with a regional mean $mCERAD_{SOT}$ of ≥1.3, indicating the presence of regional sparse-to-moderate neuritic amyloid plaques. In turn, only 1 TN cases had a similar pattern of neuropathological burden. In addition, these FP cases were reported to have a moderate to high burden of diffuse Aβ plaques, reflected in their Thal stage (i.e., 3–5). See Fig. 5 for a detailed description of these cases.

Compared to regional $mCERAD_{SOT}$-based classification (i.e., regional $mCERAD_{SOT} > 1.5$), regional VR was in agreement in 75–89.3% of cases. Lower agreement was observed for the frontal and PC/PCC ROIs, as relatively more cases (11–14% vs. 0–7%) were classified as VR+ and did not have a $mCERAD_{SOT} > 1.5$, but rather a $mCERAD_{SOT}$ between 1 and 1.5 (Sup. Table 6).

Finally, both global and regional VR positivity were associated with significantly higher mean and regional neuropathological burden as measured with the $mCERAD_{SOT}$ (Global: mean $mCERAD_{SOT}$ $W = 4$; Frontal: MFL $W = 13.5$, ACG $W = 21.5$; PC/PCC: PCG $W = 15.0$, PRC $W = 13.0$; Parietal: IPL $W = 12.0$; Temporal: STG $W = 19.5$, MTG $W = 16.0$, all $p < 0.001$; Fig. 6, Sup. Table 6).

Discussion

In the current study, we investigated the agreement between visual reads (VR) and Centiloid-based detection of early and established amyloid pathology and the utility of regional patterns of VR positivity for capturing the extent of amyloid burden beyond standard dichotomization. We found that

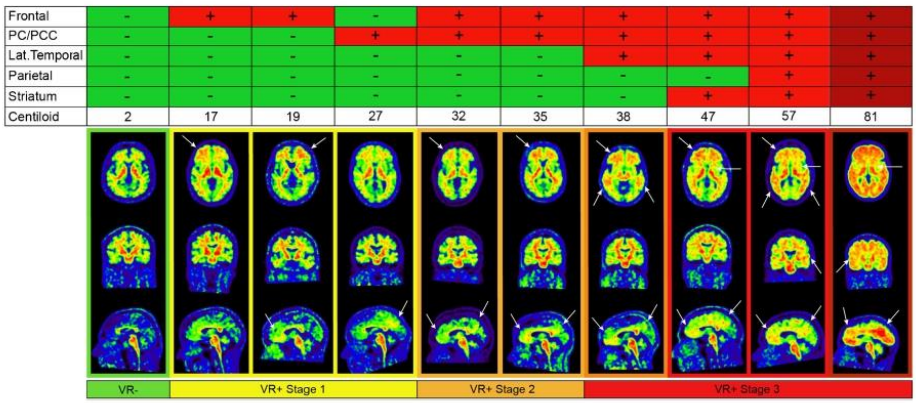

Fig. 4 Example [^{18}F]flutemetamol images. A series of 10 [^{18}F]flutemetamol scans form the ALFA+ cohort ordered based on Centiloid values are shown. Upper panel illustrates which regions were visually assessed as positive. From top to bottom, axial, coronal, and sagittal images are provided. White arrows highlight specific regional amyloid uptake. Note, that the main differences between VR- (left panel) and early amyloid accumulation (second to fourth panel) can be observed basal frontally on the axial image and in the orbitofrontal and precuneal regions on the sagittal images. PC/PCC: precuneus/posterior cingulate cortex; VR: visual read

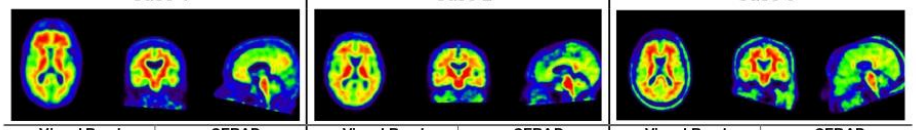

Case 1		Case 2		Case 3	
Visual Read +	$mCERAD_{SOT}$	Visual Read +	$mCERAD_{SOT}$	Visual Read +	$mCERAD_{SOT}$
Frontal	MFL: 0.7 ACG1.1	PC/PCC	PCG: 1.1 PRC: 1.4	Frontal	MFL: 1.4 ACG: 1.2
PC/PCC	PCG: 0.9 PRC: 1.0	Lateral Temporal	STG: 0.8 MTG: 1.1	PC/PCC	PCG: 0.9 PRC: 1.2
Parietal	IPC: 1.4				
Thal phase: 5		Thal phase: 3		Thal phase: 3	
Final diagnosis: LBD		Final diagnosis: AD		Final diagnosis: LBD	

Fig. 5 Visual read false positive cases. PC/PCC: precuneus/posterior cingulate cortex; MFL: midfrontal lobe; ACG: anterior cingulate gyrus; PCG: posterior cingulate gyrus; PRC: precuneus; IPC: inferior parietal cortex; STG: superior temporal gyrus; MTG: middle temporal gyrus; LBD: lewy body dementia; AD: Alzheimer's dementia

VR-based classification performed by experienced readers is in high agreement with previously proposed quantitative Centiloid (CL) cut-offs of both early and established pathology. When using VR as the reference standard, we identified an optimal cut-off (CL = 17) well within the previously proposed gray-zone band of emerging amyloid pathology (CL = 12–30). In addition, there was a clear proportional relationship between the number of visually positive regions and increases in continuous CL burden, supporting the value of regional information in capturing the degree of amyloid burden. Furthermore, we observed that regional CLs were significantly higher in those regions assessed as positive by VR. The validity of this work is supported by our analyses in the post-mortem data-set, which showed a high agreement between VR-based and neuropathological-based classification of amyloid positivity, at both global and regional level. In fact, these results suggest that VR could capture the presence of sparse-to-moderate neuritic plaques and substantial diffuse Aβ plaques.

In recent years, great emphasis has been put on improving the early identification of amyloid pathology. In a clinical trial setting, amyloid PET is increasingly used as subject selection tool and criteria are often based on visual assessment in accordance with the product label [28]. As drug interventions move towards

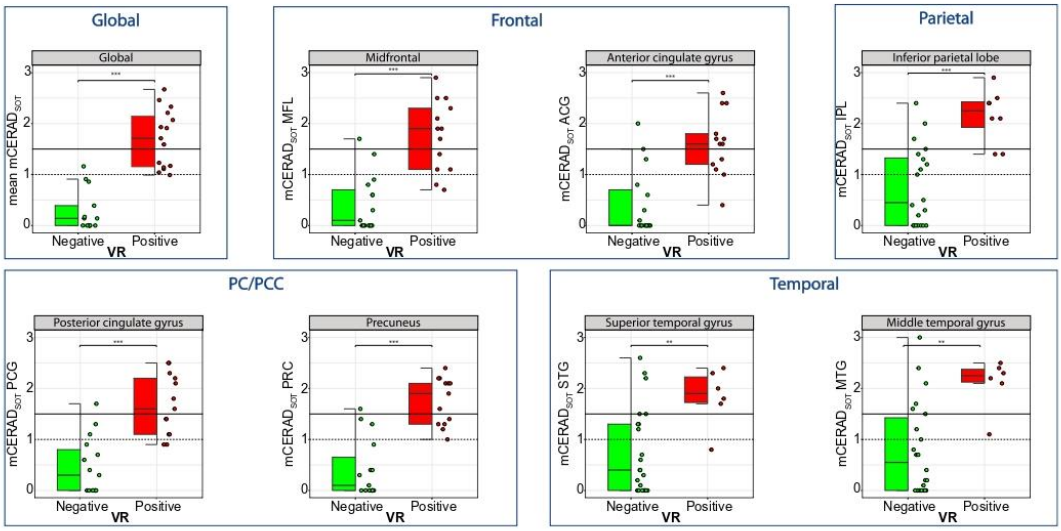

Fig. 6 Visual read against neuropathological burden measured with $mCERAD_{SOT}$. Boxplots represent the regional visual assessment (x-axis) against regional amyloid neuropathological burden (y-axis). Dotted line represents the cut-off for sparse-to-moderate ($mCERAD_{SOT}$ = 1) and the full line the cut-off for moderate-to-frequent neuritic plaques ($mCERAD_{SOT}$ > 1.5). MFL: midfrontal lobe; ACG: anterior cingulate gyrus; PCG: posterior cingulate gyrus; PRC: precuneus; IPC: inferior parietal cortex; STG: superior temporal gyrus; MTG: middle temporal gyrus; $mCERAD_{SOT}$: modfied CERAD standard of truth; VR: visual read

secondary prevention and preclinical populations [17, 29], ensuring the early detection of brain amyloid by means of VR could become crucial. In turn, identification of early pathology might also be of value for clinical use, considering the current interest in preclinical AD pathology in the memory clinic setting [22, 30]. Previous work in the clinical setting using VR as the reference to determine CL cut-offs have reported a broad range of relatively high thresholds (24–42 CL) [7, 8, 10, 11, 31], while a quantitative burden of CL > 21 has already been found to correspond to established pathology [7, 8] based on post-mortem samples. While this contrast may suggest a suboptimal VR sensitivity, the limited number of cases with emerging amyloid pathology in those studies may have limited the assessment of the true sensitivity of VR. In this work, >70% of the clinical dataset were cognitively unimpaired subjects, who are more likely to show subtle amyloid pathology, and indeed 44 subjects showed tracer uptake values within the gray-zone of amyloid burden. Therefore, this study was uniquely enriched with subjects around the expected threshold band, resulting in an observed VR-based CL cut-off of 17, with excellent sensitivity and specificity. Importantly, previous work from Su and colleagues (2018) showed that the CL quantification and consequently cut-offs vary based on local processing pipelines. They demonstrated that for a given criterion (i.e., 95% specificity), the resulting CL cut-offs ranged between 6 and 12, illustrating the value of a confidence interval in cut-off determinations [32]. Therefore, even though the optimal cut-off is calculated to be 17 in the current work, a range between 14 and 20 CL could be expected depending on the particular pipeline implementation. Nonetheless, our ROC analysis showed that this range of CL cut-offs is accompanied by a high Youden's Index (i.e., >0.9) (Sup. Table 1 and Sup. Figure 3), suggesting that such deviations in cut-offs may not significantly affect classification performance.

In addition to enriching the dataset, another unique characteristic of the study is the experience of the readers, who were familiar with research scans showing early amyloid deposition. Therefore, these readers may have been more confident than others when reading a scan with focal deposition as amyloid-positive, also contributing to a lower CL cut-off than previously reported from routine clinical cohorts. Indeed, both the intra- and inter-reader agreement were relatively high compared to previous work in a similar population [13, 33], further illustrating the experience of the readers. The inter-reader agreement analyses also showed that most of the scans with a quantitative burden above 17 CL were assessed as positive by at least 2 out of 3 readers. In addition, all readers consistently assigned visual positivity to scans with a quantitative burden of >20 CL, which is similar to previous work using one experienced reader [8]. Importantly, the regional read agreement was highly similar to the global classification agreement, supporting its utility for routine use.

The most commonly reported visually positive regions in this study, either isolated or in combination with other regions, were the precuneus and the (medial orbito) frontal cortex, including the anterior cingulate. As illustrated in Fig. 4, the sagittal plane seems to be optimal for visually detecting emerging amyloid pathology, as both these regions can be easily assessed using this orientation. While the VR [^{18}F]flutemetamol guidelines for the PC/PCC ROI already state the sagittal plane as the primary orientation for assessment, it is considered as *supportive* for the frontal ROI, where the primary orientation is the axial view. Although the axial view is an appropriate orientation to assess basal frontal uptake (example case Fig. 4 2nd panel), the sagittal view allows for the specific assessment of the medial orbitofrontal cortex (example case Fig. 4 3rd panel). The importance of these two regions is further supported by several articles in the field of amyloid staging, where PET-based regional quantitative burden has been used to identify a general order of regional involvement [16, 34]. Also, a recent review points to the importance of medial cortical regions in optimizing amyloid PET sensitivity [19]. It is important to realize that the sensitivity of medial regions is partly influenced by signal properties of PET imaging: due to their proximity to white matter and the additional gray matter signal spill-in from the contralateral hemisphere, medial regions are more frequently classified as positive in PET imaging compared to lateral counterparts, while levels of pathology are comparable [15]. This could explain why the overall quantitative burden as measured in CL units could already be relatively high, while visually the scan displays only focal deposition (example case Fig. 4, 4th panel). Therefore, this isolated or early amyloid deposition which is most often visually observed in medial cortical regions could already reflect more extensive but undetected pathological burden throughout the brain. Indeed, our post-mortem results seem to support this hypothesis, as while VR positivity in, e.g., the PC/PCC ROI corresponds to neuropathological scores indicative of sparse-to-moderate neuritic plaques, VR positivity in the lateral regions is associated with higher pathological burden. Considering that readers are now confronted with research scans more often, this knowledge can be useful to guide their assessment of early accumulation.

Beyond traditional dichotomized classification of amyloid negative/positive, reporting the number of VR+ regions to stage the severity of amyloid burden could be of value. We showed that the extent of amyloid burden in terms of number of visually positive regions and the derived VR stages related in a proportional manner to increasing CL values. More specifically, while 1 or 2 (VR+ Stages 1 and 2) visually positive regions are in line with previously proposed CL threshold of either emerging (~12 CL) or more established (~30 CL) amyloid pathology [7–9], 3 or more visually positive regions (VR+ Stage 3) are in line with CL values suggested to reflect clinical meaningful amyloid pathology (Table 2). For example, in addition to a cut-off of 26 CL for predicting clinical progression, Hanseeuw and colleagues [12] showed that in

non-demented memory clinic patients, a cut-off of 42 CL was optimal in predicting progression to dementia over a period of 6 years. This last cut-off corresponds well to the observed CL burden associated with 3 visually positive regions in this work. In addition, Amadoru and colleagues [8] concluded that a CL burden of >50 best confirmed a clinicopathological diagnosis of AD and the mean quantitative burden of patients with AD dementia can vary from 84 CL [35] to 100 CL [6]. These values are in agreement with what we observed in scans with 4 or 5 visually positive regions. Together, these correspondences indicate the extent of amyloid burden can be visually assessed and future work should determine whether it conveys prognostic information. Longitudinal data collection is necessary to determine whether regional VR has similar prognostic value as compared to quantification. Currently, the 4-year follow-up including both amyloid PET acquisition and cognitive measures of the ALFA+ cohort is being collected in collaboration with the AMYPAD Consortium [17], which will enable analyses to assess the value of regional VR in a longitudinal setting.

This work shows that VR is both sensitive enough to capture early pathology for clinical trials aimed at secondary prevention, and useful for staging a subject according to their regional amyloid burden. However, several aspects are important in order to perform the regional visual assessment in an accurate manner. The following observations can be considered when performing visual assessment of [^{18}F]flutemetamol PET images:

1. Especially in the research context, readers could benefit from focusing on the medial regions, using the sagittal view as the primary orientation for visual assessment of early amyloid pathology. Of note, a proper alignment of the images is key to ensure accurate assessment of the gray rather than the white matter signal. A suitable pivot point for all rotations is the inferior tip of the posterior corpus callosum at the junction of the hemispheres.
2. In future clinical routine, documenting the *extent* of amyloid burden could be a valuable asset in addition to the final read classification of amyloid negative/positive.

Of note, the generalizability of these results remains to be investigated in light of differences between tracers with respect to reading "signs," use of different color scales [36], and possibly distinct influence of WM uptake in the distortion of the PET signal in medial regions [15].

Some limitations of this work should be considered. First, the mean age of our clinical cohort (ADC) is relatively low. This is due to the fact that the Alzheimer Center Amsterdam is a specialized tertiary referral center, which assesses a more atypical and generally younger patients [22]. Second, it should be noted that the clinical diagnosis in this cohort was made pre-PET disclosure; thus, any discrepancies between diagnosis and the presence of amyloid pahtology could also reflect misdiagnosis. Also, the extent of amyloid burden should be considered in combination with clinical disease severity, as the presence of early amyloid pathology in patients with dementia might reflect co-pathology rather than dementia due to AD. This will be investigated within in AMYPAD consortium, where regional VR is captured for all patients participating in the Diagnostic and Patient Management Study (DPMS) [30]. Third, T1 sequences for this cohort originate from multiple scanners as part of the clinical routine, which could have introduced noise to the quantitation. However, recent work has shown that the amount of variance introduced by this methodological aspect is within the physiological scan-rescan range and lower than the within-ROI variability, suggesting a minor impact on amyloid PET studies [37]. Fourth, the majority of visual assessments in the clinical cohort was performed by one reader, while a majority visual read was available for those cases displaying emerging or focal amyloid deposition. Nonetheless, since scans with a single read represented more the extremes of the quantitative spectrum, it is likely that these cases were mostly clearly negative or positive and therefore we could assume that an additional read would not have significantly affected the results. Finally, the post-mortem data-set used in this work was only a subset of the previously reported [^{18}F]flutemetamol Phase III trial. However, by prioritizing the inclusion of cases with non-extreme CERAD neuritic plaque scores, we believe to have demonstrated with sufficient information the validity of a regional visual read and its ability to capture early pathology.

Conclusion

Visual assessment of amyloid PET scan is capable of detecting early amyloid pathology and regional visual positivity captures its extent. More specifically, we have shown that the threshold for visual read is 17 CL, with a sensitivity and specificity of ~98% and corresponds to neuropathological scores indicative of sparse-to-moderate neuritic plaques in specific brain regions. These two aspects could be highly valuable in both a research/clinical trial and future clinical routine setting. Further work should investigate the prognostic value of regional VR compared to quantitation and the comparability between amyloid radiotracers.

Supplementary Information The online version contains supplementary material available at https://doi.org/10.1007/s00259-020-05174-2.

Funding This project has received funding from the Innovative Medicines Initiative 2 Joint Undertaking under grant agreement No 115952. This Joint Undertaking receives support from the European Union's Horizon 2020 research and innovation programme and EFPIA. The ALFA Study is funded by "la Caixa" Foundation (LCF/PR/GN17/10300004) and the Alzheimer's Association and an international

anonymous charity foundation through the the TriBEKa Imaging Platform project (TriBEKa-17-519007). Additional funding has been obtained by Project RTI2018-102261-B-I00, funded by European Regional Development Fund (EDRF) / Ministry of Science and Innovation - State Research Agency (Spain).

This work also received in kind sponsoring of the PET-tracer from GE Healthcare.

FB is supported by the NIHR UCLH biomedical research centre. FB and AMW are supported by the European Union's Horizon 2020 research and innovation programme under grant agreement No. 666992.

Research of the Alzheimer Center Amsterdam is part of the neurodegeneration research program of Amsterdam Neuroscience. The clinical database structure was developed with funding from Stichting Dioraphte. Alzheimer Center Amsterdam is supported by Alzheimer Nederland and Stichting VUmc fonds.

This work also received in kind sponsoring of the PET-tracer from GE Healthcare.

Compliance with ethical standards

Conflict of interest Lyduine E. Collij; Gemma Salvadó; Mahnaz Shekari; Isadora Lopes Alves; Juhan Reimand; Alle Meije Wink; Marissa Zwan; Aida Niñerola-Baizán & Andrés Perissinotti all report no existing potential conflicts of interest relevant to this article.

Prof. Philip Scheltens received grants from GE Healthcare, Piramal, and Merck, paid to his institution; he has received speaker's fees paid to the institution Alzheimer Center, VU University Medical Center, Lilly, GE Healthcare, and Roche.

Prof. Frederik Barkhof received payment and honoraria from Bayer-Schering Pharma, Sanofi-Aventis, Genzyme, Biogen-Idec, TEVA, Merck-Serono, Novartis, Roche, Jansen Research, IXICO Ltd., GeNeuro, and Apitope Ltd. for consulting; payment from the Serono Symposia Foundation, IXICOLtd, and MedScape for educational presentations; research support via grants from EU/EFPIA Innovative Medicines Initiative Joint Undertaking (AMYPAD consortium), EuroPOND (H2020), UK MS Society, Dutch MS Society, PICTURE (IMDI-NWO), NIHR UCLH Biomedical Research Centre (BRC), ECTRIMS-MAGNIMS.

Prof. J. L. Molinuevo is currently a full-time employee of Lundbeck and priory has served as a consultant or at advisory boards for the following for-profit companies, or has given lectures in symposia sponsored by the following for-profit companies: Roche Diagnostics, Genentech, Novartis, Lundbeck, Oryzon, Biogen, Lilly, Janssen, Green Valley, MSD, Eisai, Alector, BioCross, GE Healthcare, ProMIS Neurosciences. He also received research support from the EU/EFPIA Innovative Medicines Initiative Joint Undertaking AMYPAD grant agreement n° 115952; the EU/EFPIA Innovative Medicines Initiative Joint Undertaking EPAD grant agreement n° 115736; the EU/EFPIA Innovative Medicines Initiative Joint Undertaking AETIONOMY grant n° 115568; and 'la Caixa' Foundation.

Dr. J.D. Gispert has received speaker's fees from Biogen and Philips. In addition he holds a 'Ramón y Cajal' fellowship (RYC-2013-13054) from the Spanish Ministry of Economy and Competitiveness, has received research support from the EU/EFPIA Innovative Medicines Initiative Joint Undertaking AMYPAD grant agreement n° 115952, and from Ministerio de Ciencia y Universidades (grant agreement RTI2018-102261).

Prof. BN.M. van Berckel received research support from ZON-MW, AVID radiopharmaceuticals, CTMM and Janssen Pharmaceuticals. BvB is a trainer for Piramal and GE; he receives no personal honoraria.

G Farrar, C Buckley and APL Smith are full-time employees of GE Healthcare.

MD Ikonomovic has received research funding from GE Healthcare.

No other potential conflicts of interest relevant to this article exist.

Ethical approval The ALFA study and the PET sub-study protocols and informed consent forms have been approved by the independent Ethics Committee Parc de Salut Mar Barcelona and registered at Clinicaltrials.gov (ALFA Identifier: NCT02485730; PET sub-study Identifier: NCT02685969). Both studies have been conducted in accordance with the directives of the Spanish Law 14/ 2007, of 3rd of July, on Biomedical Research (Ley 14/ 2007 de Investigación Biomédica). The medical ethics review committee of the VU University Medical Center approved the Dutch Flutemetamol study (reference number: 2012/302).

Informed consent Informed consent was obtained from all individual participants included in the study.

References

1. Salloway S, Gamez JE, Singh U, Sadowsky CH, Villena T, Sabbagh MN, et al. Performance of [(18)F]flutemetamol amyloid imaging against the neuritic plaque component of CERAD and the current (2012) NIA-AA recommendations for the neuropathologic diagnosis of Alzheimer's disease. Alzheimers Dement (Amst). 2017;9:25–34. https://doi.org/10.1016/j.dadm.2017.06.001.
2. Sabri O, Sabbagh MN, Seibyl J, Barthel H, Akatsu H, Ouchi Y, et al. Florbetaben PET imaging to detect amyloid beta plaques in Alzheimer's disease: phase 3 study. Alzheimers Dement. 2015;11: 964–74. https://doi.org/10.1016/j.jalz.2015.02.004.
3. Clark CM, Schneider JA, Bedell BJ, Beach TG, Bilker WB, Mintun MA, et al. Use of florbetapir-PET for imaging β-amyloid pathology. Jama. 2011;305:275–83.
4. Mirra SS, Heyman A, McKeel D, Sumi SM, Crain BJ, Brownlee LM, et al. The consortium to establish a registry for Alzheimer's disease (CERAD). Part II. Standardization of the neuropathologic assessment of Alzheimer's disease. Neurology. 1991;41:479–86. https://doi.org/10.1212/wnl.41.4.479.
5. Thal DR, Beach TG, Zanette M, Heurling K, Chakrabarty A, Ismail A, et al. [(18)F]flutemetamol amyloid positron emission tomography in preclinical and symptomatic Alzheimer's disease: specific detection of advanced phases of amyloid-beta pathology. Alzheimers Dement. 2015;11:975–85. https://doi.org/10.1016/j.jalz.2015.05.018.
6. Klunk WE, Koeppe RA, Price JC, Benzinger TL, Devous MD Sr, Jagust WJ, et al. The Centiloid Project: standardizing quantitative amyloid plaque estimation by PET. Alzheimers Dement. 2015;11: 1–15 e1–4. https://doi.org/10.1016/j.jalz.2014.07.003.
7. Joie R, Ayakta N, Seeley WW, Borys E, Boxer AL, DeCarli C, et al. Multisite study of the relationships between antemortem [(11)C]PIB-PET Centiloid values and postmortem measures of Alzheimer's disease neuropathology. Alzheimers Dement. 2018. https://doi.org/10.1016/j.jalz.2018.09.001.

8. Amadoru S, Dore V, McLean CA, Hinton F, Shepherd CE, Halliday GM, et al. Comparison of amyloid PET measured in Centiloid units with neuropathological findings in Alzheimer's disease. Alzheimers Res Ther. 2020;12:22. https://doi.org/10.1186/s13195-020-00587-5.
9. Salvado G, Molinuevo JL, Brugulat-Serrat A, Falcon C, Grau-Rivera O, Suarez-Calvet M, et al. Centiloid cut-off values for optimal agreement between PET and CSF core AD biomarkers. Alzheimers Res Ther. 2019;11:27. https://doi.org/10.1186/s13195-019-0478-z.
10. Battle M, Buckley C, Smith A, Farrar G, Thal D, Molineuvo JL, et al. Comparison of Centiloid scaling values with visual read assessment in a pathology verified autopsy cohort. 2019.
11. Susan Landau DK, Bullich S, De Santi S, Stephens A, Koeppe R. William Jagust. P24: Validation of highly sensitive and specific florbetaben positivity thresholds using ADNI participants and young controls. Human Amyloid Imaging Conference. 2020:94–5.
12. Hanseeuw BJ, Malotaux V, Dricot L, Quenon L, Sznajer Y, Cerman J, et al. Defining a Centiloid scale threshold predicting long-term progression to dementia in patients attending the memory clinic: an [(18)F] flutemetamol amyloid PET study. Eur J Nucl Med Mol Imaging. 2020. https://doi.org/10.1007/s00259-020-04942-4.
13. Collij L, Konijnenberg E, Reimand J, Ten Kate M, Den Braber A, Lopes Alves I, et al. Assessing amyloid pathology in cognitively normal subjects using [(18)F]Flutemetamol PET: comparing visual reads and quantitative methods. J Nucl Med. 2018. https://doi.org/10.2967/jnumed.118.211532.
14. Farrar G, Molinuevo JL, Zanette M. Is there a difference in regional read [18 F] flutemetamol amyloid patterns between end-of-life subjects and those with amnestic mild cognitive impairment? Eur J Nucl Med Mol Imaging. 2019;46:1299–308.
15. Smith A, Buckley C. [18F]flutemetamol PET image representation of Ab pathology; differences between lateral and medial image intensity for equivalent levels of pathology. 10th Human Amyloid Imaging. Miami, FL, USA. 2016.
16. Mattsson N, Palmqvist S, Stomrud E, Vogel J, Hansson O. Staging beta-amyloid pathology with amyloid positron emission tomography. JAMA Neurol. 2019. https://doi.org/10.1001/jamaneurol.2019.2214.
17. Lopes Alves I, Collij LE, Altomare D, Frisoni GB, Saint-Aubert L, Payoux P, et al. Quantitative amyloid PET in Alzheimer's disease: the AMYPAD prognostic and natural history study. Alzheimers Dement. 2020. https://doi.org/10.1002/alz.12069.
18. Collij LE, Heeman F, Salvado G, Ingala S, Altomare D, Wilde AD, et al. Multi-tracer model for staging cortical amyloid deposition using PET imaging. Neurology. 2020. https://doi.org/10.1212/WNL.0000000000010256.
19. Fantoni E, Collij L, Alves IL, Buckley C, Farrar G. The spatial-temporal ordering of amyloid pathology and opportunities for PET imaging. J Nucl Med. 2019. https://doi.org/10.2967/jnumed.119.235879.
20. Frisoni GB, Boccardi M, Barkhof F, Blennow K, Cappa S, Chiotis K, et al. Strategic roadmap for an early diagnosis of Alzheimer's disease based on biomarkers. Lancet Neurol. 2017;16:661–76. https://doi.org/10.1016/S1474-4422(17)30159-X.
21. Molinuevo JL, Gramunt N, Gispert JD, Fauria K, Esteller M, Minguillon C, et al. The ALFA project: a research platform to identify early pathophysiological features of Alzheimer's disease. Alzheimers Dement (N Y). 2016;2:82–92. https://doi.org/10.1016/j.trci.2016.02.003.
22. van der Flier WM, Scheltens P. Amsterdam dementia cohort: performing research to optimize care. J Alzheimers Dis. 2018;62:1091–111. https://doi.org/10.3233/JAD-170850.
23. Zwan MD, Bouwman FH, Konijnenberg E, van der Flier WM, Lammertsma AA, Verhey FR, et al. Diagnostic impact of [18F]flutemetamol PET in early-onset dementia. Alzheimers Res Ther. 2017;9:2. https://doi.org/10.1186/s13195-016-0228-4.
24. Desikan RS, Segonne F, Fischl B, Quinn BT, Dickerson BC, Blacker D, et al. An automated labeling system for subdividing the human cerebral cortex on MRI scans into gyral based regions of interest. Neuroimage. 2006;31:968–80. https://doi.org/10.1016/j.neuroimage.2006.01.021.
25. Buckley CJ, Sherwin PF, Smith AP, Wolber J, Weick SM, Brooks DJ. Validation of an electronic image reader training programme for interpretation of [18F]flutemetamol beta-amyloid PET brain images. Nucl Med Commun. 2017;38:234–41. https://doi.org/10.1097/MNM.0000000000000633.
26. Curtis C, Gamez JE, Singh U, Sadowsky CH, Villena T, Sabbagh MN, et al. Phase 3 trial of flutemetamol labeled with radioactive fluorine 18 imaging and neuritic plaque density. JAMA Neurol. 2015;72:287–94. https://doi.org/10.1001/jamaneurol.2014.4144.
27. Ikonomovic MD, Buckley CJ, Heurling K, Sherwin P, Jones PA, Zanette M, et al. Post-mortem histopathology underlying beta-amyloid PET imaging following flutemetamol F 18 injection. Acta Neuropathol Commun. 2016;4:130. https://doi.org/10.1186/s40478-016-0399-z.
28. Cummings J, Ritter A, Zhong K. Clinical trials for disease-modifying therapies in Alzheimer's disease: a primer, lessons learned, and a blueprint for the future. J Alzheimers Dis. 2018. https://doi.org/10.3233/JAD-179901.
29. Insel PS, Donohue MC, Sperling R, Hansson O, Mattsson-Carlgren N. The A4 study: beta-amyloid and cognition in 4432 cognitively unimpaired adults. Ann Clin Transl Neurol. 2020. https://doi.org/10.1002/acn3.51048.
30. Frisoni GB, Barkhof F, Altomare D, Berkhof J, Boccardi M, Canzoneri E, et al. AMYPAD diagnostic and patient management study: rationale and design. Alzheimers Dement. 2018. https://doi.org/10.1016/j.jalz.2018.09.003.
31. Bernard Hanseeuw VM, Dricot L, Quenon L, Cerman J, Buckley C, Farrar G, et al. P61: Defining a Centiloid scale threshold predicting long-term progression to dementia in patients attending the memory clinic: An F18-Flutemetamol amyloid-PET study. Human Amyloid Imaging Conference. 2020:211–2.
32. Su Y, Flores S, Hornbeck RC, Speidel B, Vlassenko AG, Gordon BA, et al. Utilizing the Centiloid scale in cross-sectional and longitudinal PiB PET studies. Neuroimage Clin. 2018;19:406–16. https://doi.org/10.1016/j.nicl.2018.04.022.
33. Zwan MD, Ossenkoppele R, Tolboom N, Beunders AJ, Kloet RW, Adriaanse SM, et al. Comparison of simplified parametric methods for visual interpretation of 11C-Pittsburgh compound-B PET images. J Nucl Med. 2014;55:1305–7. https://doi.org/10.2967/jnumed.114.139121.
34. Grothe MJ, Barthel H, Sepulcre J, Dyrba M, Sabri O, Teipel SJ, et al. In vivo staging of regional amyloid deposition. Neurology. 2017;89:2031–8. https://doi.org/10.1212/WNL.0000000000004643.

35. Leuzy A, Chiotis K, Hasselbalch SG, Rinne JO, de Mendonca A, Otto M, et al. Pittsburgh compound B imaging and cerebrospinal fluid amyloid-beta in a multicentre European memory clinic study. Brain. 2016;139:2540–53. https://doi.org/10.1093/brain/aww160.
36. Lundeen TF, Seibyl JP, Covington MF, Eshghi N, Kuo PH. Signs and artifacts in amyloid PET. Radiographics. 2018;38:2123–33. https://doi.org/10.1148/rg.2018180160.
37. Alessandro Palombit RM, Joules R, Wolz R. P38: Amyloid PET variability due to variation in MRI protocol and anatomical segmentation. Human Amyloid Imaging Conference. 2020;124.

Affiliations

Lyduine E. Collij[1] · Gemma Salvadó[2,3] · Mahnaz Shekari[2] · Isadora Lopes Alves[1] · Juhan Reimand[4,5,6] · Alle Meije Wink[1] · Marissa Zwan[4] · Aida Niñerola-Baizán[7] · Andrés Perissinotti[7] · Philip Scheltens[4] · Milos D. Ikonomovic[8,9,10] · Adrian P. L. Smith[11] · Gill Farrar[11] · José Luis Molinuevo[2,3,9,12,13] · Frederik Barkhof[1,14] · Christopher J. Buckley[11] · Bart N. M. van Berckel[1,15] · Juan Domingo Gispert[2,3,9,16,17] · For the ALFA study · On behalf of the AMYPAD consortium

1 Department of Radiology and Nuclear Medicine, Amsterdam UMC, Vrije Universiteit Amsterdam, De Boelelaan, 1117 Amsterdam, Netherlands

2 Barcelonaβeta Brain Research Center (BBRC), Pasqual Maragall Foundation, Barcelona, Spain

3 IMIM (Hospital del Mar Medical Research Institute), Barcelona, Spain

4 Alzheimer Center and department of Neurology, Amsterdam UMC, Vrije Universiteit Amsterdam, De Boelelaan, 1117 Amsterdam, Netherlands

5 Department of Health Technologies, Tallinn University of Technology, Tallinn, Estonia

6 Radiology Centre, North Estonia Medical Centre, Tallinn, Estonia

7 Nuclear Medicine Department, Hospital Clínic Barcelona & Biomedical Research Networking Center of Bioengineering, Biomaterials and Nanomedicine (CIBER-BBN), Barcelona, Spain

8 Department of Neurology, University of Pittsburgh, Pittsburgh, PA, USA

9 Department of Psychiatry, University of Pittsburgh, Pittsburgh, PA, USA

10 Department of Geriatric Research Education and Clinical Center, VA Pittsburgh HS, Pittsburgh, PA, USA

11 GE Healthcare, Life Sciences, Amersham, UK

12 Universitat Pompeu Fabra, Barcelona, Spain

13 CIBER Fragilidad y Envejecimiento Saludable (CIBERFES), Madrid, Spain

14 Centre for Medical Image Computing, and Queen Square Institute of Neurology, UCL, London, UK

15 Department of Radiology and Nuclear Medicine, VU University Medical Center, De Boelelaan 1117, 1108 HV Amsterdam, The Netherlands

16 Centro de Investigación Biomédica en Red de Bioingeniería, Biomateriales y Nanomedicina (CIBER-BBN), Madrid, Spain

17 Alzheimer Prevention Program, BarcelonaBeta Brain Research Center (BBRC), C/ Wellington, 30, 08005 Barcelona, Spain

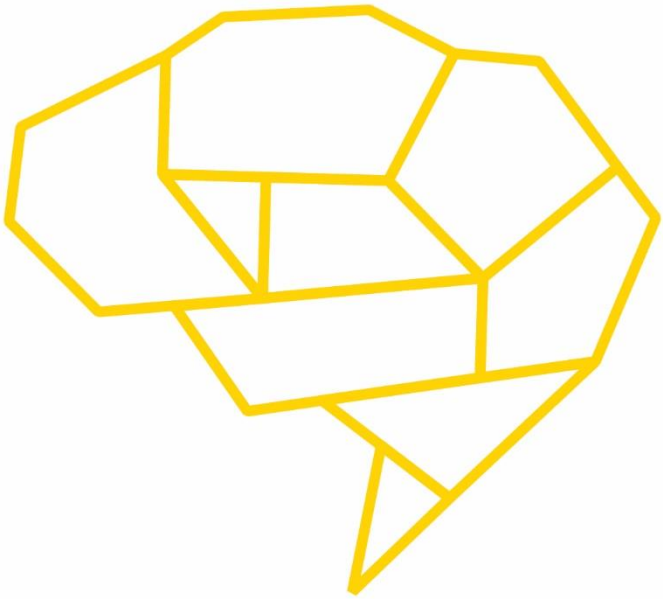

THIRD STUDY:

Age, sex and APOE-ε4 modify the balance between soluble and deposited β-amyloid in cognitively intact individuals: topographical patterns and replication across two independent cohorts

Age, sex and *APOE-ε4* modify the balance between soluble and fibrillar β-amyloid in cognitively intact individuals: topographical patterns and replication across two independent cohorts

Authors:

Raffaele Cacciaglia[1,2,3,*], Gemma Salvadó[1,2,*], José Luis Molinuevo[1,2,3,4], Mahnaz Shekari[1,2,3], Carles Falcon[1,2,5], Gregory Operto[1,2,3], Marc Suárez-Calvet[1,2,3,6], Marta Milà-Alomà[1,2,3], Arianna Sala[7], Elena Rodriguez-Vieitez[7], Gwendlyn Kollmorgen[8], Ivonne Suridjan[9], Kaj Blennow[10,11], Henrik Zetterberg[10-13], and Juan Domingo Gispert[1,2,4,5], for the Alzheimer's Disease Neuroimaging Initiative°, for the ALFA study

*These two authors contributed equally.

Authors' affiliations:

[1]Barcelonaβeta Brain Research Center (BBRC), Pasqual Maragall Foundation, 08005 Barcelona, Spain

[2]Hospital del Mar Medical Research Institute (IMIM), 08005 Barcelona, Spain

[3]Centro de Investigación Biomédica en Red de Fragilidad y Envejecimiento Saludable (CIBERFES), 28089 Madrid, Spain

[4]Universitat Pompeu Fabra, 08002 Barcelona, Spain

[5]Centro de Investigación Biomédica en Red de Bioingeniería, Biomateriales y Nanomedicina (CIBERBBN), 28089 Madrid, Spain

[6]Servei de Neurologia, Hospital del Mar, Barcelona, Spain.

[7]Department of Neurobiology, Care Sciences and Society, Division of Clinical Geriatrics, Center for Alzheimer Research, Karolinska Institutet, 141 52 Stockholm, Sweden

[8]Roche Diagnostics GmbH, Penzberg, Germany

[9]Roche Diagnostics International Lda, Rotkreuz, Switzerland

[10]Department of Psychiatry and Neurochemistry, Institute of Neuroscience and Physiology, The Sahlgrenska Academy at the University of Gothenburg, 41390 Mölndal, Sweden

[11]Clinical Neurochemistry Laboratory, Sahlgrenska University Hospital, 41390 Mölndal, Sweden

[12]UK Dementia Research Institute at UCL, WC1E 6BT London, UK

[13]Department of Neurodegenerative Disease, UCL Institute of Neurology, WC1N 3BG London, UK

°Data used in preparation of this article were obtained from the Alzheimer's Disease Neuroimaging Initiative (ADNI) database (adni.loni.usc.edu). As such, the investigators within the ADNI contributed to the design and implementation of ADNI and/or provided data but did not participate in analysis or writing of this report. A complete listing of ADNI investigators can be found at: http://adni.loni.usc.edu/wp-content/uploads/how_to_apply/ADNI_Acknowledgement_List.pdf

Number of words: 4,478

Number of tables: 2

Number of figures: 6

Number of Supplementary Data files: 1

Corresponding authors:

Juan Domingo Gispert López, Barcelonaβeta Brain Research Center, Pasqual Maragall Foundation, Wellington 30, 08005 Barcelona, Spain. Tel.: +34 933160990;

Fax: +34 932275783. E-mail: jdgispert@barcelonaneta.org

Raffaele Cacciaglia, Barcelonaβeta Brain Research Center, Pasqual Maragall Foundation, Wellington 30, 08005 Barcelona, Spain. Tel.: +34 933263188;

Fax: +34 932275783. E-mail: rcacciaglia@barcelonabeta.org

ABSTRACT

Cerebral beta-amyloid (Aβ) accumulation is the earliest detectable pathophysiological event along the Alzheimer's disease (AD) *continuum*, therefore an accurate quantification of incipient Aβ abnormality is of great importance to identify preclinical AD. Both cerebrospinal fluid (CSF) Aβ concentrations and Position Emission Tomography (PET) with specific tracers provide established biomarkers of Aβ pathology. Yet, they identify two different biological processes reflecting the clearance rate of soluble Aβ as opposed to the cerebral aggregation of insoluble Aβ fibrils. Studies have demonstrated high agreement between CSF and PET-based Aβ measurements on diagnostic and prognostic levels. However, an open question is whether risk factors known to increase AD prevalence may promote an imbalance between these biomarkers, leading to a higher cumulative Aβ cerebral aggregation for a given level of cleared Aβ in the CSF. Unveiling such interactions in cognitively unimpaired (CU) individuals shall provide novel insights into the biological pathways underlying Aβ aggregation in the brain and ultimately improve our knowledge on disease modelling. With this in mind, we assessed the impact of three major unmodifiable AD risk factors (age, *APOE-ε4* and sex) on the association between soluble and deposited Aβ in a sample of 293 middle-aged CU individuals who underwent both lumbar puncture and PET imaging using the [^{18}F]flutemetamol tracer. We looked for interactions between CSF Aβ42/40 concentrations and each of the assessed risk factors, in promoting Aβ PET uptake both in candidate regions of interest and in the whole brain. We found that, for any given level of CSF Aβ42/40, older age and female sex induced higher fibrillary plaque deposition in neocortical areas including the anterior, middle and posterior cingulate cortex. By contrast, the modulatory role of *APOE-ε4* was uniquely prominent in areas known for being vulnerable to early tau deposition, such as the entorhinal cortex and the hippocampus bilaterally. *Post hoc* three-way interactions additionally proved evidence for a synergistic effect among the risk factors on the spatial topology of Aβ deposition as a function of CSF Aβ42/40 levels. Importantly, findings were replicated in an independent sample of CU individuals derived from the ADNI cohort. Our data clarify the mechanisms underlying the higher AD prevalence associated to those risk factors and suggest that *APOE-ε4* in particular paves the way for subsequent tau spreading in the medial temporal lobe, thus favouring a spatial co-localization between Aβ and tau and increasing their synergistic interaction along the disease *continuum*.

INTRODUCTION

Alzheimer's disease (AD) is characterized by cerebral accumulation of misfolded amyloid-β (Aβ) and tau proteins along with progressive neuronal degeneration. AD has an insidious onset, with a protracted asymptomatic phase lasting about two decades prior to clinical manifestations (Sperling et al., 2011). According to recent pathophysiological models, Aβ pathology is the earliest event occurring along the Alzheimer's *continuum*, which is later followed by tau aggregation and cerebral atrophy (Jack et al., 2016). Both cerebrospinal fluid (CSF) Aβ concentrations and Position Emission Tomography (PET) with specific tracers provide established biomarkers of Aβ pathology. Several previous studies have shown good concordance between these two surrogate markers of Aβ in their diagnostic and prognostic accuracy (Fagan et al., 2006; Landau et al., 2013; Grimmer et al., 2009; Mattsson et al., 2014; Palmqvist et al., 2015). More specifically, a negative relationship between CSF Aβ and Aβ PET has been reported both *post-mortem* (Strozyk et al., 2003; Tapiola et al., 2009; La Joie et al., 2019) and *in-vivo* (Toledo et al., 2015; Schindler et al., 2018; Mattsson et al., 2015). They, however, measure two very different pools of Aβ, with CSF Aβ concentrations reflecting the production and clearance rates of soluble Aβ species from the brain, and PET detecting the cumulative load of deposited fibrillary plaques (Roberts et al., 2017; Cohen et al., 2019). It has been suggested that cumulative cerebral Aβ deposition observed in AD might stem from a dysregulation between the production and clearance of Aβ species, and that Aβ plaques may act as a "sink", hindering the transport of soluble Aβ fragments from the brain to the CSF (Mawuenyega et al., 2010; Blennow et al., 2012). In this respect, the study of factors affecting the balance between soluble and deposited Aβ may help identifying the underlying mechanisms promoting cerebral Aβ aggregation for a given level of CSF Aβ dysmetabolism. With this in mind, we investigated the impact of unmodifiable risk factors known to increase Alzheimer's dementia prevalence, such as *APOE-ε4* genotype (Liu et al., 2013), older age (Launer, 2005) and female sex (Ferretti et al., 2018) on the relationship between CSF and Aβ PET markers. We hypothesized that distinct risk factors may exacerbate cerebral Aβ accumulation (assessed by Aβ PET) as a function of incipient Aβ dysmetabolism (assessed by CSF Aβ42/40

concentrations), promoting the formation of fibrillary plaques into specific topological patterns. We tested our hypotheses in regions of vulnerability to AD proteinopathy and further examined the whole-brain using a spatially unbiased voxel-wise approach on a monocentric cohort of middle-aged cognitively unimpaired (CU) participants (ALFA sample). Furthermore, we replicated all analyses in an independent sample of CU participants derived from the Alzheimer's Disease Neuroimaging Initiative (ADNI).

METHODS

Study participants

All participants in the discovery sample were volunteers of the ALFA (ALzheimer and FAmilies) study (Clinicaltrials.gov Identifier: NCT01835717), a longitudinal monocentric research platform aiming at the identification of pathophysiological alterations in preclinical AD. The ALFA cohort entangles 2,743 CU individuals, with a Clinical Dementia Rate score of 0, most of them being first-order descendants of AD patients (Molinuevo et al., 2016). None of the subjects had a neurologic or a psychiatric diagnosis. Within this research framework, the ALFA+ is a nested study that includes advanced imaging protocols, including magnetic resonance imaging (MRI) and PET acquisitions, along with cognitive, lifestyle factors as well as fluid biomarkers. The first 293 consecutive participants of the ALFA+ study with available CSF, Aβ PET, MRI and cognitive data were included in the present work. All the tests and image acquisitions were measured within less than a year time-difference.

The replication sample included all CU ADNI participants (http://adni.loni.usc.edu/), with available Aβ CSF, [^{18}F]florbetapir Aβ PET and MRI data acquired within less than one year, resulting in a sample of 259 individuals.

ADNI is a multi-site open access dataset designed to accelerate the discovery of biomarkers to identify and track AD pathology

(adni.loni.usc.edu). The ADNI was launched in 2003 as a public-private partnership, led by Principal Investigator Michael W. Weiner, MD. The primary goal of ADNI has been to test whether serial magnetic resonance imaging (MRI), PET, other biological markers, and clinical and neuropsychological assessment can be combined to measure the progression of mild cognitive impairment (MCI) and early AD. For up-to-date information, see www.adni-info.org. All ALFA participants provided written informed consent and the study was approved by the local ethics committee and conducted according to the principles expressed in the Declaration of Helsinki. Data collection and sharing in ADNI were approved by the Institutional Review Board of each participating institution, and written informed consent was obtained from all participants.

APOE genotype

For ALFA participants, total DNA was obtained from blood cellular fraction by proteinase K digestion followed by alcohol precipitation. For ADNI, DNA was extracted by Cogenics from a 3-mL aliquot of EDTA blood (adni.loni.usc.edu/data-samples/genetic-data). Both samples were genotyped for two single nucleotide polymorphisms (SNPs), rs429358 and rs7412, to define the *APOE-ε2*, *ε3* and *ε4* alleles. For both cohorts, subjects were classified as *ε4* carriers (one or two alleles) or non-carriers. Twenty-seven participants in the ALFA cohort being homozygotes for the *ε4* allele were excluded from the present study as they were significantly younger than both non-carriers ($p<0.001$) and *APOE-ε4* heterozygotes ($p<0.001$), leading to potential inhomogeneity in the association between CSF and Aβ PET measurements (Rodrigue et al., 2012).

CSF sampling and analysis

For ALFA participants, CSF samples were obtained by lumbar puncture following standard procedures (Teunissen et al, 2014). CSF was collected into a 15mL sterile polypropylene sterile tube (Sarstedt, Nümbrecht, Germany; cat. no. 62.554.502). CSF was aliquoted in volumes of 0.5mL into sterile polypropylene tubes (0.5mL Screw Cap Micro Tube Conical Bottom; Sarstedt, Nümbrecht, Germany; cat. no. 72.730.005), and immediately frozen at −80°C. Overall, the time between collection and freezing was less than 30 minutes. All the determinations were done in aliquots that had never been previously thawed. Aβ40 as well as Aβ42 concentrations were determined with the NeuroToolKit (Roche Diagnostics International Ltd.) on cobas Elecsys e601 (Aβ42) and e411 (Aβ40) instruments at the Clinical Neurochemistry Laboratory, University of Gothenburg, Sweden. CSF collection and analyses for ADNI participants are described in the ADNI procedure manual (http://adni.loni.usc.edu/methods). Aβ40 and Aβ42 concentrations in ADNI were measured with 2D-UPLC-tandem mass-spectrometry at the University of Pennsylvania.To increase sensitivity, both in ALFA and ADNI the ratio between Aβ42 and Aβ40 was finally calculated (Lewczuk et al., 2017).

PET imaging acquisition procedures

Imaging procedures from ALFA have been described previously (Salvadó et al., 2019). In brief, Aβ PET images were acquired 90 min post-injection using [^{18}F]flutemetamol with 4 frames of 5 min each. A T1-weighted 3D-TFE sequence was acquired with a 3T Philips Ingenia CX scanner with the following sequence parameters: voxel size = 0.75 mm isotropic, field of view (FOV) = 240 x 240 x 180 mm^3, flip angle = 8º, repetition time = 9.9 ms, echo time = 4.6 ms, TI = 900 ms.

Details of ADNI imaging procedures can also been found in the website (http://adni.loni.usc.edu/methods/documents). In brief, [^{18}F]florbetapir Aβ PET images were acquired in four frames of five minutes each, 50-70 minutes post-injection. Finally, structural MRI data were acquired on 3T

scanning platforms using T1-weighted sagittal 3-dimensional magnetization-prepared rapid-acquisition gradient echo sequences (MP-RAGE).

Image preprocessing

For both cohorts, individual PET frames were co-registered to produce a mean image, which was subsequently spatially registered onto the respective structural MRI scan. Afterwards, the new segment function in SPM was employed to segment gray matter from MRI scans, which were normalized to the Montreal Neurological Institute (MNI) space, along with the PET images. We calculated the standardized uptake value ratio (SUVR) in MNI space using the whole cerebellum as reference region. Prior to statistical analysis images were smoothed with an 8-mm full width at half-maximum (FWHM) Gaussian kernel.

Regional Aβ-PET quantification

SUVRs were extracted from a-priori defined regions of interest (ROI). We selected the cortical Centiloid composite ROI (http://www.gaain.org/centiloid-project) as Aβ-sensitive cerebral region (Klunk et al., 2015), which included the following bilateral brain areas: anterior and posterior cingulate cortex, angular gyrus, posterior middle temporal gyrus, middle temporal gyrus, middle frontal gyrus, superior frontal gyrus (pars orbitalis) and the anterior subdivision of the ventral striatum. As tau-vulnerable regions, we selected the Braak stages ROIs (Braak & Braak, 1991) defined according to the Desikan-Killiany atlas (DK atlas) in Schöll et al. (2016). Figure 1 shows both the Centiloid and Braak stages ROIs mapped onto the DK atlas. For visualization purposes, the Centiolid ROIs was parceled onto the DK atlas according to a best-match visual criterion. Supplementary Table 1 shows the full list of the DK atlas labels that were used for both composite ROIs. Supplementary figure 1 shows a surface rendering of the Centilod composite ROI prior to atlas parcellation.

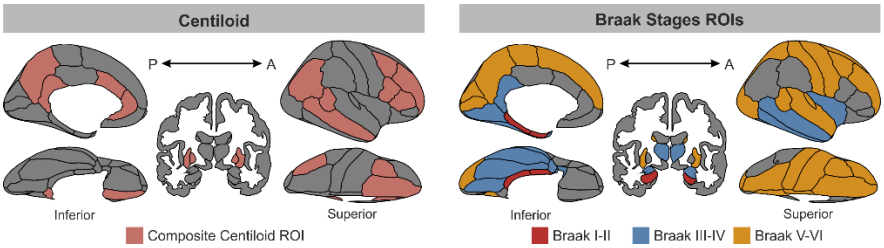

Fig. 1 Regions of interest projected onto the Desikan-Killiany atlas. Representation of both cortical and subcortical structures included in the Centiloid and Braak stages ROIs. Polygon rendering is created with the "ggseg" package in R (https://github.com/LCBC-UiO/ggseg/tree/master).

Neuropsychological assessment

Global cognitive functioning was assessed in both cohorts with the mini mental state examination test (MMSE) (Folstein et al., 1975).

Statistical analyses

Basic demographic information from both cohorts were compared using t-test for continuous variables and Chi-squared test for categorical ones.

We first looked for interactions between CSF Aβ42/40 concentrations and each of the three assessed AD risk factors (i.e., age, sex and *APOE-ε4*), in promoting cerebral Aβ deposition in regions that are selectively vulnerable to either Aβ (Centiloid composite ROI) or tau pathology (Braak stages ROIs). This first set of analyses was conducted with the SPSS software package (https://www.ibm.com/analytics/spss-statistics-software). Next, we conducted a spatially unbiased whole-brain analysis to detect interaction effects in distributed brain areas. This was achieved by performing a voxel-wise linear regression in SPM12 (Statistical Parametric Mapping, https://www.fil.ion.ucl.ac.uk/spm). For both the ROI and whole-brain analyses, we set-up three different general linear models where Aβ PET was set as dependent variable, while CSF Aβ42/40, age, sex and *APOE-ε4* status were modelled as predictors. Additionally, the interaction

term involving CSF Aβ42/40 and any of the three AD risk factors was modelled as independent variable, as follows:

$$\text{Aβ PET} = \text{CSF Aβ} + \text{age} + \text{sex} + \textit{APOE-ε4} + \text{CSF Aβ} * \textit{APOE-ε4}$$

$$\text{Aβ PET} = \text{CSF Aβ} + \text{age} + \text{sex} + \textit{APOE-ε4} + \text{CSF Aβ} * \text{age}$$

$$\text{Aβ PET} = \text{CSF Aβ} + \text{age} + \text{sex} + \textit{APOE-ε4} + \text{CSF Aβ} * \text{sex}$$

To avoid muticollinearity, continuous CSF Aβ42/40 values were centered to the group mean (Mumford et al., 2015). *APOE-ε4* was treated as categorical binary variable (*i.e.,* 0=non-carriers, 1=*ε4*-carriers). In SPM, we set parametric t-contrasts on the interaction terms, based on the hypothesis that each risk factor would exacerbate amyloid fibrillary deposition as function of CSF Aβ42/40 concentrations.

Finally, to assess the combined effects of AD risk factors, we performed additional analyses testing three-way interactions involving CSF Aβ42/40 and each pair of the tested risk factors. To this aim, we set up three different statistical models where the effects of CSF Aβ42/40 on Aβ PET were studied in combination with either *APOE-ε4* and age, *APOE-ε4* and sex, or age and sex.

$$\text{Aβ PET} = \text{CSF Aβ} + \text{age} + \text{sex} + \textit{APOE-ε4} + \text{CSF Aβ} * \textit{APOE-ε4} * \text{age}$$

$$\text{Aβ PET} = \text{CSF Aβ} + \text{age} + \text{sex} + \textit{APOE-ε4} + \text{CSF Aβ} * \textit{APOE-ε4} * \text{sex}$$

$$\text{Aβ PET} = \text{CSF Aβ} + \text{age} + \text{sex} + \textit{APOE-ε4} + \text{CSF Aβ} * \text{age} * \text{sex}$$

For the ROI analyses, results were considered significant if surviving a threshold of $p<0.05$ corrected for multiple testing using a False-Discovery Rate (FDR) approach. For the whole brain voxel-wise analysis, we set a threshold of $p<0.001$ and applied a cluster extent correction of 100

contiguous voxels (k > 100). All the above-mentioned statistical models were applied to the ADNI replication sample. Voxel-wise analyses in ADNI were masked with an inclusive mask derived from the analyses conducted in ALFA, which was generated at a liberal threshold of p<0.005 with a cluster extent of 100 voxels.

RESULTS

Sample characteristics

Demographic characteristics of both cohorts can be found in Table 1. Compared to ALFA, ADNI participants were significantly older, more educated, and harboured a lower proportion of *APOE-ε4* carriers. However, the two samples were homogeneous with respect to sex and global cognitive performance. As expected, in both cohorts CSF Aβ42/40 concentrations were negatively related to Aβ PET uptake in widespread cortical areas, while age and *APOE-ε4* were positively associated to cortical Aβ deposition (Supplementary Figure 2).

	ALFA (n=293)	**ADNI (n=259)**	**p-value**
Age, *M(SD)**	61.03(4.25)	73.70(6.39)	<0.001
Education, *M(SD)**	13.39(3.55)	16.02(2.64)	<0.001
Female sex, n(%)	183(62.4%)	141(54.4%)	0.06
***APOE-ε4*, n(%)**	143(48.8%)	72(27.8%)	<0.001
MMSE, *M(SD)***	29.14(0.99)	29.07(1.13)	0.46

Table 1 – Sample characteristics

*expressed in years.

**MMSE data for ALFA cohort were available for 235 study participants.

ROI analyses

We assessed whether AD risk factors such as age, *APOE-ε4* and female sex modulated the association between soluble and deposited Aβ in cerebral regions known for their vulnerability to either Aβ or tau pathology. Table 2 shows the results of each statistical model run for the different risk factors in each of the tested ROIs; for each model, the F-statistic and p-value of the interaction term are presented. Within the Centiloid ROI, each of the 2-Way and 3-Way interactions were significant in the ALFA cohort, while in ADNI the interaction between CSF Aβ42/40 and sex did not survive statistical correction. In Braak I/II ROIs, only the 2-Way and 3-Way interactions involving *APOE-ε4* were significant in ALFA but not the remaining models, while in ADNI no significant interactions were found. In Braak III/IV ROIs, we observed similar results as for the Centiloid ROI, that is, all interaction models being significant in ALFA with two interactions not reaching statistical significance in ADNI, those between CSF Aβ42/40 and sex as well as CSF Aβ42/40 and *APOE-ε4*. Finally, in Braak V/VI, ALFA participants displayed all significant interactions except a statistical trend for CSF Aβ42/40 x *APOE-ε4*, while for ADNI participants only the two-way interaction involving sex did not reach statistical significance. Figure 2 shows group scatterplots highlighting the modulatory role of each risk factor on the association between soluble and deposited Aβ in those ROIs, for both cohorts.

Whole brain analysis: two-way interactions

We then examined the impact of each risk factor on the association between soluble and deposited Aβ on the whole brain level by conducting voxel-wise regressions. In the ALFA cohort, we found that, for any given value of CSF Aβ42/40, *APOE-ε4* carriers displayed a higher Aβ PET retention in the bilateral anterior hippocampus extending to the entorhinal cortex, also including the inferior temporal and angular gyrus bilaterally (Fig. 3a-3c). These results were replicated in the ADNI cohort, whereby the interaction between CSF Aβ42/40 and *APOE-ε4* was significant in a topographical pattern consistent with that of ALFA, and including the right middle and inferior temporal cortex, as well as the anterior cingulate cortex (ACC) and right angular gyrus (Fig. 3d-3f).

	Centiloid ROI				Braak I/II				Braak III/IV				Braak V/VI			
	ALFA		ADNI		ALFA		ADNI		ALFA		ADNI		ALFA		ADNI	
	$F_{1,287}$	pFDR	$F_{1,251}$	pFDR	$F_{1,287}$	pFDR	$F_{1,251}$	pFDR	$F_{1,287}$	pFDR	$F_{1,251}$	pFDR	$F_{1,287}$	pFDR	$F_{1,251}$	pFDR
CSFAβ*APOE-ε4	6.89	**0.013**	6.21	**0.024**	12.73	**0.001**	0.178	0.702	10.47	**0.002**	2.80	0.142	3.58	0.071	4.83	**0.049**
CSFAβ*age	36.40	**<0.001**	8.62	**0.011**	1.28	0.269	4.44	0.062	27.48	**<0.001**	10.74	**0.008**	29.01	**<0.001**	7.79	**0.014**
CSFAβ*sex	5.51	**0.027**	0.72	0.453	1.44	0.252	0.65	0.459	6.64	**0.037**	0.58	0.810	5.07	**0.032**	1.12	0.348
CSFAβ*age* *APOE-ε4*	22.47	**0.002**	6.20	**0.002**	8.48	**<0.001**	1.71	0.219	20.20	**<0.001**	5.20	**0.010**	16.61	**<0.001**	5.38	**0.012**
CSFAβ*sex* *APOE-ε4*	5.36	**0.002**	3.75	**0.010**	5.14	**0.003**	1.49	0.244	6.69	**<0.001**	3.09	**0.020**	3.98	**0.012**	3.21	**0.017**
CSFAβ*age*sex	21.72	**0.001**	5.98	**0.012**	1.31	0.272	2.24	0.162	16.76	**0.001**	6.35	**0.012**	17.69	**<0.001**	5.90	**0.009**

Table 2 – Interactions between CSF $A\beta_{42/40}$ and each AD risk factors on Aβ-PET uptake in vulnerable ROIs.

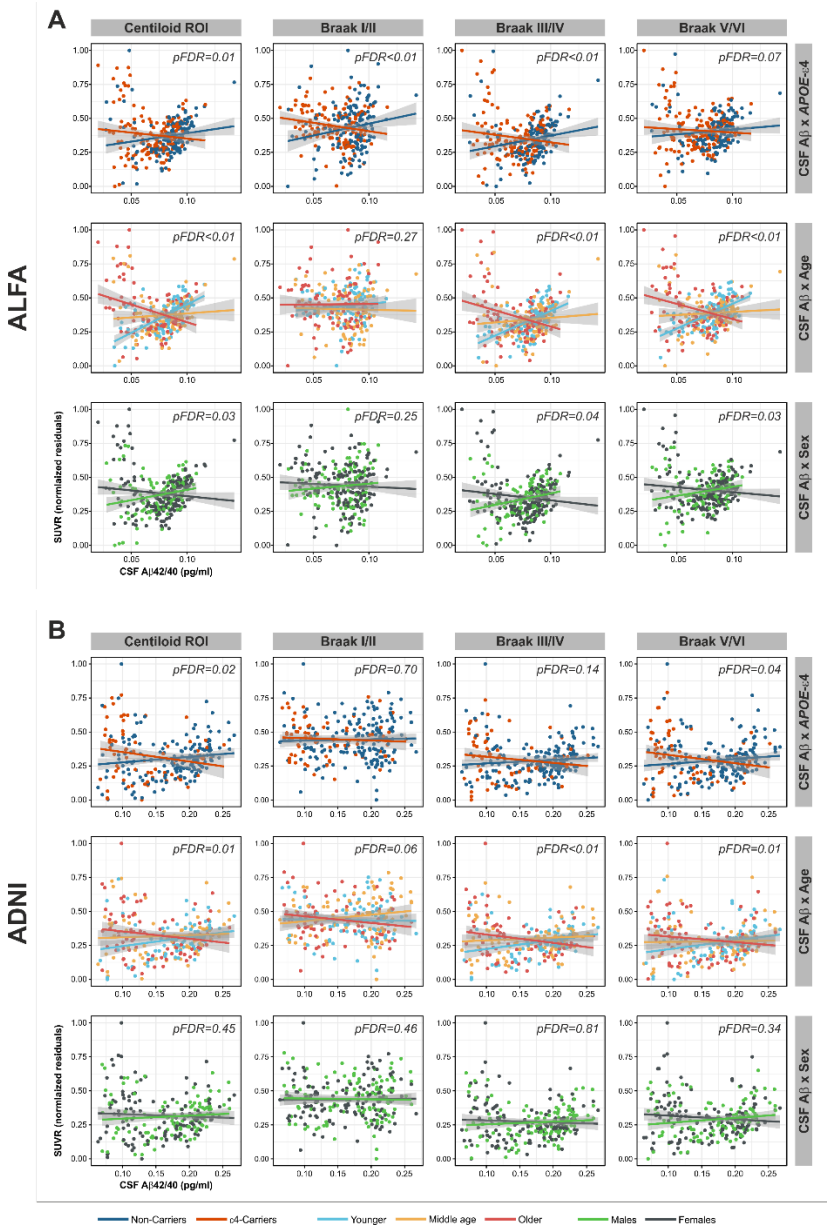

Fig. 2 *APOE-ε4*, age and sex modified the association between CSF Aβ42/40 concentrations and Aβ PET uptake quantified in regions of interest. A) Interactions assessed in the ALFA sample and **B)** in ADNI. SUVRs were residualized against the covariates of interest in each model (refer to the Statistical Analysis section). For visualization purposes, age continuous variable was broken down in three subgroups of younger, middle-aged, and older individuals, according to tercile ranking.

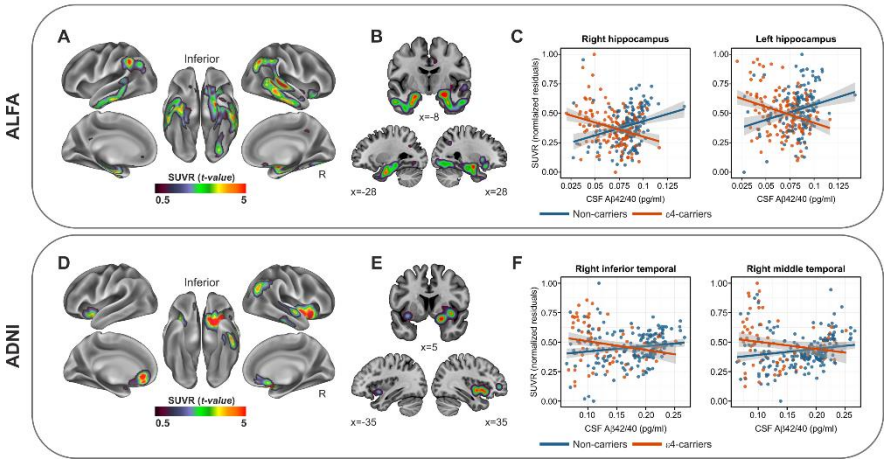

Fig. 3 *APOE-ε4* significantly modified the spatial topography of A PET as function of CSF Aβ42/40. A-B) Surface and volume rendering in ALFA participants of the Aβ PET statistical t-map resulting from the interaction model. Data indicate that compared to non-carriers, *APOE-ε4* carriers displayed higher SUVRs, for any given level of CSF Aβ42/40, in medial temporal regions including entorhinal cortex and hippocampus. **C)** Group scatterplots in ALFA participants showing the significant interaction between *APOE-ε4* and CSF Aβ42/40 in driving Aβ PET SUVRs in the right and left hippocampus. **D-E)** Surface and volume rendering in ADNI participants, of Aβ PET statistical t-map indicating that compared to non-carriers, *APOE-ε4* carriers displayed higher SUVRs, for any given level of CSF Aβ42/40, in right inferior and middle temporal as well as right insula. **F)** Group scatterplots in ADNI participants showing the significant interaction between *APOE-ε4* and CSF Aβ42/40 in driving Aβ PET SUVRs in the right inferior and middle temporal gyrus.

Next, we found that age modulated the association between CSF Aβ42/40 concentration and cortical Aβ deposition, with older individuals displaying greater SUVRs in bilateral superior frontal cortex, middle and inferior temporal areas as well as anterior and posterior cingulate cortex (PCC) (Fig. 4a-4b) in the ALFA cohort. Such a pattern of results was replicated in ADNI, with similar effects shown in older compared to younger individuals, even though the topological pattern was less widespread (Fig 4c-4d).

Finally, a similar modulatory role was observed for sex, indicating higher SUVRs in posterior areas including the cuneus, the middle cingulate cortex and middle temporal gyrus, in females compared to males (Fig. 5a-5b) in the ALFA cohort. As for the previous interactions, this interaction was replicated in ADNI, even though the spatial topography was less distributed, including the cuneus bilaterally, as shown in Fig 5c-5d.

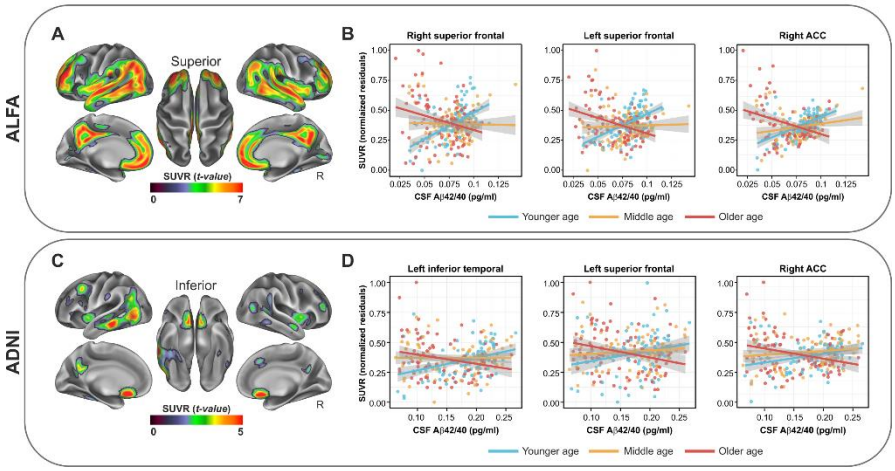

Fig. 4 Age significantly modified the association between of CSF Aβ42/40 and Aβ PET. A-B) In ALFA participants, older individuals displayed, for any given level of CSF Aβ42/40 concentration, a higher Aβ PET retention in distributed cerebral areas including inferior and superior temporal cortex as well as medial prefrontal and inferior parietal areas. **C-D)** Such an interaction was replicated in the ADNI cohort, although in a less distributed topological pattern. For visualization purposes, age continuous variable was broken down in three subgroups of younger, middle-aged, and older individuals, according to tercile ranking.

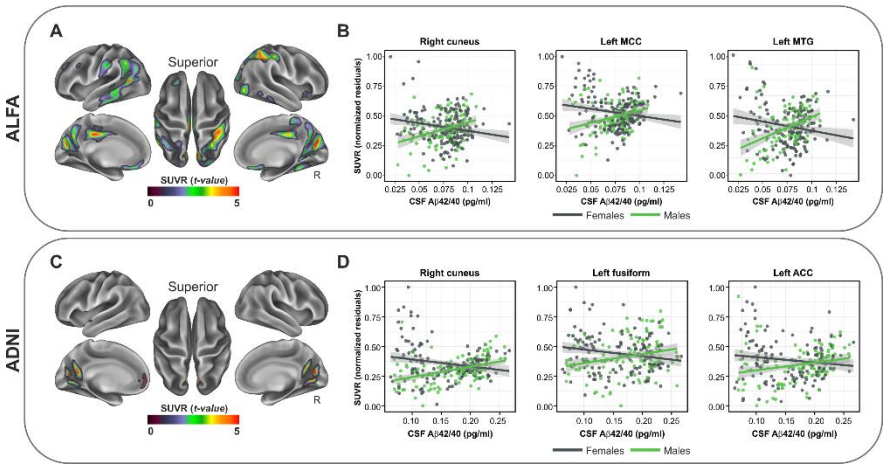

Fig. 5 Sex significantly modified the association between CSF Aβ42/40 and Aβ PET. A-B) In ALFA participants, sex significantly modulated the association between CSF Aβ42/40 and Aβ PET uptake indicating higher SUVRs in females' participants compared to males, in posterior medial regions including the precuneus and the cuneus. **C-D)** An overlapping cortical topology was found in ADNI participants indicating the same interaction effects as in ALFA. rITG=right inferior temporal gyrus; lITG=left inferior temporal gyrus; rPUT

Whole brain voxel-wise analysis on the synergistic effects of *APOE-ε4*, age and sex

In the ALFA cohort, we observed a significant three-way interaction involving CSF Aβ42/40, *APOE-ε4*, and age in lateral temporal regions, temporo-parietal junction, and PCC, indicating that the detrimental effects of *APOE-ε4* in driving a higher Aβ PET uptake as function of CSF Aβ42/40 concentrations, were stronger in older compared to younger individuals (Fig. 6a-6b). Similar patterns were significant in ADNI (Fig. 6c-6d). Next, we found a three-way interaction involving CSF Aβ42/40, age and sex, indicating that the modulatory role of age in prompting a higher Aβ PET uptake as function of CSF Aβ42/40 concentrations, were stronger in female compared to male individuals. This interaction mapped onto the orbitofrontal cortex, inferior parietal as well as anterior and posterior cingulate (Fig. 6e-6f). These findings, although less widespread, were replicated in ADNI participants as well (Fig. 6g-6h).

Finally, we found a significant three-way interaction involving CSF Aβ42/40, *APOE-ε4*, and sex, indicating that the exacerbating effects of *APOE-ε4* were more prominent in women compared to men, in inferior temporal and orbitofrontal regions (Fig. 7a-7b). This interaction was however not replicated in ADNI.

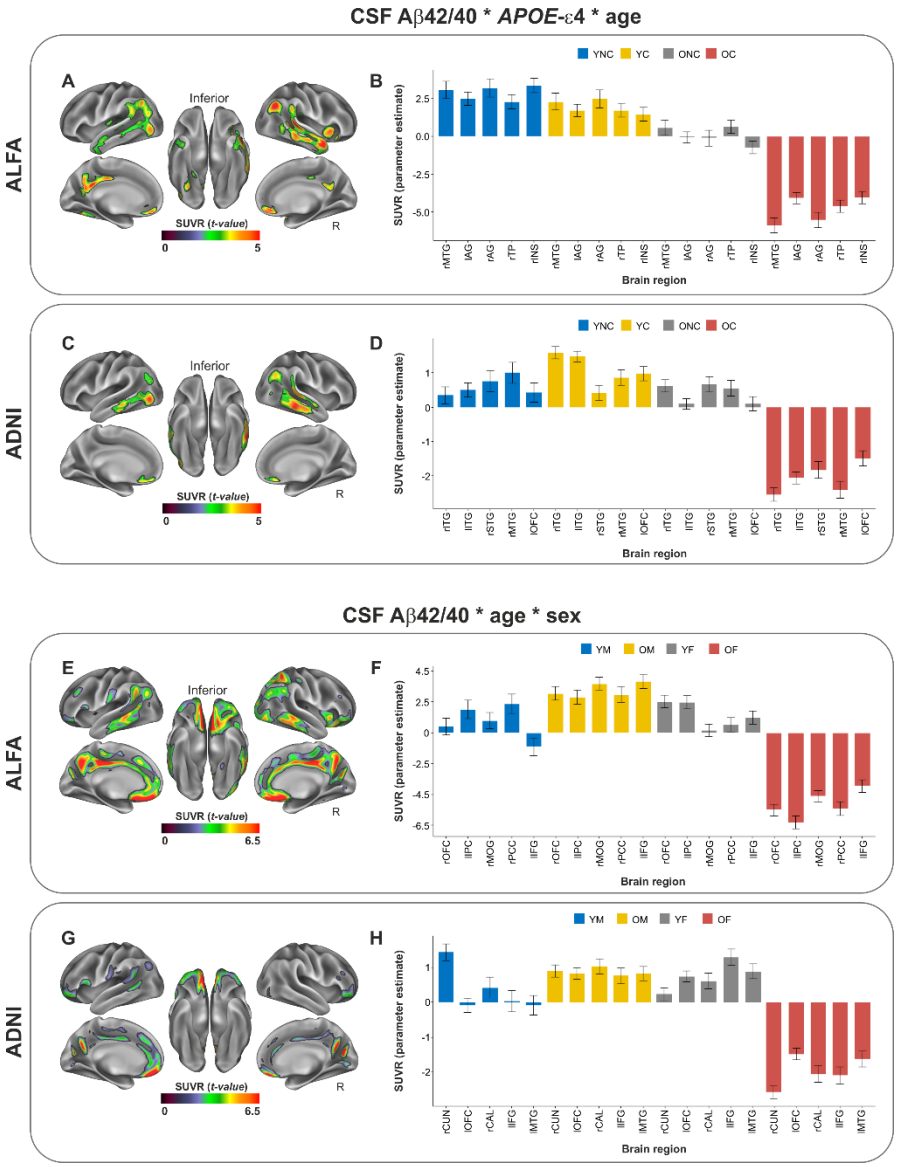

Fig. 6 Three-way interactions in both cohorts. A-B) Surface rendering and bar plots indicating three-way interactions involving CSF Aβ42/40, *APOE-ε4* and age on Aβ PET uptake in the ALFA cohort. YNC=young non-carriers; YC=young *ε4*-carriers; ONC=older non-carriers; rMTG=right middle temporal gyrus; lAG=left angular gyrus; rAG=right angular gyrus; rTP=right temporal pole. **C-D)** Same as in A-B, in the ADNI cohort. rINS=right insula; rITG=right inferior temporal gyrus; lIPG=left inferior parietal gyrus; rSTG=right superior temporal gyrus; lOFC=orbitofrontal cortex. In B) and D), bars in the plot encode the interaction between one categorical (*APOE-ε4*) and two continuous (CSF Aβ42/40, age) variables. **E-F)** Surface rendering and bar plots indicating three-way interactions involving CSF Aβ42/40, age and sex on Aβ PET uptake in the ALFA cohort. YM=young males;

OM=older males; YF=young females; OF=older females; rOFC=right orbitofrontal cortex; lIPC=left inferior parietal cortex; rMOG=right medial orbital gyrus; rPCC=right posterior cingulate cortex; lIFG=left inferior frontal gyrus; **G-H)** Same as in E-F, in the ADNI cohort. rCUN=right cuneus; lOFC=left orbitofrontal cortex; rCAL=right calcarine; lIFG=left inferior frontal gyrus; lMTG=left middle temporal gyrus. In F) and H), bars in the plot encode the interaction between one categorical (*sex*) and two continuous (CSF Aβ42/40, age) variables.

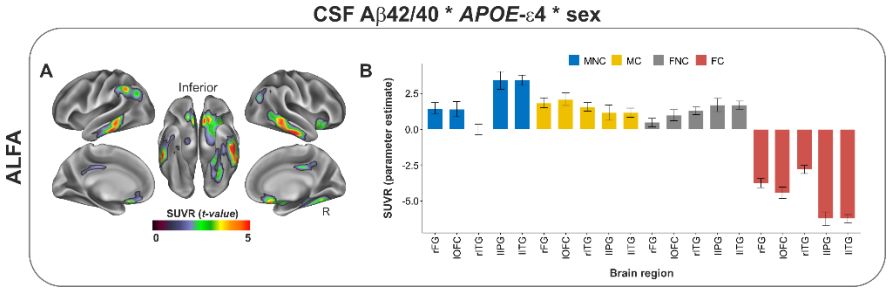

Fig. 7 Three-way interactions in the ALFA cohort. A-B) Surface rendering and bar plots indicating three-way interactions involving CSF Aβ42/40, age and sex on Aβ PET uptake in the ALFA cohort. MNC=males non-carrier; MC=males *ε4*-carriers; FNC=females non-carrier; FC=females *ε4*-carriers; FG=right fusiform gyrus; lOFC=orbitofrontal cortex; rITG=right inferior temporal gyrus; lIPG=left inferior parietal gyrus; lITG=left inferior temporal gyrus. Bars in the plot encode the interaction between two categorical (*APOE-ε4*, sex) and one continuous (CSF Aβ42/40) variables.

DISCUSSION

The present work aimed to determine whether in CU individuals, unmodifiable AD risk factors modulate the association between soluble and deposited Aβ species quantified with CSF concentrations and PET imaging, respectively. Further, our goal was to determine which brain regions are susceptible for such differential associations. We found that *APOE-ε4*, older age and female sex, all interacted with CSF Aβ42/40 concentrations, resulting in a higher fibrillary plaque deposition for any given level of CSF Aβ42/40, with each risk factor mapping onto a specific topology. Importantly, we replicated these findings in an independent cohort that differed in the PET tracers used for Aβ imaging as well as in the average age and level of progression in the preclinical AD *continuum*, thus

reinforcing the robustness and generalizability of our results. Our strategy of assessing the impact of risk factors on the association between two distinct surrogate markers of cleared and aggregated Aβ in CU individuals provide novel insights into the biological pathways underlying Aβ aggregation in the brain.

First, we observed a significant interaction between CSF Aβ42/40 and *APOE-ε4* in the Centiloid ROI as well as in Braak stages I/II and III/IV regions, in the ALFA cohort. In ADNI, this interaction was significant in the Centiloid ROI, as well as the Braak stages V/VI ROI. Whole-brain analyses conducted in the ALFA cohort confirmed that, compared to non-carriers, *APOE-ε4* carriers displayed, for any given value of CSF Aβ42/40, a higher Aβ PET retention in a symmetric pattern covering medial temporal lobe (MTL) areas including the anterior hippocampus, parahippocampus, entorhinal cortex, inferior temporal as well as the bilateral inferior parietal regions. Similarly, in ADNI this interaction covered the right middle and inferior temporal cortex, as well as the anterior cingulate cortex and right angular gyrus. These areas do not typically display Aβ accumulation in the early stages of the disease, which rather involve neocortical areas and particularly prefrontal cortex, posterior cingulate, precuneus, and inferior parietal, as shown by *in-vivo* staging (Collij et al., 2020; Mattsson et al., 2019; Grothe et al., 2017) and autopsy studies (Braak & Braak, 1991; Thal et al., 2002). Rather, the regions we found, particularly in the ALFA sample, display selective vulnerability to early tau deposition, as previously documented in patients along the Alzheimer's *continuum* (Ossenkoppele et al., 2016; Schwarz et al., 2016; Cho et al., 2016) as well as in cognitively unimpaired individuals (Johnson et al., 2016; Schöll et al., 2016). Earlier studies provide evidence for a synergistic interaction between Aβ and tau in determining functional and structural abnormalities in cognitively intact individuals (Busche & Hyman, 2020; Pascoal et al., 2017; Desikan et al., 2012; Fortea et al., 2014). According to a disease model of Aβ-induced tau hyperphosphorylation (Maia et al., 2013; Schelle et al., 2017), fibrillary Aβ initiates a pathophysiological cascade leading to tau misfolding that eventually propagates throughout the neocortex. Furthermore, one study reported that the interaction between Aβ and tau in driving a greater risk of developing AD, mapped onto inferior temporal and parietal regions, which

overlap with the regions we found (Pascoal et al., 2017). Hence, our results suggest that *APOE-ε4*, by affecting the association between soluble and deposited Aβ specifically in MTL areas, paves the way for the spread of tau in extra medial-temporal regions thus promoting later co-localization of Aβ and tau. Indeed, previous PET imaging studies have documented a higher tau deposition in *APOE-ε4* carrier AD patients compared to non-carriers (Ossenkoppele et al., 2016; Therriault et al., 2020; Tiraboschi et al., 2004). The importance of this co-localization is highlighted by evidence that the presence of tau pathology beyond the mesial temporal lobe is facilitated by the presence of Aβ in these regions (Pontecorvo et al., 2017; Jones et al., 2017; He et al., 2018; Vogel et al., 2020; Shimada et al., 2017). In turn, tau deposition in MTL regions drives subsequent neurodegeneration, brain atrophy and cognitive decline (La Joie et al., 2020; Bejanin et al, 2017). These regional effects were not detected for the interactions between CSF Aβ42/40 and age or sex, but post-hoc three-way interactions indicated that the effect of *APOE-ε4* was significantly stronger for females and older participants. Our data support earlier evidence for a combined influence of age, sex and *APOE-ε4* on the emergence of AD pathology (Mofrad et al., 2020; Li et al., 2017; Lautner et al,. 2017; Glodzik-Sobanska et al., 2009), and AD prevalence (Riedel et al., 2016; Raber et al., 2004; Farrer et al, 1997; Jarvik et al., 1995). Furthermore, our interaction effects may help to explain the faster disease progression (Mishra et al., 2018; Paranjpe et al., 2019) as well as the stronger relationship between Aβ and cognitive decline (Mormino et al., 2014; Kantarci et al., 2012; Lim et al., 2015) in *APOE-ε4* carriers compared to non-carriers. It is worth noting that, when assessing the main effects of *APOE-ε4* on Aβ PET we found, as expected, a widespread higher retention in *ε4*-carriers compared to non-carriers across regions consistent with those reported previously, namely prefrontal and midline cortical areas (Fig. S1) (Reiman et al., 2009; Toledo et al., 2019). However, as mentioned above, our interaction data between CSF Aβ42/40 and *APOE-ε4* revealed a cortical topology in different areas and precisely in MTL, tau-vulnerable, regions. Thus, our results imply that the ratio between cerebral deposited Aβ and its soluble counterpart may represent a novel biomarker putatively reflecting the imbalance between cleared and deposited Aβ in the brain, and may thus be more informative on the mechanisms of incipient Aβ pathology. Further longitudinal studies are

required to track the progression of regional Aβ PET uptake as function of CSF Aβ concentrations stratified by genetic risk, age and sex.

It is important to note that the ALFA and ADNI cohorts had significantly different age (mean age ALFA: 61.03; mean age ADNI: 73.71) and levels of cerebral Aβ load (mean Centiloid in ALFA = 2.66; mean Centiloid in ADNI = 25.71), which can be regarded as a proxy for disease progression (Palmqvist et al., 2019). Therefore, the comparison of the effect sizes across cohorts in progressive Braak stages ROIs may be indicative of the timing within the disease continuum when the effect of each of these AD risk factors may be more relevant in promoting the accumulation of Aβ in tau-vulnerable regions. In general, the sizes of effects of these AD risk factors in ADNI were progressively larger in Braak V/VI than in Braak III/IV, and nonsignificant in Braak I/II. In contrast, in ALFA, whose participants are supposed to be in earlier stages of the Alzheimer's *continuum*, the interaction effect between CSF Aβ and *APOE-ε4* was mostly prominent in Braak I/II, followed by Braak III/IV. This pattern suggests that the effect of *APOE-ε4* in promoting Aβ aggregation in entorhinal regions, which is thought to be a key event in the development of AD, may happen very early in the AD *continuum*.

Next, we reported a modulatory effect for older age in driving a higher Aβ PET uptake as a function of CSF Aβ42/40. This interaction was significant in the Centiloid ROI, Braak stages III/IV and stages V/VI, in both cohorts. Whole brain analyses yielded significant effects into the posterior cingulate, precuneus, medial prefrontal cortex including the ACC, as well as superior frontal and middle temporal areas in the ALFA cohort. Consistent effects were found in the ADNI sample even though within a more restricted topology involving ACC, PCC and middle temporal areas. Such a reduced effect in ADNI compared to that in ALFA may be due to the different age range of the two samples (ALFA= 50-73; ADNI=56-94 years). In fact, earlier studies indicate that, the effects of aging on cortical Aβ deposition drop significantly in cognitively intact individuals older than 60 years of age (*e.g.,* Rodrigue et al., 2012). Unlike the interaction findings involving *APOE-ε4*, the brain regions susceptible for the interaction between CSF Aβ42/40 and age display selective vulnerability to Aβ accumulation early in the disease

continuum (Collij et al., 2020; Mattsson et al., 2019; Braak & Braak, 1991; Thal et al., 2002). These regions overlap with the default-mode network, which is known for harboring Aβ in the initial stages of the disease, as well as in normal aging (Buckner et al., 2005, 2009; Palmqvist et al,. 2017). Interestingly, aging has been associated to a progressive disruption of the DMN, which in turn affects memory efficiency (Damoiseaux et al., 2008; Miller et al, 2008). Hence, our interaction data suggest that, as Aβ clearance rate begins to become deficient, older individuals harbor more fibrillary plaques within the DMN, which may exacerbate the effects of Aβ on cognitive performance. This hypothesis however goes beyond the scope of the present study.

Finally, we reported that sex modulated the association between soluble and deposited Aβ in the Centiloid ROI, as well as Braak stages ROIs III/IV and V/VI in the ALFA cohort, while no significant two-way interactions involving sex were retrieved in the ADNI sample using an ROI approach. Whole brain analyses yielded a significant interaction in posterior medial regions such as the PCC and cuneus, as well as middle temporal areas in ALFA, while a less distributed effect was found in ADNI, involving the cuneus bilaterally. Women represent two-thirds of the cases of late-onset AD (Beam et al., 2018). Such a higher prevalence may be ascribed to several factors, including sex-related differences in neuroinflammation burden (Hall et al., 2013), higher proportion of major depressive disorders in women (Albert, 2015) and most importantly, estrogen depletion occurring in the perimenopause (Brinton et al., 2015). Reductions in estrogen levels in women during the fifth decade and beyond, may be responsible for deficits in the brain metabolism and vascular pathogenesis. Compared to perimenopausal, post-menopausal women show more prominent brain hypometabolism, increased Aβ deposition and reduced gray matter volume, with these effects mapping onto posteromedial cortices (Mosconi et al., 2017), similarly to the brain areas that we have found in the interaction analysis. In addition, sex has been shown to modify the *APOE*-related increased risk of developing AD, with a higher proportion of MCI to AD converters in women than in men *ε4*-carriers (Altman et al., 2014). Our three-way interaction showing a greater deleterious effect of *APOE-ε4* on Aβ deposition in women than in men suggest that Aβ-dependent

mechanisms may underlie those previous observations. More in general, our three-way interaction results indicate that cognitively intact older females harbouring *APOE-ε4* may enter earlier in preclinical AD stage, thus calling for their inclusion in primary prevention strategies.

In conclusion, we show that *APOE-ε4*, age and sex modify the relationship between soluble and deposited Aβ with each risk factor promoting a higher cerebral Aβ deposition as function of CSF Aβ42/40 concentrations in specific brain regions. The interaction between CSF Aβ and *APOE-ε4* mapped onto regions that do not typically accumulate Aβ in the early preclinical AD stages, but rather show selective vulnerability to tau aggregation and atrophy early in the disease. On the other hand, both age and sex interactions showed their effects on areas of initial Aβ deposition.

These data provide novel insights into the factors mediating the balance between soluble and deposited Aβ and clarify the mechanisms underlying the higher AD prevalence associated to those risk factors.

ACKNOWLEDGEMENTS

This publication is part of the ALFA study (ALzheimer and FAmilies). The authors would like to express their most sincere gratitude to the ALFA project participants, without whom this research would have not been possible. Authors would like to thank Roche Diagnostics International Ltd. for kindly providing the kits for the CSF analysis of ALFA+ participants and GE Healthcare for kindly providing [^{18}F]flutemetamol doses of ALFA+ participants. The project leading to these results has received funding from “la Caixa” Foundation (ID 100010434), under agreement LCF/PR/GN17/50300004 and the Alzheimer’s Association and an international anonymous charity foundation through the TriBEKa Imaging Platform project (TriBEKa-17-519007). Additional support has been received from the Universities and Research Secretariat, Ministry of Business and Knowledge of the Catalan Government under the grant no. 2017-SGR-892. JDG is supported by the Spanish Ministry of Science and

Innovation (RYC-2013-13054). MSC receives funding from Instituto de Salud Carlos III (PI19/00155) and from the Spanish Ministry of Science, Innovation and Universities (Juan de la Cierva programme grant IJC2018-037478-I). KB holds the Torsten Söderberg Professorship in Medicine at the Royal Swedish Academy of Sciences, and is supported by the Swedish Research Council (#2017-00915); the Swedish Alzheimer Foundation (#AF-742881), Hjärnfonden, Sweden (#FO2017-0243); and a grant (#ALFGBG-715986) from the Swedish state under the agreement between the Swedish government and the County Councils, the ALF-agreement. HZ is a Wallenberg Scholar supported by grants from the Swedish Research Council (#2018-02532), the European Research Council (#681712), Swedish State Support for Clinical Research (#ALFGBG-720931), the Alzheimer Drug Discovery Foundation (ADDF), USA (#201809-2016862), the European Union's Horizon 2020 research and innovation programme under the Marie Skłodowska-Curie grant agreement No 860197 (MIRIADE), and the UK Dementia Research Institute at UCL.

Conflicts of interest:

JLM has served/serves as a consultant or at advisory boards for the following for-profit companies, or has given lectures in symposia sponsored by the following for-profit companies: Roche Diagnostics, Genentech, Novartis, Lundbeck, Oryzon, Biogen, Lilly, Janssen, Green Valley, MSD, Eisai, Alector, BioCross, GE Healthcare, ProMIS Neurosciences, NovoNordisk, Zambón, Cytox and Nutricia. MSC has given lectures in symposia sponsored by ROCHE DIAGNOSTICS, S.L.U. GK is a full-time employee of Roche Diagnostics GmbH. IS is a full-time employee and shareholder of Roche Diagnostics International Lda. HZ has served at scientific advisory boards for Denali, Roche Diagnostics, Wave, Samumed, Siemens Healthineers, Pinteon Therapeutics and CogRx, has given lectures in symposia sponsored by Fujirebio, Alzecure and Biogen, and is a co-founder of Brain Biomarker Solutions in Gothenburg AB (BBS), which is a part of the GU Ventures Incubator Program (outside submitted work). The rest of the authors have no conflict of interest to declare.

REFERENCES

Albert PR. Why is depression more prevalent in women? J Psychiatry Neurosci 2015; 40: 219–221.

Altmann A, Tian L, Henderson VW, Greicius MD. Sex modifies the APOE-related risk of developing Alzheimer disease. Ann Neurol 2014; 75: 563–573.

Beam CR, Kaneshiro C, Jang JY, Reynolds CA, Pedersen NL, Gatz M. Differences Between Women and Men in Incidence Rates of Dementia and Alzheimer's Disease. J Alzheimers Dis 2018; 64: 1077–1083.

Bejanin A, Schonhaut DR, La Joie R, Kramer JH, Baker SL, Sosa N, et al. Tau pathology and neurodegeneration contribute to cognitive impairment in Alzheimer's disease. Brain 2017; 140: 3286–3300.

Blennow K, Zetterberg H, Fagan AM. Fluid biomarkers in Alzheimer disease. Cold Spring Harb Perspect Med 2012; 2: a006221.

Braak H, Braak E. Neuropathological stageing of Alzheimer-related changes. Acta Neuropathol 1991; 82: 239–259.

Brinton RD, Yao J, Yin F, Mack WJ, Cadenas E. Perimenopause as a neurological transition state. Nat Rev Endocrinol 2015; 11: 393–405.

Buckner RL, Sepulcre J, Talukdar T, Krienen FM, Liu H, Hedden T, et al. Cortical hubs revealed by intrinsic functional connectivity: mapping, assessment of stability, and relation to Alzheimer's disease. J Neurosci 2009; 29: 1860–1873.

Buckner RL, Snyder AZ, Shannon BJ, LaRossa G, Sachs R, Fotenos AF, et al. Molecular, structural, and functional characterization of Alzheimer's disease: evidence for a relationship between default activity, amyloid, and memory. J Neurosci 2005; 25: 7709–7717.

Busche MA, Hyman BT. Synergy between amyloid-beta and tau in Alzheimer's disease. Nature neuroscience 2020; 23(10): 1183-93.

Cho H, Choi JY, Hwang MS, Lee JH, Kim YJ, Lee HM, et al. Tau PET in Alzheimer disease and mild cognitive impairment. Neurology 2016; 87: 375–383.

Cohen AD, Landau SM, Snitz BE, Klunk WE, Blennow K, Zetterberg H. Fluid and PET biomarkers for amyloid pathology in Alzheimer's disease. Mol Cell Neurosci 2019; 97: 3–17.

Collij LE, Heeman F, Salvadó G, Ingala S, Altomare D, de Wilde A, et al. Multitracer model for staging cortical amyloid deposition using PET imaging. Neurology 2020; 95: e1538–e1553.

Damoiseaux JS, Beckmann CF, Arigita EJS, Barkhof F, Scheltens P, Stam CJ, et al. Reduced resting-state brain activity in the 'default network' in normal aging. Cereb Cortex 2008; 18: 1856–1864.

Desikan RS, McEvoy LK, Thompson WK, Holland D, Brewer JB, Aisen PS, et al. Amyloid-β--associated clinical decline occurs only in the presence of elevated P-tau. Arch Neurol 2012; 69: 709–713.

Fagan AM, Mintun M a., Mach RH, Lee SY, Dence CS, Shah AR, et al. Inverse relation between in vivo amyloid imaging load and cerebrospinal fluid Abeta 42 in humans. Ann Neurol 2006; 59: 512–519.

Farrer LA, Cupples LA, Haines JL, Hyman B, Kukull WA, Mayeux R, et al. Effects of age, sex, and ethnicity on the association between apolipoprotein E genotype and Alzheimer disease: A meta-analysis. J Am Med Assoc 1997; 278: 1349–1356.

Ferretti MT, Iulita MF, Cavedo E, Chiesa PA, Dimech AS, Chadha AS, et al. Sex differences in Alzheimer disease — The gateway to precision medicine. Nat Rev Neurol 2018; 14: 457–469.

Folstein MF, Folstein SE, McHugh PR. "Mini-mental state": A practical method for grading the cognitive state of patients for the clinician. J Psychiatr Res 1975; 12: 189–198.

Fortea J, Vilaplana E, Alcolea D, Carmona-Iragui M, Sánchez-Saudinos M-B, Sala I, et al. Cerebrospinal fluid β-amyloid and phospho-tau biomarker interactions affecting brain structure in preclinical Alzheimer disease. Ann Neurol 2014; 76: 223–230.

Glodzik-Sobanska L, Pirraglia E, Brys M, de Santi S, Mosconi L, Rich KE, et al. The effects of normal aging and ApoE genotype on the levels of CSF biomarkers for Alzheimer's disease. Neurobiol Aging 2009; 30: 672–681.

Grimmer T, Riemenschneider M, Förstl H, Henriksen G, Klunk WE, Mathis C a., et al. Beta amyloid in Alzheimer's disease: increased deposition in

brain is reflected in reduced concentration in cerebrospinal fluid. Biol Psychiatry 2009; 65: 927–934.

Grothe MJ, Barthel H, Sepulcre J, Dyrba M, Sabri O, Teipel SJ*, et al.* In vivo staging of regional amyloid deposition. Neurology 2017; 89(20): 2031-8.

Hall JR, Wiechmann AR, Johnson LA, Edwards M, Barber RC, Winter AS, et al. Biomarkers of vascular risk, systemic inflammation, and microvascular pathology and neuropsychiatric symptoms in Alzheimer's disease. J Alzheimers Dis 2013; 35: 363–371.

He Z, Guo JL, McBride JD, Narasimhan S, Kim H, Changolkar L, et al. Amyloid-β plaques enhance Alzheimer's brain tau-seeded pathologies by facilitating neuritic plaque tau aggregation. Nat Med 2018; 24: 29–38.

Jack CR, Bennett DA, Blennow K, Carrillo MC, Feldman HH, Frisoni GB, et al. A/T/N: An unbiased descriptive classification scheme for Alzheimer disease biomarkers. Neurology 2016; 87: 539–547.

Jarvik GP, Wijsman EM, Kukull WA, Schellenberg GD, Yu C, Larson EB. Interactions of apolipoprotein E genotype, total cholesterol level, age, and sex in prediction of Alzheimer's disease: a case-control study. Neurology 1995; 45: 1092–1096.

Johnson KA, Schultz A, Betensky RA, Becker JA, Sepulcre J, Rentz D, et al. Tau positron emission tomographic imaging in aging and early Alzheimer disease. Ann Neurol 2016; 79: 110–119.

La Joie R, Ayakta N, Seeley WW, Borys E, Boxer AL, DeCarli C, et al. Multisite study of the relationships between antemortem [11 C]PIB-PET Centiloid values and postmortem measures of Alzheimer's disease neuropathology. Alzheimer's Dement 2019; 15: 205–216.

La Joie R, Visani A V, Baker SL, Brown JA, Bourakova V, Cha J, et al. Prospective longitudinal atrophy in Alzheimer's disease correlates with the intensity and topography of baseline tau-PET. Sci Transl Med 2020; 12

Jones DT, Graff-Radford J, Lowe VJ, Wiste HJ, Gunter JL, Senjem ML, et al. Tau, amyloid, and cascading network failure across the Alzheimer's disease spectrum. Cortex 2017; 97: 143–159.

Kantarci K, Lowe V, Przybelski SA, Weigand SD, Senjem ML, Ivnik RJ, et al. APOE modifies the association between Aβ load and cognition in cognitively normal older adults. Neurology 2012; 78: 232–240.

Klunk WE, Koeppe RA, Price JC, Benzinger TL, Devous MD, Jagust WJ, et al. The Centiloid project: Standardizing quantitative amyloid plaque estimation by PET. Alzheimer's Dement 2015; 11: 1-15.e4.

Landau SM, Lu M, Joshi AD, Pontecorvo M, Mintun M a., Trojanowski JQ, et al. Comparing positron emission tomography imaging and cerebrospinal fluid measurements of β-amyloid. Ann Neurol 2013; 74: 826–836.

Launer LJ. The epidemiologic study of dementia: a life-long quest? Neurobiol Aging 2005; 26: 335–340.

Lautner R, Insel PS, Skillbäck T, Olsson B, Landén M, Frisoni GB, et al. Preclinical effects of APOE ε4 on cerebrospinal fluid Aβ42 concentrations. Alzheimers Res Ther 2017; 9: 87.

Lewczuk P, Matzen A, Blennow K, Parnetti L, Molinuevo JL, Eusebi P, et al. Cerebrospinal Fluid Aβ42/40 Corresponds Better than Aβ42 to Amyloid PET in Alzheimer's Disease. J Alzheimers Dis 2017; 55: 813–822.

Li G, Shofer JB, Petrie EC, Yu C-E, Wilkinson CW, Figlewicz DP, et al. Cerebrospinal fluid biomarkers for Alzheimer's and vascular disease vary by age, gender, and APOE genotype in cognitively normal adults. Alzheimers Res Ther 2017; 9: 48.

Lim YY, Villemagne VL, Pietrzak RH, Ames D, Ellis KA, Harrington K, et al. APOE ε4 moderates amyloid-related memory decline in preclinical Alzheimer's disease. Neurobiol Aging 2015; 36: 1239–1244.

Liu CC, Kanekiyo T, Xu H, Bu G. Apolipoprotein e and Alzheimer disease: Risk, mechanisms and therapy. Nat Rev Neurol 2013; 9: 106–118.

Maia LF, Kaeser SA, Reichwald J, Hruscha M, Martus P, Staufenbiel M, et al. Changes in amyloid-β and Tau in the cerebrospinal fluid of transgenic mice overexpressing amyloid precursor protein. Sci Transl Med 2013; 5: 194re2.

Mawuenyega KG, Sigurdson W, Ovod V, Munsell L, Kasten T, Morris JC, et al. Decreased clearance of CNS beta-amyloid in Alzheimer's disease. Science 2010; 330: 1774.

Mattsson N, Insel PS, Landau S, Jagust W, Donohue M, Shaw LM, et al. Diagnostic accuracy of CSF Ab42 and florbetapir PET for Alzheimer's disease. Ann Clin Transl Neurol 2014; 1: 534–543.

Mattsson N, Palmqvist S, Stomrud E, Vogel J, Hansson O. Staging β - Amyloid Pathology with Amyloid Positron Emission Tomography. JAMA Neurol 2019; 76: 1319–1329.

Mattsson N, Insel PS, Donohue M, Landau S, Jagust WJ, Shaw LM, et al. Independent information from cerebrospinal fluid amyloid-beta and florbetapir imaging in Alzheimer's disease. Brain: a journal of neurology 2015; 138(Pt 3): 772-83.

Miller SL, Celone K, DePeau K, Diamond E, Dickerson BC, Rentz D, et al. Age-related memory impairment associated with loss of parietal deactivation but preserved hippocampal activation. Proc Natl Acad Sci U S A 2008; 105: 2181–2186.

Mishra S, Blazey TM, Holtzman DM, Cruchaga C, Su Y, Morris JC, et al. Longitudinal brain imaging in preclinical Alzheimer disease: impact of APOE ε4 genotype. Brain 2018; 141: 1828–1839.

Mofrad BR, Tijms BM, Scheltens P, Barkhof F, van der Flier WM, Sikkes SAM*, et al.* Sex differences in CSF biomarkers vary by Alzheimer disease stage and APOE epsilon4 genotype. Neurology 2020; 95(17): e2378-e88.

Molinuevo JL, Gramunt N, Gispert JD, Fauria K, Esteller M, Minguillon C, et al. The ALFA project: A research platform to identify early pathophysiological features of Alzheimer’s disease. Alzheimer’s Dement Transl Res Clin Interv 2016; 2: 82–92.

Mormino EC, Betensky RA, Hedden T, Schultz AP, Ward A, Huijbers W, et al. Amyloid and APOE ε4 interact to influence short-term decline in preclinical Alzheimer disease. Neurology 2014; 82: 1760–1767.

Mosconi L, Berti V, Quinn C, McHugh P, Petrongolo G, Varsavsky I, et al. Sex differences in Alzheimer risk: Brain imaging of endocrine vs chronologic aging. Neurology 2017; 89: 1382–1390.

Mumford JA, Poline J-B, Poldrack RA. Orthogonalization of regressors in FMRI models. PLoS One 2015; 10: e0126255.

Ossenkoppele R, Schonhaut DR, Schöll M, Lockhart SN, Ayakta N, Baker SL, et al. Tau PET patterns mirror clinical and neuroanatomical variability in Alzheimer’s disease. Brain 2016; 139: 1551–1567.

Palmqvist S, Insel PS, Stomrud E, Janelidze S, Zetterberg H, Brix B, et al. Cerebrospinal fluid and plasma biomarker trajectories with increasing

amyloid deposition in Alzheimer's disease. EMBO Mol Med 2019; 11: 1–13.

Palmqvist S, Scholl M, Strandberg O, Mattsson N, Stomrud E, Zetterberg H*, et al.* Earliest accumulation of beta-amyloid occurs within the default-mode network and concurrently affects brain connectivity. Nature communications 2017; 8(1): 1214.

Palmqvist S, Zetterberg H, Mattsson N, Johansson P, Minthon L, Blennow K, et al. Detailed comparison of amyloid PET and CSF biomarkers for identifying early Alzheimer disease. Neurology 2015; 85: 1240–1249.

Paranjpe MD, Chen X, Liu M, Paranjpe I, Leal JP, Wang R, et al. The effect of ApoE ε4 on longitudinal brain region-specific glucose metabolism in patients with mild cognitive impairment: a FDG-PET study. NeuroImage Clin 2019; 22: 101795.

Pascoal TA, Mathotaarachchi S, Shin M, Benedet AL, Mohades S, Wang S, et al. Synergistic interaction between amyloid and tau predicts the progression to dementia. Alzheimers Dement 2017; 13: 644–653.

Pontecorvo MJ, Devous MD, Navitsky M, Lu M, Salloway S, Schaerf FW, et al. Relationships between flortaucipir PET tau binding and amyloid burden, clinical diagnosis, age and cognition. Brain 2017; 140: 748–763.

Raber J, Huang Y, Ashford JW. ApoE genotype accounts for the vast majority of AD risk and AD pathology. Neurobiol Aging 2004; 25: 641–650.

Reiman EM, Chen K, Liu X, Bandy D, Yu M, Lee W, et al. Fibrillar amyloid-beta burden in cognitively normal people at 3 levels of genetic risk for Alzheimer's disease. Proc Natl Acad Sci U S A 2009; 106: 6820–6825.

Riedel BC, Thompson PM, Brinton RD. Age, APOE and sex: Triad of risk of Alzheimer's disease. J Steroid Biochem Mol Biol 2016; 160: 134–147.

Roberts BR, Lind M, Wagen AZ, Rembach A, Frugier T, Li QX, et al. Biochemically-defined pools of amyloid-β in sporadic Alzheimer's disease: Correlation with amyloid PET. Brain 2017; 140: 1486–1498.

Rodrigue KM, Kennedy KM, Devous MDS, Rieck JR, Hebrank AC, Diaz-Arrastia R, et al. β-Amyloid burden in healthy aging: regional distribution and cognitive consequences. Neurology 2012; 78: 387–395.

Salvadó G, Molinuevo JL, Brugulat-Serrat A, Falcon C, Grau-Rivera O, Suárez-Calvet M, et al. Centiloid cut-off values for optimal agreement

between PET and CSF core AD biomarkers. Alzheimer's Res Ther 2019; 11: 1–12.

Schelle J, Häsler LM, Göpfert JC, Joos TO, Vanderstichele H, Stoops E, et al. Prevention of tau increase in cerebrospinal fluid of APP transgenic mice suggests downstream effect of BACE1 inhibition. Alzheimers Dement 2017; 13: 701–709.

Schindler SE, Gray JD, Gordon BA, Xiong C, Batrla-Utermann R, Quan M, et al. Cerebrospinal fluid biomarkers measured by Elecsys assays compared to amyloid imaging. Alzheimer's Dement 2018: 1–10.

Schöll M, Lockhart SN, Schonhaut DR, O'Neil JP, Janabi M, Ossenkoppele R, et al. PET Imaging of Tau Deposition in the Aging Human Brain. Neuron 2016; 89: 971–982.

Schwarz AJ, Yu P, Miller BB, Shcherbinin S, Dickson J, Navitsky M, et al. Regional profiles of the candidate tau PET ligand 18F-AV-1451 recapitulate key features of Braak histopathological stages. Brain 2016; 139: 1539–1550.

Shimada H, Kitamura S, Shinotoh H, Endo H, Niwa F, Hirano S, et al. Association between Aβ and tau accumulations and their influence on clinical features in aging and Alzheimer's disease spectrum brains: A [(11)C]PBB3-PET study. Alzheimer's Dement (Amsterdam, Netherlands) 2017; 6: 11–20.

Sperling RA, Aisen PS, Beckett LA, Bennett DA, Craft S, Fagan AM, et al. Toward defining the preclinical stages of Alzheimer's disease. Alzheimer's Dement 2011; 7: 280–292.

Strozyk D, Blennow K, White LR, Launer LJ. CSF Aß 42 levels correlate with amyloid-neuropathology in a population-based autopsy study. Neurology 2003; 60: 652–656.

Tapiola T, Alafuzoff I, Herukka S-K, Parkkinen L, Hartikainen P, Soininen H, et al. Cerebrospinal Fluid β-Amyloid 42 and Tau Proteins as Biomarkers of Alzheimer-Type Pathologic Changes in the Brain. Arch Neurol 2009; 66: 382–389.

Teunissen CE, Tumani H, Engelborghs S, Mollenhauer B. Biobanking of CSF: international standardization to optimize biomarker development. Clin Biochem 2014; 47: 288–292.

Thal DR, Rüb U, Orantes M, Braak H. Phases of Aβ-deposition in the human brain and its relevance for the development of AD. Neurology 2002; 58: 1791–1800.

Therriault J, Benedet AL, Pascoal TA, Mathotaarachchi S, Chamoun M, Savard M, et al. Association of Apolipoprotein e ϵ4 with Medial Temporal Tau Independent of Amyloid-β. JAMA Neurol 2020; 77: 470–479.

Tiraboschi P, Hansen LA, Masliah E, Alford M, Thal LJ, Corey-Bloom J. Impact of APOE genotype on neuropathologic and neurochemical markers of Alzheimer disease. Neurology 2004; 62: 1977–1983.

Toledo JB, Bjerke M, Da X, Landau SM, Foster NL, Jagust W, et al. Nonlinear Association Between Cerebrospinal Fluid and Florbetapir F-18 β-Amyloid Measures Across the Spectrum of Alzheimer Disease. JAMA Neurol 2015; 72: 571–581.

Toledo JB, Habes M, Sotiras A, Bjerke M, Fan Y, Weiner MW, et al. APOE Effect on Amyloid-β PET Spatial Distribution, Deposition Rate, and Cut-Points. J Alzheimers Dis 2019; 69: 783–793.

Vogel JW, Iturria-Medina Y, Strandberg OT, Smith R, Levitis E, Evans AC, et al. Spread of pathological tau proteins through communicating neurons in human Alzheimer's disease. Nat Commun 2020; 11: 2612.

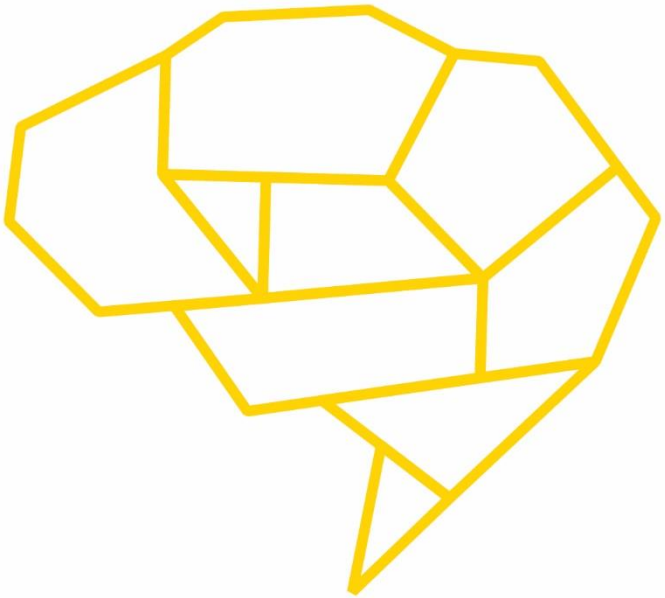

FOURTH STUDY:

Cerebral amyloid-β load is associated with neurodegeneration and gliosis: Mediation by p-tau and interactions with risk factors early in the Alzheimer's continuum

Received: 8 July 2020 | Revised: 6 October 2020 | Accepted: 24 October 2020

DOI: 10.1002/alz.12245

Alzheimer's & Dementia®
THE JOURNAL OF THE ALZHEIMER'S ASSOCIATION

RESEARCH ARTICLE

Cerebral amyloid-β load is associated with neurodegeneration and gliosis: Mediation by p-tau and interactions with risk factors early in the Alzheimer's *continuum*

Gemma Salvadó[1,2] | **Marta Milà-Alomà**[1,2,3,4] | **Mahnaz Shekari**[1,2,3] | **Carolina Minguillon**[1,2,4] | **Karine Fauria**[1,4] | **Aida Niñerola-Baizán**[5,6] | **Andrés Perissinotti**[5,6] | **Gwendlyn Kollmorgen**[7] | **Christopher Buckley**[8] | **Gill Farrar**[8] | **Henrik Zetterberg**[9,10,11,12] | **Kaj Blennow**[9,10] | **Marc Suárez-Calvet**[1,2,4,13] | **José Luis Molinuevo**[1] | **Juan Domingo Gispert**[1,2,3,6] | **for the ALFA study***

[1] Barcelonaβeta Brain Research Center (BBRC), Pasqual Maragall Foundation, Barcelona, Spain

[2] IMIM (Hospital del Mar Medical Research Institute), Barcelona, Spain

[3] Universitat Pompeu Fabra, Barcelona, Spain

[4] Centro de Investigación Biomédica en Red de Fragilidad y Envejecimiento Saludable (CIBERFES), Madrid, Spain

[5] Nuclear Medicine Department, Hospital Clínic Barcelona, Barcelona, Spain

[6] Centro de Investigación Biomédica en Red Bioingeniería, Biomateriales y Nanomedicina, (CIBER-BBN), Barcelona, Spain

[7] Roche Diagnostics GmbH, Penzberg, Germany

[8] GE Healthcare, Life Sciences, Amersham, UK

[9] Department of Psychiatry and Neurochemistry, Institute of Neuroscience and Physiology, University of Gothenburg, Mölndal, Sweden

[10] Clinical Neurochemistry Laboratory, Sahlgrenska University Hospital, Mölndal, Sweden

[11] Department of Neurodegenerative Disease, UCL Institute of Neurology, Queen Square, London, UK

[12] UK Dementia Research Institute at UCL, London, UK

[13] Servei de Neurologia, Hospital del Mar, Barcelona, Spain

Correspondence
Juan Domingo Gispert, Alzheimer Prevention Program, BarcelonaBeta Brain Research Center (BBRC), C/ Wellington, 30, 08005, Barcelona, Spain.
Email: jdgispert@barcelonabeta.org

*The complete list of collaborators of the ALFA Study can be found in the acknowledgements section.

Funding information
The project leading to these results has received funding from "la Caixa" Foundation (ID 100010434), under agreement LCF/PR/GN17/50300004 and the Alzheimer's Association and an international anonymous charity foundation through the TriBEKa Imag-

Abstract

Introduction: The association between cerebral amyloid-β accumulation and downstream CSF biomarkers is not fully understood, particularly in asymptomatic stages.

Methods: In 318 cognitively unimpaired participants, we assessed the association between amyloid-β PET (Centiloid), and cerebrospinal fluid (CSF) biomarkers of several pathophysiological pathways. Interactions by Alzheimer's disease risk factors (age, sex and *APOE-ε4*), and the mediation effect of tau and neurodegeneration were also investigated.

Results: Centiloids were positively associated with CSF biomarkers of tau pathology (p-tau), neurodegeneration (t-tau, NfL), synaptic dysfunction (neurogranin) and neuroinflammation (YKL-40, GFAP, sTREM2), presenting interactions with age (p-tau, t-tau, neurogranin) and sex (sTREM2, NfL). Most of these associations were mediated by p-tau, except for NfL. The interaction between sex and amyloid-β on sTREM2 and NfL was also tau-independent.

ing Platform project (TriBEKa-17-519007). Additional support has been received from the Universities and Research Secretariat, Ministry of Business and Knowledge of the Catalan Government under the grant no. 2017-SGR-892. MSC received funding from the European Union's Horizon 2020 Research and Innovation Program under the Marie Sklodowska-Curie action grant agreement No 752310, and currently receives funding from Instituto de Salud Carlos III (PI19/00155) and from the Spanish Ministry of Science, Innovation and Universities (Juan de la Cierva Programme grant IJC2018-037478-I). JDG is supported by the Spanish Ministry of Science and Innovation (RYC-2013-13054). HZ is a Wallenberg Scholar supported by grants from the Swedish Research Council (#2018-02532), the European Research Council (#681712), Swedish State Support for Clinical Research (#ALFGBG-720931), the Alzheimer Drug Discovery Foundation (ADDF), USA (#201809-2016862), and the UK Dementia Research Institute at UCL. KB holds the Torsten Söderberg Professorship in Medicine at the Royal Swedish Academy of Sciences, and is supported by the Swedish Research Council (#2017-00915), the Alzheimer Drug Discovery Foundation (ADDF), USA (#RDAPB-201809-2016615), the Swedish Alzheimer Foundation (#AF-742881), Hjärnfonden, Sweden (#FO2017-0243), a grant (#ALFGBG-715986) from the Swedish state under the agreement between the Swedish government and the County Councils, the ALF-agreement, and European Union Joint Program for Neurodegenerative Disorders (JPND2019-466-236).

Discussion: Early amyloid-β accumulation has a tau-independent effect on neurodegeneration and a tau-dependent effect on neuroinflammation. Besides, sex has a modifier effect on these associations independent of tau.

KEYWORDS
[^{18}F]flutemetamol, Alzheimer, biomarkers, glial activation, inflammation, modulation, neuronal injury, preclinical

1 | BACKGROUND

The pathological hallmarks of Alzheimer's disease (AD) are amyloid-β (Aβ) plaques and neurofibrillary tau tangles. According to the amyloid cascade hypothesis, Aβ accumulation is the earliest pathological event, which can start decades before symptoms, and it is followed by tau accumulation and neurodegeneration.[1] In addition, recent studies have reported the involvement of many other downstream pathophysiological processes during the early stages of the Alzheimer's *continuum*, even in asymptomatic individuals, including neuroinflammation, synaptic dysfunction and neuronal injury.[2,3]

Recent advances in the development of novel biomarkers have enabled us and others to track some of these processes through cerebrospinal fluid (CSF) or plasma biomarkers.[4–10] Studying the early changes in these biomarkers and their relationship with the main pathological hallmarks of Alzheimer's disease (AD) would allow us to better understand the role of these processes in the progression of AD. Understanding these mechanisms, especially in the earliest stages, can also be informative on novel possible drug targets for the prevention of AD.

In a previous study, we found that after CSF Aβ42/40 becomes positive, there is a steep increase in tau-related (phosphorylated tau [p-tau]) and synaptic dysfunction (neurogranin) CSF biomarkers and, to a lesser extent, in axonal injury (neurofilament light [NfL] and total tau [t-tau]) and glial biomarkers (soluble triggering receptor on myeloid cells 2 [sTREM2], YKL40, glial fibrillary acidic protein [GFAP]).[11] Despite the novelty of these findings, there were still important questions to be addressed. First, to assess whether cerebral Aβ deposition, as measured by Aβ PET, would also be associated with CSF biomarkers of downstream pathophysiological mechanisms. To this regard, it is important to note that Aβ measured in CSF and in PET probe different pools of Aβ,[12] and that aggregated Aβ (or Aβ load, as measured by Aβ PET) may have a different effect than soluble Aβ (as measure by CSF Aβ42/40). Second, to investigate whether age, sex and *APOE-ε4* status, the main unmodifiable AD risk factors, had also a modulation effect over the association between Aβ PET and the rest of CSF biomarkers. Finally, since these CSF biomarkers show a high level of collinearity at early asymptomatic AD stages, it remained to be determined to what extent these associations represented unique downstream alterations associated to Aβ or were driven by other correlated biomarkers. In this respect, we hypothesized that CSF p-tau would mediate several associations between cerebral Aβ load and CSF biomarkers.

With this in mind, we aimed to analyze the relationship between Aβ accumulation in the brain measured with [^{18}F]flutemetamol Aβ

RESEARCH IN CONTEXT

1. **Systematic review**: The authors reviewed the literature using traditional (eg. PubMed) sources. Several studies have been recently published about the association between novel CSF biomarkers for Alzheimer's disease (AD) and core AD biomarkers (ie. amyloid-β, t-tau and p-tau). Relevant citations are appropriately cited.
2. **Interpretation**: Unlike previous studies, we studied a wide range of biomarkers reflecting several pathophysiological mechanisms, we focused in the very early stages of the disease, and we assessed the modifier effects of AD risk factors. Moreover, we tested how tau pathology mediated the association between amyloid-β pathology and downstream neurodegeneration and neuroinflammation.
3. **Future directions**: This is a cross-sectional study. We will conduct a longitudinal study of these participants, which will allow us to have a better understanding of the evolution of these biomarkers in the early stages of AD.

PET and multiple biological pathways measured in CSF in the early Alzheimer's *continuum*. We also studied whether these associations were modified by the main risk factors for AD: age, sex and *APOE-ε4* status. We hypothesized that Aβ PET is associated with several downstream pathophysilogical processes, and these association are modified by age, sex and *APOE-ε4* status. Moreover, we assessed whether these associations were mediated by biomarkers of tau pathology and neurodegeneration. We hypothesized that CSF p-tau would mediate several associations between cerebral Aβ load and CSF biomarkers. To achieve these aims, we analyzed CSF biomarkers reflecting multiple Alzheimer's pathophysiological, including: tau pathology (CSF p-tau), neuronal injury (CSF t-tau and NfL), synaptic dysfunction (CSF neurogranin), inflammation and glial activation (sTREM2, YKL-40, GFAP, S100b and interleukin 6 [IL-6]), and also total α-synuclein.[2,4] All these analyses were performed in a cohort of 318 cognitively unimpaired participants. Remarkably, these participants had a relatively low mean [^{18}F]flutemetamol Aβ PET uptake, which allowed us to study very early pathophysiological changes associated with a low load of cerebral Aβ deposition.

2 | MATERIALS AND METHODS

2.1 | Participants

Participants of this study were part of the ALFA+ cohort, nested in the ALFA (for ALzheimer's and FAmilies) parent cohort.[13] The ALFA cohort was established as a research platform to characterize preclinical AD in 2,743 cognitively unimpaired individuals, aged between 45 and 75 years old, and enriched for family history of sporadic AD. ALFA+ participants were selected for a more comprehensive evaluation including a lumbar puncture (LP) and a [^{18}F]flutemetamol Aβ PET. All ALFA+ participants were cognitively unimpaired with a Mini-Mental State Examination (MMSE) above 26 and a Clinical Dementia Rating (CDR) of zero and were enriched for *APOE- ε4* allele carriership and family history of AD. We also measured delayed free recall from Free and Cued Selective Reminding Test (FCSRT, see Supplementary Material).[14] For this study, we included the first 318 consecutive participants that had usable CSF and Aβ PET data acquired in less than a year.

2.2 | CSF sampling

CSF Aβ_{42} was measured using the Elecsys® β- amyloid(1-42),[15] while t-tau and p-tau were measured using the electrochemiluminescence immunoassays Elecsys® Total-Tau and Phospho-Tau(181P) CSF on a fully automated cobas e 601 instrument (Roche Diagnostics International Ltd., Rotkreuz, Switzerland). The rest of the biomarkers (Aβ_{40}, NfL, neurogranin, YKL-40, GFAP, sTREM2, S100b, IL-6 and α-synuclein) were measured with robust prototype assays as part of the NeuroToolKit (Roche Diagnostics International Ltd., Rotkreuz, Switzerland) on a cobas e 411 and e 601 instruments). All available CSF biomarkers were used in this study. All measurements were performed at the Clinical Neurochemistry Laboratory, Sahlgrenska University Hospital, Mölndal, Sweden, by board-certified laboratory technicians who were blinded to diagnostic and other clinical data.

2.3 | Image acquisition

Imaging acquisition and preprocessing protocols have been described previously.[16] Briefly, all participants had a [^{18}F]flutemetamol PET scan and a T1-weighted MRI acquired within one year. PET imaging was conducted in a Siemens Biograph mCT (Siemens, Munich, Germany), following a cranial CT scan for attenuation correction. Participants were injected with 185 MBq (range 166.5 to 203.5 MBq) of [^{18}F]flutemetamol, and four frames of 5 min each were acquired 90 min post-injection. Finally, the T1-weighted 3D-Turbo field echo (TFE) sequence was acquired in a Philips 3 T Ingenia CX scanner (Philips, Amsterdam, Netherlands).

2.4 | Image processing

PET images were pre-processed following the standard Centiloid pipeline using Statistical parametric mapping (SPM12).[17] In brief, PET frames were first realigned and summed to obtain a unique PET image, which was then co-registered with the available T1-weighted MRI scan of the same participant. Then, MRIs were normalized to the MNI space, and the same transformation was then applied to the PET image. All PET images were visually inspected as a quality control procedure.

The intensity normalization was performed using the whole cerebellum as reference region, provided by the Centiloid working group on the GAAIN website (http://www.gaain.org/centiloid-project). We quantified the global Aβ load using the standard Centiloid region of interest (ROI) that can also be found on the GAAIN website. The ratio of standardized uptake values (SUVr) were transformed to Centiloids using a previously validated linear regression.[16] From T1-weighted images we derived normalized hippocampal volumes as described in the Supplementary Materials.

2.5 | Statistical analyses

CSF biomarker determination were inspected before performing any correlation studies with [^{18}F]flutemetamol PET uptake. Extreme values in CSF were excluded as specified in[11] (Supplementary Materials). We tested for normality of the distribution for each biomarker using the Kolmogorov-Smirnov test and visual inspection of histograms. Those CSF biomarkers that did not follow a normal distribution $\log_{10}$-transformed and Centiloid values were also $\log_2$-transformed. Cross-correlation between all CSF biomarkers were calculated using Pearson's correlation.

The first main analysis of this study aimed to assess the direct associations between Aβ load in the brain and all CSF biomarkers available. To this aim, we used each of the of the CSF biomarkers as variable of interest (dependent variable), and Aβ load (ie. Centiloids) as the independent variable in univariate general linear models (GLM). Age, sex, education and *APOE-ε4* status were added as covariates for all the models as shown in the following equation:

$$CSF\ biomarker \sim 1 + age + sex + education + APOE\varepsilon4 + \log(CL)$$

We also tested interaction effects between global cerebral Aβ load in the brain and main AD risk factors (ie, age, sex and *APOE-ε4* status) on each CSF biomarker. To test age interactions, we used a GLM model including a new variable that resulted from the product of age and Centiloids. To display the results of this interaction we divided the population in three age groups, using the tertiles of age, although this was not used for any statistical analysis. To test sex and *APOE-ε4* status interactions, we performed ANCOVAs using the same covariates as the previous models. The equations for the interaction are shown below:

$$CSF\ biomarker \sim 1 + sex + education + APOE\varepsilon4 + age * \log(CL)$$

$$CSF\ biomarker \sim 1 + age + education + APOE\varepsilon4 + sex * \log(CL)$$

$$CSF\ biomarker \sim 1 + age + sex + education + APOE\varepsilon4 * \log(CL)$$

As a complementary analysis we repeated the previous analyses replacing *log(CL)* by CSF Aβ42/40 ratio both only including the Aβ positive sub-group, as the association between CSF Aβ42/40 ratio and the rest of CSF biomarkers showed a change of slope in the Aβ positivity threshold (Figure S3).

Finally, we performed a mediation analysis between cerebral Aβ load and each of the CSF biomarkers using p-tau and/or NfL as mediators. The aim of this analysis was to understand whether the associations previously found between Aβ deposition and the other CSF biomarkers were partially, fully or not at all mediated by these biomarkers. We used the PROCESS version 3.4.1 toolbox from SPSS (www.processmacro.org)[18] to perform these analyses. In each model, Centiloid values were included as independent variable, CSF biomarkers as dependent variable, using the same covariates as in the previous analyses. Both p-tau and NfL were included as mediators in all initial models (except the one studying NfL), but discarded if they did not show a significant mediation effect. As a complementary analysis, we also repeated mediation models using CSF Aβ42/40 ratio as independent variable in the Aβ positive sub-group defined by CSF.

Finally, we repeated the main and interaction models including the significant mediators as covariates in each of the models to see whether these associations remained after adjusting by their mediators.

Other additional analyses regarding imaging biomarkers of neurodegeneration (hippocampal volumes) and cognition (MMSE and FCSRT) are presented in the Supplementary Materials, as well as Aβ PET analyses including only Aβ positive participants. Statistical significance was set at $P < .05$ without corrections for multiple comparisons for all analyses.

2.6 | Ethical statement

The ALFA+ study (ALFA-FPM-0311) was approved by the Independent Ethics Committee "Parc de Salut Mar," Barcelona, and registered at Clinicaltrials.gov (Identifier: NCT02485730). All participants signed the study's informed consent form that had also been approved by the Independent Ethics Committee "Parc de Salut Mar," Barcelona.

3 | RESULTS

Participants' demographics, CSF biomarker levels and PET measurements are summarized in Table 1. Their mean age was 61.4 years old, with a majority of women (62.6%) and more than half of the participants were *APOE-ε4* carriers (52.8%). The mean time difference between PET and LP was 97 days. Mean Aβ deposition for the whole cohort in the brain was low (mean CL: 2.7, range: −23.9 to 81.6). Importantly, those considered to be Aβ positive also have a low Aβ deposition compared to other cohorts (mean CL: 16.4, n = 109, Table S4), showing the early stage in the Alzheimer's *continuum* of this population. This can also be seen in the distribution of our participants in the A/T/(N) classification (Table S1).[19] All CSF biomarkers but sTREM2 were $\log_{10}$-transformed for following analyses as were not normally distributed.

CSF levels for the different biomarkers were highly correlated. Except for CSF IL-6, the rest of CSF biomarkers showed a significant correlation between them with high values (Figure S1).

TABLE 1 Participants' demographics and CSF and PET measures

N = 318	Mean (SD)
Demographics	
Age (years) [range]	61.4 (4.6) [50.4 to 74.3]
Women, n(%)	199 (62.6)
Education (years)	13.4 (3.5)
APOE-ε4 carriers, n(%)	168 (52.8)
Time difference LP - PET (days)	96.7 (67.4)
MMSE	29.2 (1.0)
FCSRT - Delayed free recall	11.6 (2.1)
CSF measures	
$A\beta_{1-42}$ (pg/mL) [range]	1328 (569) [307 to 3595]
$A\beta_{1-40}$ (ng/mL)	17.6 (5.0)
p-tau (pg/mL)	16.1 (6.3)
t-tau (pg/mL)	198 (68)
NfL (pg/mL)	81.5 (26.8)
Neurogranin (pg/mL)	805 (323)
GFAP (ng/mL)	7.5 (2.3)
YKL-40 (ng/mL)	148 (53)
sTREM2 (ng/mL)	7.9 (2.3)
S100b (ng/mL)	1.01 (0.22)
IL-6 (pg/mL)	3.8 (1.4)
α-synuclein (pg/mL)	199 (81)
PET measures	
Centiloids [range]	2.7 (16.6) [−23.9, 81.6]

Mean (SD) values are shown unless otherwise stated.
Aβ, amyloid-β; FCSRT, Free and Cued Selective Reminding Test; GFAP, glial fibrillary acidic protein; IL-6, interleukin 6; LP, lumbar puncture; MMSE, Mini-Mental State Examination; NfL, neurofilament light; p-tau, phosphorylated tau; SD, standard deviation; sTREM2, soluble triggering receptor on myeloid cells 2 (TREM2); t-tau; total tau.

3.1 | Associations of CSF biomarkers with cerebral Aβ load

In our global main analysis, we calculated the association between a global measure of Aβ load in the brain and all CSF biomarkers (Table 2). CSF p-tau, t-tau, NfL, neurogranin, GFAP, YKL-40, and sTREM2 showed a significant positive correlation with Centiloids. CSF S100b, IL-6 and α-synuclein did not show significant association. Similar associations were found when we took into account only the Aβ positive participants, except for CSF neurogranin and sTREM2 that became non-significant (Table S5).

For comparison purposes, we also repeated this analysis using CSF Aβ42/40 ratio as biomarker Aβ pathology, instead of Aβ PET. For this analysis we only included Aβ positive subjects. Similar results were found with this approach with only a significant association with α-synuclein as a difference (Table 2). Effect sizes found using CSF Aβ42/40 ratio were bigger than with those found using Aβ PET. However, this increase in effect sizes was also seen in PET analyses when we only considered Aβ positive subjects (Table S5). Therefore, we could say that analyses using CSF Aβ42/40 ratio were very similar to those using Aβ PET, although only considering Aβ positive participants.

3.2 | Age, sex, and APOE-ε4 interactions with Aβ load on CSF biomarkers

The first interaction effect tested in the association between Centiloids and CSF biomarkers was age. We found that this interaction was significant for CSF p-tau, t-tau and neurogranin (Table 2 and Figure 1). This was also true when we only included Aβ positive subjects (Table S5). Age-interaction also shows a trend to significance on sTREM2 and IL-6. All CSF biomarkers showed a more pronounced positive association with Centiloids with older age. No significant interactions with age were observed using CSF Aβ42/40 as a marker of Aβ pathology when only studying Aβ positive subjects (Table 2).

Regarding the interaction between sex and Centiloids, it was only significant for CSF NfL and sTREM2 (Table 2 and Figure 2). In both cases, women presented a higher correlation between CSF levels and Centiloids. Together with these two biomarkers, YKL-40 also showed a sex interaction when only Aβ positive participants were included (Table S5). In contrast, the sex interaction with CSF Aβ42/40 was also significant for CSF NfL and IL-6 for Aβ positive subjects (Table 2).

On the contrary, none of the CSF biomarkers showed a significant interaction between *APOE-ε4* status and Centiloids (both with the whole sample and Aβ positive participants). However, the interaction between CSF Aβ42/40 and *APOE-ε4* status was significant for α-synuclein in Aβ positive subjects (Table 2).

3.3 | Mediation effects of tau and neuronal injury biomarkers

Here, we tested whether the association between Centiloids and CSF biomarkers were mediated by tau pathology and/or neuronal injury, as measured by CSF p-tau and CSF NfL, respectively. We performed the mediation on those CSF biomarkers that showed a significant or a trend to a significant effect in the main association analyses (ie. CSF NfL, GFAP, YKL-40, and sTREM2). We did not include CSF t-tau or neurogranin in this analysis due to its high colinearity with CSF p-tau, ($r>0.9$, Figure S1). Figure 3 shows the final models whose mediators (CSF p-tau and/or NfL) showed at least a trend to significance in the mediation path. First, we observed that the Centiloids effect on CSF NfL was only partially mediated by CSF p-tau. This is shown by the

TABLE 2 Main and interactions effects of Aβ on CSF biomarkers

	Main effect		Age interaction		Sex interaction (F > M)		*APOE-ε4* interaction (C > NC)	
	Effect size [95% CI]	*P*	Effect size [95% CI]	*P*	Effect size [95% CI]	*P*	Effect size [95% CI]	*P*
Aβ PET (all subjects)								
p-tau	**0.30 [0.19 to 0.41]**	**<.001**	**0.17 [0.06 to 0.28]**	**.003**	0.06 [−0.05 to 0.17]	.302	−0.03 [−0.14 to 0.09]	.651
t-tau	**0.28 [0.17 to 0.39]**	**<.001**	**0.13 [0.02 to 0.24]**	**.017**	0.03 [−0.08 to 0.14]	.584	−0.04 [−0.15 to 0.07]	.483
NfL	**0.25 [0.14 to 0.36]**	**<.001**	0.07 [−0.04 to 0.18]	.201	**0.11 [0.00 to 0.22]**	**.045**	0.02 [−0.09 to 0.13]	.736
Neurogranin	**0.15 [0.04 to 0.26]**	**.009**	**0.12 [0.01 to 0.23]**	**.031**	0.04 [−0.07 to 0.15]	.451	−0.03 [−0.14 to 0.08]	.584
GFAP	**0.18 [0.07 to 0.29]**	**.001**	0.04 [−0.07 to 0.15]	.461	0.04 [−0.07 to 0.15]	.527	−0.04 [−0.15 to 0.07]	.452
YKL-40	**0.21 [0.10 to 0.32]**	**<.001**	0.06 [−0.05 to 0.17]	.261	0.10 [−0.01 to 0.21]	.085	−0.02 [−0.13 to 0.09]	.681
sTREM2	**0.13 [0.02 to 0.24]**	**.026**	0.11 [−0.00 to 0.22]	.051	**0.13 [0.02 to 0.24]**	**.021**	−0.04 [−0.15 to 0.07]	.522
S100b	0.09 [−0.03 to 0.20]	.130	−0.01 [−0.12 to 0.10]	.819	0.06 [−0.05 to 0.17]	.293	−0.07 [−0.18 to 0.04]	.229
IL-6	0.06 [−0.06 to 0.17]	.326	0.09 [−0.02 to 0.20]	.099	−0.01 [−0.12 to 0.10]	.857	0.01 [−0.10 to 0.12]	.856
α-synuclein	0.07 [−0.04 to 0.18]	.216	0.09 [−0.02 to 0.20]	.112	0.04 [−0.07 to 0.15]	.479	−0.11 [−0.21 to 0.01]	.065
CSF $Aβ_{42/40}$ ratio (Aβ positive subjects)								
p-tau	**−0.57 [−0.76, −0.38]**	**<.001**	−0.18 [0.37, 0.02]	.072	0.03 [−0.16, 0.22]	.758	0.19 [−0.01, 0.37]	.067
t-tau	**−0.54 [−0.73, −0.35]**	**<.001**	−0.14 [0.32, 0.06]	.172	0.02 [−0.17, 0.21]	.851	0.15 [−0.05, 0.33]	.153
NfL	**−0.34 [−0.53, −0.14]**	**.001**	−0.05 [−0.23, 0.15]	.655	**−0.20 [−0.38, −0.00]**	**.047**	0.15 [−0.05, 0.34]	.135
Neurogranin	**−0.48 [−0.67, −0.29]**	**<.001**	−0.08 [−0.27, 0.11]	.405	0.01 [−0.19, 0.20]	.951	0.19 [−0.00, 0.38]	.051
GFAP	**−0.27 [−0.46, −0.08]**	**.005**	0.10 [−0.10, 0.29]	.323	0.08 [−0.12, 0.27]	.432	−0.01 [−0.20, 0.18]	.935
YKL-40	**−0.46 [−0.65, −0.27]**	**<.001**	0.02 [−0.17, 0.21]	.867	0.01 [−0.18, 0.21]	.884	0.02 [−0.17, 0.21]	.820
sTREM2	**−0.19 [−0.38, −0.00]**	**.046**	−0.02 [−0.21, 0.17]	.815	−0.06 [−0.25, 0.13]	.533	−0.09 [−0.28, 0.11]	.382
S100b	−0.08 [−0.27, 0.11]	.405	0.20 [−0.00, 0.38]	.051	0.07 [−0.13, 0.26]	.498	−0.14 [−0.33, 0.05]	.260
IL-6	−0.08 [−0.27, 0.11]	.413	−0.11 [−0.29, 0.09]	.290	**−0.25 [−0.43, −0.04]**	**.017**	0.12 [−0.07, 0.31]	.230
α-synuclein	**−0.34 [−0.53, −0.15]**	**.001**	−0.01 [−0.20, 0.19]	.952	−0.02 [−0.21, 0.17]	.829	**0.20 [0.00, −0.38]**	**.047**

Aβ was assessed both with PET and CSF. In the analysis using CSF $Aβ_{42/40}$ ratio, only Aβ positive subjects were assessed due change of slopes between this Aβ marker and the rest of the CSF biomarkers in the Aβ cut-off for positivity (see Figure S2). Aβ positive participants' were defined as having CSF $Aβ_{42/40}$ ratio below 0.071.[11] Effect sizes are calculated as standardized betas. Significant effects ($P < .05$) are shown in bold. Models included age, sex, education and *APOE-ε4* status as covariates. Of note, the sign is reversed in the CSF analysis due to the inverse relationship between CSF Aβ and Aβ PET.
Aβ, amyloid-β; C, carrier; CI, confidence interval; F, female; GFAP, glial fibrillary acidic protein; IL-6, interleukin 6; M, male; NC, non-carrier; NfL, neurofilament light; p-tau, phosphorylated tau; sTREM2, soluble triggering receptor on myeloid cells 2 (TREM2); t-tau, total tau.

fact that the Centiloids direct effect on CSF NfL still showed a trend effect after adjusting by CSF p-tau (40.5% of total effect). In contrast, we found that the effect of Centiloids on CSF sTREM2 was fully mediated by CSF p-tau, but not by CSF NfL. Regarding GFAP and YKL-40, both had a significant two-step indirect effect of p-tau and NfL (ie. Centiloids → p-tau → GFAP/YKL-40 and Centiloids → NfL → GFAP/YKL-40); and also a three-step indirect effect of p-tau and NfL (ie. Centiloids → p-tau → NfL → GFAP/YKL-40). However, the biggest effect in both cases was seen in the indirect path involving p-tau (ie, Centiloids → p-tau → GFAP/YKL-40, GFAP: 56.6% and YKL-40: 95.3% of the total effect).

Similar results were observed when using CSF Aβ42/40 as independent variable in Aβ positive participants (Figure 3). CSF p-tau also mediated the association between CSF Aβ42/40 and NfL, but in this case, CSF Aβ42/40 direct effect on NfL was no longer significant. CSF GFAP was also mediated by both p-tau (66.2% of the total effect) and NfL (30.8% of the total effect). On the other hand, CSF YKL-40 was only mediated by p-tau. Finally, we did not perform the mediation analysis with CSF sTREM2 in this case, as it did not show a significant total effect.

3.4 | Associations between CSF biomarkers and Aβ load after adjusting for mediators

Finally, we repeated the main association models as well as the ones including interaction effects but adjusting by the significant mediators found in the previous analyses. These analyses were only repeated for those CSF biomarkers and associations that were significant in the main analyses using Aβ PET. These analyses had the objective of disentangling whether these associations or interactions were independent of p-tau and/or NfL indirect effects. As shown in Table 3, none of the main associations between Aβ load and the CSF biomarkers studied remained significant after adjusting by their specific mediators. Similarly, CSF NfL and age interaction became non-significant after including mediators as covariates. Finally, we found that the interaction effect

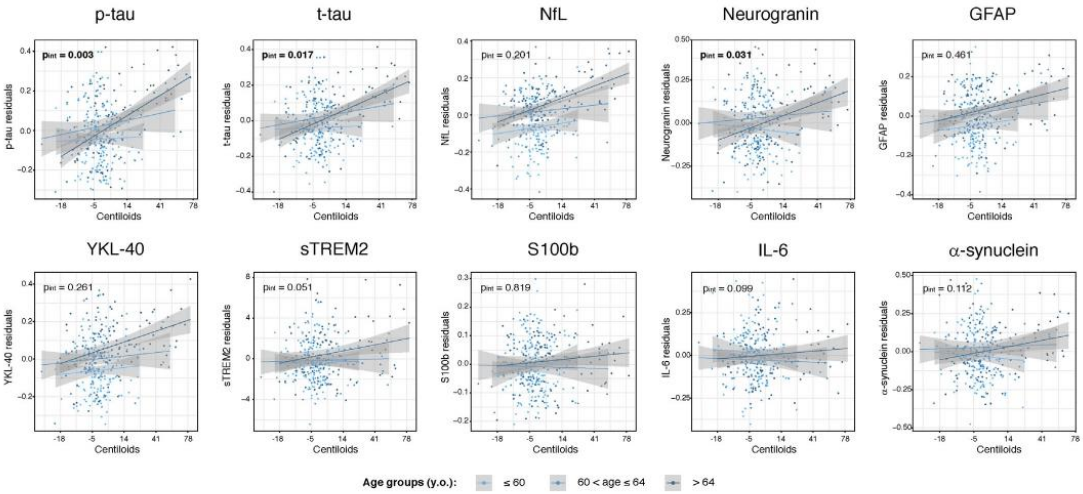

FIGURE 1 Age and Aβ interaction effects on CSF biomarkers. CSF biomarkers residuals, after adjusting by covariates (sex, education, and *APOE-ε4* status), are compared to global Aβ load measured as Centiloids. Light, medium and dark blue colors depict the three age groups (tertiles): below 60, between 60 and 64 and, above 64 years old, respectively. These groups were used for visualization purposes only. *P*-value of each interaction effect is shown in the upper left corner. Statistically significant effects ($P < .05$) are shown in bold. x axis is depicted in logarithmic scale. Aβ, amyloid-β; GFAP, glial fibrillary acidic protein; IL-6, interleukin 6; NfL, neurofilament light; p-tau, phosphorylated tau; sTREM2, soluble triggering receptor on myeloid cells 2 (TREM2); t-tau, total tau

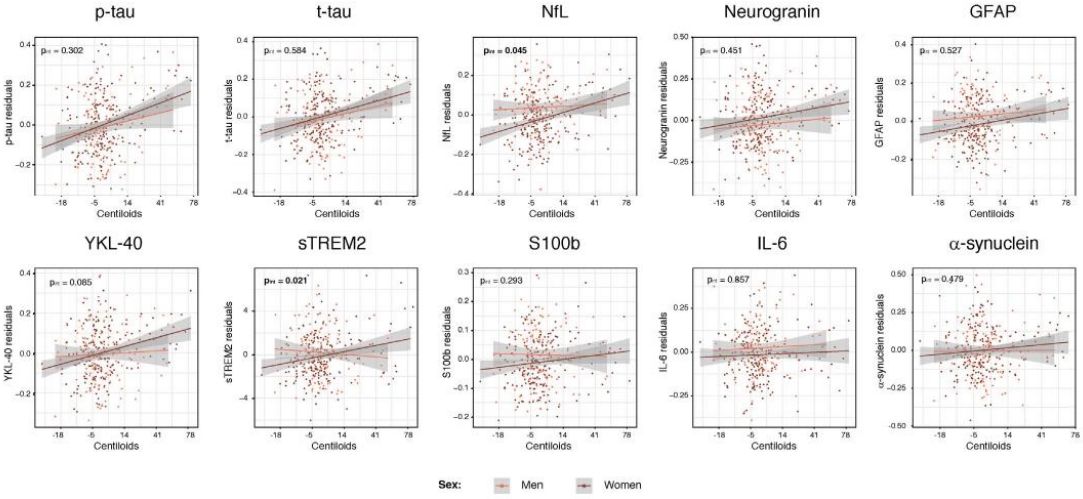

FIGURE 2 Sex and Aβ interaction effects on CSF biomarkers. CSF biomarkers residuals, after adjusting by covariates (age, education, and *APOE-ε4* status), are compared to global Aβ load measured as Centiloids. Colors represent the two sex groups, with women depicted in dark coral. *P*-value of each interaction effect is shown in the upper left corner. Statistically significant effects ($P < .05$) are shown in bold. x axis is depicted in logarithmic scale. Aβ, amyloid-β; GFAP, glial fibrillary acidic protein; IL-6, interleukin 6; NfL, neurofilament light; p-tau, phosphorylated tau; sTREM2, soluble triggering receptor on myeloid cells 2 (TREM2); t-tau, total tau

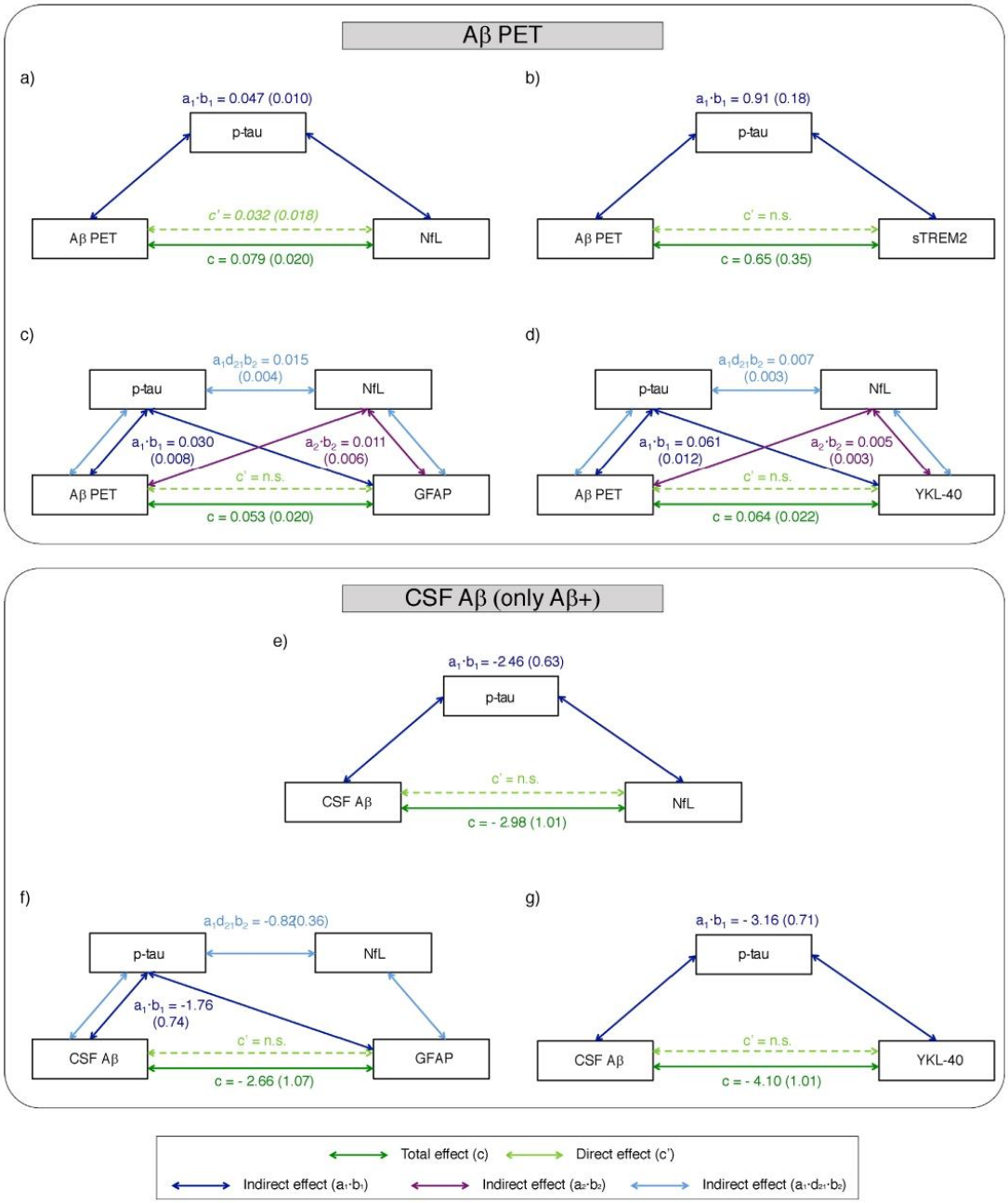

FIGURE 3 Aβ mediated effects on CSF biomarkers. Models of mediation for CSF NfL (A,E), sTREM2 (B), GFAP (C,F) and YKL-40 (D,G) with Aβ PET (upper part) and CSF Aβ (lower part). Models with CSF Aβ as independent variable only included Aβ positive participants (n = 109). The values of each path show the effect (SE). Total effect between Aβ load and each CSF biomarker is shown in dark green (path c); direct effect, after adjusting by mediators, is shown in light green (path c'); and indirect effects are shown in dark blue (path a_1b_1, mediation effect of p-tau), in purple (path a_2b_2, mediation effect of NfL) and in light blue (path $a_1 \cdot d_{21} \cdot b_2$, mediation effect of p-tau and NfL). All paths depicted are significant ($P < .05$), except for direct effect between Aβ and NfL that showed a trend to significance ($P < .10$, in italics). All paths are adjusted by covariates (age, sex, education, and *APOE-ε4* status). Aβ, amyloid-β; GFAP, glial fibrillary acidic protein; IL-6, interleukin 6; NfL, neurofilament light; p-tau, phosphorylated tau; sTREM2, soluble triggering receptor on myeloid cells 2 (TREM2).

TABLE 3 Main and interactions effects of Aβ load on CSF biomarkers after adjusting by specific mediators

	Main effect		Age interaction		Sex interaction (F > M)	
CSF biomarker	Effect size [95% CI]	P	Effect size [95% CI]	P	Effect size [95% CI]	P
NfL (adj p-tau)	0.10 [−0.01 to 0.21]	.082	0.00 [−0.11 to 0.11]	.958	0.10 [−0.01 to 0.21]	.077
GFAP (adj p-tau & NfL)	−0.01 [−0.12 to 0.10]	.853	-	-	-	-
YKL-40 (adj p-tau & NfL)	−0.03 [−0.14 to 0.08]	.632	-	-	-	-
sTREM2 (adj p-tau)	−0.05 [−0.16 to 0.06]	.410	-	-	**0.13 [0.02 to 0.24]**	**.023**

Association parameters between CSF biomarkers and global Aβ deposition for the main and interaction effects after adjusting by significant mediators. Only those associations that were significant without mediators (shown in Table 2) were tested. Effect sizes are calculated as standardized betas. Significant effects ($P < .05$) are shown in bold.
Aβ, amyloid-β; CI, confidence interval; F, female; GFAP, glial fibrillary acidic protein; M, male; NfL, neurofilament light; p-tau, phosphorylated tau; sTREM2, soluble triggering receptor on myeloid cells 2 (TREM2).

between sex and Aβ load on CSF sTREM2 was still significant after adjusting by CSF p-tau.

4 | DISCUSSION

In this study, we investigated the relationship between Aβ load in the brain, as measured by PET, and CSF biomarkers of pathophysiological processes downstream to Aβ in a cohort of cognitively unimpaired participants. Remarkably, some of them were in a very early stage of the Alzheimer's *continuum*, as shown by a very low load of Aβ load. Our first finding was that markers of tau pathology (CSF p-tau), neuronal injury (CSF t-tau and NfL), synaptic dysfunction (CSF neurogranin), and neuroinflammation (CSF GFAP, YKL-40, and sTREM2) showed a positive association with Aβ load, even at this early stage. Interestingly, we found that age and sex, but not *APOE-ε4* status, had a modulatory influence on some of these relationships. There was a stronger association between Aβ PET and CSF biomarkers in older individuals and in women. Finally, as some of these CSF biomarkers were highly correlated, we performed mediation analyses to disentangle the ones driving the observed associations. We found that the association of Aβ PET with CSF NfL, a marker of neuronal injury, was only partially mediated by tau pathology (CSF p-tau) suggesting a direct effect of Aβ deposition on neurodegeneration. In contrast, almost all the associations of Aβ PET with inflammatory markers (ie. CSF GFAP, YKL-40, and sTREM2), as well as their respective interactions with AD risk factors, were mediated by CSF biomarkers of tau pathology (CSF p-tau), alone or in combination with neuronal injury (CSF NfL). The only exception was the interaction between sex and Aβ load on CSF sTREM2 (and between sex and CSF NfL, at a trend level) that remained significant after correction for CSF p-tau.

Previously, it was reported in older subjects with cognitive impairment associations between Aβ PET and several CSF biomarkers, including CSF p-tau, t-tau, neurogranin, NfL and YKL-40.[20,21] However, less is known in preclinical Alzheimer. Herein, we extend these findings to younger individuals without objective cognitive impairment associations. In line with our findings, a recent study by Palmqvist et al. showed changes in CSF p-tau, neurogranin, NfL, and YKL-40 associated with Aβ load measured with PET.[20] Similar results were also found in another recent study by Bos et al., in which the authors reported an association between CSF Aβ and NfL, neurogranin and YKL-40 in cognitively unimpaired participants.[21] With respect to these reports, our sample is younger (mean age of 61.4 vs 72.1 years old) and does not include mild cognitive impairment (MCI) patients. Importantly, we included a relatively high percentage of individuals (25%, see Table S1) that were Aβ positive (as defined by CSF Aβ42/40) but still tau negative (as defined by CSF p-tau). It can thus be considered that our study focuses on an earlier stage in the Alzheimer's *continuum* and in late-/middle-aged individuals, when Alzheimer's pathology most likely starts. In addition, we also detected associations between Aβ load and additional neuroinflammatory markers (CSF GFAP and sTREM2) that, to the best of our knowledge, have not been previously described. It is important to note that the vast majority of these associations remained significant even when we only analyzed Aβ positive participants, both measuring CSF Aβ42/40 and Aβ PET load (see Table 2 and Table S5).

Mounting evidence suggests that women are at increased risk of AD,[22] but the biological explanation of this difference is still unknown. Neither Aβ load nor its accumulation over time seem to be the cause as multiple studies found no difference in Aβ by sex,[23–26] which is replicated in our study (data not shown). In our previous study, we found that CSF NfL was significantly lower than in women.[11] But in the present study we discovered that this difference was related to Aβ load; as we revealed that CSF NfL levels had a steeper increase in women with higher Aβ load than men, with women having lower CSF NfL with low Aβ load but higher CSF NfL with high Aβ load. This effect was also seen even after correcting for CSF p-tau (trend level) or when measuring Aβ pathology in the CSF. Previous studies already reported higher levels of neurodegeneration in women,[27,28] particularly in *APOE-ε4* carriers, and have been related to their worse clinical output, although this was not replicated in all cases.[26] Our result confirmed this in a younger and earlier in the Alzheimer's *continuum* population. What is new in our study is that we find that these differences are related to Aβ pathology load and irrespective of tau pathology. This result suggests that women may show a tighter coupling between Aβ pathology and neurodegeneration, which may contribute to explain their higher risk of AD, independently of their tau levels.

Another novelty of our study was finding an interaction between sex and Aβ load on sTREM2. Women presented more elevated levels of

CSF sTREM2 with increasing Aβ load than men, although their global measures did not differ.[11] Of note, this difference in slope with increasing Aβ was independent of tau pathology. Whether this is a protective or detrimental effect for women against Aβ cannot be stated. The role of microglial activation, and in particular of TREM2-mediated microglia function, in AD is still not fully understood, and it has been suggested that could have different effects depending on the stage of the disease, being beneficial at early stages but detrimental at later ones.[3,29–31] Sex differences in microglial activation have been reported before in mice.[32] Also, recently early sex differential patterns of atrophy were related to glial biomarkers with a greater impact in areas of the Papez circuit in women and greater impact in men in lateral parietal and paracentral areas.[33]

We also found an interaction between age and Aβ load on p-tau and t-tau, suggesting that for the same levels of Aβ PET-measured pathology, older individuals have increased tau pathology. To the best of our knowledge, this has not been reported before and, therefore, needs replication. However, multiple hypotheses may explain this behavior. On one hand, older subjects have an increased probability to have other comorbidities which can decrease their resistance to tau pathology and neurodegeneration.[34] On another hand, it is possible that biological pathways that may help to slow-down the spreading of tau pathology once Aβ is present (ie. glial activation), become less effective in older ages.[35] CSF neurogranin, sTREM2 and IL-6 (the two last at a trend level) also had a significant Aβ*age interaction, however, these interactions became non-significant when we adjusted by tau pathology. This suggests that their initial relationship was mainly driven by the actual interaction of age and Aβ on p-tau.

The association between CSF NfL, a marker of neuronal injury, and Aβ PET or CSF Aβ has been reported before.[11,20,21] However, whether this association is mediated by tau pathology is unknown and, therefore, we conducted a mediation analysis. Interestingly, we found a tau-dependent but also a relevant tau-independent effect of Aβ PET on CSF NfL (40.5% of the total effect, Figure 3). This is in line with a recent publication that shows a direct effect of Aβ accumulation on CSF NfL levels and neurodegeneration in AD-regions in a rat model with minimal tau pathology.[36] In the same study, these results were replicated in humans even when accounting for tau pathology. Altogether, this result suggests that Aβ load has, at least, a partial direct effect on neurodegeneration in early stages of Alzheimer's *continuum*. It is important to note, that this Aβ-direct effect over CSF NfL did not remain significant when we studied this model using CSF Aβ42/40 in positive participants. We speculate that there may be two reasons underlying these findings, which are not mutually exclusive. First, that soluble Aβ changes first triggers tau metabolism changes and, after that, neurodegeneration occurs. This is supported by the fact that there is an active secretion of p-tau in response of Aβ early changes.[37–40] Second, there is the possibility that Aβ-direct effect on neurodegeneration may be most important in later stages of the Alzheimer's *continuum*, when the progression of AD pathology can still be tracked by PET and no longer by CSF Aβ and due to other mechanisms, such as inflammation or actual physical damage by the plaques. Then, after both Aβ and tau pathology increase, this association may be fully driven by tau pathology, which agrees with previous studies finding a direct association between tau -but not Aβ- and neurodegeneration.[41,42] However, longitudinal investigations in participants in the very early stages of the Alzheimer's *continuum* are needed to confirm this hypothesis.

Overall, three markers of neuroinflammation showed associations with Aβ pathology in this study: one related to microglial activation (sTREM2), and two related to astroglial reactivity (YKL-40 and GFAP). sTREM2 is the soluble ectodomain of the TREM2 receptor, mainly expressed in microglia in the central nervous system. Previous studies have shown that CSF sTREM2 levels are elevated in late asymptomatic (once participants have changes in tau-related biomarkers) and early symptomatic stages of familial and sporadic AD.[43–47] Recently, we found that CSF sTREM2 was increased in Aβ and tau positive cognitively unimpaired individuals but not in those that were Aβ positive but tau negative.[11] Considering that Aβ PET changes later than CSF Aβ,[48–50] the associations that we observe here between Aβ PET and CSF sTREM2 reinforce the idea that CSF sTREM2 increases are not as soon as the first changes in CSF Aβ42/40. Also supporting this hypothesis, we found that CSF sTREM2 only showed an association with CSF Aβ42/40 in our cohort when Aβ-positive participants were considered, suggesting that this association may relate to later stages of preclinical AD pathophysiology. Our mediation analyses allowed us to determine, whether this association was possibly due to collinearity with other CSF biomarkers or a singular association with Aβ PET load. The fact that this association was fully mediated by CSF p-tau is in line with the hypothesis that CSF sTREM2 increases with the early changes in tau biomarkers.

We also found associations between cerebral Aβ load -and CSF Aβ- and astroglial markers (YKL-40 and GFAP). To our knowledge, this is the first study to show an association between Aβ load and CSF GFAP, although we previously showed this association with CSF Aβ42/40.[11] On the other hand, previous studies only reported associations between CSF YKL-40 with tau levels but not with Aβ in CSF,[51,52] except for our previous study only in Aβ positive participants.[11] To this regard, and like CSF sTREM2, we found the association between astroglial markers and Aβ to be fully mediated by p-tau levels. This pinpoints the importance of this analysis to understand the underlying associations between a set of CSF biomarkers that were highly correlated. The fact that p-tau fully mediated the association between Aβ and astroglial markers is in line with the hypothesis that levels of glial markers parallel those of tau biomarkers.[43–47,51,52] Some of these previous publications also found an association of glial markers, not only with tau, but also with markers of neuronal injury (ie, t-tau and NfL) and imaging markers of neurodegeneration.[43,45,46,52,53] In line with these, we also found CSF NfL to mediate the association between Aβ load and astroglial markers, but not CSF sTREM2. However, both for CSF GFAP and YKL-40, the effect size of this mediation was considerably lower than that of CSF p-tau (GFAP: p-tau effect = 56.6%; YKL-40: p-tau effect = 95.3%). Moreover, NfL mediation effect did not remain significant when only Aβ positive subjects were studied. Such a weak association may be explained by the almost complete lack of neurodegeneration positive individuals in our sample: only three participants (0.9%) were A+T+N+, see Table S1).[19] The follow-up of these participants will

enable us to study whether this association is replicated when they will be more advanced in the Alzheimer's *continuum*. Altogether, we hypothesize that the neuroinflammatory response in this early phase of AD probably follows the early changes of tau pathology and, to a lower extent, of neurodegeneration. Of note, in the mediation analysis, we used CSF NfL, and not CSF t-tau, as a marker of neurodegeneration due to the colinearity observed between the latter and p-tau (r>0.98, Figure S1). Moreover, recent publications suggest that CSF NfL may be a better neurodegeneration biomarker than CSF t-tau for AD.[54–56]

In this study, we considered the associations, and interactions, found between Aβ-downstream CSF biomarkers and Aβ load as the main results. However, we also performed complementary analyses using CSF Aβ42/40 ratio as a proxy of Aβ pathology. In these last analyses, we focused on Aβ positive participants only, as we found that associations between CSF Aβ and the rest of CSF biomarkers were highly modified by Aβ status (see Figure S3). However, even only focusing in a subset of participants, we found that the results of Aβ main effects on the other CSF biomarkers to be very similar. On the contrary, many of the interactions found between AD risk factors and Aβ load were not significant with CSF Aβ and, also other became significant such as with *APOE-ε4* status on α-synuclein when using CSF Aβ. This result may be related to the fact that, although both measures are usually used as Aβ biomarkers, they are measuring different pools of Aβ,[12] and although they are usually used as indistinguishable clinical biomarkers, differences between them has shown to have consequences on future tau deposition.[57] Therefore, it is possible that AD risk factors affect differently the Aβ production/clearance imbalance (as measured in CSF) and Aβ plaque production (as measured in PET), as we have seen in a previous study of our group with *APOE-ε4* status.[58]

The main strengths of this study are: (1) the availability of many different CSF biomarkers that allowed us to study, in the same individuals, the relationship between Aβ and many other pathophysiological processes, which their role in the AD development is still unknown; (2) the inclusion of many cognitively unimpaired participants with low or very low levels of Aβ deposited in the brain resulting in an increased statistical power to detect the earliest changes in the Alzheimer's *continuum*; and (3) the comparison between associations with Aβ both measured in PET and in CSF. Nonetheless, there are also some limitations to note. The cross-sectional design of this study gives us a picture of all the processes occurring but cannot tell us its implications on future developments. In particular, it is worth noting that mediation models in cross-sectional data do not allow testing for causality. This will be analyzed in the follow-up of these participants that is already on-going. Another limitation was the high correlation between almost all CSF biomarkers that makes it difficult to disentangle each specific association with Aβ. Finally, due to the exploratory nature of this study, we did not correct for multiple comparisons. Worth to note, all main associations survived FDR-correction, but none of the interaction effects did, which may be due to limited statistical power. Further investigations are needed to validate these results in independent cohorts.

As a conclusion, our results suggest that Aβ deposition in the brain is associated with many biological pathways in very early stages of the Alzheimer's *continuum*, notably including neurodegeneration, even after accounting for the effect of tau physiopathology. On the other hand, tau, alone or in combination with neurodegeneration, fully accounts for the observed association between Aβ deposition and glial response. From a clinical point of view, a better understanding of the pathophysiological mechanisms triggered by early AD pathology may provide novel insights to develop therapeutical strategies to interfere with the course of the disease in preclinical AD stages. Our results may help to better understand the sequence of events that occur in preclinical Alzheimer, which can be very valuable in trials design. More specifically, our results suggest that removing deposited Aβ in the brain may impact on future neurodegeneration. And also that targeting tau pathology, may have consequences on other pathophysiological mechanisms in Alzheimer's, such as inflammation, even at the earliest stages of the Alzheimer's *continuum*. Finally, in the context of precision medicine for future AD treatments, as suggested by our results, it may be important to also take into account subject's characteristics that may modify the course of these mechanisms, such as age or sex.

ACKNOWLEDGMENTS

This publication is part of the ALFA study (ALzheimer and FAmilies). The authors would like to express their most sincere gratitude to the ALFA project participants and relatives without whom this research would have not been possible. Collaborators of the ALFA study are: Annabella Beteta, Raffaele Cacciaglia, Alba Cañas, Carme Deulofeu, Ruth Dominguez, Maria Emilio, Carles Falcon, Sherezade Fuentes, Oriol Grau-Rivera, Laura Hernandez, Gema Huesa, Jordi Huguet, Eider M. Arenaza-Urquijo, Paula Marne, Tania Menchón, Grégory Operto, Albina Polo, Sandra Pradas, Aleix Sala-Vila, Gonzalo Sánchez-Benavides, Anna Soteras, Marc Vilanova and Natalia Vilor-Tejedor. The authors thank Roche Diagnostics International Ltd. for providing the kits to measure CSF biomarkers and GE Healthcare for providing the doses for [^{18}F]flutemetamol PET. ELECSYS, COBAS, and COBAS E are trademarks of Roche.

CONFLICT OF INTERESTS

JLM is currently a full time employee of H. Lundbeck A/S and priory has served as a consultant or at advisory boards for the following for-profit companies, or has given lectures in symposia sponsored by the following for-profit companies: Roche Diagnostics, Genentech, Novartis, Lundbeck, Oryzon, Biogen, Lilly, Janssen, Green Valley, MSD, Eisai, Alector, BioCross, GE Healthcare, ProMIS Neurosciences. HZ has served at scientific advisory boards for Denali, Roche Diagnostics, Wave, Samumed, Siemens Healthineers, Pinteon Therapeutics and CogRx, has given lectures in symposia sponsored by Fujirebio, Alzecure and Biogen, and is a co-founder of Brain Biomarker Solutions in Gothenburg AB (BBS), which is a part of the GU Ventures Incubator Program (outside submitted work). KB has served as a consultant, at advisory boards, or at data monitoring committees for Abcam, Axon, Biogen, JOMDD/Shimadzu. Julius Clinical, Lilly, MagQu, Novartis, Roche Diagnostics, and Siemens Healthineers, and is a co-founder of Brain Biomarker Solutions in Gothenburg AB (BBS), which is a part of the GU Ventures Incubator Program. GK is a full time employee

of Roche Diagnostics GmbH. The remaining authors declare that they have no conflict of interest.

REFERENCES

1. Jack CR, Knopman DS, Jagust WJ, et al. Tracking pathophysiological processes in Alzheimer's disease: an updated hypothetical model of dynamic biomarkers. *Lancet Neurol* 2013;12:207-216.
2. Milà-Alomà M, Suárez-Calvet M, Molinuevo JL. Latest advances in cerebrospinal fluid and blood biomarkers of Alzheimer's disease. *Ther Adv Neurol Disord* 2019;12:1-23. https://doi.org/10.1177/https.
3. Heneka MT, Carson MJ, El Khoury J, et al. Neuroinflammation in Alzheimer's disease. *Lancet Neurol* 2015;14:388-405.
4. Molinuevo JL, Ayton S, Batrla R, Bednar MM, Bittner T, Cummings J, Fagan AM, Hampel H, Mielke MM, Mikulskis A, O'Bryant S, Scheltens P, Sevigny J, Shaw LM, Soares HD, Tong G, Trojanowski JQ, Zetterberg H, Blennow K. Current state of Alzheimer's fluid biomarkers. *Acta Neuropathologica* 2018;136(6):821-853. http://doi.org/10.1007/s00401-018-1932-x.
5. Palmqvist S, Insel PS, Stomrud E, et al. Cerebrospinal fluid and plasma biomarker trajectories with increasing amyloid deposition in Alzheimer's disease. *EMBO Mol Med* 2019;11:e11170. https://doi.org/10.15252/emmm.201911170.
6. Fagan AM, Xiong C, Jasielec MS, et al. Longitudinal change in CSF biomarkers in autosomal-dominant Alzheimer's disease. *Sci Transl Med* 2014;6:226ra30. https://doi.org/10.1126/scitranslmed.3007901.
7. Schindler SE, Li Y, Todd KW, et al. Emerging cerebrospinal fluid biomarkers in autosomal dominant Alzheimer's disease. *Alzheimers Dement* 2019;15:655-665.
8. McDade E, Wang G, Gordon BA, et al. Longitudinal cognitive and biomarker changes in dominantly inherited Alzheimer disease. *Neurology* 2018;91:E1295-E306.
9. Fleisher AS, Chen K, Quiroz YT, et al. Associations between biomarkers and age in the presenilin 1 E280A autosomal dominant Alzheimer disease kindred: a cross-sectional study. *JAMA Neurol* 2015;72:316-324.
10. Lleó A, Alcolea D, Martínez-Lage P, et al. Longitudinal cerebrospinal fluid biomarker trajectories along the Alzheimer's disease continuum in the BIOMARKAPD study. *Alzheimers Dement* 2019;15:742-753.
11. Milà-Alomà M, Salvadó G, Gispert JD, et al. Amyloid-β, tau, synaptic, neurodegeneration and glial biomarkers in the preclinical stage of the Alzheimer's continuum. *Alzheimers Dement* 2020;16:1358-1371.
12. Roberts BR, Lind M, Wagen AZ, et al. Biochemically-defined pools of amyloid-β in sporadic Alzheimer's disease: correlation with amyloid PET. *Brain* 2017;140:1486-1498.
13. Molinuevo JL, Gramunt N, Gispert JD, et al. The ALFA project: a research platform to identify early pathophysiological features of Alzheimer's disease. *Alzheimers Dement* 2016;2:82-92.
14. Buschke H, Kuslansky G, Katz M, et al. Screening for dementia with the Memory Impairment Screen. *Neurology* 1999;52:231-238.
15. Bittner T, Zetterberg H, Teunissen CE, et al. Technical performance of a novel, fully automated electrochemiluminescence immunoassay for the quantitation of β-amyloid (1-42) in human cerebrospinal fluid. *Alzheimers Dement* 2016;12:517-526.
16. Salvadó G, Molinuevo JL, Brugulat-Serrat A, et al. Centiloid cut-off values for optimal agreement between PET and CSF core AD biomarkers. *Alzheimers Res Ther* 2019;11:27. https://doi.org/10.1186/s13195-019-0478-z.
17. Klunk WE, Koeppe RA, Price JC, et al. The Centiloid project: standardizing quantitative amyloid plaque estimation by PET. *Alzheimers Dement* 2015;11:1-15.e4. https://doi.org/10.1016/j.jalz.2014.07.003.
18. Hayes AF. *Introduction to Mediation, Moderation, and Conditional Process Analysis: A Regression-Based Approach*. 2nd ed. New York, NY: Guilford Press; 2018.
19. Jack CR, Bennett DA, Blennow K, et al. A/T/N: an unbiased descriptive classification scheme for Alzheimer disease biomarkers. *Neurology* 2016;87:539-547.
20. Palmqvist S, Insel PS, Stomrud E, et al. Cerebrospinal fluid and plasma biomarker trajectories with increasing amyloid deposition in Alzheimer's disease. *EMBO Mol Med* 2019;11:e11170. https://doi.org/10.15252/emmm.201911170.
21. Bos I, Vos S, Verhey F, Scheltens P, et al. Cerebrospinal fluid biomarkers of neurodegeneration, synaptic integrity, and astroglial activation across the clinical Alzheimer's disease spectrum. *Alzheimers Dement* 2019;15:644-654.
22. Fisher DW, Bennett DA, Dong H. Sexual dimorphism in predisposition to Alzheimer's disease. *Neurobiol Aging* 2018;70:308-324.
23. Buckley RF, Mormino EC, Amariglio RE, et al. Sex, amyloid, and APOE ε4 and risk of cognitive decline in preclinical Alzheimer's disease: Findings from three well-characterized cohorts. *Alzheimers Dement* 2018;14:1193-1203.
24. Altmann A, Tian L, Henderson VW, Greicius MD. Sex modifies the APOE-related risk of developing Alzheimer disease. *Ann Neurol* 2014;75:563-573.
25. Weiner MW, Veitch DP, Aisen PS, et al. 2014 Update of the Alzheimer's Disease Neuroimaging Initiative: a review of papers published since its inception. *Alzheimers Dement* 2015;11:e1-120. https://doi.org/10.1016/j.jalz.2014.11.001.
26. Jack CR, Wiste HJ, Weigand SD, et al. Age, sex, and APOE ε4 effects on memory, brain structure, and β-Amyloid across the adult life Span. *JAMA Neurol* 2015;72:511-519.
27. Sampedro F, Vilaplana E, de Leon MJ, et al. APOE-by-sex interactions on brain structure and metabolism in healthy elderly controls. *Oncotarget* 2015;6:26663-26674.
28. Holland D, Desikan RS, Dale AM, McEvoy LK. Higher rates of decline for women and apolipoprotein e ε4 carriers. *Am J Neuroradiol* 2013;34:2287-2293.
29. Hamelin L, Lagarde J, Dorothée G, et al. Distinct dynamic profiles of microglial activation are associated with progression of Alzheimer's disease. *Brain* 2018;141:1855-1870.
30. Parhizkar S, Arzberger T, Brendel M, et al. Loss of TREM2 function increases amyloid seeding but reduces plaque-associated ApoE. *Nat Neurosci* 2019;22:191-204.
31. Gratuze M, Leyns CEG, Holtzman DM. New insights into the role of TREM2 in Alzheimer's disease. *Mol Neurodegener* 2018;13:66. https://doi.org/10.1186/s13024-018-0298-9.
32. Yang JT, Wang ZJ, Cai HY, et al. Sex differences in neuropathology and cognitive behavior in APP/PS1/tau Triple-transgenic mouse model of Alzheimer's disease. *Neurosci Bull* 2018;34:736-746.
33. Falcon C, Grau-Rivera O, Suárez-Calvet M, et al. Sex differences of longitudinal brain changes in cognitively unimpaired adults. *J Alzheimers Dis* 2020;1-9. https://doi.org/10.3233/JAD-160256.
34. Arenaza-Urquijo EM, Vemuri P. Resistance vs resilience to Alzheimer disease. *Neurology* 2018;90:695-703.
35. Iram T, Trudler D, Kain D, et al. Astrocytes from old Alzheimer's disease mice are impaired in Aβ uptake and in neuroprotection. *Neurobiol Dis* 2016;96:84-94.
36. Kang MS, Aliaga AA, Shin M, et al. Amyloid-beta modulates the association between neurofilament light chain and brain atrophy in Alzheimer's disease. *Mol Psychiatry* 2020. https://doi.org/10.1038/s41380-020-0818-1.
37. Chai X, Dage JL, Citron M. Constitutive secretion of tau protein by an unconventional mechanism. *Neurobiol Dis* 2012;48:356-366.
38. Karch CM, Jeng AT, Goate AM. Extracellular Tau levels are influenced by variability in Tau that is associated with tauopathies. *J Biol Chem* 2012;287:42751-42762.
39. Pooler AM, Phillips EC, Lau DHW, Noble W, Hanger DP. Physiological release of endogenous tau is stimulated by neuronal activity. *EMBO Rep* 2013;14:389-394.

40. Sato C, Barthélemy NR, Mawuenyega KG, et al. Tau kinetics in neurons and the human central nervous system. *Neuron* 2018;97:1284-1298.e7.
41. Iaccarino L, Tammewar G, Ayakta N, et al. Local and distant relationships between amyloid, tau and neurodegeneration in Alzheimer's disease. *NeuroImage Clin* 2018;17:452-464.
42. Ossenkoppele R, Schonhaut DR, Schöll M, et al. Tau PET patterns mirror clinical and neuroanatomical variability in Alzheimer's disease. *Brain* 2016;139:1551-1567.
43. Suárez-Calvet M, Caballero MÁA, Kleinberger G, et al. Early changes in CSF sTREM2 in dominantly inherited Alzheimer's disease occur after amyloid deposition and neuronal injury. *Sci Transl Med* 2016;8:34-38.
44. Suárez-Calvet M, Morenas-Rodríguez E, Kleinberger G, et al. Early increase of CSF sTREM2 in Alzheimer's disease is associated with tau related-neurodegeneration but not with amyloid-β pathology. *Mol Neurodegener* 2019;14:1-14. https://doi.org/10.1186/s13024-018-0301-5.
45. Rauchmann BS, Schneider-Axmann T, Alexopoulos P, Perneczky R. CSF soluble TREM2 as a measure of immune response along the Alzheimer's disease continuum. *Neurobiol Aging* 2019;74:182-190.
46. Suárez-Calvet M, Kleinberger G, Araque Caballero MÁ, et al. sTREM 2 cerebrospinal fluid levels are a potential biomarker for microglia activity in early-stage Alzheimer's disease and associate with neuronal injury markers. *EMBO Mol Med* 2016;8:466-476.
47. Heslegrave A, Heywood W, Paterson R, et al. Increased cerebrospinal fluid soluble TREM2 concentration in Alzheimer's disease. *Mol Neurodegener* 2016;11:3. https://doi.org/10.1186/s13024-016-0071-x.
48. Schindler SE, Gray JD, Gordon BA, et al. Cerebrospinal fluid biomarkers measured by Elecsys assays compared to amyloid imaging. *Alzheimers Dement* 2018;14:1460-1469.
49. Hansson O, Seibyl J, Stomrud E, et al. CSF biomarkers of Alzheimer's disease concord with amyloid-β PET and predict clinical progression: a study of fully automated immunoassays in BioFINDER and ADNI cohorts. *Alzheimers Dement* 2018;14:1470-1481.
50. Shaw LM, Waligorska T, Fields L, et al. Derivation of cutoffs for the Elecsys ® amyloid β (1-42) assay in Alzheimer's disease. *Alzheimers Dement* 2018;10:698-705.
51. Gispert JD, Monté GC, Suárez-Calvet M, et al. The APOE ε4 genotype modulates CSF YKL-40 levels and their structural brain correlates in the continuum of Alzheimer's disease but not those of sTREM2. *Alzheimers Dement* 2017;6:50-59.
52. Alcolea D, Martínez-Lage P, Sánchez-Juan P, et al. Amyloid precursor protein metabolism and inflammation markers in preclinical Alzheimer disease. *Neurology* 2015;85:626-633.
53. Alcolea D, Vilaplana E, Pegueroles J, et al. Relationship between cortical thickness and cerebrospinal fluid YKL-40 in predementia stages of Alzheimer's disease. *Neurobiol Aging* 2015;36:2018-2023.
54. Kern S, Syrjanen JA, Blennow K, et al. Association of cerebrospinal fluid neurofilament light protein with risk of mild cognitive impairment among individuals without cognitive impairment. *JAMA Neurol* 2019;76:1413-1422.
55. Mattsson-Carlgren N, Leuzy A, Janelidze S, et al. The implications of different approaches to define AT(N) in Alzheimer disease. *Neurology* 2020;94:e2233-e2244.
56. Sugarman MA, Zetterberg H, Blennow K, et al. A longitudinal examination of plasma neurofilament light and total tau for the clinical detection and monitoring of Alzheimer's disease. *Neurobiol Aging* 2020;94:60-70.
57. Reimand J, Collij L, Scheltens P, Bouwman F, Ossenkoppele R. Association of amyloid-β CSF/PET discordance and tau load five years later. *Neurology* 2020;95:e2648-e2657.
58. Cacciaglia R, Molinuevo JL, Salvadó G, et al. Impact of the APOE gene on amyloid deposition in participants with abnormal soluble amyloid levels. AAIC, 2020.

SUPPORTING INFORMATION

Additional supporting information may be found online in the Supporting Information section at the end of the article.

How to cite this article: Salvadó G, Milà-Alomà M, Shekari M, et al. Cerebral amyloid-β load is associated with neurodegeneration and gliosis: Mediation by p-tau and interactions with risk factors early in the Alzheimer's continuum. *Alzheimer's Dement*. 2020;1-13. https://doi.org/10.1002/alz.12245

SUMMARY OF RESULTS

In this thesis we have presented four different studies all related to Aβ deposition in early stages of the Alzheimer's *continuum* and its downstream consequences. Our overall objective was related to further advance the characterization of Aβ PET alterations observable in these early stages of the disease. First, we looked at the capability of Aβ PET to detect the earliest signs of Aβ pathology both using quantification and visual assessment (studies 1 and 2, respectively). Second, we studied how AD risk factors affect cerebral amyloid aggregation by associating two different Aβ biomarkers (study 3). And, finally, in our last study, we investigated the associations between Aβ PET and CSF biomarkers of multiple downstream pathophysiological mechanisms. The roles in these associations of AD risk factors and indirect effects of other biomarkers were also studied.

The main objective of our first study was to derive standard thresholds of Aβ PET to detect the earliest signs of Aβ pathology. To this aim, we capitalized on having CSF Aβ measurements in the same participants, and the well-established fact that CSF Aβ dyshomeostasis occurs earlier in the disease progression than cerebral Aβ accumulation. Two different cohorts were merged to study the whole AD spectrum, with a particular emphasis in subjects with low-intermediate Aβ load. Using this dataset, we maximized the agreement between Aβ PET global measures and dichotomized CSF biomarkers using previously established thresholds. This analysis gave two thresholds as a result: 12 Centiloids (CL) when comparing with dichotomized CSF Aβ and, around 30 CL when dichotomized CSF tau/Aβ ratios were used.

Following these results, we wanted to elucidate whether visual assessment could also detect this early Aβ load. To do so, two cohorts that covered the whole Alzheimer's *continuum* with available [^{18}F]flutemetamol PET scans were studied. Our results demonstrated that visual assessment performed by highly trained reader(s) led to high accuracy ($\kappa \geq 0.88$) in determining Aβ positivity compared to thresholds derived in the first study, which were significantly lower than previously derived cut-offs for positive visual reads. Moreover, when the quantification threshold was derived against visual

read assessment classification, we found a value, 17 CL, which was within the range of the two thresholds in the first work. Further, we also observed high agreement (89.3%) on assessing Aβ positivity when studying an independent sample with neuropathological information (n=28).

In this second study the role of regional visual assessment was also investigated. First, we observed that the number of regions visually assessed as positive was associated with the global Aβ load measured with quantification (χ^2=303.71, df=5, p<0.001). Further, comparing subjects with a particular region assessed as positive or negative, a significant difference in regional quantification was also proven (all p<0.001). These results were also confirmed in the neuropathological sample comparing the continuous measure of $mCERAD_{SOT}$ between both groups (all p<0.01). Finally, the most common patterns of regional Aβ positivity were described. In summary, frontal or precuneus/posterior cingulate alone first and after in conjunction, were the first areas to be assessed as positive in our staging model (VR stages 1 and 2, respectively). Followed by a final stage in which these regions plus any other of the cortical and/or striatal areas were assessed as positive (VR stage 3). We also detected that the sagittal plane seemed to be optimal to assess the earliest regions. These results led us to propose this approach as a regional staging method to monitor the spread of Aβ pathology across the brain. Being entirely based on visual reading, this method would be suitable to be applied in clinical practice without the need of quantitative approaches.

In the third study, the role of AD risk factors as modifiers of cerebral Aβ aggregation for a given level of Aβ dyhomeostasis was investigated. Using two independent cohorts of cognitively unimpaired participants, our study showed that older age, female sex and *APOE-ε4* carriership increased the Aβ PET load, for any given level of CSF Aβ. Interestingly, the brain areas in which these risk factors facilitated Aβ aggregation were different. Particularly, older age and female sex, displayed increased Aβ load in areas such as precuneus and posterior cingulate, which are well-known areas of Aβ deposition. On the other hand, *APOE-ε4* carriership showed increased Aβ deposition mainly in the medial temporal lobe which is a key region for early tau accumulation and neurodegeneration in AD. In all cases

these patterns were more widespread in the ALFA+ participants, which were also younger and had less Aβ in the brain, than in the ADNI participants, thus supporting that these effects might be more prominent in the early AD *continuum*.

On the final study presented, we investigated Aβ-downstream effects in the early stages of the Alzheimer's *continuum*. Our results indicate that CSF biomarkers related to tau pathology, neurodegeneration and glial activation are positively associated with Aβ load measured with PET, even when measured in cognitively unimpaired participants. Further, our analyses indicated that some of these associations were also modified by AD risk factors. Specifically, we observed a tighten association between Aβ load and tau and synaptic dysfunction markers in older participants. A marker of microglial activation, sTREM2, also showed a trend to stiffen the association with Aβ load in older participants. Also, steeper increases in CSF NfL, neurodegeneration marker, and sTREM2 levels were detected in women for increasing Aβ load. No significant modifier effects were observed for *APOE-ε4* carriership.

On top of these, the main novelty in this study was discovering a direct association between Aβ load and NfL, a marker of neurodegeneration, independent of p-tau. On the other hand, associations between glial activation markers and Aβ load, they were all found to be fully mediated by CSF levels of p-tau and NfL.

PUBLICATIONS' REPORT

Four manuscripts have been included in the preparation of this thesis, three of them have been already published in international scientific journals, and another one is currently under revision at the present time.

The first study, entitled "Centiloid cut-off values for optimal agreement between PET and CSF core AD biomarkers", was published in the journal

Alzheimer's Research & Therapy (IF: 6.116, Q1) in 2019. The presenter of this thesis is the first author of this study, as she conceptualized the study; performed the main analyses; discussed the results and contributed to the writing and revision of the manuscript. This work has not been included in any other PhD thesis.

The second study included is entitled: "Visual assessment of [^{18}F]flutemetamol PET images can detect early amyloid pathology and grade its extent" and was published in the *European Journal of Nuclear Medicine and Molecular Imaging* (IF: 7.081, Q1) in 2021. This work was the result of a tight collaboration between our group and a Dutch research group in which data from both centers was used. The thesis presenter is a co-first author together with Lyduine E. Collij. The specific work of Gemma Salvadó in this study included the conceptualization of the project; analysis of the data, such as the quantification of all PET images included in this work, performance of statistical analyses; critical discussion and interpretation of the results and; revision of the manuscript. The other co-first author, also played a main role in this work not only contributing with data from her center, but also working together in the conceptualization of the study; analysis of the data, such as performing the visual analysis of all PET images, as well as many statistical analyses; critical discussion of the results and writing of the manuscript. This work has also been included in the PhD thesis of Lyduine E. Collij.

The third study is entitled: "Age, sex and *APOE-ε4* modify the balance between soluble and deposited β-amyloid in cognitively intact individuals: topographical patterns and replication across two independent cohorts" and is currently under review. This study also came as a tight collaboration, in this case within our center, between the thesis presenter and Dr. Cacciaglia. In this case, the work of Gemma Salvadó consisted on contributing to the conceptualization of the project; performing analysis of the data, such as the preprocessing of all the images, as well as conducting a vast part of the statistical analyses; critical discussion of the results and its interpretation and; finally, the revision of the manuscript. This work has not been included in any other PhD thesis.

Finally, the last study, entitled "Cerebral amyloid-β load is associated with neurodegeneration and gliosis: Mediation by p-tau and interactions with risk factors early in the Alzheimer's *continuum*", was published in the journal *Alzheimer's & Dementia* (IF: 17.127, Q1) in 2021. The presenter of this thesis is the first author of this study as she conducted the main tasks of this study including: the conceptualization of the study; performance of the analyses; discussion of the results and writing of the manuscript. This work has not been included in any other PhD thesis.

Yours sincerely,

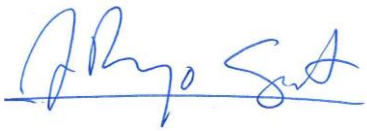

Dr. Juan Domingo Gispert López

Dr. José Luis Molinuevo Guix

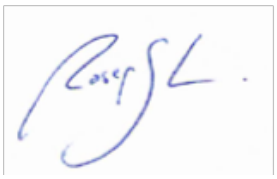

Dra. Roser Sala Llonch

DISCUSSION

DISCUSSION

Alterations in amyloid-β (Aβ) are thought to be the earliest, or one of the earliest, detectable feature of Alzheimer's disease (AD). Aβ PET allows the identification of Aβ in the brain, even in cognitively unimpaired individuals. Throughout this thesis, we have used Aβ PET to address three main objectives: first, to detect the earliest signs of pathological cerebral Aβ deposition; second, to assess how the main non-modifiable risk factors for Alzheimer's dementia affect the amount and pattern of Aβ deposition and, finally, to characterize pathophysiological pathways triggered by early Aβ deposition. In this chapter we will jointly discuss the results that we have presented in previous chapters and in the context of current literature of the field.

THE ALFA COHORT

To contextualize the results of this thesis, we have first to introduce the cohort of participants used to perform this thesis' research. The reason for this is that the particularities of the ALFA cohort have been key to address the objectives of this thesis, especially focused on the earliest stages of the Alzheimer's *continuum*. This particular emphasis on early phases of AD makes our work unique of its kind.

The ALFA cohort was assembled to investigate the pathophysiological events that occur at the early stages of the Alzheimer's *continuum* (Molinuevo *et al.*, 2016). To be able to detect these early stages of the disease, participants were selected to be (late) middle-aged cognitively unimpaired participants, most of which were offspring of AD patients. Further, in the nested ALFA+ subsample, which was used in all our studies, participants were preferentially selected to be *APOE-ε4* carriers and have a positive family history of AD. These characteristics increased the

proportion of participants in the preclinical stage of the Alzheimer's *continuum* (Sperling *et al.*, 2011*b*).

With the advantage of this dataset available, the main focus of this thesis was to study the earliest stages of the Alzheimer's *continuum* and, in particular, those events related to the first signs of cerebral Aβ deposition. Most of the studies in the literature involve clinical samples of AD patients and controls. Whilst this approach allows the detection of the main features of the disease, it is not adequate to detect the earliest alterations. Nonetheless, the early stages of the Alzheimer's *continuum* have gained more attention in recent years as they are thought to be a window of opportunity for intervention (Sperling *et al.*, 2014*b*). Similar approaches have been followed in other cohort studies like the Adult children Study by the Washington University in Sant Louis (Coats and Morris, 2005), the Winsconsin Registry for Alzheimer's Prevention (Sager *et al.*, 2005), the Biomarkers for Older Controls at Risk for Alzheimer's Disease study at Johns Hopkins (Levy *et al.*, 2004), the Baltimore Longitudinal Study of Aging, Prevention (Shock *et al.*, 1984), and the Australian Blood, Imaging, and Lifestyle study (Ellis *et al.*, 2009). Finally, it also allows the study of the whole *continuum* if participants are followed longitudinally, as is the case of ALFA+ participants. In summary, the use of the ALFA+ cohort was crucial for the development of the studies presented.

DEFINITION OF Aβ PET POSITIVITY

To study the natural history of Aβ deposition or the effect of pharmacological interventions on Aβ load, quantification is fundamental. However, many factors significantly affect PET-derived measures of Aβ burden, like the tracer used to obtain the images, how the regions of interest (ROIs) are drawn or the pre-processing pipeline used to quantify them. To improve the comparability of the estimates of Aβ PET burden, the Centiloid project was designed and the Centiloid scale (CL) was proposed as a tool for direct comparison of Aβ load across centers (Klunk *et al.*, 2015). In our

studies, the CL method was adopted and allowed us to either validate our results in independent samples or to pool quantitative Aβ measurements from different sources to extend our findings in the ALFA cohort to the full spectrum of AD. In addition, reporting our results in CL units, being these absolute, facilitates their comparability to the rest of the literature.

PET quantification

Our first study was specifically designed to detect these first signs of Aβ deposition in the brain and, ultimately, classify subjects as Aβ positive or negative. To this aim, we operationalized an Aβ PET threshold that maximized the agreement with dichotomized cerebrospinal fluid (CSF) values. The idea behind this strategy was to approximate, as much as possible, the classification that would have been obtained if we had used CSF Aβ, which is supposed to be the earliest marker of Aβ alterations in AD (Bateman *et al.*, 2012*b*, Jack *et al.*, 2013*b*; Palmqvist *et al.*, 2016).

Another remarkable characteristic of our study that also helped to detect early signs of cerebral Aβ was the sample that was studied. As previously stated, our study included a large number of participants with low-intermediate Aβ load, which allowed having a good representation of the range in which the most sensitive thresholds were expected. However, we considered that it was necessary to cover the whole AD spectrum to avoid stability problems and also, to confirm our results in more typical cases. To this aim, we also added an extra clinical cohort -ADNI - that included participants with higher Aβ pathology. As shown in the sensitivity analyses, the exclusion of these subjects could lead to much lower thresholds, which may be more related to noise than to an actual signal. In conclusion, the derivation of Aβ thresholds is sensitive to the studied samples (Jack *et al.*, 2017).

These two characteristics of the study allowed us to derive a low and, in turn, specific threshold at 12 CL. Even though this threshold could seem too low, this value is supported by two other recent studies that were published during the development of this thesis. During the preparation of our first manuscript, *La Joie* and colleagues presented a threshold of 12.2

CL derived against neuropathology (La Joie *et al.*, 2019). In particular, this value corresponded to the boundary of CERAD moderate-to-frequent neuritic plaques, advocating for a sensitive although robust threshold. In line with this, a more recent study also using neuropathological measures adopted a threshold of 10 CL to discard the existence of neuritic plaques (Amadoru *et al.*, 2020). Therefore, both studies corroborated our finding using completely different methodological approaches. A third study using neuropathology data also proposed a threshold of 24.1 CL but it was not strictly derived against it and, also, used a more limited number of cases, which supports the idea that the population selected for these type of studies is key (Navitsky *et al.*, 2018). Also, a very recent study suggested just a slightly higher threshold (15-18.5 CL) to be the lowest threshold to have clinical relevance as to be related to future Aβ accumulation and cognitive decline (Farrell *et al.*, 2021). And, another reported 13.5 CL, very close to our 12 CL, as the cut-off to differentiate Aβ negative subjects from subjects with early Aβ deposition (Bullich *et al.*, 2020).

Recent studies have derived Centiloid thresholds with other objectives. Remarkably, two studies used longitudinal data to derive a threshold with significant prognostic value. In one of these studies, the authors indicated that the probability to progress from cognitively unimpaired to mild cognitive decline (MCI) or dementia in five years increased from 5% to 12% if baseline Aβ PET was above 26 CL (van der Kall *et al.*, 2020). And another similar study also estimated that the Centiloid value that optimally predicted the progression to dementia in six years, yielding also a threshold of 26 CL (Hanseeuw *et al.*, 2020). These thresholds are in remarkable agreement with the one derived in our study against dichotomized tau/Aβ ratios (25-30 CL). The aim of this calculation in our study was to derive a more specific threshold that would be related to established pathology. But in views of its accordance with these two more recent studies, it suggests the appropriateness of the use of our second threshold (25-30 CL) with prognostic objectives.

PET visual assessment

Visual assessment is the other typical method to assess an Aβ PET scan. It is more often used in the clinical setting and it is the only EMA- and FDA-approved method to classify a scan as positive or negative. As it was operationalized to detect moderate-to-frequent plaques using the CERAD classification, it has been usually considered to be less reliable to early signs of Aβ deposition (La Joie *et al.*, 2019). Furthermore, the few studies that had previously compared visual assessment with Centiloid quantification had proposed high thresholds of positivity (from 25 CL up to 40 CL) (Leuzy *et al.*, 2016; Rowe *et al.*, 2017; La Joie *et al.*, 2019; Amadoru *et al.*, 2020; Hanseeuw *et al.*, 2020), which also discouraged the use of visual read for the assessment of early Aβ pathology.

However, and due to the characteristics of the previously published studies, we suspected that the sensitivity of visual assessment could be higher than what was originally thought. As we hypothesized, the capability to detect early signs of Aβ deposition with this method was demonstrated in our second study. This was firstly validated by the CL threshold matching a positive visual read in our study (17 CL). And further confirmed by the results of our additional analysis against neuropathology, which suggested that visual assessment, performed by highly trained readers, could capture the presence of sparse- to-moderate neuritic plaques. Noteworthy, this quantification threshold was between the range (15-18.5 CL) proposed for a very recent study to be the lowest to predict future cognitive decline (Farrell *et al.*, 2021). Altogether, advocating for the use of visual assessment also in the early stages of AD.

Two main properties may have favoured the detection of lower Aβ burden by visual assessment in our study. First, the selection of participants, which included a considerable number of participants with low-intermediate Aβ load and, second, the experience of our readers. This first characteristic is in contrast with previous studies that only included few subjects in this range (La Joie *et al.*, 2019; Amadoru *et al.*, 2020; Hanseeuw *et al.*, 2020). Particularly, only six participants were included in one of these studies in the range of 12-24 CL (La Joie *et al.*, 2019). Important to note, the majority of these cases (72%) were assessed as visually positive, although not for

all readers. This is in agreement with our results, suggesting that low Aβ load can be detected by visual assessment. However, it also suggests that some readers, maybe those less used to review these early cases which are more frequent in population studies than in clinical samples, may fail at detecting the subtle signs of Aβ pathology. Another strength of our study is that the three readers of our study had previously reviewed a large number of Aβ [^{18}F]flutemetamol PET scans, including a large number of dubious cases. This characteristic may have also fostered the detection of earlier signs of Aβ in our study.

CHARACTERIZATION OF REGIONAL Aβ DEPOSITION

Until this point, we have only discussed Aβ positivity as a global measure. However, multiple studies, including one with the involvement of our group (Collij *et al.*, 2020), have demonstrated advantages of classifying participants in ordinal categories -or stages- based on regional information from Aβ PET scans (Fantoni *et al.*, 2020). Among others, these studies showed associations with CSF biomarkers, neuropathological Aβ markers, and also predicted cognitive decline, supporting its use over dichotomization of global Aβ load for some research applications (Grothe *et al.*, 2017; Hanseeuw *et al.*, 2018; Mattsson *et al.*, 2019; Collij *et al.*, 2020; Jelistratova *et al.*, 2020; Teipel *et al.*, 2020).

Staging model

Besides, all the studies mentioned above used regional quantification to address this goal. Thus, no study had used regional information derived from regional visual assessment, although it is performed *as per* guidelines description, relegating regional analyses to the research setting only. To address this issue, in our second study we aimed to disentangle whether regional visual assessment could give more granular information about Aβ

load than global dichotomization. All our analyses supported the value of regional assessment, as we showed associations with both global and regional Aβ load measured with quantification. And it was also confirmed in the neuropathological cases. Thus, suggesting that regional visual assessment could serve to grade the Aβ extent and, therefore, give a more comprehensive grading of Aβ deposition in the brain. As far as we know, the utility of regional visual assessment was not previously investigated although it is routinely performed in the clinics. In addition, a very recent paper, contemporaneous with ours, suggested that the number of regions visually assessed as positive may have an impact on future cognitive decline (Kim *et al.*, 2021). Therefore, our recommendation to use this resource would provide extra information, useful for prognostics, without requiring extra effort from readers.

Finally, also in the second study, we described regional patterns of Aβ positivity. Observing which regions were more usually assessed as positive allowed us to describe a progression on regional positivity similar to what was previously done with the quantitative staging methods. Our staging model, based on visual assessment, may be of utility for the clinical setting as it gives an idea comparable to quantification depending on the pattern observed in the Aβ PET scan. Further, it may also be of utility for readers less used to dubious cases as we propose to focus on particular areas to detect the earliest signs of pathology (*e.g.* precuneus/posterior cingulate and orbitofrontal cortex in the sagittal plane). It is important to note, though, that only cross-sectional data was involved in this project. Therefore, the validity of this method for prognostics needs to be tested in longitudinal studies. This is planned to be investigated with the longitudinal data of the ALFA+ study in the context of the Amyloid Imaging to Prevent Alzheimer's Disease (AMYPAD) Consortium (Lopes Alves *et al.*, 2020).

Different patterns of Aβ deposition

The relevance of regional Aβ information is also highlighted by the results of our third study, in which we compared the global CSF Aβ levels with regional Aβ PET load. Multiple studies had previously investigated the associations between CSF Aβ and Aβ PET (Palmqvist *et al.*, 2014, 2015,

2016; Toledo *et al.*, 2015). In broad strokes, the main objective of many of these studies was to assess the agreement between both methods to detect Aβ pathology. However, none had previously investigated how these associations could inform us about differences in regional patterns of Aβ deposition, for similar CSF Aβ levels, associated with Alzheimer's dementia risk factors. This was a key novelty in the approach of our study.

Our hypothesis of increased Aβ deposition with increased AD risk was confirmed for all three risk factors: older age, female sex and carriership of the *APOE-ε4* genotype. However, the pattern of higher deposition was not homogeneous for all AD risk factors investigated. These differences between AD-risk factors advocate for different biological mechanisms behind this increased Aβ deposition, which would have been unnoticed without the regional information.

On one hand, older age and female sex demonstrated to be associated with higher Aβ deposition in areas known for their early Aβ accumulation, such as precuneus, anterior and posterior cingulate or the orbitofrontal lobe (Palmqvist *et al.*, 2017). This result suggests an additive effect of these Alzheimer's dementia risk factors on Aβ deposition.

On the other hand, a completely different behaviour was observed for *APOE-ε4* carriers. In our study, *APOE-ε4* carriers had higher Aβ deposition in brain areas that do not primarily accumulate amyloid, but are vulnerable to early tau deposition (Braak and Braak, 1991). This specific localisation points out a possible explanation of the interplay between Aβ, the *APOE-ε4* allele and tau (Therriault *et al.*, 2020*b*). In particular, we hypothesize that the increased Aβ deposition on these early tau accumulation regions may pave the way for tau to spread across the brain. Previous neuropathological studies have suggested that the increased levels of tau in *APOE-ε4* carriers are only due to their higher levels of Aβ pathology (Mungas *et al.*, 2014; Serrano-Pozo *et al.*, 2015). And recent *in vivo* studies have shown that the Aβ-independent effect of this allele on tau can be only observed in these early regions (Therriault *et al.*, 2020*a*; Salvadó *et al.*, 2021). Further, tau propagation seems to be accelerated in areas with elevated Aβ load (Vogel *et al.*, 2020). Taking all these findings together, it seems reasonable to think

that tau tangles in the medial temporal lobe (MTL), may be more easily spread through the neocortex in *APOE-ε4* carriers due to their higher amount of deposited Aβ on the MTL. However, this is a new hypothesis and, therefore, should be further confirmed with tau PET information and in a longitudinal settings.

Finally, it is also important to note that, again, the selection of participants in this study was key for our objective. Including participants with higher Aβ load may have blurred the analysis, as Aβ is known to reach a *plateau* in more advanced stages of the disease (Jack *et al.*, 2013*b*) thus making it harder to detect these early effects. With this line of thinking, in this study, we used the ALFA+ cohort for the main results and cognitively unimpaired participants of ADNI for confirmatory analysis. Although similar results were observed in both cohorts, the regions showing significant interactions were less spread in the latter. Multiple factors may explain this discrepancy, such as the use of different PET tracer, different scanners or different CSF Aβ markers. However, it is also conceivable that the earlier stage of ALFA+ participants have allowed us to better capture these effects than in more advanced subjects in the ADNI cohort. Noteworthy, although both samples were selected to be cognitively unimpaired, they have significant differences in terms of age, *APOE-ε4* carriership and, most importantly, in Aβ load, with more elevated values in the ADNI cohort.

DOWNSTREAM Aβ MECHANISMS

Aβ has a central role in the progression of AD pathophysiology as it is considered to be the earliest detectable hallmark of the disease, which might spark the pathological cascade that characterizes AD. In particular, Aβ has been suggested as a trigger of tau pathology, which, in turn, seems to drive synapse dysfunction and neurodegeneration (Jack *et al.*, 2013*a*). However, multiple additional pathophysiological mechanisms, such as neuroinflammation, have been reported to be altered with the emergence of Aβ and tau and have been proposed to play an important role in this

cascade of events (Heneka *et al.*, 2015; Arranz and De Strooper, 2019). The very recent development of biomarkers for several of these mechanisms has fostered the research to understand their role in the Alzheimer's *continuum*, with the main aim of developing novel drug candidates against AD (Zetterberg and Bendlin, 2020).

Our objective in our last study was, not only to investigate the associations between some of these novel biomarkers and cerebral Aβ load, but also to discover mediation effects among them. Further, we also aimed at exploring whether some of the associations between Aβ load and the other biomarkers were modified by Alzheimer's dementia risk factors, as could be hypothesised based on the results of Study 3. Two coetaneous studies looked at associations between some similar biomarkers and Aβ pathology -either measured in CSF or PET-, but two important differences have to be noted (Bos *et al.*, 2019, Palmqvist *et al.*, 2019*a*). Firstly, only direct associations were investigated in these two studies, hampering a deeper interpretation of the biological relationships between Aβ and the other biomarkers. Secondly, our study included only cognitively unimpaired participants enriched for AD risk factors whereas previous studies included participants of the whole spectrum. Although the latter permits a more general view of the behaviour of these biomarkers across the Alzheimer's *continuum*, our framework allowed us to perform a more focused analysis in the earliest stages of the disease. Knowledge about pathophysiological mechanisms in these early phases will be of utmost importance for designing future clinical trials (Sperling *et al.*, 2014*a*).

The strong relationship between Aβ and tau is well established in the literature (Jack *et al.*, 2013*a*, Alcolea *et al.*, 2015*a*, Palmqvist *et al.*, 2019*a*). In our study, we also found this association even in the earliest stages of the Alzheimer's *continuum*, thus corroborating previous results of our group using CSF Aβ (Milà-Alomà *et al.*, 2020*a*). One novelty in this study was the finding that this association strengthened in older subjects. Although this has not been reported before, multiple factors could explain this behaviour. First, older participants are more prone to have concomitant morbidities, which may reduce their brain resilience to Aβ and facilitate tau production and/or spreading. On the other hand, some mechanisms reduce cerebral

Aβ deposition or its detrimental effects, such as glial activation, might be impaired at older ages. This, in turn, may also facilitate the increase of tau pathology for similar levels of Aβ load.

Regarding neurodegeneration, it is well-established that has a tight association with tau but poor with Aβ (Iaccarino *et al.*, 2018; La Joie *et al.*, 2020). In our population, however, we did find a significant direct (*i.e.* independent of p-tau) association between Aβ load and CSF NfL, which is a marker of neurodegeneration. In light of the previous literature, our findings suggest that such an Aβ-driven mechanism directly associated with neurodegeneration occurs in the earliest stages of the Alzheimer's *continuum*, whereas, neurodegeneration may be driven by tau in later stages of the disease, in which previous studies were focused. Our results support the role for tau pathology as the main, but not only, mediator of the relationship between Aβ and neurodegeneration. This was an important novelty of our study that deserves further validation with a similar population. A major potential implication of this finding is that removal of Aβ deposited in the brain in its earliest stages might prevent future neurodegeneration, either directly or by preventing tau pathology.

Also in regards of the association between Aβ and neurodegeneration, our study revealed an interaction effect with sex. Thus, indicating that for higher Aβ load, the Aβ-derived neurodegeneration was higher in women. Previous studies have reported higher hypometabolism and atrophy in women, especially in *APOE-ε4* carriers (Holland *et al.*, 2013; Sampedro *et al.*, 2015), but little data exist on its relationship with Aβ. On top of that, the sex-interaction in our study showed only a trend to significance after accounting for CSF p-tau levels, suggesting that this effect may be partly mediated by their also higher tau pathology. This would be in line with previous findings by Buckley *et al.* that showed that higher global Aβ load was associated with higher ERC tau burden in women (Buckley *et al.*, 2019*b*). Further, other studies have also associated this higher Aβ load with higher cognitive decline in women (Buckley *et al.*, 2018), suggested to be related with their higher tau in the medial temporal lobe (Buckley *et al.*, 2020). Given the tight relationship between neurodegeneration and cognitive function, our results seem to be in line with previous literature. Due to the borderline significance

of this result, though, we suspect that Aβ may have also a direct higher effect on neurodegeneration in women, independent of tau. However, no previous study has shown this tau-independent effect and, therefore, further research is needed to confirm it.

Interesting relationships were also observed between CSF glial activation markers and Aβ load. First, increased Aβ load was associated with higher levels of markers of both micro- and astroglia. These associations with Aβ PET burden confirmed what our group previously found using CSF Aβ in the same population, although only in the Aβ positive group (Milà-Alomà *et al.*, 2020*a*). Our findings suggest an early involvement of glial activity in the progression of the Alzheimer's *continuum*, once Aβ plaques are deposited into the brain. Recent studies, almost contemporary to our project, also observed elevated levels of CSF glial markers with increased Aβ pathology (Bos *et al.*, 2019, Palmqvist *et al.*, 2019*a*). But these two studies reported these findings in older and later in the disease stage population. Furthermore, they only presented one astroglial marker, CSF YKL-40, whereas in our case we were able to replicate this result and to describe significant relationships with two other glial markers: sTREM2 and GFAP, a microglial and astroglial activity marker, respectively. It is important to note, though, that these markers may be involved in very various biological pathways with different -even opposed- effects in the brain (Heneka *et al.*, 2015; Webers *et al.*, 2020). Further, glial activation may promote antagonistic effects in different moments of the disease, with an initial beneficial effect but with a detrimental effect at later stages due to their promotion of chronic inflammation. Therefore, their role in this specific stage of the disease is unknown, as well as their contribution to participants' clinical progression. For this reason, it is of utmost importance to further investigate the natural history of the dynamics of these glial markers and their relation to subjects' clinical evolution in the Alzheimer's *continuum* in longitudinal settings.

One important novelty of our study was to investigate possible mediators of the associations between Aβ and glial markers. Through this approach, we were able to reveal, for the first time, that these previously observed associations could be fully accounted for by an indirect association with

CSF p-tau levels. Therefore, it can be hypothesized that p-tau, and not Aβ, is driving the glial response. Previous studies with sTREM2 already pointed at this direction showing elevated levels of this marker only after the first signs of tau pathology (Suárez-Calvet *et al.*, 2016, 2019). In our study, astroglial activity (*i.e.* GFAP and YKL-40) markers showed a similar, although not identical, relationship to sTREM2.

Regarding interactions with risk factors for Alzheimer's dementia, our study revealed that the coupling between Aβ load and sTREM2 was tighter in women. Of note, this effect was independent of tau pathology. Sex differences in glial activation have never been reported before in humans, although one study with transgenic mice also found increased neuroinflammation in females (Yang *et al.*, 2018). Also, important sex-differences in microglial structure and function have been described in mouse brains (Guneykaya *et al.*, 2018). Although it has to be noted that the differences between these studies and ours are non-trivial, they both pinpoint the necessity to further investigate glial activation differences by sex as they may play an important role in the different risk of developing AD observed between sexes and, maybe, also constitute a useful way forward for precision medicine against AD (Ferretti *et al.*, 2018, 2020). Noteworthy, is still unknown whether these differences may cause beneficial or detrimental responses, which also warrants further research in this topic.

Finally, only ALFA+ participants were included in our last study. This was due to the novelty of the CSF biomarkers studied, which prevented us to replicate it with other publicly available cohorts. Although associations between CSF biomarkers of some of the pathophysiological mechanisms were also published during the execution of our study (Bos *et al.*, 2019, Palmqvist *et al.*, 2019*a*), our analysis allowed us to investigate in detail these relationships in the earliest stages of the disease. Our results advocate for associations between Aβ and neurodegeneration, synaptic dysfunction and glial activation, even with a low cerebral Aβ load. Thus, emphasizing the presence in the earliest stages of the AD *continuum* of these pathophysiological events that have been previously described in clinical stages of AD. Further research will be necessary to unravel the beneficial or detrimental effects of these mechanisms in the course of the

disease. To this aim, the longitudinal follow-up of these participants, which is already planned, will be of utmost importance.

In summary, the research that has been performed in the context of this PhD thesis has rendered important results concerning the detection of early Aβ alterations, the relevance of the regional spread of Aβ deposition in the brain and, the study of pathophysiological pathways altered related to Aβ. As to the early detection of Aβ pathology, the research here included has contributed to recent developments that have shown that relatively low Centiloid values, much lower than what was previously thought, may be specifically associated with Aβ abnormalities and be detected by visual assessment. In relation to the exploitation of the regional information in Aβ scans, we have proposed a staging method based on the visual assessment of brain regions, and its potential to predict clinical progression is currently being evaluated. Besides, we have revealed the differential effect of *APOE-ε4*, as compared to the other main risk factors for Alzheimer's dementia, to foster Aβ deposition in key areas for the spread of tau pathology in early AD, which may have important consequences for future neurodegeneration and cognitive decline. Finally, the analysis of associations among different pathophysiological alterations has also rendered results suggesting the existence of independent Aβ-driven and tau-driven mechanisms of neurodegeneration. The most important implication of this result is that removal of early Aβ deposition from the brain may have synergistic effects on future cognitive decline by preventing both direct and indirect mechanisms associated with neurodegeneration. On the other hand, p-tau, alone or in combination with neurodegeneration, fully accounted for the observed association between Aβ deposition and glial response.

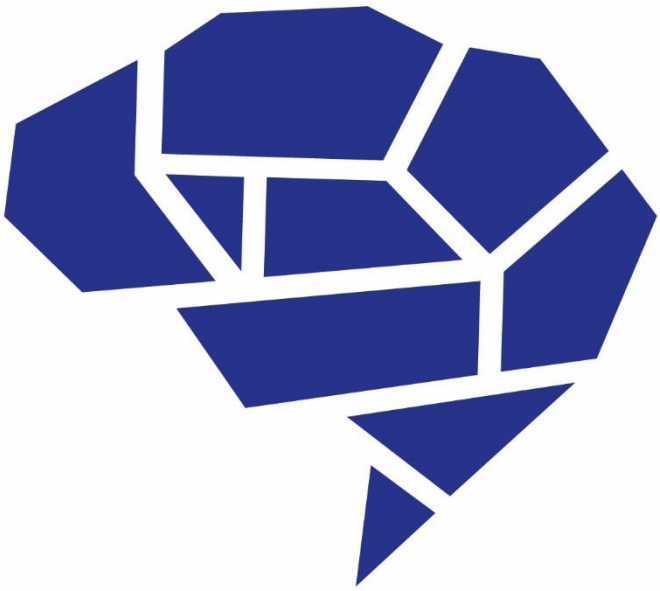

CONCLUSIONS

CONCLUSIONS

1. Global Aβ PET quantification can detect early signs of Aβ deposition with high accuracy through significantly lower quantitative cut-offs than previously thought.

2. Visual assessment of Aβ PET can detect early Aβ pathology and grade its extent using regional information.

3. Older age, female sex and *APOE-ε4* carriership promote early Aβ deposition in different regions of the brain for the same levels of Aβ dyshomeostasis. The first two risk factors increment Aβ deposition in areas of early Aβ accumulation, whereas *APOE-ε4* carriership was associated with the spread of Aβ to areas vulnerable to early tau pathology, thus potentially promoting its propagation in the brain.

4. Aβ deposition has a tau-independent effect on neurodegeneration and a tau-dependent effect on neuroinflammation in the earliest stages of the Alzheimer's *continuum*.

PUBLICATIONS

Publications included in this tesis

1. **Salvadó G**, *et al.* Centiloid cut-off values for optimal agreement between PET and CSF core AD biomarkers, Alzheimer's Res Ther, 2019; 11(1):27
2. Collij LE*, **Salvadó G***, *et al.* Visual assessment of [18F]flutemetamol PET images can detect early amyloid pathology and grade its extent, Eur J Nucl Med Mol Imaging, 2021
3. Cacciaglia R*, **Salvadó G***, *et al.* Age, sex and APOE-ε4 modify the balance between soluble and deposited amyloid-β in cognitively intact individuals: topographical patterns and replication across two independent cohorts, *submitted*
4. **Salvadó G**, *et al.* Cerebral amyloid-β load is associated with neurodegeneration and gliosis: Mediation by p-tau and interactions with risk factors early in the Alzheimer's *continuum*, Alzheimer's and Dementia, 2021

*Authors contributed equally

Other publications

5. **Salvadó G**, Brugulat-Serrat A, Sudre CH, Grau-Rivera O, Suárez-Calvet M, Falcon C, *et al.* Spatial patterns of white matter hyperintensities associated with Alzheimer ' s disease risk factors in a cognitively healthy middle-aged cohort, Alzheimers Res Ther 2019; 11(1):12
6. Brugulat-Serrat A*, **Salvadó G***, Sudre CH, Grau-Rivera O, Suárez-Calvet M, Falcon C, *et al.* Patterns of white matter hyperintensities associated with cognition in middle-aged cognitively healthy individuals, Brain Imaging Behav 2020; 14(5):2012-2023

7. Brugulat-Serrat A*, **Salvadó G***, Operto G, Cacciaglia R, Sudre CH, Grau-Rivera O, *et al.* White matter hyperintensities mediate gray matter volume and processing speed relationship in cognitively unimpaired participants, Hum Brain Mapp 2020; 41(5): 1309–1322

8. Grau-Rivera O, Operto G, Falcón C, Sánchez-Benavides G, Cacciaglia R, Brugulat-Serrat A, Gramunt N, **Salvadó G**, *et al.* Association between insomnia and cognitive performance, gray matter volume, and white matter microstructure in cognitively unimpaired adults, Alzheimer's Res Ther 2020; 12(1): 1–14

9. Milà-Alomà M, **Salvadó G**, Gispert JD, Vilor-Tejedor N, Grau-Rivera O, Sala-Vila A, *et al.* Amyloid-β, tau, synaptic, neurodegeneration and glial biomarkers in the preclinical stage of the Alzheimer's continuum, Alzheimer's and Dementia 2020; 16(10):1358-1371

10. Collij LE*, Heeman F*, **Salvadó G**, Ingala S, Altomare D, de Wilde A, *et al.* Multitracer model for staging cortical amyloid deposition using PET imaging, Neurology 2020; 95(11): e1538–e1553

11. Arenaza-Urquijo EM, **Salvadó G**, Operto G, Minguillón C, Sánchez-Benavides G, Crous-Bou M, *et al.* Association of years to parent's sporadic onset and risk factors with neural integrity and Alzheimer's biomarkers, Neurology 2020; 95(15):e2065-e2074

12. Ingala S, Mazzai L, Sudre CH, **Salvadó G**, Brugulat-Serrat A, Wottschel V, *et al.* The relation between APOE genotype and cerebral microbleeds in cognitively unimpaired middle- and old-aged individuals, Neurobiol Aging 2020; 95:104– 114

13. Suárez-Calvet M, Karikari TK, Ashton NJ, Lantero Rodríguez J, Milà-Alomà M, Gispert JD, **Salvadó G**, Minguillon C, Fauria K, *et al.* Novel tau biomarkers phosphorylated at T181, T217 or T231 rise in the initial stages of the preclinical Alzheimer's continuum when only subtle changes in Aβ pathology are detected, EMBO Mol Med. 2020;12(12):e12921

14. Sánchez-Benavides, **Salvadó G**, Arenaza-Urquijo EM, Grau-Rivera O, Suárez-Calvet M, Milà-Alomà M, *et al.* Quantitative informant- and self-

reports of subjective cognitive decline predict Amyloid-β PET-outcomes in cognitively unimpaired individuals independently of age and *APOE-ε4*, Alzheimer's & Dementia: Diagnosis, Assessment & Disease Monitoring, 2020 Nov 11;12(1):e12127

15. Milà-Alomà M, **Salvadó G**, Shekari M, Grau-Rivera O, Sala-Vila A, Sánchez-Benavides G, *et al.* Comparative Analysis of Different Definitions of Amyloid-β Positivity to Detect Early Downstream Pathophysiological Alterations in Preclinical Alzheimer, J Prev Alzheimer's Dis 2021;8(1):68-77

16. **Salvadó G***, Grothe MJ*, Groot C, Moscoso A, Schöll M, Gispert JD, *et al.* Differential effects of *APOE-ε2* and *APOE-ε4* alleles on PET-measured amyloid-β and tau deposition in older individuals without dementia, Eur J Nucl Med Mol Imaging 2021 Feb 1

17. Grau-Rivera O, Navalpotro-Gomez I, Sánchez-Benavides G, Suárez-Calvet M, Milà-Alomà M, Arenaza-Urquijo EM, **Salvadó G**, *et al.* Association of weight change with cerebrospinal fluid biomarkers and amyloid positron emission tomography in preclinical Alzheimer's disease, Alzheimers Res Ther. 2021 Feb 17;13(1):46

18. Cortes-Canteli M*, Gispert JD*, **Salvadó G**, Toribio-Fernandez R, Tristão-Pereira C, Falcon C, Oliva B, Mendiguren J, Fernandez-Friera L, Sanz J, Garcia-Ruiz JM, Fernandez-Ortiz A, Sanchez-Gonzalez J, Ibanez B, Molinuevo JL, Fuster V. Subclinical Atherosclerosis and Brain Metabolism in Middle-Aged Individuals: The PESA Study, J Am Coll Cardiol. 2021 Feb 23;77(7):888-898

19. Sala-Vila A,..., **Salvadó G**, *et al.* Docosahexaenoic acid intake relates to better cerebrovascular and neurodegeneration neuroimaging phenotypes in middle aged adults at increased genetic risk of Alzheimer's disease, Am J Clin Nutr. 2021 Mar 18

20. Bucci M.*, Savitcheva I.*, Farrar G.*, **Salvadó G**, *et al.* A multisite analysis of the concordance between visual image interpretation and quantitative analysis of [^{18}F]flutemetamol amyloid PET images, Eur J Nucl Med Mol Imaging 2021 Apr 12

21. Lopes-Alves I, Heeman F, **Salvadó G**, *et al.* Strategies to reduce sample sizes in Alzheimer's disease primary and secondary prevention trials using longitudinal amyloid PET imaging, Alzheimers Res Ther, 2021 Apr 19

22. **Salvadó G***, Ferreira D*, *et al.* The protective gene dose effect of the *APOE-ε2* allele on gray matter volume in cognitively unimpaired participants, *submitted*

23. Milà-Alomà M, Shekari M, **Salvadó G**, *et al.* Cognitively unimpaired individuals with low burden of Aβ pathology have a distinct CSF biomarker profile, *submitted*

24. Alemany S*, Crous-Bou M*,..., **Salvadó G**, *et al*. Air pollution and biomarkers of Alzheimer's disease in cognitively unimpaired individuals, *submitted*

25. Collij LE, Mastenbroek SE, **Salvadó G**, *et al.* Regional amyloid accumulation predicts memory decline in initially cognitively unimpaired individuals, *submitted*

26. Milà-Alomà M, Brinkmalm A, Ashton NJ, Kvartsberg H, Shekari M, Operto G, **Salvadó G**, *et al.* CSF synaptic biomarkers increase in preclinical Alzheimer's and are differentially associated with neurodegeneration markers, *submitted*

27. Gispert JD*, Lopes-Alves I*, Buckley C, Heeman F, Bullich S, **Salvadó G**, *et al.* β-amyloid PET Imaging in the AMYPAD Project: Implementing Quantitative Imaging in Clinical Trials and Clinical Practice, *submitted*

28. Benedet AL*, Milà-Alomà M*, Vrillon A, Ashton NJ, Karikari TK, Hourregue C, Cognat E, Dumurgier J, **Salvadó G**, *et al.*, Plasma GFAP is an earlier and more specific biomarker of amyloid-β pathology than CSF GFAP, *submitted*

29. Collij LE, **Salvadó G**, *et al.*, Data-driven evidence for three distinct trajectories of amyloid-β accumulation, *submitted*

30. **Salvadó G**, *et al.*, Brain alterations in the early Alzheimer's *continuum* with amyloid- β, tau, glial and neurodegeneration CSF markers, *submitted*

APPENDIX: RESUM EN CATALÀ

■ INTRODUCCIÓ

La malaltia d'Alzheimer és un trastorn neurodegeneratiu caracteritzat per l'acumulació de plaques de beta amiloide (Aβ) i cabdells neurofibril·lars de tau en el cervell (Scheltens *et al.*, 2016). Es creu que l'acumulació d'aquestes dues proteïnes comporta mort neuronal, que acaba conduint a neurodegeneració i, conseqüentment, a la disfunció cognitiva. Aquestes dues proteïnes poden ser mesurades en estudis de neuropatologia, que fins fa relativament pocs anys era la única manera de diagnosticar definitivament la malaltia d'Alzheimer. Tanmateix, en les últims anys s'han desenvolupat biomarcadors *in vivo* per ambdues proteïnes, de manera que aquest diagnòstic es pot portar a terme abans de la mort (Jagust, 2018; Zetterberg and Blennow, 2021). Aquest ha sigut un desenvolupament clau en camp de l'Alzheimer ja que una gran proporció de casos classificats degut als símptomes cognitius com demència deguda provablement a l'Alzheimer mostraven signes d'altres patologies en el moment de l'estudi patològic (Beach *et al.*, 2012). Per altra banda, i potser inclús més important, l'ús de biomarcadors ha beneficiat el diagnosis precoç (Frisoni *et al.*, 2017), ja que el dipòsit d'aquestes dues proteïnes pot començar fins a una vintena d'anys abans de l'aparició de qualsevol símptoma clínic (Jack *et al.*, 2013*a*).

Gràcies a l'aparició de biomarcadors *in vivo*, el camp de recerca en Alzheimer ha anat movent progressivament el seu interès cap a estadis més inicials de la malaltia. Actualment, la malaltia d'Alzheimer ja no es conceptualitza només en l'estadi de demència, sinó més com a un continu. Aquest continu està dividit en tres estadis principals: el preclínic, en el que hi ha patologia Alzheimer en el cervell però cap tipus de símptoma cognitiu; el deteriorament cognitiu lleu degut a Alzheimer, en el qual hi ha símptomes cognitius però no afecten a les activitats del

dia a dia; i, finalment, la demència d'Alzheimer, en la que els símptomes cognitius ja afecten a aquestes activitats del dia a dia (Jack *et al.*, 2013*a*). En els últims anys l'estadi preclínic ha rebut més i més atenció ja que representa una finestra d'actuació per a provar noves intervencions preventives (Sperling *et al.*, 2014*a*). Tot i això, s'ha de tenir en compte que aquest estadi no és fàcil de diagnosticar, ja que no té cap símptoma clínic, només canvis patològics inicials. Per a fer-ho, doncs, els biomarcadors *in vivo* són claus.

Actualment, hi ha un cert consens sobre l'ordre en què els principals biomarcadors utilitzats en l'estudi de l'Alzheimer comencen a tenir nivells anormals en el transcurs la malaltia (Jack *et al.*, 2013*a*). Els dos primers biomarcadors en esdevenir anormals estan relacionats amb la mesura de l'amiloide-β (Aβ), primer mesurat en el líquid cefalorraquidi (LCR) i poc després, mesurat amb l'ús de la tomografia per emissió de positrons (PET) (Palmqvist *et al.*, 2016). Aquests van seguits pels biomarcadors encarregats de mesurar els nivells d'acumulació de la proteïna tau que poden mesurar-se també en el LCR o amb PET. I després, per biomarcadors de neurodegeneració que tradicionalment es valorava amb una ressonància magnètica (RM) o un PET de fluorodeoxiglucosa (FDG), tot i que en els últims anys han aparegut marcadors en LCR i sang com els neurofilaments lleugers (NfL). Finalment, l'últim biomarcador en esdevenir anormal és la cognició, que marca la transició cap a l'estadi de deteriorament cognitiu lleu. Tanmateix, és important tenir en compte que hi ha moltes altres vies patofisiològiques alterades durant el continu de la malaltia d'Alzheimer que no estan incloses en aquest marc conceptual. Un exemple important és la neuroinflamació, que ha mostrat alteracions inclús en estadis inicials de la malaltia (Suárez-Calvet *et al.*, 2016; Suárez-Calvet *et al.*, 2016). En els últims anys, l'aparició de nous biomarcadors per algunes d'aquestes vies metabòliques han mostrat la seva utilitat en el camp de la recerca de la malaltia d'Alzheimer (Molinuevo *et al.*, 2018*a*; Milà-Alomà *et al.*, 2019; Zetterberg and Bendlin, 2020). Però encara hi ha moltes incògnites sobre el seu comportament, sobretot en etapes incipients del continu de l'Alzheimer. És important fer notar, que un millor coneixement sobre aquestes vies no només ens proporciona un

coneixement més detallat de la malaltia, sinó que a més, pot donar peu al desenvolupament de nous tractaments que tinguin altres blancs d'actuació que no siguin ni la proteïna Aβ ni la tau.

En relació a la tècnica de PET d'Aβ, hi ha dues maneres d'avaluar-la: visualment o utilitzant mètodes automàtics de quantificació. En l'avaluació visual, que és l'únic mètode aprovat per la *Food and Drug Administration* (FDA) i la *European Medicines Agency* (EMA), els participants són únicament classificats com Aβ positius o Aβ negatius, sense tenir en compte la informació regional. La quantificació, per altra banda, pot proporcionar informació més refinada i detallada, ja que permet una mesura continua i regional de la càrrega d'Aβ, cosa que pot ser útil per a detectar els primers signes de la seva acumulació. Tanmateix, la quantificació de PET d'Aβ té altres limitacions. La més important és la comparabilitat, cosa que complica la transferència directa de coneixement entre estudis. Aquesta es complica quan entren en joc diferent traçadors, escàners i/o protocols d'adquisició i processament de la imatge. Per sobreposar-se a aquest problemes, es va desenvolupar el projecte Centiloid (Klunk *et al.*, 2015). L'escala Centiloid és similar a l'escala Centígrada en el sentit que té dos punts d'ancoratge a 0 i a 100, que en l'escala Centiloid corresponen a la càrrega mitjana d'Aβ d'un grup de subjectes joves sans, i a la d'un grup de subjectes amb demència d'Alzheimer, respectivament. D'aquesta manera, uns valors baixos de Centiloid (CL) representen una baixa o nul·la càrrega d'Aβ, mentre que valors alts de CL impliquen una càrrega alta de la proteïna en forma de placa en el cervell.

Un altre mètode per mesurar els nivells de patologia Aβ és mesurar-ho utilitzant LCR. Estudis previs comparant la classificació dicotòmica entre aquest biomarcador i el PET d'Aβ han demostrat una alta comparabilitat (Landau *et al.*, 2013; Palmqvist *et al.*, 2014, 2015). Tanmateix, ambdós biomarcadors presenten importants diferències entre ells. Primerament, és conegut que el LCR i el PET mesuren diferents tipus d'Aβ (Roberts *et al.*, 2017); en el cas del LCR mesura el desequilibri entre la producció i l'eliminació d'Aβ, mentre que els traçadors PET només s'uneixen a les plaques denses d'Aβ i tenen poca

afinitat per les plaques difuses o l'Aβ soluble (Rowe and Villemagne, 2013). Un altra diferència important entre ambdós biomarcadors és el seu rang dinàmic. Per una banda, el LCR presenta un rang ampli en els baixos nivells de patologia Aβ mentre que en el PET aquest rang és curt. El contrari passa amb els nivells alt de patologia, en el LCR s'observa un *plateau* mentre que el PET presenta un gran rang dinàmic en aquests nivells. Aquestes característiques resulten en uns nivells anormals primer en el LCR que en les imatges PET (Palmqvist *et al.*, 2016), cosa que suggereix que el LCR semblaria més apropiat per una mesura incipient i sensible d'Aβ. No obstant, també hi ha estudis suggerint que els llindars de positivitat utilitzats en PET poden ser massa alts, i que trobar-ne de nous més baixos podria ajudar a detectar indicis més inicials i/o subtils d'amiloïdosis (Villeneuve *et al.*, 2015).

En aquesta tesis doctoral ens hem centrat a investigar els canvis més incipients en el continu de la malaltia d'Alzheimer associats a la patologia d'Aβ i les seves conseqüències derivades. Amb aquest objectiu global, primer hem utilitzat el PET d'Aβ per a millorar la detecció inicial de patologia amiloide, utilitzant la quantificació i l'avaluació visual. Després, hem investigat si algunes característiques biològiques, com són diferents factors de risc per la demència d'Alzheimer, poden augmentar l'acumulació d'Aβ en forma de plaques per a nivells similars d'Aβ en LCR. Finalment, hem investigat diversos mecanismes patofisiològics derivats de l'acumulació incipient d'Aβ observant les associacions entre la càrrega d'Aβ i diferents biomarcadors novells en LCR.

OBJECTIUS

L'objectiu global d'aquesta Tesis doctoral és:

Investigar el dipòsit d'Aβ en les fases inicials del continu de la malaltia d'Alzheimer i els seus efectes derivats.

Amb aquest propòsit, els objectius específics són:

1. Establir llindars sensibles al dipòsit anormal d'Aβ utilitzant la quantificació d'imatges PET d'Aβ.
2. Determinar la precisió i la sensibilitat de l'avaluació visual de PETs d'Aβ per detectar signes inicials de dipòsit cerebral d'Aβ.
3. Investigar les diferències entre la dishomeostàsis d'Aβ soluble i el dipòsit d'Aβ en relació amb factors de risc establerts per a la demència d'Alzheimer.
4. Descriure els mecanismes patofisiològics derivats del dipòsit inicial d'Aβ en el cervell utilitzant biomarcadors novells en LCR.

RESULTATS I DISCUSSIÓ

El treball presentat en aquesta tesis es focalitza en el dipòsit d'Aβ en etapes incipients del continu de la malaltia d'Alzheimer i els seus efectes derivats. Per a fer-ho, s'han inclòs quatre treballs dels que presentem a continuació els resultats i la seva interpretació.

El nostre primer objectiu era el de millorar la detecció d'Aβ incipient utilitzant la quantificació de PETs d'Aβ. Amb aquesta meta, hem derivat diferents llindars de positivitat comparant les mesures contínues de PET d'Aβ amb els valors dicotomitzats de biomarcadors d'Alzheimer en LCR, utilitzant llindars en LCR prèviament validats (Hansson *et al.*, 2018; Schindler *et al.*, 2018).

Amb aquest anàlisis, vam trobar dos llindars de Centiloid diferents que poden servir com a frontera de dos estadis diferent de patologia amiloide: un a 12 CL, que marca la transició entre l'absència de patologia i l'existència d'una patologia subtil; i un altre a 30 CL indicant la presència establerta de patologia. Aquests llindars es corresponen amb el que es va trobar en dos estudis neuropatològics contemporanis al nostre estudi (Joie *et al.*, 2018; Amadoru *et al.*, 2020). El llindar més baix es correspon, en el nostre estudi, al què maximitza l'exactitud de classificació comparant amb les mesures dicotomitzades d'Aβ en el LCR. Per altra banda, el llindar superior, que pretenia ser més específic, va ser derivat contra mesures dicotomitzades del ràtio tau/Aβ, que són més apropiades per descriure el conjunt de tot el continu de la malaltia d'Alzheimer. És important d'emfatitzar que en aquest treball es van incloure participants que cobrien tot el rang del continu de la malaltia d'Alzheimer, assegurant d'incloure participants en els estadis més incipients de la malaltia. D'aquesta manera, vam maximitzar el nombre de subjectes en el que anomenem àrea gris (càrrega baixa-intermitja d'Aβ), el que va permetre derivar llindars molt sensibles per la detecció incipient de la patologia Aβ.

Perseguint un objectiu similar, el segon treball presentat volia investigar si el PET d'Aβ era capaç de detectar patologia incipient d'Aβ, però en aquest cas utilitzant l'avaluació visual. És important de destacar que, tot i que la quantificació és el mètode més emprat en recerca, l'avaluació visual és encara l'únic mètode acceptat per les agències del medicament (FDA i EMA) per classificar un individu com Aβ positiu o Aβ negatiu en la clínica. D'aquesta manera, i donat el creixent interès per a detectar els primers signes de patologia amiloide per assaigs clínics, és de vital importància avaluar la sensitivitat d'aquesta mesura, i millorar-la si és possible. Els nostres resultats suggereixen que l'avaluació visual feta per experts altament entrenats pot detectar els primers signes de patologia amiloide amb una exactitud similar a la quantificació. Per ser més específics, l'avaluació visual va demostrar una alta exactitud en classificar subjectes quan es va comparar amb els llindars derivats en l'estudi previ. I quan es va derivar un llindar quantitatiu utilitzant l'avaluació visual com a referència, es va trobar un valor, 17 CL, que es troba comprès entre els altres dos llindars.

A destacar, els nostres resultats van ser corroborats en una petita mostra independent de subjectes amb informació neuropatològica, que és el *gold standard* per avaluar patologia amiloide. En concret, l'avaluació visual va concordar amb la classificació neuropatològica en el 89% de casos (25/28). I en els tres casos que no van coincidir es va tractar de falsos positius, que tot i ser classificats com a negatius en l'estudi neuropatològic mostraven un nivell elevat de patologia (Mirra *et al.*, 1991; Ikonomovic *et al.*, 2016). Suggerint, així, que l'avaluació visual podia detectar nivells dispersos-moderats de patologia. Així, tots els nostres resultats indiquen que l'avaluació visual pot detectar càrrega incipient de patologia amiloide.

Una altra novetat important del nostre estudi va ser l'avaluació visual a nivell regional. Els nostres anàlisis van demostrar que el nombre de regions classificades com a positives en l'avaluació visual estava associada amb la càrrega total d'amiloide quantificada amb l'escala Centiloid. Tot i que aquest pot ser un resultat fins a un cert punt previsible, aquesta troballa recolza l'ús de l'avaluació visual regional ja que permet qualificar l'extensió d'Aβ en el cervell. Aquesta eina podria ser de molta utilitat per estadiar subjectes i rastrejar la progressió de la malaltia. Tanmateix, aquesta hipòtesis hauria de ser corroborada en un estudi longitudinal. És també destacable, que la classificació regional visual també mostrava associacions amb la quantificació regional, tant en les imatges PET com en la valoració neuropatològica. Finalment, i de manera més inesperada, vam descobrir uns patrons regionals de positivitat molt específics. Vam observar que només s'observaven un conjunt limitat de combinacions de regions avaluades com a positives, de manera que vam proposar un model d'estadiatge. En particular, els patrons observats majoritàriament eren: les regions frontals o precuni/cingulat posterior en solitari (estadi 1) o en combinació (estadi 2); i finalment, aquestes dues regions conjuntament amb qualsevol altra de les regions corticals o l'estriat (estadi 3). Aquests estadis mostraven una correlació significativa amb la quantificació global. Conjuntament, aquestes troballes reforcen la hipòtesis del valor pronòstic de l'avaluació visual regional i clarifiquen els patrons regionals de positivitats esperables en la clínica.

En el següent estudi vàrem investigar si factors de risc establerts per a la demència d'Alzheimer podien augmentar el dipòsit d'Aβ en el cervell per a nivells similar d' Aβ en el LCR. En ell vam observar que tres dels majors factors de risc per aquesta malaltia -edat avançada, sexe femení i ser portador d'un al·lel *APOE-ε4*- estaven associats amb un increment de càrrega d'Aβ, mesurada en imatges PET, pels mateixos nivells d'Aβ en el LCR; recolzant la idea que contribueixen d'aquesta manera a augmentar l'acumulació d'Aβ en forma de plaques. A destacar, les àrees en les que aquestes diferències apareixen són diferents depenent del factor de risc estudiat. En particular, ser portador d'un al·lel *APOE-ε4* maximitza la càrrega d'Aβ dipositada en regions no típicament afectades per l'Aβ en les etapes incipients, sinó en àrees en les que apareix inicialment la proteïna tau (Braak and Braak, 1991; Schöll *et al.*, 2016). Això ens induí a pensar que aquest al·lel pot facilitar l'expansió d'aquesta proteïna fora del còrtex entorinal gràcies, precisament, a l'augment d'Aβ en aquesta localització, augmentant així la interacció sinergètica entre Aβ i tau (Mungas *et al.*, 2014). Això, unit a l'augment de càrrega global d'Aβ ja àmpliament conegut, pot ser una de les raons per l'augment en el risc de la malaltia d'Alzheimer per als portadors d'aquest al·lel. Per altra banda, l'edat avançada mostrà un augment del dipòsit d'Aβ en àrees relacionades amb l'inici d'acumulació d'aquesta proteïna com el cingulat posterior o el precuni (Palmqvist *et al.*, 2017). Unes regions similars són les que també presentaven una càrrega incrementada d'Aβ en les dones, tot i que menys extenses. Considerant tots els nostres resultats de manera general, el nostre estudi revelà possibles vies biològiques per les quals els factors les característiques estudiades augmenten diferencialment el risc de desenvolupar la malaltia d'Alzheimer.

En l'últim estudi presentat, l'objectiu era entendre les relacions entre l'Aβ dipositat i múltiples vies patofisiològiques secundàries en la malaltia d'Alzheimer en els estadis inicials de la malaltia, utilitzant biomarcadors novells en LCR. La importància d'aquest tipus d'estudis resideix en el fet d'intentar desxifrar quins canvis ocorren en els moments inicials de la malaltia; cosa que pot ser útil per a poder dissenyar futurs estudis clínics. Es poden extreure múltiples conclusions del nostre últim treball. El primer que vam trobar van ser associacions entre l'Aβ dipositat i biomarcadors en LCR de patologia tau, disfunció sinàptica, neurodegeneració i inflamació. Aquesta

troballa estén a individus més joves i sense símptomes cognitius els resultats prèviament reportats en dos estudis contemporanis al nostre (Bos *et al.*, 2019, Palmqvist *et al.*, 2019*a*). A més, també mostràvem associacions amb certs biomarcadors de neuroinflamació -GFAP i sTREM2- que no havien sigut descrits abans. Aquests resultats emfatitzen la importància de la neuroinflamació ens estadis inicials del continu de la malaltia d'Alzheimer i demostren que hi ha moltes alteracions biològiques en el cervell abans que aparegui qualsevol símptoma cognitiu.

En uns anàlisis addicionals vam investigar amb més profunditat les relacions entre el dipòsit d'Aβ i els mecanismes patofisiològics derivats. Estudiant les relacions entre patologia Aβ, tau i neurodegeneració, vam observar que l'associació entre Aβ i el marcador de neurodegeneració estava parcialment derivada per la patologia tau. Tanmateix, el més interessant és que hi ha una part de la associació entre Aβ i neurodegeneració que no depenia de tau. La literatura prèvia suggereix una relació més estreta entre neurodegeneració i patologia tau que amb Aβ; tanmateix, la majoria d'aquests estudis estan centrats en etapes més tardanes de la malaltia (Iaccarino *et al.*, 2018; La Joie *et al.*, 2020). La nostra hipòtesis és que hi ha una relació directe entre Aβ i neurodegeneració en etapes inicials del continu, però aquesta és sobrepassada per la relació entre tau i neurodegeneració en etapes més avançades. Pel que fa a les relacions entre inflamació i patologia Aβ, els nostres resultats apuntaven a que aquestes depenien totalment de la patologia tau. Aquest resultat està en línia amb la hipòtesis, prèviament publicada, que els nivells de marcadors de glia van en paral·lel d'aquells relacionats amb la patologia tau (Suárez-Calvet et al., 2016, 2019; Rauchmann et al., 2019).

Finalment, en aquest últim treball també ens vam interessar pel paper modulador de certs factors de risc de la malaltia d'Alzheimer en les relacions entre els diferents biomarcadors. Amb aquest anàlisi vam observar que les relacions entre sTREM2, un marcador d'activitat de micròglia, i Aβ eren més importants en dones que en homes. NfL, un biomarcador de neurodegeneració, mostrava una relació similar. Aquest últim fet pot contribuir a explicar el major risc de desenvolupar la malaltia per part de les dones, independentment de la càrrega de tau (Fisher et al., 2018). Aquest

fet també està en conjunció amb previs estudis que mostren que les dones amb patologia Aβ presenten un major declini cognitiu que els homes (Buckley *et al.*, 2018), donada la íntima relació entre neurodegeneració i cognició (Nelson *et al.*, 2012). Per altra banda, el fet de si el major augment d'activitat microglial en dones amb càrrega d'Aβ és un efecte protector o perjudicial encara és desconegut i mereix una investigació més profunda.

Pel que fa a interaccions amb l'edat, vam observar un major nivell de patologia tau per a càrregues incrementals d'Aβ en individus d'avançada edat. Això suggereix que, un cop comença a acumular-se l'Aβ, les persones d'edat avançada semblen ser més susceptibles a la patologia tau. Tot i ser la primera vegada que es descriu aquest tipus de relació, hi ha algunes explicacions plausibles per aquest fet. Primer, és possible que altres co-patologies, més probables en gent d'edat avançada, facin el cervell més susceptible a la patologia tau un cop ja hi hagi Aβ. Segon, també és possible que altres mecanismes biològics, com ara la neuroinflamació, vagin disminuint la seva capacitat protectores en edats més avançades. Tanmateix, cal més recerca per replicar aquests resultats i confirmar les nostres hipòtesis.

En conclusió, el nostre treball contribueix a expandir el nostre coneixement sobre el dipòsit incipient d'Aβ en el cervell i els seus efectes derivats. Per ser més precisos, primer preteníem millorar la detecció incipient d'Aβ utilitzant la imatge PET. Per fer-ho, primer hem derivat llindars, significativament inferiors als prèviament publicats, utilitzant la quantificació de les imatges en una escala estàndard, fàcilment traduïbles a altres traçadors i mètodes de processament. Segon, hem demostrat que l'avaluació visual, pràctica habitual en la clínica, pot detectar el dipòsit incipient d'Aβ i, més important, qualificar la seva extensió. La informació regional, que ja es recull en el marc clínic, ha demostrat proveir informació extra que pot relacionar-se amb la càrrega d'Aβ mesurada amb la quantificació. També hem pogut observar que tres factors de risc per desenvolupar la malaltia d'Alzheimer -avançada edat, sexe femení i l'al·lel *APOE-ε4*- augmenten el dipòsit d'Aβ en forma de placa. Això apunta cap a un possible mecanisme biològic pel qual aquest factors podrien augmentar el risc de desenvolupar la malaltia Alzheimer. I, finalment, en l'últim estudi hem demostrat que la càrrega d'Aβ està associada

amb múltiples vies patofisiològiques, fins i tot en nivells baixos de patologia amiloide. Com a conclusió final, podem dir que les imatges PET d'Aβ són una eina molt valuosa per la detecció incipient de la patologia amiloide i ens permeten entendre una mica millor els fenòmens inicials que ocorren en la etapa preclínica de la malaltia d'Alzheimer.

CONCLUSIONS

1. La quantificació global del PET d' Aβ pot detectar els primers signes de dipòsit d'Aβ amb una gran precisió utilitzant llindars quantitatius significativament menors dels prèviament utilitzats.

2. L'avaluació visual dels PETs d'Aβ pot detectar els primers signes de patologia Aβ i quantificar la seva extensió utilitzant informació regional.

3. Les condicions d'edat avançada, sexe femení o ser portador d'almenys un al·lel *APOE-ε4* promou el dipòsit incipient d'Aβ en diferents regions del cervell per nivells similar de deshomeòstasi d'Aβ. En el cas de les dues primeres condicions, l'increment de dipòsit d'Aβ es produeix en àrees d'acumulació inicial d'Aβ; mentre que en cas de ser portador d'un al·lel *APOE-ε4* està associat amb l'extensió de l'Aβ en regions vulnerables a la patologia tau incipient i, per tant, pot contribuir a l'extensió de l'última pel cervell.

4. El dipòsit d'Aβ té un efecte independent de tau sobre la neurodegeneració i un efecte totalment dependent de tau sobre la neuroinflamació en les primeres fases del continu de l'Alzheimer.

ACKNOWLEDGEMENTS

Voldria començar aquesta secció dient que aquí vull expressar uns agraïments per la gent que ha estat al meu costat en aquests últims quatre anys, independentment de la seva relació, directa o indirecta, amb la ciència duta a terme, perquè al final és tan important treballar quan cal, com saber desconnectar.

Als primers als que he de mencionar en aquest apartat no poden ser altres que els meus directors, el Dr. Juan Domingo Gispert i el Dr. José Luis Molinuevo. Us agraeixo de la manera més profunda i sincera tot el heu fet per mi aquests últims anys. Ambdós m'heu ajudat immensament a evolucionar com a investigadora, pels coneixements que m'heu transmès, però sobretot per forçar-me a sortir de la meva zona de confort -tot i les meves reticències- per a que descobrís del que sóc capaç. Tot i això, el que valoro per sobre de tot és el suport que m'heu donat en l'aspecte més personal. I és que la suma de les vostres personalitats totalment complementàries ha sigut vital. Gràcies Juando per compartir aquesta passió per descobrir i anar sempre una mica més enllà; he gaudit molt de les estones de discussió tot fent una mica de ciència. Y a ti, José Luis, quiero agradecerte la manera que tienes de mirar la vida, haciendo que todo parezca más fácil para los que te rodean. Siempre nos quedará *la Cervecita*.

També m'agradaria tenir unes paraules d'agraïment per la meva tutora, la Dra. Roser Sala-Llonch, per estar sempre disposada a ajudar-me en tot i en tot moment malgrat la distància.

Vull fer un especial agraïment a tots els participants, especialment als de l'estudi ALFA, que amb el seu temps i esforç han permès que es pogués fer la investigació presentada en aquesta tesi. Res d'això seria possible sense vosaltres.

Durant aquests anys he tingut la sort de compartir moltes estones de lleure al costat de companys i companyes, molts dels quals ja considero amics.

Per fer aquesta part he estat remirant fotos del que hem compartit, i realment és impossible resumir-ho tot aquí. Tanmateix, intentaré plasmar encara que sigui una petita part, els sentiments que em venen al cap quan faig memòria d'aquests darrers anys. Carol, abans de res et demano perdó per haver sigut tan *plasta*. També, t'he de donar gràcies perquè sense tu segurament mai hauria arribat a BBRC. Però per si això fos poc, t'agraeixo tots els bons moments compartits, que no són pocs: GA's, AAIC's, post-AAIC's, dormides en llits i en sofàs, retards en aeroports, *big packages*, pràctiques de presentacions i, sobretot, moltes i moltes converses i confidències regades amb alguna que altra cervesa. Espero poder seguir gaudint, com a mínim, d'això últim. Carles, a tu et recordo com la primera persona de BBRC que vaig conèixer i la primera que em va acollir. Gràcies per la teva infinita paciència a l'hora d'explicar-me el processat d'imatges i per totes les tardes acompanyades d'un tros de xocolata. Greg, *merci* per haver sigut durant molt temps el meu *personal trainer*, per haver tingut paciència en els meus pitjors moments de forma, i per tots els entrenaments on conversàvem de ciència i de no ciència mentre m'arrossegaves fins al Fòrum. Aquests últims anys haurien sigut més difícils de suportar sense aquests petits moments de *kit-kat*. Anna, gràcies per haver format part del primer *PhD team* del grup fent que les coses fossin molt més fàcils per mi amb els teus consells de *senior PhD*. *Grazas* Gema, por compartir la pasión por la física, el baile y el vermut. Espero poder reanudar todas las actividades "extraescolares" cuando el mundo vuelva a la normalidad. Karine, a tu et vull agrair tot l'afecte i la confiança cap a mi que sempre m'has demostrat, més i tot de la que tinc jo mateixa. Mahnaz and Marta, you form part of my other PhD team, thanks for many lessons learned together, and for forgiving me not knowing when to arrive at the airport. Raffa, gràcies per compartir amb mi l'amor a l'*APOE* donant lloc a un gran treball. Nat, amb tu comparteixo un altre amor, per un país en aquest cas. Per això t'he d'agrair, per sobre de tot, haver-me ajudat a tornar a Àmsterdam. Ana Belén, tot i que en molts moments m'he queixat de totes les fotos que he hagut de suportar, t'agraeixo la teva tasca de divulgació, però sobretot la manera amb la que ho fas. I també a la resta de persones amb les que he compartit moments durant aquests anys: partits de *volley*, fit, entrenaments, congressos, reunions, cerveses, cerques de claus d'apartaments, terrassetes i incomptables anècdotes que

han quedat gravades a la meva memòria. Finalment, vull agrair a tota la gent de la Fundació Pasqual Maragall i de BBRC -als que han estat, als que estan i als que estaran- per fer seguir creixent aquest projecte tan especial.

A l'Aida, al Domènec i al Javier agraeixo haver-me batejat en el camp de la neuroimatge. Segurament, aquesta aventura no hauria començat si no fos perquè em vau acollir al grup de biofísica fa uns anys. Gràcies per donar-me l'oportunitat d'iniciar-me en aquest món i tenir la paciència necessària per ensenyar-me les bases per començar a recórrer aquest camí.

To the whole AMYPAD family, and the WP7 in particular, as these four years would have been completely different without being part of this amazing group. I especially appreciate the closeness between people and the eagerness to work for a future without Alzheimer's. Within this amazing group of people, I would like to mention some in particular. Gill and Chris, thanks for making this path easier and more enjoyable. I hope we can meet again and enjoy Miami's sun together soon. Elena, gracias por acogerme en mi primer congreso cuando estaba completamente perdida. Siempre es un placer coincidir contigo científica y personalmente, y espero seguir haciéndolo en el futuro.

A Silvia, por obligarme casi, a seguir este camino cuando estaba a punto de tirar la toalla. Gracias por tener más fe en mi que yo misma.

A los badminton *core*: Jaime, Juanjo y Dani. Por todos los *clears* hechos para relajar tensiones y las cervezas posteriores para recuperar fuerzas.

Als petits de la casa, Mateu i Gabriel i a la meva padrina Montse, per regalar-me unes tardes d'estiu plenes d'escalf quan més ho necessitava.

A tota la colla de físics per totes les estones de distracció tan necessàries per aguantar el procés d'una tesis. Per les cerveses, els vermuts, les esquiades, els caminos, els caps d'any, les calçotades, els festivals de primavera, els Sant Alberts, les festes de Gràcia (i de Sants) i tants altres records inesborrables. Gràcies Raquel, Monty, Pérez, Joan, Popep, Fran,

Gràcia, Adri, Alba's, Víctor, Isma i Irene. Un especial record cap al grup de viatges - Toni, Elis i Grau- que espero que recuperem aviat, sigui per visitar-nos a les nostres noves destinacions o per descobrir llocs nous. I finalment vull dedicar unes paraules a dues persones amb qui he compartit casa i molt més. Gràcies Sergi, per ser un gran suport al principi d'aquest camí. Iván, a ti te agradezco los vermuts preparando la comida, los Polonia en el sofá y nuestras listas de reproducción para limpiar la casa. Pero sobretodo *dankon* por tantas conversaciones en las que intentábamos arreglar la ciencia, el mundo, e incluso nuestras vidas.

Gràcies Mar, perquè tot i la distància física, sempre t'he sentit molt a prop.

A les de tota la vida: Anna, Marina, Àngela i Sònia, perquè tot és més fàcil quan algú et coneix millor que tu mateix. I especialment, gràcies Marina per fer-me escampar la boira en amb les nostres passejades en els moments més grisos.

A lot of happy memories come to my mind when I remember the time spent in the Netherlands. First, I would like to thank Dr. Frederik Barkhof and Dr. Rik Ossenkoppele for giving me the opportunity to live the Amsterdam life twice (even if it meant being there during a pandemic). I especially would like to thank Rik for having such a comprehensive and helpful attitude when the situation got complicated. Second, to all the people that have made my months there unforgettable: Daniele, Silvia, Juhan, Viktor, Ifrah, Denise, Yvonne, Luigi, Emma's, Colin, Fiona, Linda, Ellen, Diana, Anita, Ilse, Ilona, Sophie and Timothy. A part of my heart will always be in Amsterdam and this is in part because of you.

And, finally, to my Dutch family: Isa and Lyduine. The whole AMYPAD experience would have not been the same without you. In my first visit to the Netherlands I had the opportunity to get to know you, and that was an important part of why I wanted to come back later. I'm deeply thankful for all the moments we've lived together these last years, which are countless, and I hope we can continue sharing many more in the future. On these moments we had lived some interesting experiences: sunbathing in January in Miami, eating *pimientos* in Barcelona or *bitterballen* in Amsterdam, virtual *vermuts* during a pandemic or wine tastings in Friday's

afternoons and, maybe, even some science in between. But my most valuable honor is to be able to call you my friends. Thank you for making me feel *gezellig* by your side.

A la Bàrbara per ser, a part d'una amiga excepcional, la meva *coach* científica. Per ser la persona -i ja és difícil- que més vegades m'ha dit: "Escriu!" en els últims quatre anys. Però sobretot, gràcies per les hores i hores dedicades a escoltar les meves històries, des de les més científiques com les més profanes.

I per últim, als meus tres pilars: Jaume, Maria i Marta. No hi ha manera possible d'agrair-vos tot el que heu fet per mi; així que només diré gràcies per ser-hi sempre, per acompanyar-me en els bons moments però sobretot per estirar de mi en els pitjors. Només espero poder seguir al vostre costat molts anys més. Com a vegades diem, vosaltres sou aquell tipus de família que tenim el privilegi d'escollir.

Per acabar, vull dedicar aquesta tesi als meus pares i als meus avis. I aquí les paraules sobren.

Gràcies, gracias, grazas, eskerrik asko, dankon, thank you, merci, grazie, dank je, danke, مـ تـ شـ كـ رم, obrigada

REFERENCES

Alcolea D, Martínez-Lage P, Sánchez-Juan P, Olazarán J, Antúnez C, Izagirre A, et al. Amyloid precursor protein metabolism and inflammation markers in preclinical Alzheimer disease. Neurology 2015; 85: 626–633.

Alcolea D, Vilaplana E, Pegueroles J, Montal V, Sánchez-Juan P, González-Suárez A, et al. Relationship between cortical thickness and cerebrospinal fluid YKL-40 in predementia stages of Alzheimer's disease. Neurobiol Aging 2015; 36: 2018–2023.

Alcolea D, Vilaplana E, Suárez-calvet M, Illán-gala I, Sánchez-valle R, García-ribas G, et al. CSF sAPPb, YKL-40, and neurofilament light in frontotemporal lobar degeneration. Neurology 2017; 89: 178–188.

Altmann A, Tian L, Henderson VW, Greicius MD. Sex modifies the APOE-related risk of developing Alzheimer disease. Ann Neurol 2014; 75: 563–573.

Alzheimer A. Uber eine eigenartige Erkrankung der Hirnrinde. Allg Zeitschrift fur Psychiatr und phychish- Gerichtl Medizin 1907; 64: 146–148.

Amadoru S, Doré V, McLean CA, Hinton F, Shepherd CE, Halliday GM, et al. Comparison of amyloid PET measured in Centiloid units with neuropathological findings in Alzheimer's disease. Alzheimers Res Ther 2020; 12: 22.

Andersson E, Janelidze S, Lampinen B, Nilsson M, Leuzy A, Stomrud E, et al. Blood and cerebrospinal fluid neurofilament light differentially detect neurodegeneration in early Alzheimer's disease. Neurobiol Aging 2020; 95: 143–153.

Andreasen N, Minthon L, Vanmechelen E, Vanderstichele H, Davidsson P, Winblad B, et al. Cerebrospinal fluid tau and Abeta42 as predictors of development of Alzheimer's disease in patients with mild cognitive impairment. Neurosci Lett 1999; 273: 5–8.

Arnsten AFT, Datta D, Tredici K Del, Braak H. Hypothesis: Tau pathology is an initiating factor in sporadic Alzheimer's disease. Alzheimer's Dement 2020: 1–10.

Arranz AM, De Strooper B. The role of astroglia in Alzheimer's disease: pathophysiology and clinical implications. Lancet Neurol 2019; 18: 406–414.

Arriagada P V, Growdon JH, Hedley-Whyte ET, Hyman BT. Neurofibrillary tangles but not senile plaques parallel duration and severity of Alzheimer's disease. Neurology 1992; 42: 631–639.

Barthel H, Gertz HJ, Dresel S, Peters O, Bartenstein P, Buerger K, et al. Cerebral amyloid-b PET with florbetaben (18F) in patients with Alzheimer's disease and healthy controls: A multicentre phase 2 diagnostic study. Lancet Neurol 2011; 10: 424–435.

Barthélemy NR, Bateman RJ, Hirtz C, Marin P, Becher F, Sato C, et al. Cerebrospinal fluid phospho-tau T217 outperforms T181 as a biomarker for the differential diagnosis of Alzheimer's disease and PET amyloid-positive patient identification. Alzheimers Res Ther 2020; 12: 26.

Bateman RJ, Xiong C, Benzinger TLS, Fagan AM, Goate A, Fox NC, et al. Clinical and biomarker changes in dominantly inherited Alzheimer's disease. N Engl J Med 2012; 367: 795–804.

Bateman RJ, Xiong C, Benzinger TLS, Fagan AM, Goate A, Fox NC, et al. Clinical and biomarker changes in dominantly inherited Alzheimer's disease. N Engl J Med 2012; 367: 795–804.

Battle MR, Buckley CJ, Smith APL, Farrar G, Thal DR, Molinuevo JL. Comparison of Centiloid Scaling Values with Visual Read Assessment in a Pathology Verified Autopsy Cohort. In: EANM. 2019

Beach TG, Monsell SE, Phillips LE, Kukull W. Accuracy of the clinical diagnosis of Alzheimer disease at National Institute on Aging Alzheimer Disease Centers, 2005-2010. J Neuropathol Exp Neurol 2012; 71: 266–273.

Bejanin A, Schonhaut DR, La Joie R, Kramer JH, Baker SL, Sosa N, et al. Tau pathology and neurodegeneration contribute to cognitive impairment in Alzheimer's disease. Brain 2017; 140: 3286–3300.

Belloy ME, Napolioni V, Greicius MD. A Quarter Century of APOE and Alzheimer's Disease: Progress to Date and the Path Forward. Neuron 2019; 101: 820–838.

Bischof GN, Jessen F, Fliessbach K, Dronse J, Hammes J, Neumaier B, et al. Impact of tau and amyloid burden on glucose metabolism in Alzheimer's disease. Ann Clin Transl Neurol 2016; 3: 934–939.

Bittner T, Zetterberg H, Teunissen CE, Ostlund RE, Militello M, Andreasson U, et al. Technical performance of a novel, fully automated electrochemiluminescence immunoassay for the quantitation of β-amyloid (1-42) in human cerebrospinal fluid. Alzheimer's Dement 2016; 12: 517–526.

Blennow K, Shaw LM, Stomrud E, Mattsson N, Toledo JB, Buck K, et al. Predicting clinical decline and conversion to Alzheimer's disease or dementia using novel Elecsys Aβ(1–42), pTau and tTau CSF immunoassays. Sci Rep 2019; 9: 1–11.

Blennow K, Wallin A, Agren H, Spenger C, Siegfried J, Vanmechelen E. Tau protein in cerebrospinal fluid: a biochemical marker for axonal degeneration in Alzheimer disease? Mol Chem Neuropathol 1995; 26: 231–245.

Blennow K, Zetterberg H. Biomarkers for Alzheimer's disease: current status and prospects for the future. J Intern Med 2018; 284: 643–663.

Bos I, Vos S, Verhey F, Scheltens P, Teunissen C, Engelborghs S, et al. Cerebrospinal fluid biomarkers of neurodegeneration, synaptic integrity, and astroglial activation across the clinical Alzheimer's disease spectrum. Alzheimer's Dement 2019; 15: 644–654.

Boyle PA, Yu L, Leurgans SE, Wilson RS, Brookmeyer R, Schneider JA, et al. Attributable risk of Alzheimer's dementia attributed to age-related neuropathologies. Ann Neurol 2019; 85: 114–124.

Braak H, Alafuzoff I, Arzberger T, Kretzschmar H, Tredici K. Staging of Alzheimer disease-associated neurofibrillary pathology using paraffin sections and immunocytochemistry. Acta Neuropathol 2006; 112: 389–404.

Braak H, Braak E. Neuropathological stageing of Alzheimer-related changes. Acta Neuropathol 1991; 82: 239–259.

Braak H, Braak E. Frequency of stages of Alzheimer-related lesions in different age categories. Neurobiol Aging 1997; 18: 351–357.

Braak H, Thal DR, Ghebremedhin E, Del Tredici K. Stages of the pathologic process in alzheimer disease: Age categories from 1 to 100 years. J Neuropathol Exp Neurol 2011; 70: 960–969.

Braak H, Del Tredici K. The pathological process underlying Alzheimer's disease in individuals under thirty. Acta Neuropathol 2011; 121: 171–181.

Bradshaw EM, Chibnik LB, Keenan BT, Ottoboni L, Raj T, Tang A, et al. CD33 Alzheimer's disease locus: altered monocyte function and amyloid biology. Nat Neurosci 2013; 16: 848–850.

Brier MR, Gordon B, Friedrichsen K, McCarthy J, Stern A, Christensen J, et al. Tau and Ab imaging, CSF measures, and cognition in Alzheimer's disease. Sci Transl Med 2016; 8: 1–10.

de Bruijn RFAG, Bos MJ, Portegies MLP, Hofman A, Franco OH, Koudstaal PJ, et al. The potential for prevention of dementia across two decades: the prospective, population-based Rotterdam Study. BMC Med 2015; 13: 132.

Bu G. Apolipoprotein e and its receptors in Alzheimer's disease: Pathways, pathogenesis and therapy. Nat Rev Neurosci 2009; 10: 333–344.

Buckley RF, Mormino EC, Amariglio RE, Properzi MJ, Rabin JS, Lim YY, et al. Sex, amyloid, and APOE ε4 and risk of cognitive decline in preclinical Alzheimer's disease: Findings from three well-characterized cohorts. Alzheimer's Dement 2018; 14: 1193–1203.

Buckley RF, Mormino EC, Chhatwal J, Schultz AP, Rabin JS, Rentz DM, et al. Associations between baseline amyloid, sex, and APOE on subsequent tau accumulation in cerebrospinal fluid. Neurobiol Aging 2019; 78: 178–185.

Buckley RF, Mormino EC, Rabin JS, Hohman TJ, Landau S, Hanseeuw BJ, et al. Sex Differences in the Association of Global Amyloid and Regional Tau Deposition Measured by Positron Emission Tomography in Clinically Normal Older Adults. JAMA Neurol 2019; 76: 542–551.

Buckley RF, Scott MR, Jacobs HIL, Schultz AP, Properzi MJ, Amariglio RE, et al. Sex Mediates Relationships Between Regional Tau Pathology and Cognitive Decline. Ann Neurol 2020: 1–12.

Bullich S, Roe-Vellve N, Marquie M, Barthel H, Villemagne V, Sanabria A, et al. Early detection of amyloid load using 18F-Florbetaben PET. J Nucl Med 2020; 61: 1–15.

Cacciaglia R, Molinuevo JL, Falcón C, Brugulat-Serrat A, Sánchez-Benavides G, Gramunt N, et al. Effects of APOE-ε4 allele load on brain morphology in a cohort of middle-aged healthy individuals with enriched

genetic risk for Alzheimer's disease. Alzheimer's Dement 2018; 14: 902–912.

Cai Z, Hussain MD, Yan L-J. Microglia, neuroinflammation, and beta-amyloid protein in Alzheimer's disease. Int J Neurosci 2014; 124: 307–321.

Casaletto KB, Elahi FM, Bettcher BM, Neuhaus J, Bendlin BB, Asthana S, et al. Neurogranin, a synaptic protein, is associated with memory independent of Alzheimer biomarkers. Neurology 2017; 89: 1782–1788.

Chetelat G, Desgranges B, de la Sayette V, Viader F, Berkouk K, Landeau B, et al. Dissociating atrophy and hypometabolism impact on episodic memory in mild cognitive impairment. Brain 2003; 126: 1955–1967.

Cho H, Choi JY, Hwang MS, Kim YJ, Lee HM, Lee HS, et al. In vivo cortical spreading pattern of tau and amyloid in the Alzheimer disease spectrum. Ann Neurol 2016; 80: 247–258.

Clark CM, Schneider JA, Bedell BJ, Beach TG, Bilker WB, Mintun MA, et al. Use of florbetapir-PET for imaging beta-amyloid pathology. JAMA 2011; 305: 275–283.

Coats M, Morris JC. Antecedent biomarkers of Alzheimer's disease: the adult children study. J Geriatr Psychiatry Neurol 2005; 18: 242–244.

Cohen AD, Landau SM, Snitz BE, Klunk WE, Blennow K, Zetterberg H. Fluid and PET biomarkers for amyloid pathology in Alzheimer's disease. Mol Cell Neurosci 2019; 97: 3–17.

Collij LE, Heeman F, Salvadó G, Ingala S, Altomare D, de Wilde A, et al. Multitracer model for staging cortical amyloid deposition using PET imaging. Neurology 2020; 95: e1538–e1553.

Corder EH, Saunders AM, Risch NJ, Strittmatter WJ, Schmechel DE, Gaskell PC, et al. Protective effect of apolipoprotein E type 2 allele for late onset Alzheimer disease. Nat Genet 1994; 7: 180–184.

Craig-Schapiro R, Perrin RJ, Roe CM, Xiong C, Carter D, Cairns NJ, et al. YKL-40: a novel prognostic fluid biomarker for preclinical Alzheimer's disease. Biol Psychiatry 2010; 68: 903–912.

Cummings J, Lee G, Ritter A, Sabbagh M, Zhong K. Alzheimer's disease drug development pipeline: 2020. Alzheimer's Dement Transl Res Clin Interv 2020; 6: 1–29.

Damoiseaux JS, Seeley WW, Zhou J, Shirer WR, Coppola G, Karydas A, et al. Gender modulates the APOE ε4 effect in healthy older adults: Convergent evidence from functional brain connectivity and spinal fluid tau levels. J Neurosci 2012; 32: 8254–8262.

DeCarli C, Massaro J, Harvey D, Hald J, Tullberg M, Au R, et al. Measures of brain morphology and infarction in the framingham heart study: establishing what is normal. Neurobiol Aging 2005; 26: 491–510.

Deture MA, Dickson DW. The neuropathological diagnosis of Alzheimer's disease. Mol Neurodegener 2019; 14: 1–18.

Dickerson BC, Bakkour A, Salat DH, Feczko E, Pacheco J, Greve DN, et al. The cortical signature of Alzheimer's disease: Regionally specific cortical thinning relates to symptom severity in very mild to mild AD dementia and is detectable in asymptomatic amyloid-positive individuals. Cereb Cortex 2009; 19: 497–510.

Dumitrescu L, Barnes LL, Thambisetty M, Beecham G, Kunkle B, Bush WS, et al. Sex differences in the genetic predictors of Alzheimer's pathology. Brain 2019; 142: 2581–2589.

Duyckaerts C, Delatour B, Potier MC. Classification and basic pathology of Alzheimer disease. Acta Neuropathol 2009; 118: 5–36.

Ellis KA, Bush AI, Darby D, De Fazio D, Foster J, Hudson P, et al. The Australian Imaging, Biomarkers and Lifestyle (AIBL) study of aging: Methodology and baseline characteristics of 1112 individuals recruited for a longitudinal study of Alzheimer's disease. Int Psychogeriatrics 2009; 21: 672–687.

Van der Elst W, van Boxtel MPJ, van Breukelen GJP, Jolles J. Rey's verbal learning test: normative data for 1855 healthy participants aged 24-81 years and the influence of age, sex, education, and mode of presentation. J Int Neuropsychol Soc 2005; 11: 290–302.

Ewers M, Franzmeier N, Suárez-Calvet M, Morenas-Rodriguez E, Caballero MAA, Kleinberger G, et al. Increased soluble TREM2 in cerebrospinal fluid is associated with reduced cognitive and clinical decline in Alzheimer's disease. Sci Transl Med 2019; 11

Fagan AM, Mintun M a., Mach RH, Lee SY, Dence CS, Shah AR, et al. Inverse relation between in vivo amyloid imaging load and cerebrospinal fluid Abeta 42 in humans. Ann Neurol 2006; 59: 512–519.

Fagan AM, Xiong C, Jasielec MS, Bateman RJ, Goate AM, Benzinger TLS, et al. Longitudinal change in CSF biomarkers in autosomal-dominant Alzheimer's disease. Sci Transl Med 2014; 6

Falcon C, Monté-Rubio GC, Grau-Rivera O, Suárez-Calvet M, Sánchez-Valle R, Rami L, et al. CSF glial biomarkers YKL40 and sTREM2 are associated with longitudinal volume and diffusivity changes in cognitively unimpaired individuals. NeuroImage Clin 2019; 23: 101801.

Fan Z, Brooks DJ, Okello A, Edison P. An early and late peak in microglial activation in Alzheimer's disease trajectory. Brain 2017; 140: 792–803.

Fan Z, Okello AA, Brooks DJ, Edison P. Longitudinal influence of microglial activation and amyloid on neuronal function in Alzheimer's disease. Brain 2015; 138: 3685–3698.

Fantoni E, Collij L, Lopes Alves I, Buckley C, Farrar G. The Spatial-Temporal Ordering of Amyloid Pathology and Opportunities for PET Imaging. J Nucl Med 2020; 61: 166–171.

Farfel JM, Yu L, De Jager PL, Schneider JA, Bennett DA. Association of APOE with tau-tangle pathology with and without β-amyloid. Neurobiol Aging 2016; 37: 19–25.

Farrell ME, Jiang S, Schultz AP, Properzi MJ, Price JC, Becker JA, et al. Defining the Lowest Threshold for Amyloid-PET to Predict Future Cognitive Decline and Amyloid Accumulation. Neurology 2021; 96: e619–e631.

Farrer LA, Cupples LA, Haines JL, Hyman B, Kukull WA, Mayeux R, et al. Effects of age, sex, and ethnicity on the association between apolipoprotein E genotype and Alzheimer disease: A meta-analysis. J Am Med Assoc 1997; 278: 1349–1356.

Ferretti MT, Iulita MF, Cavedo E, Chiesa PA, Dimech AS, Chadha AS, et al. Sex differences in Alzheimer disease — The gateway to precision medicine. Nat Rev Neurol 2018; 14: 457–469.

Ferretti MT, Martinkova J, Biskup E, Benke T, Gialdini G, Nedelska Z, et al. Sex and gender differences in Alzheimer's disease: current challenges and implications for clinical practice. Eur J Neurol 2020; 27: 928–943.

Fisher DW, Bennett DA, Dong H. Sexual dimorphism in predisposition to Alzheimer's disease. Neurobiol Aging 2018; 70: 308–324.

Frisoni GB, Boccardi M, Barkhof F, Blennow K, Cappa S, Chiotis K, et al. Strategic roadmap for an early diagnosis of Alzheimer's disease based on biomarkers. Lancet Neurol 2017; 16: 661–676.

Galasko D, Chang L, Motter R, Clark CM, Kaye J, Knopman D, et al. High cerebrospinal fluid tau and low amyloid β42 levels in the clinical diagnosis of Alzheimer disease and relation to apolipoprotein E genotype. Arch Neurol 1998; 55: 937–945.

Ghebremedhin E, Schultz C, Thal DR, Rüb U, Ohm TG, Braak E, et al. Gender and age modify the association between APOE and AD-related neuropathology. Neurology 2001; 56: 1696–1701.

Giannakopoulos P, Herrmann FR, Bussière T, Bouras C, Kövari E, Perl DP, et al. Tangle and neuron numbers, but not amyloid load, predict cognitive status in Alzheimer's disease. Neurology 2003; 60: 1495–1500.

Gispert JD, Monté GC, Falcon C, Tucholka A, Rojas S, Sánchez-Valle R, et al. CSF YKL-40 and pTau181 are related to different cerebral morphometric patterns in early AD. Neurobiol Aging 2016; 38: 47–55.

Gispert JD, Monté GC, Suárez-Calvet M, Falcon C, Tucholka A, Rojas S, et al. The APOE ε4 genotype modulates CSF YKL-40 levels and their structural brain correlates in the continuum of Alzheimer's disease but not those of sTREM2. Alzheimer's Dement Diagnosis, Assess Dis Monit 2017; 6: 50–59.

Gómez-Isla T, Hollister R, West H, Mui S, Growdon JH, Petersen RC, et al. Neuronal loss correlates with but exceeds neurofibrillary tangles in Alzheimer's disease. Ann Neurol 1997; 41: 17–24.

Gratuze M, Leyns CEG, Holtzman DM. New insights into the role of TREM2 in Alzheimer's disease. Mol Neurodegener 2018; 13: 1–16.

Grothe MJ, Teipel SJ, Dyrba M, Sepulcre J, Sabri O, Barthel H. In vivo staging of regional amyloid deposition. Neurology 2017; 89: 2031–2038.

Guerreiro R, Wojtas A, Bras J, Carrasquillo M, Rogaeva E, Majounie E, et al. TREM2 variants in Alzheimer's disease. N Engl J Med 2013; 368: 117–127.

Guillozet AL, Weintraub S, Mash DC, Mesulam MM. Neurofibrillary tangles, amyloid, and memory in aging and mild cognitive impairment. Arch Neurol 2003; 60: 729–736.

Guneykaya D, Ivanov A, Hernandez DP, Haage V, Wojtas B, Meyer N, et al. Transcriptional and Translational Differences of Microglia from Male and Female Brains. Cell Rep 2018; 24: 2773-2783.e6.

Halaas NB, Henjum K, Blennow K, Dakhil S, Idland A-V, Nilsson LN, et al. CSF sTREM2 and Tau Work Together in Predicting Increased Temporal Lobe Atrophy in Older Adults. Cereb Cortex 2020; 30: 2295–2306.

Hanseeuw BJ, Betensky RA, Mormino EC, Schultz AP, Sepulcre J, Becker JA, et al. PET staging of amyloidosis using striatum. Alzheimer's Dement 2018; 14: 1281–1292.

Hanseeuw BJ, Malotaux V, Dricot L, Quenon L, Sznajer Y, Cerman J, et al. Defining a Centiloid scale threshold predicting long-term progression to dementia in patients attending the memory clinic: an [18F] flutemetamol amyloid PET study. Eur J Nucl Med Mol Imaging 2020

Hansson O, Lehmann S, Otto M, Zetterberg H, Lewczuk P. Advantages and disadvantages of the use of the CSF Amyloid β (Aβ) 42/40 ratio in the diagnosis of Alzheimer's Disease. Alzheimer's Res Ther 2019; 11: 1–15.

Hansson O, Seibyl J, Stomrud E, Zetterberg H, Trojanowski JQ, Bittner T, et al. CSF biomarkers of Alzheimer's disease concord with amyloid-β PET and predict clinical progression: A study of fully automated immunoassays in BioFINDER and ADNI cohorts. Alzheimer's Dement 2018: 1–12.

Hansson O, Zetterberg H, Buchhave P, Londos E, Blennow K, Minthon L. Association between CSF biomarkers and incipient Alzheimer's disease in patients with mild cognitive impairment: a follow-up study. Lancet Neurol 2006; 5: 228–234.

Hardy JA, Higgins GA. Alzheimer's disease: The amyloid cascade hypothesis. Science (80-) 1992; 256: 184–185.

He Z, Guo JL, McBride JD, Narasimhan S, Kim H, Changolkar L, et al. Amyloid-β plaques enhance Alzheimer's brain tau-seeded pathologies by facilitating neuritic plaque tau aggregation. Nat Med 2018; 24: 29–38.

Hebert LE, Weuve J, Scherr PA, Evans DA. Alzheimer disease in the United States (2010-2050) estimated using the 2010 census. Neurology 2013; 80: 1778–1783.

Hedden T, Gabrieli JDE. Insights into the ageing mind: A view from cognitive neuroscience. Nat Rev Neurosci 2004; 5: 87–96.

Heneka MT, Carson MJ, Khoury J El, Landreth GE, Brosseron F, Feinstein DL, et al. Neuroinflammation in Alzheimer's disease. Lancet Neurol 2015; 14: 388–405.

Hohman TJ, Dumitrescu L, Barnes LL, Thambisetty M, Beecham G, Kunkle B, et al. Sex-specific association of apolipoprotein e with cerebrospinal fluid levels of tau. JAMA Neurol 2018; 75: 989–998.

Holland D, Desikan RS, Dale AM, McEvoy LK. Higher rates of decline for women and apolipoprotein e ε4 carriers. Am J Neuroradiol 2013; 34: 2287–2293.

Honig LS, Vellas B, Woodward M, Boada M, Bullock R, Borrie M, et al. Trial of Solanezumab for Mild Dementia Due to Alzheimer's Disease. N Engl J Med 2018; 378: 321–330.

Iaccarino L, Tammewar G, Ayakta N, Baker SL, Bejanin A, Boxer AL, et al. Local and distant relationships between amyloid, tau and neurodegeneration in Alzheimer's Disease. NeuroImage Clin 2018; 17: 452–464.

Ikonomovic MD, Buckley CJ, Heurling K, Sherwin P, Jones P a., Zanette M, et al. Post-mortem histopathology underlying β-amyloid PET imaging following flutemetamol F 18 injection. Acta Neuropathol Commun 2016; 4: 130.

Insel PS, Donohue MC, Sperling R, Hansson O, Mattsson-Carlgren N. The A4 study: β-amyloid and cognition in 4432 cognitively unimpaired adults. Ann Clin Transl Neurol 2020; 7: 776–785.

Iwatsubo T, Odaka A, Suzuki N, Mizusawa H, Nukina N, Ihara Y. Visualization of A beta 42(43) and A beta 40 in senile plaques with end-specific A beta monoclonals: evidence that an initially deposited species is A beta 42(43). Neuron 1994; 13: 45–53.

Jack CR, Bennett D a., Blennow K, Carrillo MC, Dunn B, Haeberlein SB, et al. NIA-AA Research Framework: Toward a biological definition of Alzheimer's disease. Alzheimer's Dement 2018; 14: 535–562.

Jack CR, Bennett DA, Blennow K, Carrillo MC, Feldman HH, Frisoni GB, et al. A/T/N: An unbiased descriptive classification scheme for Alzheimer disease biomarkers. Neurology 2016; 87: 539–547.

Jack CR, Knopman DS, Jagust WJ, Petersen RC, Weiner MW, Aisen PS, et al. Tracking pathophysiological processes in Alzheimer's disease: An

updated hypothetical model of dynamic biomarkers. Lancet Neurol 2013; 12: 207–216.

Jack CR, Lowe VJ, Weigand SD, Wiste HJ, Senjem ML, Knopman DS, et al. Serial PIB and MRI in normal, mild cognitive impairment and Alzheimers disease: Implications for sequence of pathological events in Alzheimers disease. Brain 2009; 132: 1355–1365.

Jack CR, Wiste HJ, Weigand SD, Knopman DS, Mielke MM, Vemuri P, et al. Different definitions of neurodegeneration produce similar amyloid/neurodegeneration biomarker group findings. Brain 2015; 138: 3747–3759.

Jack CR, Wiste HJ, Weigand SD, Knopman DS, Vemuri P, Mielke MM, et al. Age, sex, and APOE ϵ4 effects on memory, brain structure, and β-Amyloid across the adult life Span. JAMA Neurol 2015; 72: 511–519.

Jack CR, Wiste HJ, Weigand SD, Therneau TM, Lowe VJ, Knopman DS, et al. Defining imaging biomarker cut points for brain aging and Alzheimer's disease. Alzheimer's Dement 2017; 13: 205–216.

Jack CRJ, Knopman DS, Jagust WJ, Petersen RC, Weiner MW, Aisen PS, et al. Tracking pathophysiological processes in Alzheimer's disease: an updated hypothetical model of dynamic biomarkers. Lancet Neurol 2013; 68: 497–501.

Jack CRJ, Wiste HJ, Weigand SD, Therneau TM, Lowe VJ, Knopman DS, et al. Predicting future rates of tau accumulation on PET. Brain 2020

Jagust W. Is amyloid-β harmful to the brain? Insights from human imaging studies. Brain 2016; 139: 23–30.

Jagust W. Imaging the evolution and pathophysiology of Alzheimer disease. Nat Rev Neurosci 2018

Janelidze S, Mattsson N, Palmqvist S, Smith R, Beach TG, Serrano GE, et al. Plasma P-tau181 in Alzheimer's disease: relationship to other biomarkers, differential diagnosis, neuropathology and longitudinal progression to Alzheimer's dementia. Nat Med 2020; 26: 379–386.

Janelidze S, Stomrud E, Palmqvist S, Zetterberg H, Van Westen D, Jeromin A, et al. Plasma β-amyloid in Alzheimer's disease and vascular disease. Sci Rep 2016; 6: 1–11.

Janelidze S, Stomrud E, Smith R, Palmqvist S, Mattsson N, Airey DC, et al. Cerebrospinal fluid p-tau217 performs better than p-tau181 as a biomarker of Alzheimer's disease. Nat Commun 2020; 11: 1683.

Jansen WJ, Ossenkoppele R, Knol DL, Tijms BM, Scheltens P, Verhey FRJ, et al. Prevalence of cerebral amyloid pathology in persons without dementia: A meta-analysis. JAMA - J Am Med Assoc 2015; 313: 1924–1938.

Jelistratova I, Teipel SJ, Grothe MJ. Longitudinal validity of PET-based staging of regional amyloid deposition. Hum Brain Mapp 2020; 41: 4219–4231.

Joie R La, Ayakta N, Seeley WW, Borys E, Boxer AL, DeCarli C, et al. Multisite study of the relationships between antemortem [11C]PIB-PET Centiloid values and postmortem measures of Alzheimer's disease neuropathology. Alzheimer's Dement 2018: 1–12.

La Joie R, Ayakta N, Seeley WW, Borys E, Boxer AL, DeCarli C, et al. Multisite study of the relationships between antemortem [11 C]PIB-PET Centiloid values and postmortem measures of Alzheimer's disease neuropathology. Alzheimer's Dement 2019; 15: 205–216.

La Joie R, Visani A V, Baker SL, Brown JA, Bourakova V, Cha J, et al. Prospective longitudinal atrophy in Alzheimer's disease correlates with the intensity and topography of baseline tau-PET. Sci Transl Med 2020; 12

van der Kall LM, Truong T, Burnham SC, Doré V, Mulligan RS, Bozinovski S, et al. Association of β-amyloid level, clinical progression and longitudinal cognitive change in normal older individuals. Neurology 2020: 10.1212/WNL.0000000000011222.

van der Kant R, Goldstein LSB, Ossenkoppele R. Amyloid-β-independent regulators of tau pathology in Alzheimer disease. Nat Rev Neurosci 2020; 21: 21–35.

Kern S, Syrjanen JA, Blennow K, Zetterberg H, Skoog I, Waern M, et al. Association of Cerebrospinal Fluid Neurofilament Light Protein with Risk of Mild Cognitive Impairment among Individuals Without Cognitive Impairment. JAMA Neurol 2019; 76: 187–193.

Kester MI, Teunissen CE, Crimmins DL, Herries EM, Ladenson JH, Scheltens P, et al. Neurogranin as a Cerebrospinal Fluid Biomarker for

Synaptic Loss in Symptomatic Alzheimer Disease. JAMA Neurol 2015; 72: 1275–1280.

Khalil M, Teunissen CE, Otto M, Piehl F, Sormani MP, Gattringer T, et al. Neurofilaments as biomarkers in neurological disorders. Nat Rev Neurol 2018; 14: 577–589.

Kim SE, Lee B, Jang H, Chin J, Khoo CS, Choe YS, et al. Cognitive trajectories of patients with focal ß-amyloid deposition. Alzheimers Res Ther 2021; 7: 13:48.

Klunk WE, Engler H, Nordberg A, Wang Y, Blomqvist G, Holt DP, et al. Imaging Brain Amyloid in Alzheimer's Disease with Pittsburgh Compound-B. Ann Neurol 2004; 55: 306–319.

Klunk WE, Koeppe RA, Price JC, Benzinger TL, Devous MD, Jagust WJ, et al. The Centiloid project: Standardizing quantitative amyloid plaque estimation by PET. Alzheimer's Dement 2015; 11: 1-15.e4.

Kuhlmann J, Andreasson U, Pannee J, Bjerke M, Portelius E, Leinenbach A, et al. CSF Aβ1–42– an excellent but complicated Alzheimer's biomarker – a route to standardisation. Clin Chim Acta 2017; 467: 27–33.

Kvartsberg H, Duits FH, Ingelsson M, Andreasen N, Öhrfelt A, Andersson K, et al. Cerebrospinal fluid levels of the synaptic protein neurogranin correlates with cognitive decline in prodromal Alzheimer's disease. Alzheimers Dement 2015; 11: 1180–1190.

Lagarde J, Sarazin M, Bottlaender M. In vivo PET imaging of neuroinflammation in Alzheimer's disease. J Neural Transm 2018; 125: 847–867.

Landau SM, Lu M, Joshi AD, Pontecorvo M, Mintun M a., Trojanowski JQ, et al. Comparing positron emission tomography imaging and cerebrospinal fluid measurements of β-amyloid. Ann Neurol 2013; 74: 826–836.

Landau SM, Thomas BA, Thurfjell L, Schmidt M, Margolin R, Mintun M, et al. Amyloid PET imaging in Alzheimer's disease: A comparison of three radiotracers. Eur J Nucl Med Mol Imaging 2014; 41: 1398–1407.

Lehmann M, Ghosh PM, Madison C, Laforce RJ, Corbetta-Rastelli C, Weiner MW, et al. Diverging patterns of amyloid deposition and hypometabolism in clinical variants of probable Alzheimer's disease. Brain 2013; 136: 844–858.

Leuzy A, Chiotis K, Hasselbalch SG, Rinne JO, De Mendonça A, Otto M, et al. Pittsburgh compound B imaging and cerebrospinal fluid amyloid-β in a multicentre European memory clinic study. Brain 2016; 139: 2540–2553.

Leuzy A, Chiotis K, Lemoine L, Gillberg PG, Almkvist O, Rodriguez-Vieitez E, et al. Tau PET imaging in neurodegenerative tauopathies—still a challenge. Mol Psychiatry 2019; 24: 1112–1134.

Levy JA, Bergeson J, Putnam K, Rosen V, Cohen R, Lalonde F, et al. Context-specific memory and apolipoprotein E (ApoE) epsilon 4: cognitive evidence from the NIMH prospective study of risk for Alzheimer's disease. J Int Neuropsychol Soc 2004; 10: 362–370.

Liesinger AM, Graff-Radford NR, Duara R, Carter RE, Hanna Al-Shaikh FS, Koga S, et al. Sex and age interact to determine clinicopathologic differences in Alzheimer's disease. Acta Neuropathol 2018; 136: 873–885.

Lifke V, Kollmorgen G, Manuilova E, Oelschlaegel T, Hillringhaus L, Widmann M, et al. Elecsys(®) Total-Tau and Phospho-Tau (181P) CSF assays: Analytical performance of the novel, fully automated immunoassays for quantification of tau proteins in human cerebrospinal fluid. Clin Biochem 2019; 72: 30–38.

Lin C-H, Li C-H, Yang K-C, Lin F-J, Wu C-C, Chieh J-J, et al. Blood NfL: A biomarker for disease severity and progression in Parkinson disease. Neurology 2019; 93: e1104–e1111.

Liu CC, Kanekiyo T, Xu H, Bu G. Apolipoprotein e and Alzheimer disease: Risk, mechanisms and therapy. Nat Rev Neurol 2013; 9: 106–118.

Livingston G, Huntley J, Sommerlad A, Ames D, Ballard C, Banerjee S, et al. Dementia prevention, intervention, and care: 2020 report of the Lancet Commission. Lancet 2020; 396: 413–446.

Lopes Alves I, Collij LE, Altomare D, Frisoni GB, Saint-Aubert L, Payoux P, et al. Quantitative amyloid PET in Alzheimer's disease: the AMYPAD prognostic and natural history study. Alzheimer's Dement 2020; 16: 750–758.

Lyman M, Lloyd DG, Ji X, Vizcaychipi MP, Ma D. Neuroinflammation: The role and consequences. Neurosci Res 2014; 79: 1–12.

Maass A, Landau S, Horng A, Lockhart SN, Rabinovici GD, Jagust WJ, et al. Comparison of multiple tau-PET measures as biomarkers in aging and Alzheimer's disease. Neuroimage 2017; 157: 448–463.

Marquié M, Siao Tick Chong M, Antón-Fernández A, Verwer EE, Sáez-Calveras N, Meltzer AC, et al. [F-18]-AV-1451 binding correlates with postmortem neurofibrillary tangle Braak staging. Acta Neuropathol 2017; 134: 619–628.

Masdeu JC. Future Directions in Imaging Neurodegeneration. Curr Neurol Neurosci Rep 2017; 17: 9.

Masliah E, Mallory M, Hansen L, DeTeresa R, Alford M, Terry R. Synaptic and neuritic alterations during the progression of Alzheimer's disease. Neurosci Lett 1994; 174: 67–72.

Mattsson-Carlgren N, Leuzy A, Janelidze S, Palmqvist S, Stomrud E, Strandberg O, et al. The implications of different approaches to define AT(N) in Alzheimer disease. Neurology 2020; 94: e2233–e2244.

Mattsson N, Andreasson U, Persson S, Carrillo MC, Collins S, Chalbot S, et al. CSF biomarker variability in the Alzheimer's Association quality control program. Alzheimers Dement 2013; 9: 251–261.

Mattsson N, Ewers M, Rich K, Kaiser E, Mulugeta E, Rose E. CSF Biomarkers and Incipient Alzheimer Disease. JAMA 2009; 302: 385–393.

Mattsson N, Palmqvist S, Stomrud E, Vogel J, Hansson O. Staging β - Amyloid Pathology with Amyloid Positron Emission Tomography. JAMA Neurol 2019; 76: 1319–1329.

McDade E, Wang G, Gordon BA, Hassenstab J, Benzinger TLS, Buckles V, et al. Longitudinal cognitive and biomarker changes in dominantly inherited Alzheimer disease. Neurology 2018; 91: E1295–E1306.

Medeiros R, LaFerla FM. Astrocytes: conductors of the Alzheimer disease neuroinflammatory symphony. Exp Neurol 2013; 239: 133–138.

Meyer PF, McSweeney M, Gonneaud J, Villeneuve S. AD molecular: PET amyloid imaging across the Alzheimer's disease spectrum: From disease mechanisms to prevention. In: Progress in Molecular Biology and Translational Science. 2019. p. 63–106

Mielke MM, Hagen CE, Xu J, Chai X, Vemuri P, Lowe VJ, et al. Plasma phospho-tau181 increases with Alzheimer's disease clinical severity and is associated with tau- and amyloid-positron emission tomography. Alzheimers Dement 2018; 14: 989–997.

Milà-Alomà M, Salvadó G, Gispert JD, Vilor-Tejedor N, Grau-Rivera O, Sala-Vila A, et al. Amyloid-β, tau, synaptic, neurodegeneration and glial biomarkers in the preclinical stage of the Alzheimer's continuum. Alzheimer's Dement 2020: 1–14.

Milà-Alomà M, Salvadó G, Shekari M, Grau-Rivera O, Sala-Vila A, Sánchez-Benavides G, et al. Comparative Analysis of Different Definitions of Amyloid-β Positivity to Detect Early Downstream Pathophysiological Alterations in Preclinical Alzheimer. J Prev Alzheimer's Dis 2020; in press

Milà-Alomà M, Suárez-Calvet M, Molinuevo JL. Latest advances in cerebrospinal fluid and blood biomarkers of Alzheimer's disease. Ther Adv Neurol Disord 2019; 12: 1–23.

Mills SM, Mallmann J, Santacruz AM, Fuqua A, Carril M, Aisen PS, et al. Preclinical trials in autosomal dominant AD: implementation of the DIAN-TU trial. Rev Neurol (Paris) 2013; 169: 737–743.

Minoshima S, Giordani B, Berent S, Frey KA, Foster NL, Kuhl DE. Metabolic reduction in the posterior cingulate cortex in very early Alzheimer's disease. Ann Neurol 1997; 42: 85–94.

Mirra SS, Heyman A, McKeel D, Sumi SM, Crain BJ, Brownlee LM, et al. The Consortium to Establish a Registry for Alzheimer's Disease (CERAD). Part II. Standardization of the neuropathologic assessment of Alzheimer's disease. Neurology 1991; 41: 479–486.

Mitchell TW, Mufson EJ, Schneider JA, Cochran EJ, Nissanov J, Han L-Y, et al. Parahippocampal tau pathology in healthy aging, mild cognitive impairment, and early Alzheimer's disease. Ann Neurol 2002; 51: 182–189.

Mofrad RB, Tijms BM, Scheltens P, Barkhof F, van der Flier WM, AM Sikkes S, et al. Sex differences in CSF biomarkers vary by Alzheimer's disease stage and APOE ε4 genotype. Neurology 2020: 10.1212/WNL.0000000000010629.

Molinuevo JL, Ayton S, Batrla R, Bednar MM, Bittner T, Cummings J, et al. Current state of Alzheimer's fluid biomarkers. Springer Berlin Heidelberg; 2018

Molinuevo JL, Ayton S, Batrla R, Bednar MM, Bittner T, Cummings J, et al. Current state of Alzheimer's fluid biomarkers. Springer Berlin Heidelberg; 2018

Molinuevo JL, Gramunt N, Gispert JD, Fauria K, Esteller M, Minguillon C, et al. The ALFA project: A research platform to identify early pathophysiological features of Alzheimer's disease. Alzheimer's Dement Transl Res Clin Interv 2016; 2: 82–92.

Molinuevo JL, Minguillon C, Rami L, Gispert JD. The Rationale Behind the New Alzheimer's Disease Conceptualization: Lessons Learned During the Last Decades. J Alzheimers Dis 2018; 62: 1067–1077.

Morris E, Chalkidou A, Hammers A, Peacock J, Summers J, Keevil S. Diagnostic accuracy of18F amyloid PET tracers for the diagnosis of Alzheimer's disease: a systematic review and meta-analysis. Eur J Nucl Med Mol Imaging 2016; 43: 374–385.

Mortamais M, Ash JA, Harrison J, Kaye J, Kramer J, Randolph C, et al. Detecting cognitive changes in preclinical Alzheimer's disease: A review of its feasibility. Alzheimer's Dement 2017; 13: 468–492.

Motter R, Vigo-Pelfrey C, Kholodenko D, Barbour R, Johnson-Wood K, Galasko D, et al. Reduction of beta-amyloid peptide42 in the cerebrospinal fluid of patients with Alzheimer's disease. Ann Neurol 1995; 38: 643–648.

Mungas D, Tractenberg R, Schneider JA, Crane PK, Bennett DA. A 2-process model for neuropathology of Alzheimer's disease. Neurobiol Aging 2014; 35: 301–308.

Musiek ES, Holtzman DM. Origins of Alzheimer's disease: Reconciling cerebrospinal fluid biomarker and neuropathology data regarding the temporal sequence of amyloid-beta and tau involvement. Curr Opin Neurol 2012; 25: 715–720.

Nagy ZS, Esiri MM, Jobst KA, Johnston C, Litchfield S, Sim E, et al. Influence of the apolipoprotein E genotype on amyloid deposition and neurofibrillary tangle formation in Alzheimer's disease. Neuroscience 1995; 69: 757–761.

Nakamura A, Kaneko N, Villemagne VL, Kato T, Doecke J, Doré V, et al. High performance plasma amyloid-β biomarkers for Alzheimer's disease. Nature 2018; 554: 249–254.

Navitsky M, Joshi AD, Kennedy I, Klunk WE, Rowe CC, Wong DF, et al. Standardization of amyloid quantitation with florbetapir standardized uptake value ratios to the Centiloid scale. Alzheimer's Dement 2018; 14: 1565–1571.

Nelson PT, Alafuzoff I, Bigio EH, Bouras C, Braak H, Cairns NJ, et al. Correlation of Alzheimer disease neuropathologic changes with cognitive status: a review of the literature. J Neuropathol Exp Neurol 2012; 71: 362–381.

Nelson PT, Dickson DW, Trojanowski JQ, Jack CR, Boyle PA, Arfanakis K, et al. Limbic-predominant age-related TDP-43 encephalopathy (LATE): consensus working group report. Brain 2019; 142: 1503–1527.

Neu SC, Pa J, Kukull W, Beekly D, Kuzma A, Gangadharan P, et al. Apolipoprotein E genotype and sex risk factors for Alzheimer disease: A meta-analysis. JAMA Neurol 2017; 74: 1178–1189.

Ngandu T, Lehtisalo J, Solomon A, Levälahti E, Ahtiluoto S, Antikainen R, et al. A 2 year multidomain intervention of diet, exercise, cognitive training, and vascular risk monitoring versus control to prevent cognitive decline in at-risk elderly people (FINGER): A randomised controlled trial. Lancet 2015; 385: 2255–2263.

Norton S, Matthews FE, Barnes DE, Yaffe K, Brayne C. Potential for primary prevention of Alzheimer's disease: an analysis of population-based data. Lancet Neurol 2014; 13: 788–794.

Okamura N, Harada R, Ishiki A, Kikuchi A, Nakamura T, Kudo Y. The development and validation of tau PET tracers: current status and future directions. Clin Transl imaging 2018; 6: 305–316.

Olsson B, Lautner R, Andreasson U, Öhrfelt A, Portelius E, Bjerke M, et al. CSF and blood biomarkers for the diagnosis of Alzheimer's disease: a systematic review and meta-analysis. Lancet Neurol 2016; 15: 673–684.

Ossenkoppele R, Schonhaut DR, Baker SL, O'Neil JP, Janabi M, Ghosh PM, et al. Tau, amyloid, and hypometabolism in a patient with posterior cortical atrophy. Ann Neurol 2015; 77: 338–342.

Ossenkoppele R, Schonhaut DR, Schöll M, Lockhart SN, Ayakta N, Baker SL, et al. Tau PET patterns mirror clinical and neuroanatomical variability in Alzheimer's disease. Brain 2016; 139: 1551–1567.

Ossenkoppele R, Schonhaut DR, Schöll M, Lockhart SN, Ayakta N, Baker SL, et al. Tau PET patterns mirror clinical and neuroanatomical variability in Alzheimer's disease. Brain 2016; 139: 1551–1567.

Oyama F, Shimada H, Oyama R, Ihara Y. Apolipoprotein E genotype, Alzheimer's pathologies and related gene expression in the aged population. Mol Brain Res 1995; 29: 92–98.

Palmqvist S, Insel PS, Stomrud E, Janelidze S, Zetterberg H, Brix B, et al. Cerebrospinal fluid and plasma biomarker trajectories with increasing amyloid deposition in Alzheimer's disease. EMBO Mol Med 2019; 11: 1–13.

Palmqvist S, Insel PS, Stomrud E, Janelidze S, Zetterberg H, Brix B, et al. Cerebrospinal fluid and plasma biomarker trajectories with increasing amyloid deposition in Alzheimer's disease. EMBO Mol Med 2019; 11: 1–13.

Palmqvist S, Mattsson N, Hansson O. Cerebrospinal fluid analysis detects cerebral amyloid-β accumulation earlier than positron emission tomography. Brain 2016; 139: 1226–1236.

Palmqvist S, Schöll M, Strandberg O, Mattsson N, Stomrud E, Zetterberg H, et al. Earliest accumulation of β-amyloid occurs within the default-mode network and concurrently affects brain connectivity. Nat Commun 2017; 8

Palmqvist S, Zetterberg H, Blennow K, Vestberg S, Andreasson U, Brooks DJ, et al. Accuracy of brain amyloid detection in clinical practice using cerebrospinal fluid β-Amyloid 42: A cross-validation study against amyloid positron emission tomography. JAMA Neurol 2014; 71: 1282–1289.

Palmqvist S, Zetterberg H, Mattsson N, Johansson P, Minthon L, Blennow K, et al. Detailed comparison of amyloid PET and CSF biomarkers for identifying early Alzheimer disease. Neurology 2015; 85: 1240–1249.

Pascoal TA, Therriault J, Benedet AL, Savard M, Lussier FZ, Chamoun M, et al. 18F-MK-6240 PET for early and late detection of neurofibrillary tangles. Brain 2020; 143: 2818–2830.

Pontecorvo MJ, Devous MD, Navitsky M, Lu M, Salloway S, Schaerf FW, et al. Relationships between flortaucipir PET tau binding and amyloid burden, clinical diagnosis, age and cognition. Brain 2017; 140: 748–763.

Portelius E, Zetterberg H, Skillbäck T, Törnqvist U, Andreasson U, Trojanowski JQ, et al. Cerebrospinal fluid neurogranin: relation to cognition and neurodegeneration in Alzheimer's disease. Brain 2015; 138: 3373–3385.

Preische O, Schultz SA, Apel A, Kuhle J, Kaeser SA, Barro C, et al. Serum neurofilament dynamics predicts neurodegeneration and clinical progression in presymptomatic Alzheimer's disease. Nat Med 2019; 25: 277–283.

Price JL, Morris JC. Tangles and plaques in nondemented aging and 'preclinical' alzheimer's disease. Ann Neurol 1999; 45: 358–368.

Prince M, Bryce R, Albanese E, Wimo A, Ribeiro W, Perrin CP. The global prevalence of latent tuberculosis: A systematic review and meta-analysis. Alzheimer's Dement 2013; 9: 63–75.

Rauchmann BS, Schneider-Axmann T, Alexopoulos P, Perneczky R. CSF soluble TREM2 as a measure of immune response along the Alzheimer's disease continuum. Neurobiol Aging 2019; 74: 182–190.

Raz N, Lindenberger U, Rodrigue KM, Kennedy KM, Head D, Williamson A, et al. Regional brain changes in aging healthy adults: general trends, individual differences and modifiers. Cereb Cortex 2005; 15: 1676–1689.

Reiman EM. Fluorodeoxyglucose positron emission tomography: Emerging roles in the evaluation of putative Alzheimer's disease-modifying treatments. Neurobiol Aging 2011; 32: S44–S47.

Reiman EM, Arboleda-Velasquez JF, Quiroz YT, Huentelman MJ, Beach TG, Caselli RJ, et al. Exceptionally low likelihood of Alzheimer's dementia in APOE2 homozygotes from a 5,000-person neuropathological study. Nat Commun 2020; 11: 667.

Reiman EM, Chen K, Alexander GE, Caselli RJ, Bandy D, Osborne D, et al. Correlations between apolipoprotein E ε4 gene dose and brain-imaging measurements of regional hypometabolism. Proc Natl Acad Sci U S A 2005; 102: 8299–8302.

Reiman EM, Chen K, Liu X, Bandy D, Yu M, Lee W, et al. Fibrillar amyloid-beta burden in cognitively normal people at 3 levels of genetic risk for Alzheimer's disease. Proc Natl Acad Sci U S A 2009; 106: 6820–6825.

Reiman EM, Jagust WJ. Brain imaging in the study of Alzheimer's disease. Neuroimage 2012; 61: 505–516.

Roberts BR, Lind M, Wagen AZ, Rembach A, Frugier T, Li QX, et al. Biochemically-defined pools of amyloid-β in sporadic Alzheimer's disease: Correlation with amyloid PET. Brain 2017; 140: 1486–1498.

Roher AE, Lowenson JD, Clarke S, Wolkow C, Wang R, Cotter RJ, et al. Structural alterations in the peptide backbone of beta-amyloid core protein may account for its deposition and stability in Alzheimer's disease. J Biol Chem 1993; 268: 3072–3083.

Rowe CC, Ackerman U, Browne W, Mulligan R, Pike KL, O'Keefe G, et al. Imaging of amyloid beta in Alzheimer's disease with 18F-BAY94-9172, a novel PET tracer: proof of mechanism. Lancet Neurol 2008; 7: 129–135.

Rowe CC, Doré V, Jones G, Baxendale D, Mulligan RS, Bullich S, et al. 18F-Florbetaben PET beta-amyloid binding expressed in Centiloids. Eur J Nucl Med Mol Imaging 2017; 44: 2053–2059.

Rowe CC, Villemagne VL. Brain amyloid imaging. J Nucl Med Technol 2013; 41: 11–18.

Sabri O, Sabbagh MN, Seibyl J, Barthel H, Akatsu H, Ouchi Y, et al. Florbetaben PET imaging to detect amyloid beta plaques in Alzheimer's disease: Phase 3 study. Alzheimer's Dement 2015; 11: 964–974.

Sager MA, Hermann B, La Rue A. Middle-aged children of persons with Alzheimer's disease: APOE genotypes and cognitive function in the Wisconsin Registry for Alzheimer's Prevention. J Geriatr Psychiatry Neurol 2005; 18: 245–249.

Saint-Aubert L, Almkvist O, Chiotis K, Almeida R, Wall A, Nordberg A. Regional tau deposition measured by [(18)F]THK5317 positron emission tomography is associated to cognition via glucose metabolism in Alzheimer's disease. Alzheimers Res Ther 2016; 8: 38.

Salloway S, Gamez JE, Singh U, Sadowsky CH, Villena T, Sabbagh MN, et al. Performance of [18F]flutemetamol amyloid imaging against the neuritic plaque component of CERAD and the current (2012) NIA-AA recommendations for the neuropathologic diagnosis of Alzheimer's disease. Alzheimer's Dement Diagnosis, Assess Dis Monit 2017; 9: 25–34.

Salvadó G, Grothe MJ, Groot C, Moscoso A, Schöll M, Gispert JD, et al. Differential effects of APOE-ε2 and APOE-ε4 alleles on PET-measured amyloid-β and tau deposition in older individuals without dementia. Eur J Nucl Med Mol Imaging 2021; 16

Sampedro F, Vilaplana E, J de LM, Alcolea D, Pegueroles J, Montal V, et al. APOE-by-sex interactions on brain structure and metabolism in healthy elderly controls. Oncotarget 2015; 6: 26663–26674.

Scheltens P, Blennow K, Breteler MMB, de Strooper B, Frisoni GB, Salloway S, et al. Alzheimer's disease. Lancet 2016; 388: 505–517.

Scheltens P, Leys D, Barkhof F, Huglo D, Weinstein HC, Vermersch P, et al. Atrophy of medial temporal lobes on MRI in 'probable' Alzheimer's disease and normal ageing: diagnostic value and neuropsychological correlates. J Neurol Neurosurg Psychiatry 1992; 55: 967–972.

Schindler SE, Gray JD, Gordon BA, Xiong C, Batrla-Utermann R, Quan M, et al. Cerebrospinal fluid biomarkers measured by Elecsys assays compared to amyloid imaging. Alzheimer's Dement 2018: 1–10.

Schindler SE, Li Y, Todd KW, Herries EM, Henson RL, Gray JD, et al. Emerging cerebrospinal fluid biomarkers in autosomal dominant Alzheimer's disease. Alzheimer's Dement 2019; 15: 655–665.

Schöll M, Lockhart SN, Schonhaut DR, O'Neil JP, Janabi M, Ossenkoppele R, et al. PET Imaging of Tau Deposition in the Aging Human Brain. Neuron 2016; 89: 971–982.

Schwarz CG, Senjem ML, Gunter JL, Kemp BJ, Spychalla AJ, Vemuri P, et al. Optimizing PiB-PET SUVR change-over-time measurement by a large-scale analysis of longitudinal reliability, plausibility, separability, and correlation with MMSE. Neuroimage 2017; 144: 113–127.

Selkoe DJ. Alzheimer disease and aducanumab: adjusting our approach. Nat Rev Neurol 2019; 15: 365–366.

Selkoe DJ, Hardy J. The amyloid hypothesis of Alzheimer's disease at 25 years. EMBO Mol Med 2016; 8: 595–608.

Serrano-Pozo A, Qian J, Monsell SE, Betensky RA, Hyman BT. APOEε2 is associated with milder clinical and pathological Alzheimer disease. Ann Neurol 2015; 77: 917–929.

Shaw LM, Vanderstichele H, Knapik-Czajka M, Clark CM, Aisen PS, Petersen RC, et al. Cerebrospinal fluid biomarker signature in alzheimer's disease neuroimaging initiative subjects. Ann Neurol 2009; 65: 403–413.

Shaw LM, Waligorska T, Fields L, Korecka M, Figurski M, Trojanowski JQ, et al. Derivation of cutoffs for the Elecsys ® amyloid β (1–42) assay in Alzheimer's disease. Alzheimer's Dement Diagnosis, Assess Dis Monit 2018: 1–8.

Shi Y, Yamada K, Liddelow SA, Smith ST, Zhao L, Luo W, et al. ApoE4 markedly exacerbates tau-mediated neurodegeneration in a mouse model of tauopathy. Nature 2017; 549: 523–527.

Shock NW, Greulich richard c, Costa PTJ, Andres R, Lakatta EG, Arenberg D, et al. Normal Human Aging: The Baltimore Longitudinal Study of Aging. NIH Publ No 84-2450 1984

Sjögren M, Blomberg M, Jonsson M, Wahlund LO, Edman A, Lind K, et al. Neurofilament protein in cerebrospinal fluid: a marker of white matter changes. J Neurosci Res 2001; 66: 510–516.

Skillbäck T, Farahmand B, Bartlett JW, Rosén C, Mattsson N, Nägga K, et al. CSF neurofilament light differs in neurodegenerative diseases and predicts severity and survival. Neurology 2014; 83: 1945–1953.

Sperling R, Mormino E, Johnson K. The evolution of preclinical Alzheimer's disease: Implications for prevention trials. Neuron 2014; 84: 608–622.

Sperling RA, Aisen PS, Beckett LA, Bennett DA, Craft S, Fagan AM, et al. Toward defining the preclinical stages of Alzheimer's disease. Alzheimer's Dement 2011; 7: 280–292.

Sperling RA, Aisen PS, Beckett LA, Bennett DA, Craft S, Fagan AM, et al. Toward defining the preclinical stages of Alzheimer's disease: Recommendations from the National Institute on Aging-Alzheimer's Association workgroups on diagnostic guidelines for Alzheimer's disease. Alzheimer's Dement 2011; 7: 280–292.

Sperling RA, Mormino EC, Johnson KA. The Evolution of Preclinical Alzheimer's Disease: Implications for Prevention Trials. Neuron 2014; 84: 608–622.

Sperling RA, Rentz DM, Johnson KA, Karlawish J, Donohue M, Salmon DP, et al. The A4 Study: Stopping AD before Symptoms Begin? Sci Transl Med 2014; 6

Spina S, La Joie R, Petersen C, Nolan AL, Cuevas D, Cosme C, et al. Comorbid neuropathological diagnoses in early vs late-onset Alzheimer's disease. Medrxiv 2020

Stelzmann RA, Norman Schnitzlein H, Reed Murtagh F. An english translation of alzheimer's 1907 paper, "über eine eigenartige erkankung der hirnrinde". Clin Anat 1995; 8: 429–431.

Suárez-Calvet M, Caballero MÁA, Kleinberger G, Bateman RJ, Fagan AM, Morris JC, et al. Early changes in CSF sTREM2 in dominantly inherited Alzheimer's disease occur after amyloid deposition and neuronal injury. Sci Transl Med 2016; 8: 34–38.

Suárez-Calvet M, Morenas-Rodríguez E, Kleinberger G, Schlepckow K, Caballero MÁA, Franzmeier N, et al. Early increase of CSF sTREM2 in Alzheimer's disease is associated with tau related-neurodegeneration but not with amyloid-β pathology. Mol Neurodegener 2019; 14: 1–14.

Suárez-Calvet M, Karikari TK, Ashton nicholas j, Lantero-Rodríguez J, Milà-Alomà M, Gispert JD, et al. Novel tau biomarkers phosphorylated at T181, T217 or T231 rise in the initial stages of the preclinical Alzheimer's continuum when only subtle changes in Ab pathology are detected. EMBO Mol Med 2020

Suárez-Calvet M, Kleinberger G, Araque Caballero MÁ, Brendel M, Rominger A, Alcolea D, et al. sTREM 2 cerebrospinal fluid levels are a potential biomarker for microglia activity in early-stage Alzheimer's disease and associate with neuronal injury markers. EMBO Mol Med 2016; 8: 466–476.

Swardfager W, Lanctôt K, Rothenburg L, Wong A, Cappell J, Herrmann N. A meta-analysis of cytokines in Alzheimer's disease. Biol Psychiatry 2010; 68: 930–941.

Tarawneh R, D'Angelo G, Crimmins D, Herries E, Griest T, Fagan AM, et al. Diagnostic and Prognostic Utility of the Synaptic Marker Neurogranin in Alzheimer Disease. JAMA Neurol 2016; 73: 561–571.

Teipel SJ, Temp AGM, Levin F, Dyrba M, Grothe MJ. Association of PET-based stages of amyloid deposition with neuropathological markers of Aβ pathology. Ann Clin Transl Neurol 2020

Terry RD, Masliah E, Salmon DP, Butters N, DeTeresa R, Hill R, et al. Physical basis of cognitive alterations in Alzheimer's disease: synapse loss is the major correlate of cognitive impairment. Ann Neurol 1991; 30: 572–580.

Thal DR, Beach TG, Zanette M, Lilja J, Heurling K, Chakrabarty A, et al. Estimation of amyloid distribution by [18F]flutemetamol PET predicts the neuropathological phase of amyloid β-protein deposition. Acta Neuropathol 2018; 136: 557–567.

Thal DR, Rüb U, Orantes M, Braak H. Phases of Aβ-deposition in the human brain and its relevance for the development of AD. Neurology 2002; 58: 1791–1800.

Thal DR, Rüb U, Schultz C, Sassin I, Ghebremedhin E, Del Tredici K, et al. Sequence of Aβ-protein deposition in the human medial temporal lobe. J Neuropathol Exp Neurol 2000; 59: 733–748.

Therriault J, Benedet AL, Pascoal TA, Mathotaarachchi S, Chamoun M, Savard M, et al. Association of Apolipoprotein e ϵ4 with Medial Temporal Tau Independent of Amyloid-β. JAMA Neurol 2020; 77: 470–479.

Therriault J, Benedet AL, Pascoal TA, Mathotaarachchi S, Savard M, Chamoun M, et al. APOEε4 potentiates the relationship between amyloid-β and tau pathologies. Mol Psychiatry 2020

Thijssen EH, La Joie R, Wolf A, Strom A, Wang P, Iaccarino L, et al. Diagnostic value of plasma phosphorylated tau181 in Alzheimer's disease and frontotemporal lobar degeneration. Nat Med 2020; 26: 387–397.

Thorsell A, Bjerke M, Gobom J, Brunhage E, Vanmechelen E, Andreasen N, et al. Neurogranin in cerebrospinal fluid as a marker of synaptic degeneration in Alzheimer's disease. Brain Res 2010; 1362: 13–22.

Toledo JB, Bjerke M, Da X, Landau SM, Foster NL, Jagust W, et al. Nonlinear association between Cerebrospinal fluid and florbetapir F-18 β-amyloid measures across the spectrum of Alzheimer disease. JAMA Neurol 2015; 72: 571–581.

Vandenberghe R, Van Laere K, Ivanoiu A, Salmon E, Bastin C, Triau E, et al. 18F-flutemetamol amyloid imaging in Alzheimer disease and mild cognitive impairment: a phase 2 trial. Ann Neurol 2010; 68: 319–329.

Varnum MM, Ikezu T. The classification of microglial activation phenotypes on neurodegeneration and regeneration in Alzheimer's disease brain. Arch Immunol Ther Exp (Warsz) 2012; 60: 251–266.

Vemuri P, Knopman DS, Lesnick TG, Przybelski SA, Mielke MM, Graff-Radford J, et al. Evaluation of amyloid protective factors and alzheimer disease neurodegeneration protective factors in elderly individuals. JAMA Neurol 2017; 74: 718–726.

Villemagne VL, Burnham S, Bourgeat P, Brown B, Ellis KA, Salvado O, et al. Amyloid-β deposition, neurodegeneration, and cognitive decline in

sporadic Alzheimer's disease: A prospective cohort study. Lancet Neurol 2013; 12: 357–367.

Villemagne VL, Ong K, Mulligan RS, Holl G, Pejoska S, Jones G, et al. Amyloid imaging with (18)F-florbetaben in Alzheimer disease and other dementias. J Nucl Med 2011; 52: 1210–1217.

Villeneuve S, Rabinovici GD, Cohn-Sheehy BI, Madison C, Ayakta N, Ghosh PM, et al. Existing Pittsburgh Compound-B positron emission tomography thresholds are too high: Statistical and pathological evaluation. Brain 2015; 138: 2020–2033.

Vogel JW, Iturria-Medina Y, Strandberg OT, Smith R, Levitis E, Evans AC, et al. Spread of pathological tau proteins through communicating neurons in human Alzheimer's disease. Nat Commun 2020; 11: 2612.

Wang H, Shen X, Li J, Suckling J, Tan C, Wang Y, et al. Clinical and biomarker trajectories in sporadic Alzheimer's disease: A longitudinal study. Alzheimer's Dement Diagnosis, Assess Dis Monit 2020; 12: 1–10.

Webers A, Heneka MT, Gleeson PA. The role of innate immune responses and neuroinflammation in amyloid accumulation and progression of Alzheimer's disease. Immunol Cell Biol 2020; 98: 28–41.

Weintraub S, Wicklund AH, Salmon DP. The neuropsychological profile of Alzheimer disease. Cold Spring Harb Perspect Med 2012; 2: a006171.

Wellington H, Paterson RW, Portelius E, Törnqvist U, Magdalinou N, Fox NC, et al. Increased CSF neurogranin concentration is specific to Alzheimer disease. Neurology 2016; 86: 829–835.

Weston PSJ, Poole T, O'Connor A, Heslegrave A, Ryan NS, Liang Y, et al. Longitudinal measurement of serum neurofilament light in presymptomatic familial Alzheimer's disease. Alzheimers Res Ther 2019; 11: 19.

Weston PSJ, Poole T, Ryan NS, Nair A, Liang Y, Macpherson K, et al. Serum neurofilament light in familial Alzheimer disease: A marker of early neurodegeneration. Neurology 2017; 89: 2167–2175.

Whitwell JL, Josephs KA, Murray ME, Kantarci K, Przybelski SA, Weigand SD, et al. MRI correlates of neurofibrillary tangle pathology at autopsy: a voxel-based morphometry study. Neurology 2008; 71: 743–749.

Whitwell JL, Martin P, Graff-Radford J, Machulda MM, Senjem ML, Schwarz CG, et al. The role of age on tau PET uptake and gray matter

atrophy in atypical Alzheimer's disease. Alzheimer's Dement 2019; 15: 675–685.

Wong DF, Rosenberg PB, Zhou Y, Kumar A, Raymont V, Ravert HT, et al. In vivo imaging of amyloid deposition in Alzheimer disease using the radioligand 18F-AV-45 (florbetapir [corrected] F 18). J Nucl Med 2010; 51: 913–920.

Yang JT, Wang ZJ, Cai HY, Yuan L, Hu MM, Wu MN, et al. Sex Differences in Neuropathology and Cognitive Behavior in APP/PS1/tau Triple-Transgenic Mouse Model of Alzheimer's Disease. Neurosci Bull 2018; 34: 736–746.

Zetterberg H, Bendlin BB. Biomarkers for Alzheimer's disease—preparing for a new era of disease-modifying therapies. Mol Psychiatry 2020

Zetterberg H, Blennow K. Moving fluid biomarkers for Alzheimer ' s disease from research tools to routine clinical diagnostics. Mol Neurodegener 2021; 16: 1–7.

Zetterberg H, Mörtberg E, Song L, Chang L, Provuncher GK, Patel PP, et al. Hypoxia due to cardiac arrest induces a time-dependent increase in serum amyloid β levels in humans. PLoS One 2011; 6: e28263.

Zetterberg H, Skillbäck T, Mattsson N, Trojanowski JQ, Portelius E, Shaw LM, et al. Association of cerebrospinal fluid neurofilament light concentration with Alzheimer disease progression. JAMA Neurol 2016; 73: 60–67.

Zhao N, Ren Y, Yamazaki Y, Qiao W, Li F, Felton LM, et al. Alzheimer's Risk Factors Age, APOE Genotype, and Sex Drive Distinct Molecular Pathways. Neuron 2020: 727–742.